

AD-A084 416

AD A089416

MANUFACTURING METHODS AND TECHNOLOGY
(MANTECH) PROGRAM

TECHNICAL
LIBRARY

SERVICE LIFE DETERMINATION FOR THE UH-60A (BLACKHAWK)
HELICOPTER ELASTOMERIC BEARINGS

Seymour A. Hatch
CR Industries
Mechanical Products Division
Engineering Facilities
2517 Pan Am Boulevard
Elk Grove Village, IL 60007

April 1980

FINAL REPORT

Contract No. DAAG46-78-C-0029



Approved for public release;
distribution unlimited

United States Army
AVIATION RESEARCH AND DEVELOPMENT COMMAND

-- 2 OF 2
-- 1 - AD NUMBER: A089416
--48 - SBI SITE HOLDING SYMBOL: TAV
-- 2 - FIELDS AND GROUPS: 1/3.1, 11/10, 13/9
-- 3 - ENTRY CLASSIFICATION: UNCLASSIFIED
-- 5 - CORPORATE AUTHOR: CR INDUSTRIES ELK GROVE VILLAGE IL MECHANICAL
PRODUCTS DIV
-- 6 - UNCLASSIFIED TITLE: SERVICE LIFE DETERMINATION FOR THE UH-60A
(BLACKHAWK) HELICOPTER ELASTOMETRIC BEARINGS.
-- 8 - TITLE CLASSIFICATION: UNCLASSIFIED
-- 9 - DESCRIPTIVE NOTE: FINAL REPT.,
--10 - PERSONAL AUTHORS: HATCH,SEYMOUR A. ;
--11 - REPORT DATE: APR , 1980
--12 - PAGINATION: 246P MEDIA COST: \$ 11.00 PRICE CODE: AC
--15 - CONTRACT NUMBER: DAAG46-78-C-0029
--18 - MONITOR ACRONYM: USAAVRADCOM,AMMRC
--19 - MONITOR SERIES: TR-80-F-8,TR-80-24
--20 - REPORT CLASSIFICATION: UNCLASSIFIED
--21 - SUPPLEMENTARY NOTE: REPORT ON MANUFACTURING METHODS AND
TECHNOLOGY (MANTECH) PROGRAM.
--23 - DESCRIPTORS: *MANUFACTURING, *TECHNOLOGY TRANSFER,
*METHODOLOGY, *BEARINGS, *ELASTOMERS, FATIGUE(MECHANICS),
<<P FOR NEXT PAGE>> OR <<ENTER NEXT COMMAND>>
MSG RECEIVED

Y
1a ROW=24 COL= 01

<Ctrl>H For Help

N Poll

The findings in this report are not to be construed as an official
Department of the Army position, unless so designated by other
authorized documents.

Mention of any trade names or manufacturers in this report
shall not be construed as advertising nor as an official
endorsement or approval of such products or companies by
the United States Government.

DISPOSITION INSTRUCTIONS

Destroy this report when it is no longer needed.
Do not return it to the originator.

UNCLASSIFIED

SECURITY CLASSIFICATION OF THIS PAGE (When Data Entered)

REPORT DOCUMENTATION PAGE		READ INSTRUCTIONS BEFORE COMPLETING FORM
1. REPORT NUMBER AVRADCOM-80-F-8	2. GOVT ACCESSION NO.	3. RECIPIENT'S CATALOG NUMBER
4. TITLE (and Subtitle) SERVICE LIFE DETERMINATION FOR THE UH-60A (BLACKHAWK) HELICOPTER ELASTOMERIC BEARINGS		5. TYPE OF REPORT & PERIOD COVERED Final Report
		6. PERFORMING ORG. REPORT NUMBER
7. AUTHOR(s) Seymour A. Hatch		8. CONTRACT OR GRANT NUMBER(s) DAAG-46-78-C-0029
9. PERFORMING ORGANIZATION NAME AND ADDRESS CR Industries Mechanical Products Division 2515-2517 Pan Am Blvd. Elk Grove Village, IL 60007		10. PROGRAM ELEMENT, PROJECT, TASK AREA & WORK UNIT NUMBERS D/A Project: 1757095 AMCMS Code: 1498.94.587095 Agency Accession: (YYS)
11. CONTROLLING OFFICE NAME AND ADDRESS Army Aviation Research & Development St. Louis, MO 63166 Command		12. REPORT DATE April, 1980
14. MONITORING AGENCY NAME & ADDRESS(if different from Controlling Office) Army Materials & Mechanics Research Center Watertown, MA 02131		13. NUMBER OF PAGES 272
		15. SECURITY CLASS. (of this report) Unclassified
		15a. DECLASSIFICATION/DOWNGRADING SCHEDULE N/A
16. DISTRIBUTION STATEMENT (of this Report) Approved for public release; distribution unlimited.		
17. DISTRIBUTION STATEMENT (of the abstract entered in Block 20, if different from Report)		
18. SUPPLEMENTARY NOTES AMMRC TR 80-24		
19. KEY WORDS (Continue on reverse side if necessary and identify by block number) UH-60A Helicopter Elastomers Predictions Helicopters Bearing Blackhawk Fatigue Life expectancy Finite Element		
20. ABSTRACT (Continue on reverse side if necessary and identify by block number) The contract with AMMRC calls for developing an improved method of predicting the service life of elastomeric bearings in general with specific reference to the Blackhawk main rotor bearings. One object of this study is to develop a correlation between a bearing that has sustained some endurance damage and its remaining service life based on its appearance. The second objective is to develop an analytical capability to predict the		

UNCLASSIFIED

SECURITY CLASSIFICATION OF THIS PAGE(When Data Entered)

Block No. 20

ABSTRACT

service life of bearings without the necessity for testing.

An endurance rating for an appropriate elastomer is determined by testing a series of 13 test specimens. The test specimen and the Blackhawk main rotor bearings are analysed by finite element methods. A procedure is developed for relating the complex strain history of the Blackhawk bearings to the endurance data so that a life prediction can be made for the main rotor bearings without testing. The main rotor bearings are then tested and experimental and analytical results compared.

UNCLASSIFIED

SECURITY CLASSIFICATION OF THIS PAGE(When Data Entered)

FOREWARD

This project was accomplished as part of the U. S. Army Aviation Research and Development Command Manufacturing Technology program. The primary objective of this program is to develop, on a timely basis, manufacturing processes, techniques, and equipment for use in production of Army Material. Comments are solicited on the potential utilization of the information contained herein as applied to present and/or future production programs. Such comments should be sent to: U. S. Army Aviation Research and Development Command, ATTN: DRSAV-EXT, P. O. Box 209, St. Louis, MO 63166.

The work described in this report was accomplished under a contract let and monitored by the U. S. Army Materials and Mechanics Research Center (DAAG46-78-C-0029).

PREFACE

The author is grateful for the contributions of the following individuals:

Dr. Barnard Halpin -- Coordination of this project for the Army Material and Mechanics Research Center.

J.P. Morley -- Coordination of this project for CR Industries.

E.M. Skroch -- Supervision and reporting of test work.

T.G. Mueller -- Material recommendations, testing and reporting.

S. Rengarajan -- Finite element modeling, data reduction and general assistance.

Mrs. Olga Kriz -- Typing this report.

INDEX OF REPORT SECTIONS

SECTION	TITLE	PAGE
	FORWARD.....	3
	PREFACE.....	5
1.	OUTLINE OF OBJECTIVES.....	9
2.	METHODOLOGY OF FINITE ELEMENT ANALYSIS AT CR INDUSTRIES.....	27
3.	ANALYSIS OF ENDURANCE STRAINS.....	47
4.	ANALYSIS OF THE AMMRC FATIGUE SPECIMEN.....	71
5.	EXPERIMENTAL DATA ON AMMRC ENDURANCE SPECIMEN.....	97
6.	ANALYSIS OF THE BLACKHAWK MAIN ROTOR THRUST BEARING.....	113
7.	ANALYSIS OF THE SHELL STRESSES IN AN ALTERNATE BLACKHAWK MAIN ROTOR THRUST BEARING.....	145
8.	ANALYSIS OF THE BLACKHAWK MAIN ROTOR SPHERICAL BEARING.....	171
9.	TEST RESULTS ON THE BLACKHAWK MAIN ROTOR BEARINGS.....	225
10.	TEST RESULTS ON THE BLACKHAWK MAIN ROTOR SPHERICAL BEARING WITH ON-OFF CENTRIFUGAL FORCE AS THE ONLY LOADING MODE.....	241
11.	TEST RESULTS ON THE ALTERNATE BLACKHAWK MAIN ROTOR THRUST BEARING WITH ON-OFF CENTRIFUGAL FORCE AS THE ONLY LOADING MODE.....	253
12.	SUMMARY AND CONCLUSIONS.....	269

SECTION 1.
OUTLINE OF OBJECTIVES

OUTLINE OF OBJECTIVES

The main rotor elastomeric bearings used on the Blackhawk model helicopter are flight critical hardware. It is imperative that their service life be predictable and well known. Correctly applied elastomeric bearings should degrade gradually and give some visual indication of their remaining life. Blackhawk main rotor bearings are to be replaced on an "on condition basis". It is, therefore, important to be able to correlate the appearance of a bearing with its remaining service life.

Under this contract two sets of Blackhawk main rotor bearings (see Figs. 1, 2 & 3) will be endurance tested to Sikorsky Aircraft's load and motion specification S.E.S. 701059 Rev. 4. Fig. 4, 5 & 6 show the proposed blocks of endurance testing that will be used. During the test the free heights, spring rates and photographic appearance of the bearings will be recorded. The unaccelerated test will be run for the equivalent of 1500 hrs. of helicopter flight or until a red line value is reached for any of the above. Fig. 7

& 8 are basic line drawings of the existing test rigs that will be used for this testing. Photographs of these rigs are shown in Fig. 9 & 10.

Because of the high cost of running full scale endurance tests, it is very desirable that a method be developed for predicting the service life of these bearings and all military elastomeric bearings in general. The most reliable tool that we have at this point for making these predictions is a complete analysis of the strain in the elastomeric bearings by finite element analysis (F.E.A.) followed by a correlation of the resulting strain histories to basic endurance data. Because of the complexity of these bearings, it is usually found that some modeling compromises must be made in order that the problem can be handled on even the largest available computers. Our experience on the other hand, shows that these compromises must be intelligently made, for the results of F.E.A. are no better than the model from which they are generated.

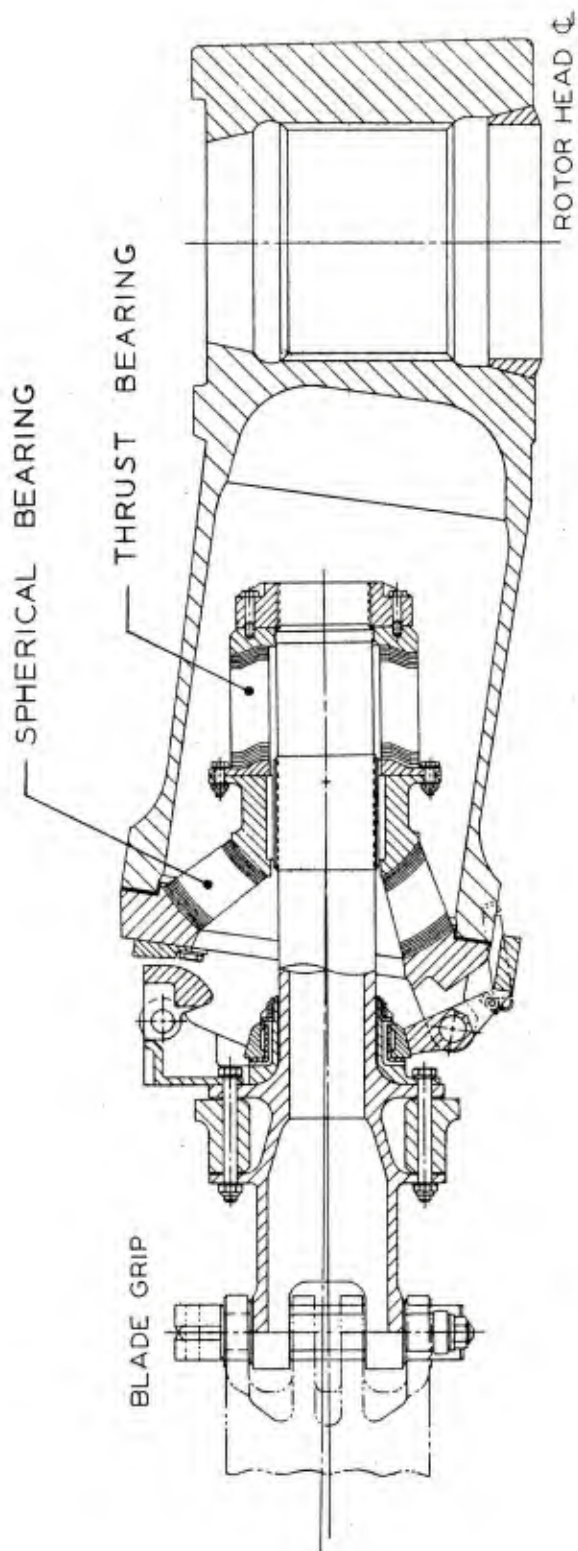
In order to get this project started on a firm basis, a relatively simple endurance test specimen will be designed. The simplicity of this specimen will allow a F.E.A. to be performed with a fine grid mesh with relatively few modeling compromises. This model will be used first to study modeling compromises that can be made so that good results can be

obtained from a relatively coarse mesh model. This skill will be needed later to model the full scale Blackhawk elastomeric bearings for F.E.A. Next, thirteen endurance test specimens will be fabricated and tested for "first damage" according to the tentative test plan in Fig. 11. An endurance life rule will be generated for the elastomer from the data from these tests. A F.E.A. will be made for the full scale Blackhawk main rotor elastomeric bearings and the strain history in the full scale endurance test bearings generated. In generating this strain history it will at first be assumed that strains can be combined as time-space vectors and that "first damage" can be predicted by Miner's Rule for accumulated damage. The basic elastomer endurance life data previously generated will be used to predict the main rotor E.B. "first damage" point. This "first damage" point will be correlated with full scale testing.

Elastomeric bearings are in general three-dimensional bodies loaded in three-dimensional space. Because of computational limitations it is usually necessary to apply a finite element program that was written to analyze axisymmetric objects of revolution that are loaded either axisymmetrically or by simple rotational loading rules such as a sine loading rule, but not both. These restrictions are not a severe handicap in the

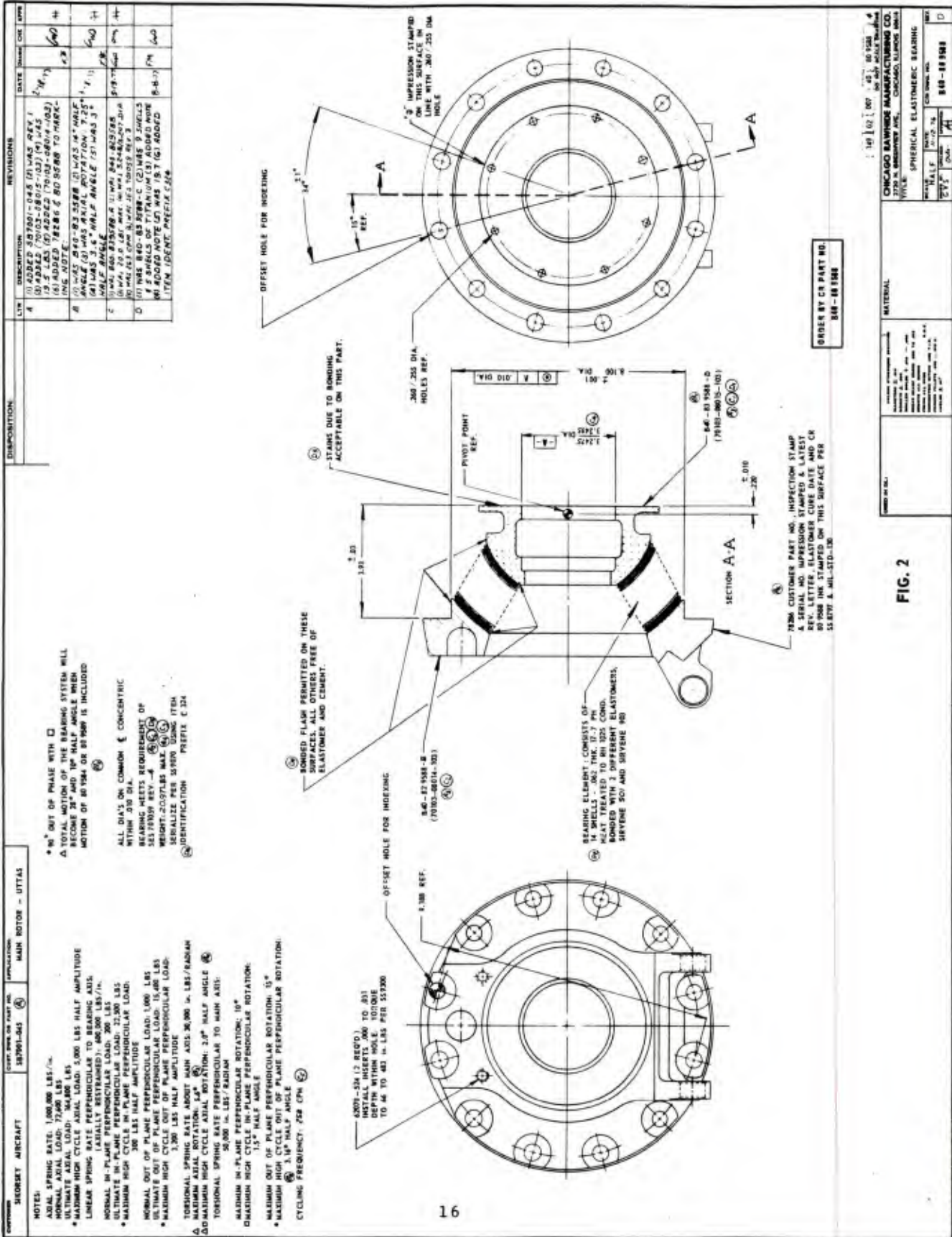
case of the thrust bearing and its loading system (see Fig. 3). For the spherical bearing (see Fig. 2) it will not be possible to include a complete loading system in any one computer solution. The elastomer strains from several runs that form a complete loading case must be combined as time-space vectors. This technique yields useful results in the case of elastomer strains, but can not be used to find the maximum shell stress in the spherical bearing. This maximum stress has been found experimentally with strain gages to occur when the combined centrifugal force (C.F.) and cocking rotation (lead-lag or flap) is applied to the bearing.

The two principal modes of failure of elastomeric bearings are elastomer endurance degradation and metal fatigue. The major effort in this project will be directed towards predicting elastomer damage. The endurance test on full scale bearings will, however, yield valuable endurance data on metal shells. To show the usefulness of F.E.A. in predicting metal fatigue in some types of elastomeric bearings a special fatigue test will be run on a thrust bearing that can be completely analyzed.



BLACKHAWK MAIN ROTOR BEARINGS LAYOUT

FIG. 1



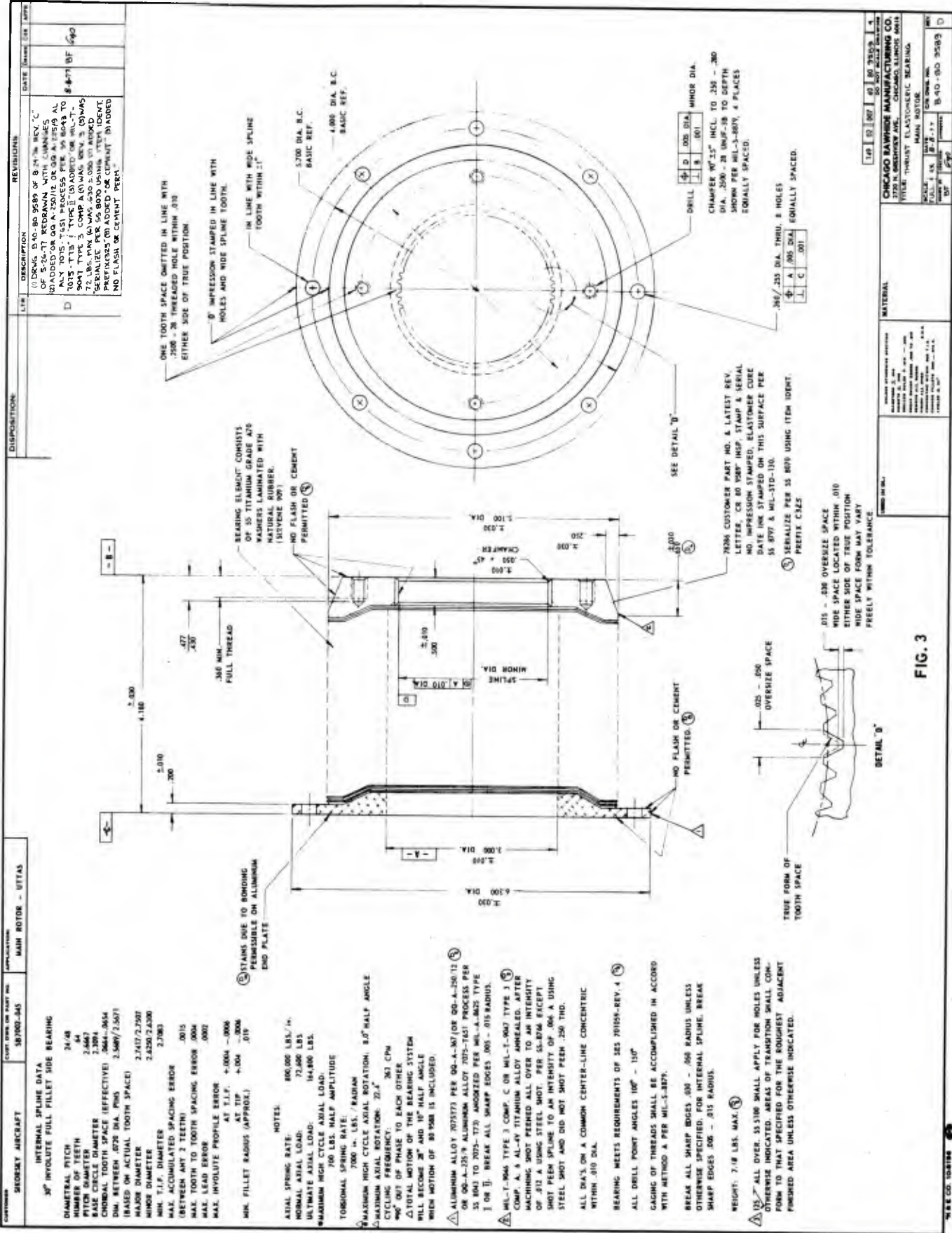


FIG. 3

BLACKHAWK MAIN ROTOR E.B. ENDURANCE LIFE TEST BLOCK I

S.E.S. CONDITION NO. (S.E.S. Rev. 4-4-74)	TIME HRS. PER 100 BLOCK	CONE ANGLE θ_x	FLAP ANGLE $\pm\theta_x$	HUNT ANGLE θ_y	PITCH ANGLE $\pm\theta_z$	AXIAL LOAD T_c	PERPENDICULAR LOAD (POUNDS) $\pm V_n$
10	1.5 ⁰	-4.32 ⁰	5.0 ⁰	0	1.5 ⁰	-5.72 ⁰	6.49 ⁰
1, 30, 50 & 57	3.8		4.5				1,196
9, 28, 29, 51 & 58	17.9		4.0				
8, 27, 33	13.1		3.65				
38 & 40	3.0		3.5				
20 & 26	2.4		3.4				
19, 21 & 39	9.2		3.3				
18	9.1		3.15				
25, 34 & 37	4.6		2.97				
7, 17, 31 & 35	14.4		2.9				
16 & 22	2.1		2.72				
2, 24 & 36	2.5		2.59				
6, 11, 12, 15 & 23	5.6		2.5				
13 & 14	2.4		1.4				
3	1.2		1.44				
32	3.0		1.3				
4 & 5	2.9	-4.32	1.2	0	1.5	6.49	68,000
					-5.72		1,026
							1,026
							1,196
Total hrs. per hr. block	98.92						

Cycling Frequency: 263 CPM.
 Phasing: $\pm\theta_y$ & $\pm\theta_z$ in phase, $\pm\theta_x$ & $\pm V_n$ both out of phase with θ_z by 90°
 θ_z & $\pm\theta_z$ proportioned between the thrust and spherical bearings according to their relative spring rates.

FIG. 4

BLACKHAWK MAIN ROTOR E.B. ENDURANCE LIFE TEST BLOCK II

S.E.S. CONDITION NO. (S.E.S.Rev.4 of 4)	CYCLES @ 258 RPM/100 HR.	CONE ANGLE θ_x	FLAP ANGLE $\pm\theta_x$	HUNT ANGLE θ_y	PITCH ANGLE θ_z	$\pm\theta_z$	AXIAL LOAD Vn	PERPENDICULAR LOAD (POUNDS) $\pm Vn$
41	1.5	-3.18°	12.0°	2.9°	1.5°	3.60°	14.4°	68,000 LBS.
42	3	-3.18	11.0	2.9	3.70	13.5		1,608
43	6	-2.69	10.0	2.7	3.90	12.5		1,598
44	36	-2.09	9.0	2.4	4.10	11.5		1,579
45	77	-1.46	8.0	2.1	4.25	10.5		1,540
46	340	-0.86	7.0	1.8	4.40	9.5		1,500
47	1,548	0.55	6.0	1.1	4.55	8.5		1,431
48	1,703	1.33	5.5	0.8	4.60	8.0		1,373
49	4,644	2.0	5.0	0.4	4.70	7.5		2,176
52	1.5	0.55	8.0	1.1	3.60	14.4		1,334
53	29	1.11	7.0	0.9	3.85	12.6		1,979
54	433	1.34	6.0	0.6	4.15	10.9		1,470
55	1,858	2.11	5.5	0.4	4.30	10.0		2,503
56	6,037	2.45	5.0	0.2	1.5	4.45	68,000	1,315

BLACKHAWK MAIN ROTOR E.B. ENDURANCE LIFE TEST BLOCK III

CONDITION (S.E.S.Rev.4 of 4-4-74)100 HR.	CYCLES / FLAP ANGLE $\pm\theta_x$	CONE ANGLE θ_x	HUNT ANGLE θ_y	PITCH ANGLE (1) θ_z	AXIAL LOAD (LBS.) $\pm T_c$	PERPENDICULAR LOAD (POUNDS) $\pm V_n$
Start/Stop (2)	300	-8.5°	0	$\pm 10^{\circ}$	11.5°	0
On/Off Centrifugal	200	0	0	0	11.5	0
Control Check	400	-8.5	0	0	-3.5	24.5
Rotor Overspeed	100	0	0	0	11.5	0
					41,000	41,000
					0	0

Cycling Frequencies: Will be between 1 & 10 CPM.

- 1) θ_z & $\pm\theta_z$ proportioned between the thrust and spherical bearings according to their relative spring rates.
- 2) $\pm\theta_y$ & $\pm T_c$ in phase for Start/Stop test.

FIG. 6

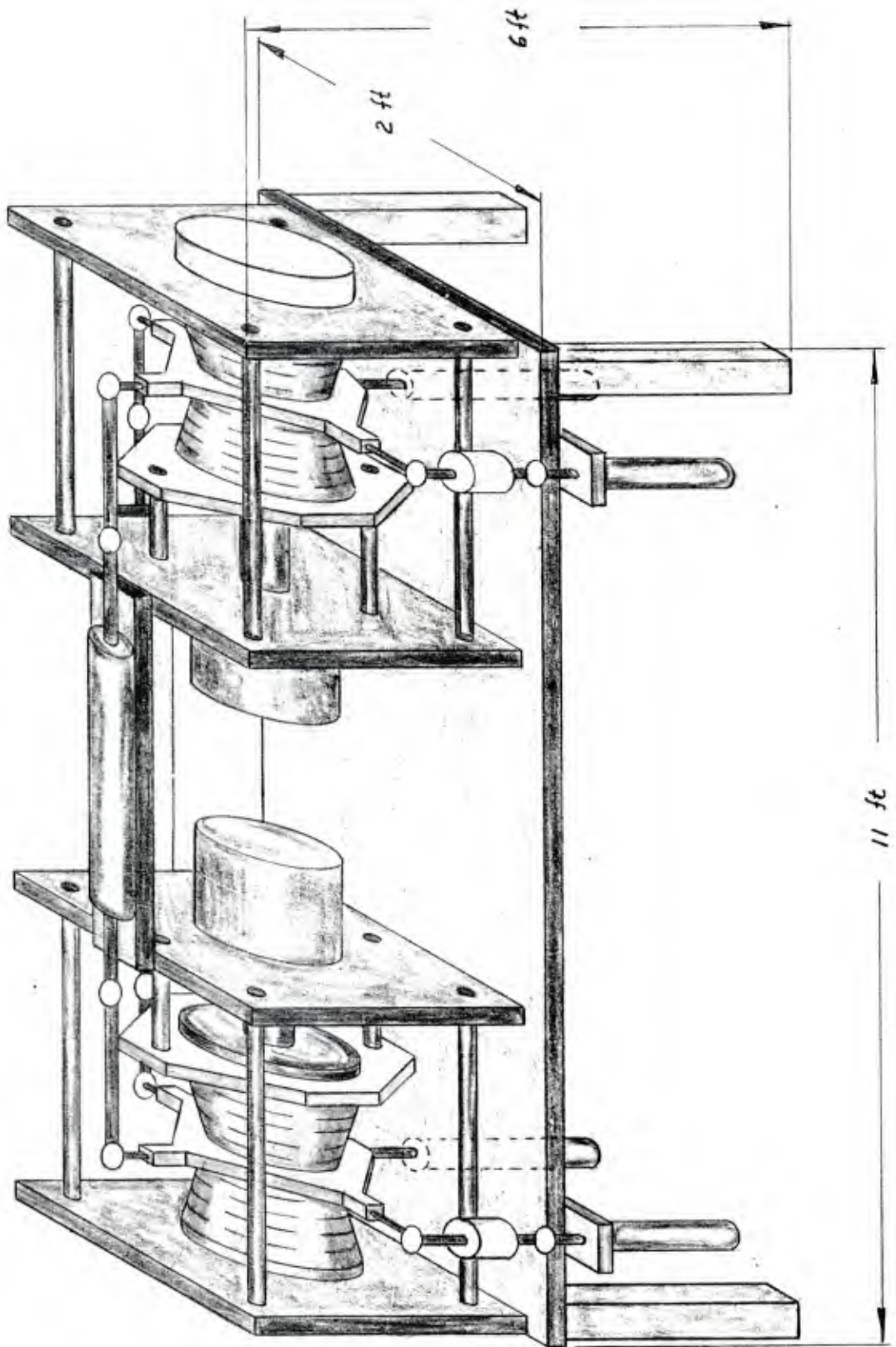


FIG. 7 BLADE RETENTION BEARING FATIGUE TEST STAND

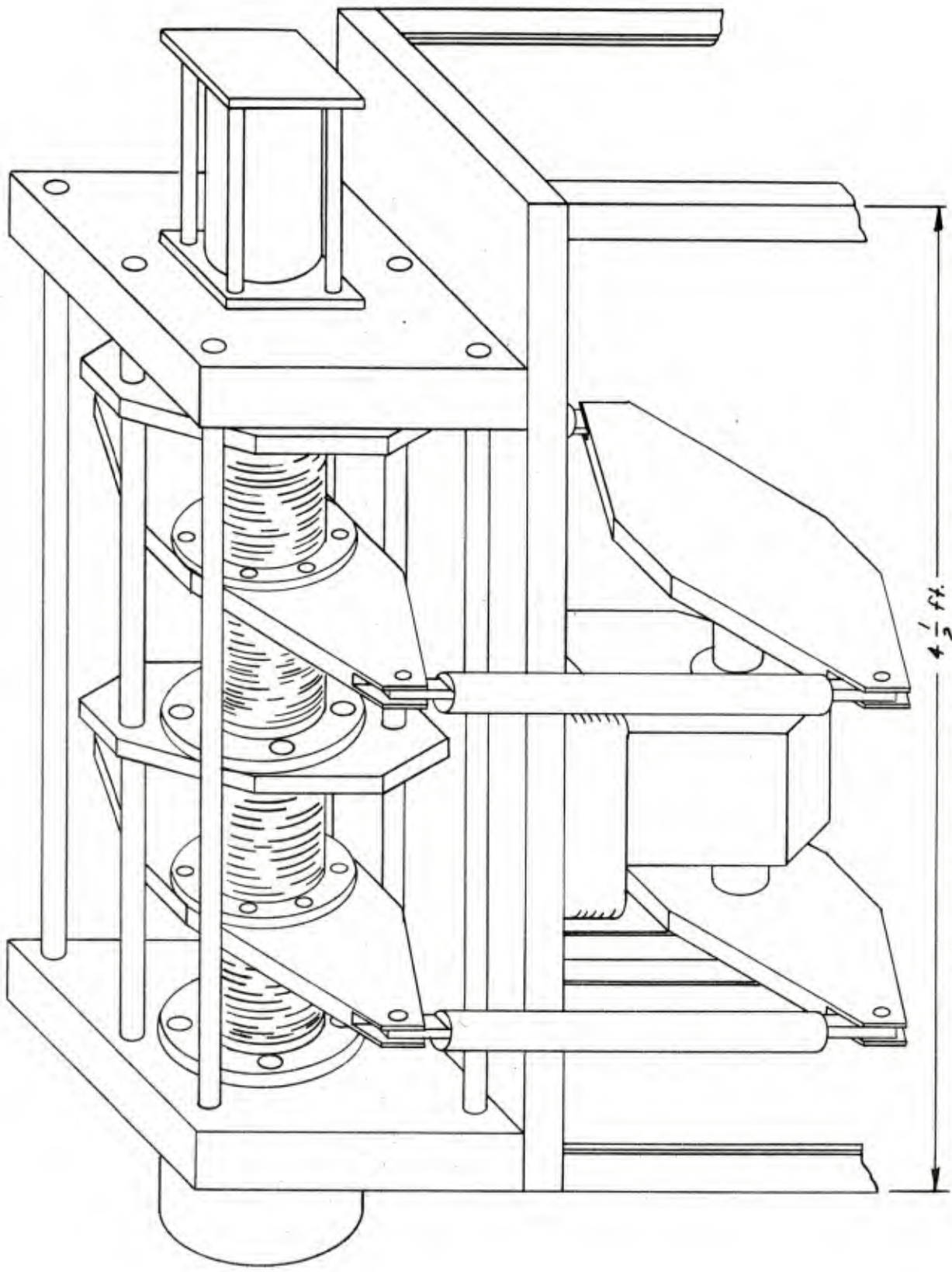
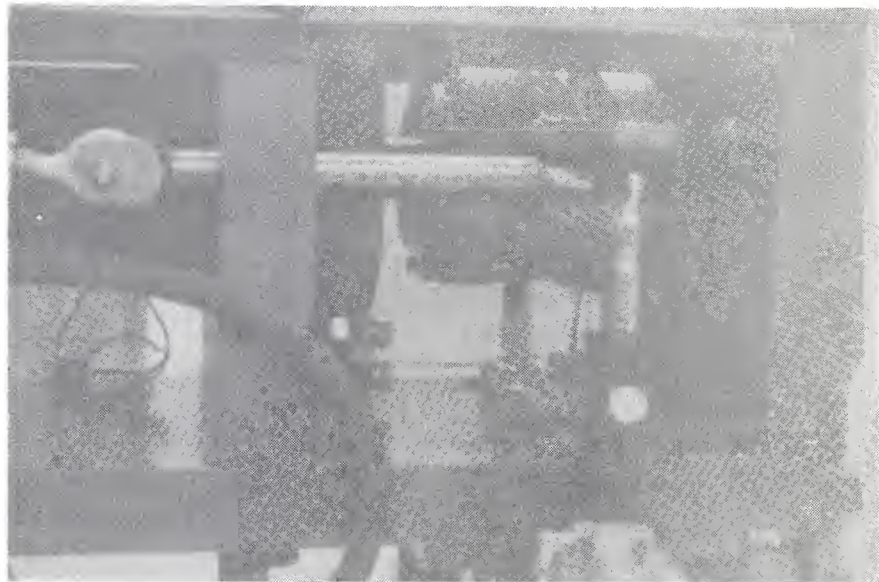
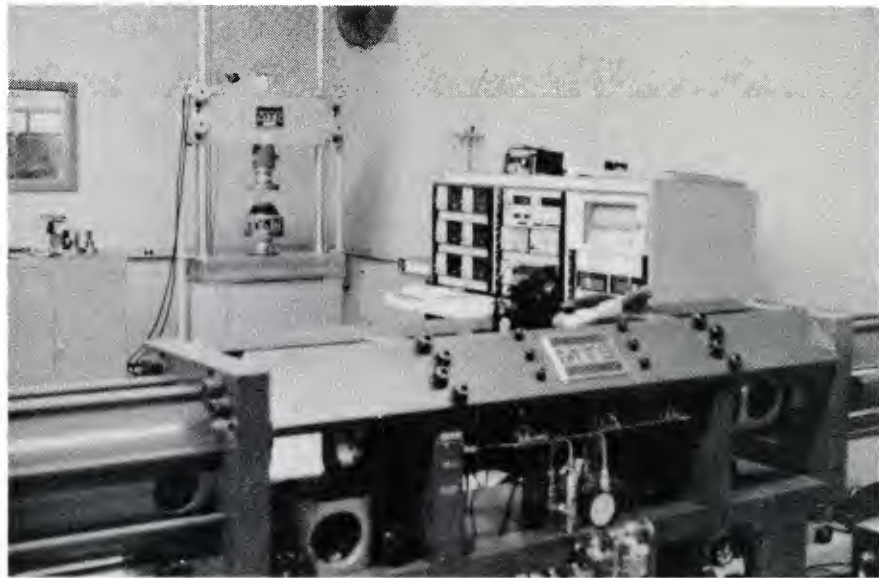
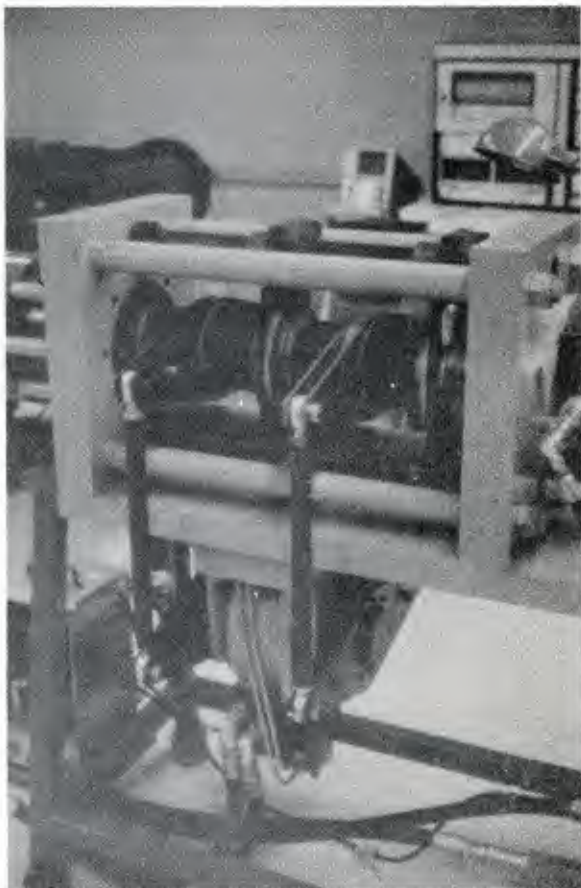


FIG. 8 THRUST BEARING FATIGUE TEST STAND



**SPHERICAL BEARING
TEST RIG.
FIGURE 9**



THRUST BEARING

TEST RIG.

FIGURE 10

TENTATIVE ENDURANCE SPECIMEN TEST PLAN

<u>Test No.</u>	<u>Hours</u>
1	2
2	3
3	5
4	10
5	20
6	30
7	50
8	100
9	200
10	300
11	500
12	1000
13	<u>1500</u> <u>3720</u>

NOTE: Loads for the first test will be estimates based on the results of the F.E.A. of this part. Loads for subsequent test will be chosen to obtain a good distribution of data.

Fig. 11.

SECTION 2.
METHODOLOGY OF FINITE ELEMENT
ANALYSIS AT CR INDUSTRIES

This section will cover the mechanics of utilizing finite element analysis that are currently employed by CR Industries. The essential basis for our finite element program is Texgap controlled by E. B. Becker and R. S. Dunham at the University of Texas (see enclosed cover sheet for the program manual in Figure 1). The library elements used for our work are solid two-dimensional ring elements with the third displacement handled by one of the following rules; plane stress, plane strain, axial symmetry with no tangential displacement, axial symmetry with a constant tangential displacement and axial symmetry with tangential displacement following a sinusoidal distribution.

In order to have a meaningful solution with the above program, loading conditions must be restricted to those that are compatible with the chosen third dimension displacement condition. Plane strain and plane stress problems are normally well known. With the tangential displacement set to zero problems with axisymmetrical models and loading conditions are handled. Constant tangential displacement handles axial torsion on an axisymmetrical model. Sinusoidal tangential displacements are used to handle lateral loading cases and non-axial twisting or rotation on an axisymmetrical model. Unfortunately the complete set of boundary conditions chosen for each problem case must be

totally compatible with the displacement restriction used-- combination types of loadings are not allowed in a single program run.

The most useful element for laminated elastomeric bearing work is the "Quad", which is a four node quadratic displacement solid ring element that can handle Poisson's ratio as close to $\frac{1}{2}$ as desired. Also useful at times, is the "Tri" ring element, which is a three node quadratic displacement solid element that also allows Poisson's ratio to approach or equal $\frac{1}{2}$. Other elements available are "Quad 8", "Liner", "Case" and "Crack".

The program has a good mesh generator for developing two-dimensional nodal points in both rectangular and polar co-ordinates. For some complex problems, however, it has been found desirable to supplement the programs mesh generation with a pre-processing mesh generation program that feeds the main program. The program has a nice looping feature that aids in establishing connectivity, element assignment, material deployment and establishing boundary conditions. These features expedite the generation of the two-dimensional model that is needed for each problem solved by this finite element program. This model is supplied to the main program as an input data program.

The computation work for our finite element analysis is done on our IBM 370 computer located at Elgin, Illinois.

The operating system accepts card image programs supplied by a remote Tektronix 4051 terminal located at Elk Grove Village, Illinois. See Figure 2 for a sample input program. In processing a job the main computer pulls from storage a binary copy of the finite element program and produces a line printer file and a graphics data file. Both files are accessible at Elk Grove Village.

Finite element data is retained through line printing done at Elgin and graphics data plotted at Elk Grove Village. See Figure 3 for a sample element model plot. A sample of the output stress and strain, as line printed, is shown in Figure 4. The maximum and minimum stress and strains are calculated for each material. A sample of this summary is shown in Figure 5. Because of the tedium of reading 75 pages of computer line print, it is normal practice to plot the pertinent strain value from the line output with the graphics terminal. See Figure 6 for a sample strain plot.

Interactive graphics can be used at CR Industries for model preparation. The part to be analysed is first drawn on the Tektronix 4051 CRT and into a data base by a CAD (Computer Aided Design) program (see Fig. 7 & 8). Auxiliary element model construction lines are added and the pertinent coordinate points are queried (see Fig. 9) for use in the input data program. After the input data program is assembled, it can

be read by our off-line preview program and a preview model generated (see Fig. 10, 11, 12 & 13). This debugging aid can save a considerable amount of mainframe time.

The following CR Industries capabilities result in a powerful elastomer bearing analysis tool:

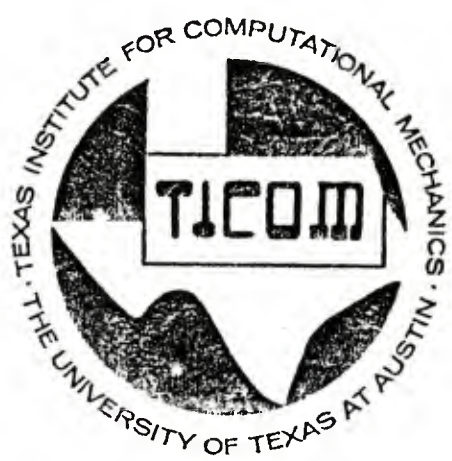
- A) A finite element program with solid elements for use with elastomeric material which have Poisson's ratios that approach $\frac{1}{2}$.
- B) Large main-frame computational capability.
- C) Direct data input to a remote terminal.
- D) Graphics output both to a CRT and hardcopy.
- E) Interactive graphics input during model preparation.
- F) Off-line verification of both the input data program and the element model.
- G) Personnel skilled in modeling finite element problems and interpreting the resulting output.

TEXGAP—THE TEXAS GRAIN ANALYSIS PROGRAM

by R. S. Dunham and E. B. Becker

TICOM REPORT 73-1

Final Report
to the
United Technology Company
Sunnyvale, California
and
Air Force Rocket Propulsion Lab
Edwards, California



THE TEXAS INSTITUTE *for* COMPUTATIONAL MECHANICS
THE UNIVERSITY OF TEXAS AT AUSTIN

August, 1973

FIG. 1

```

1:$ ELASTOMERIC THRUST BEARING TEST PROGRAM - MODEL 2;
2:SETUP,4
3:RUBBER,1,850,.5
4:STEEL,2,3E7,.3
5:TITANM,3,15E6,.3
6:END,MATERIAL
7:1,1,3,2
8:1.5,2.5,2.5,1.5
9:0,0,5,.5
10:1,2,3,7
11:1.5,2.5,2.5,1.5
12:1.5,.5,.65,.65
13:1,7,3,8
14:1.5,2.5,2.5,1.5
15:.65,.65,1.15,1.15
16:END,GRID
17:ILoop,2,1
18:QUAD,3,1,1
19:QUAD,1,1,2
20:QUAD,2,1,3
21:QUAD,1,1,4
22:QUAD,2,1,5
23:QUAD,1,1,6
24:QUAD,3,1,7
25:IEHD
26:ILoop,2,1
27:BC,SLOPE,1,1,1
28:BC,PRESSURE,1,7,3,7000
29:IEHD
30:EHd,ELEMENTS
31:PLOT,ELEMENTS,1.25,-.5,2.75,1.5,10
32:AXISYM
33:STOP

```

FIG. 2

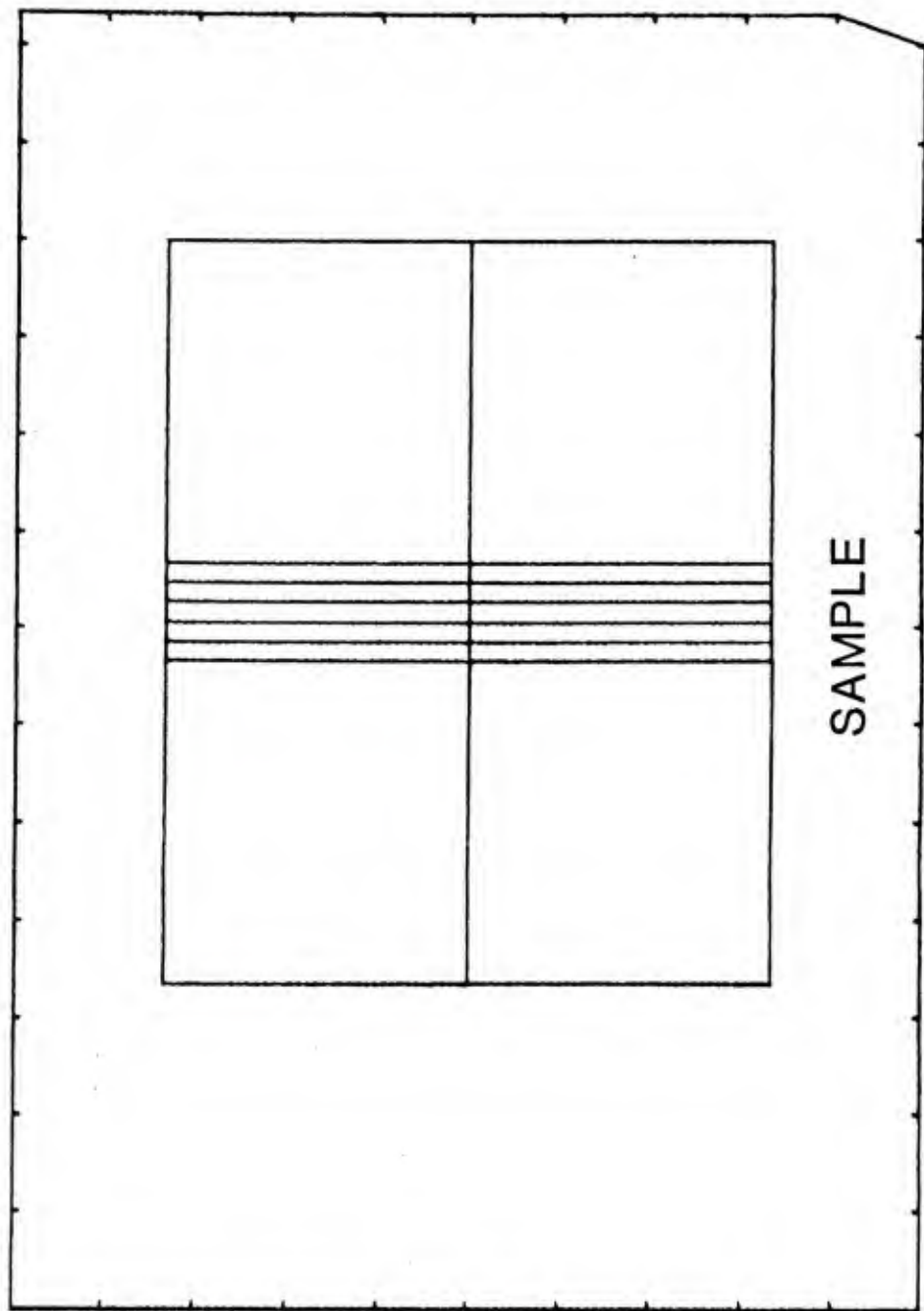


FIG. 3

DISPLACEMENTS FOR QUAD(LINER) NO 1

	J	RADIAL	AXIAL	TZD EZO	TRD ERO	TZD EZO	MAX	MIN	TAUMAX
1	1	0.2127D-03	-0.3512D-24	0.0	HCCP	0.3010D-03			
2	1	0.3049D-03	-0.6972D-24	0.0		-0.4416D-03			
2	2	0.2987D-03	-0.3319D-03	0.0		-0.9962D-03			
1	2	0.2766D-03	-0.1229D-03	0.0		-0.2856D-04			
		0.2444D-03	-0.7432D-24	0.0					
		0.3035D-03	-0.1565D-03	0.0					
		0.2868D-03	-0.2453D-03	0.0					
		0.2169D-03	-0.7851D-04	0.0					
MIDSIDE STRESS AND STRAINS FOR QUAD(LINER) NO 1									
SIDE	R	Z	TRR ERR	TZZ EZZ	TCO EOO	TRZ ERZ	TRD ERO	TZD EZO	TAUMAX
1	1.7500	0.0	0.8435D-03	-0.7015D-04	0.3261D-03	-0.7182D-02	0.0	0.0	
			0.1845D-03	-0.4966D-05	0.1015D-05	-0.7374D-03	0.0	0.0	
2	2.0000	0.2500	0.5184D-03	-0.2505D-03	0.2238D-03	-0.5239D-04	0.0	0.0	
			0.2505D-03	-0.1169D-04	0.6867D-04	-0.1750D-03	0.0	0.0	
3	1.7500	0.5000	-0.5236D-04	-0.4414D-03	0.1639D-03	-0.1245D-03	0.0	0.0	
			0.5236D-04	-0.3030D-02	0.1058D-04	-0.3310D-03	0.0	0.0	
4	1.5000	0.2500	-0.9377D-04	-0.2459D-03	0.1446D-03	-0.5737D-04	0.0	0.0	
			0.4131D-04	-0.2459D-03	0.1446D-03	-0.5737D-04	0.0	0.0	
DISPLACEMENTS FOR QUAD(LINER) NO 2									
SIDE	R	Z	TRR ERR	TZZ EZZ	TCO EOO	TRZ ERZ	TRD ERO	TZD EZO	TAUMAX
1	1	0.3049D-03	-0.6972D-24	0.0	HCCP	-0.4416D-03			
	2	0.3394D-03	-0.3835D-24	0.0		-0.2519D-03			
3	1	0.3299D-03	-0.1238D-03	0.0		-0.7317D-04			
	2	0.2987D-03	-0.3319D-03	0.0		-0.9962D-03			
	2	0.3618D-03	-0.7085D-24	0.0					
	3	0.3831D-03	-0.6597D-04	0.0					
	3	0.3131D-03	-0.2404D-03	0.0					
	3	0.3C35D-03	-0.1565D-03	0.0					
MIDSIDE STRESS AND STRAINS FOR QUAD(LINER) NO 2									
SIDE	R	Z	TRR ERR	TZZ EZZ	TCO EOO	TRZ ERZ	TRD ERO	TZD EZO	TAUMAX
1	2.2500	0.0	0.7251D-03	-0.5822D-04	0.6550D-03	0.6872D-02	0.0	0.0	
			0.1670D-03	-0.4872D-03	0.1608D-03	0.1191D-04	0.0	0.0	
2	2.5000	0.2500	-0.8070D-02	-0.3420D-04	0.1206D-04	0.2803D-03	0.0	0.0	
			0.8070D-02	-0.4148D-04	0.2477D-03	0.1532D-03	0.0	0.0	
3	2.2500	0.5000	-0.131D-04	-0.6931D-04	0.4500D-03	0.4859D-04	0.0	0.0	
			0.6931D-04	-0.4403D-03	0.1392D-03	0.6718D-03	0.0	0.0	
4	2.0000	0.2500	-0.5047D-23	-0.1015D-05	0.7374D-03	0.1164D-03	0.0	0.0	
			0.2594D-03	-0.6639D-03	0.1518D-03	0.2937D-03	0.0	0.0	
			0.2594D-03	-0.6639D-03	0.1518D-03	0.5091D-04	0.0	0.0	
			0.2601D-03	-0.6645D-03	0.1518D-03	0.9246D-03	0.0	0.0	

FIG. 4

MATERIAL NO.	1	QUANTITY	R	Z	ELEM	MAXIMUM	F	Z	ELEM	MINIMUM
RADIAL STRESS	1.0500	0.0575	7	-0.1415329D 04	2.000	0.575	8	-0.1232979D 05		
AXIAL STRESS	1.0500	0.0575	7	-0.1464780D 04	2.000	0.575	7	-0.1237981D 05		
HOOP STRESS	1.0500	0.0575	7	-0.1460910D 04	2.000	0.575	7	-0.1236888D 05		
TAURZ STRESS	1.0750	0.0530	3	0.3278019D 03	1.750	0.620	11	-0.3322344D 03		
TAURO STRESS	2.0000	0.0635	12	0.0	2.000	0.635	12	0.0		
TAUZO STRESS	2.0000	0.0635	12	0.0	2.000	0.635	12	0.0		
MAX STRESS	1.0500	0.0575	7	-0.1415322D 04	2.000	0.575	8	-0.1232979D 05		
MIN STRESS	1.0500	0.0575	7	-0.1464786D 04	2.000	0.575	8	-0.1237981D 05		
MAX SHEAR	1.0750	0.0620	11	0.3324266D 03	1.500	0.515	3	0.2448620D 02		
RADIAL STRAIN	2.0500	0.0635	12	0.0260573D-01	1.750	0.500	3	0.5235667D-04		
AXIAL STRAIN	1.0500	0.0635	11	-0.1697301D-01	2.250	0.620	12	-0.5434087D-01		
HOOP STRAIN	2.0500	0.0575	8	0.7841879D-02	1.500	0.635	11	-0.1160334D-01		
GAMRZ STRAIN	1.0750	0.0530	3	C.1156348D 01	1.750	0.620	11	-0.1172592D 01		
GAMRO STRAIN	2.0000	0.0635	12	0.0	2.000	0.635	12	0.0		
GAMZO STRAIN	2.0000	0.0635	12	0.0	2.000	0.635	12	0.0		
MAX STRAIN	1.0750	0.0620	11	0.5669476D 00	2.000	0.515	4	0.6557656D-01		
MIN STRAIN	1.0500	0.0515	3	-0.1732509D-01	2.250	0.650	12	-0.6066723D 00		
MAX SHEAR	1.0750	0.0620	11	0.11732700 01	1.500	0.515	3	0.8642186D-01		
MATERIAL NO.	2	QUANTITY	R	Z	ELEM	MAXIMUM	F	Z	ELEM	MINIMUM
RADIAL STRESS	2.0000	0.0545	5	0.1250774D 05	2.500	0.605	10	0.1435560D 04		
AXIAL STRESS	1.0500	0.0545	5	-0.1527446D 04	2.000	0.545	6	-0.1336281D 05		
HOOP STRESS	2.0250	0.0620	10	0.7323177D 04	1.750	0.590	9	0.5844664D 04		
TAURZ STRESS	1.0750	0.0590	9	0.33335668D 03	1.750	0.560	5	-0.330834D 03		
TAURO STRESS	2.0000	0.0605	10	0.0	2.000	0.605	10	0.0		
TAUZO STRESS	2.0000	0.0605	10	0.0	2.000	0.605	10	0.0		
MAX STRESS	2.0000	0.0545	5	0.125C742D 05	2.500	0.545	6	0.1435733D 04		
MIN STRESS	1.0500	0.0545	5	-0.1527556D 04	2.000	0.545	6	-0.1236284D 05		
MAX SHEAR	2.0000	0.0545	5	0.0124512D 05	2.500	0.545	6	0.1585767D 04		
RADIAL STRAIN	2.0000	0.0605	9	0.4751134D-03	2.500	0.545	6	-0.322631D-05		
AXIAL STRAIN	1.0500	0.0605	9	-0.1321124D-03	2.000	0.545	6	-0.6040460-03		
HOOP STRAIN	2.0250	0.0605	6	0.259465D-03	1.750	0.590	9	0.1958407D-03		
GAMRZ STRAIN	1.0750	0.0590	9	C.2889179D-04	1.750	0.560	5	-0.2860723D-04		
GAMRO STRAIN	2.0000	0.0605	10	0.0	2.000	0.605	10	0.0		
GAMZO STRAIN	2.0000	0.0605	10	0.0	2.000	0.605	10	0.0		
MAX STRAIN	2.0000	0.0605	9	0.4751153D-03	2.500	0.545	6	-0.4321377D-05		
MIN STRAIN	1.0500	0.0605	9	-0.1321370D-03	2.000	0.545	6	-0.6040355D-03		
MAX SHEAR	2.0000	0.0545	5	0.1077711D-02	2.500	0.545	6	0.1374332D-03		

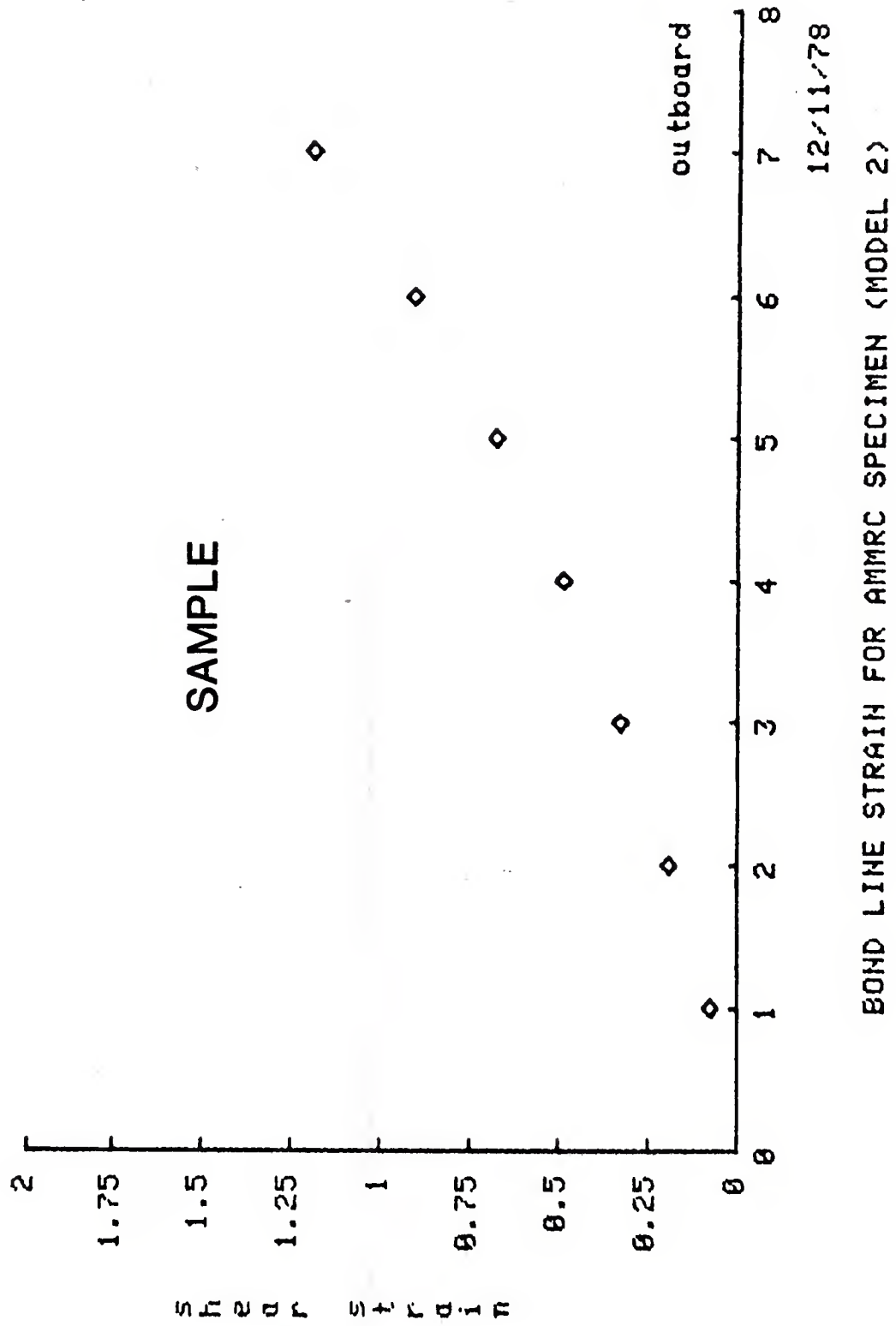
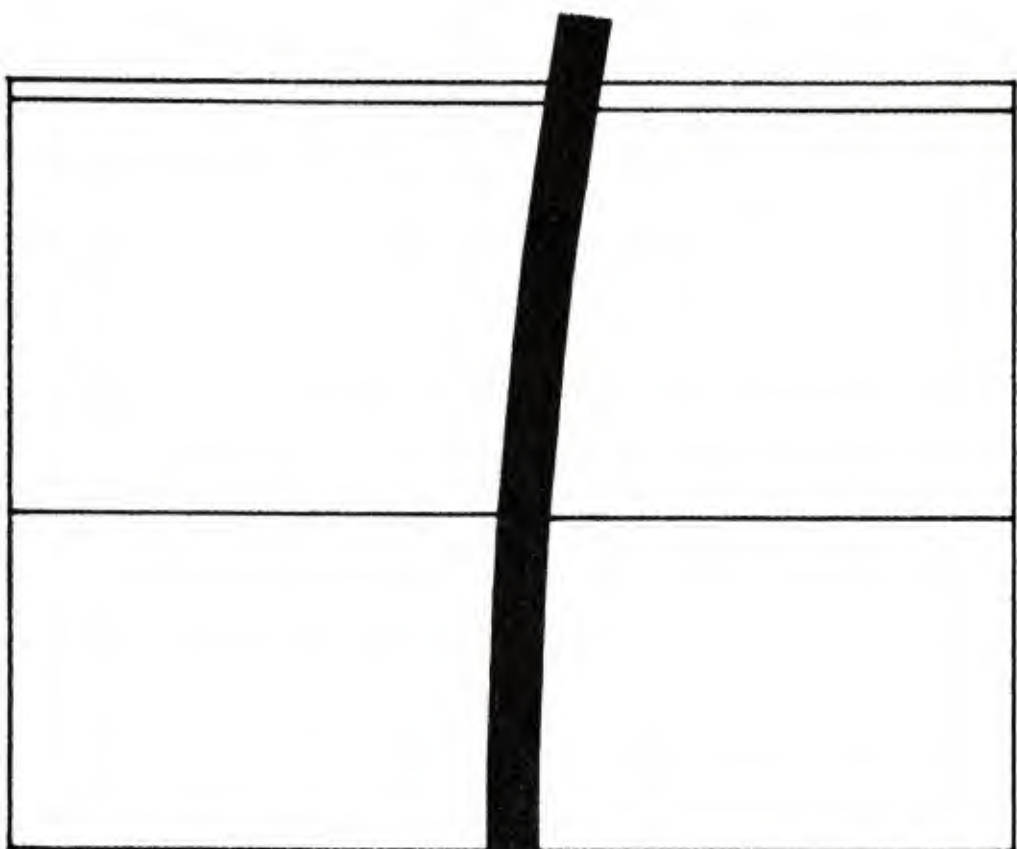
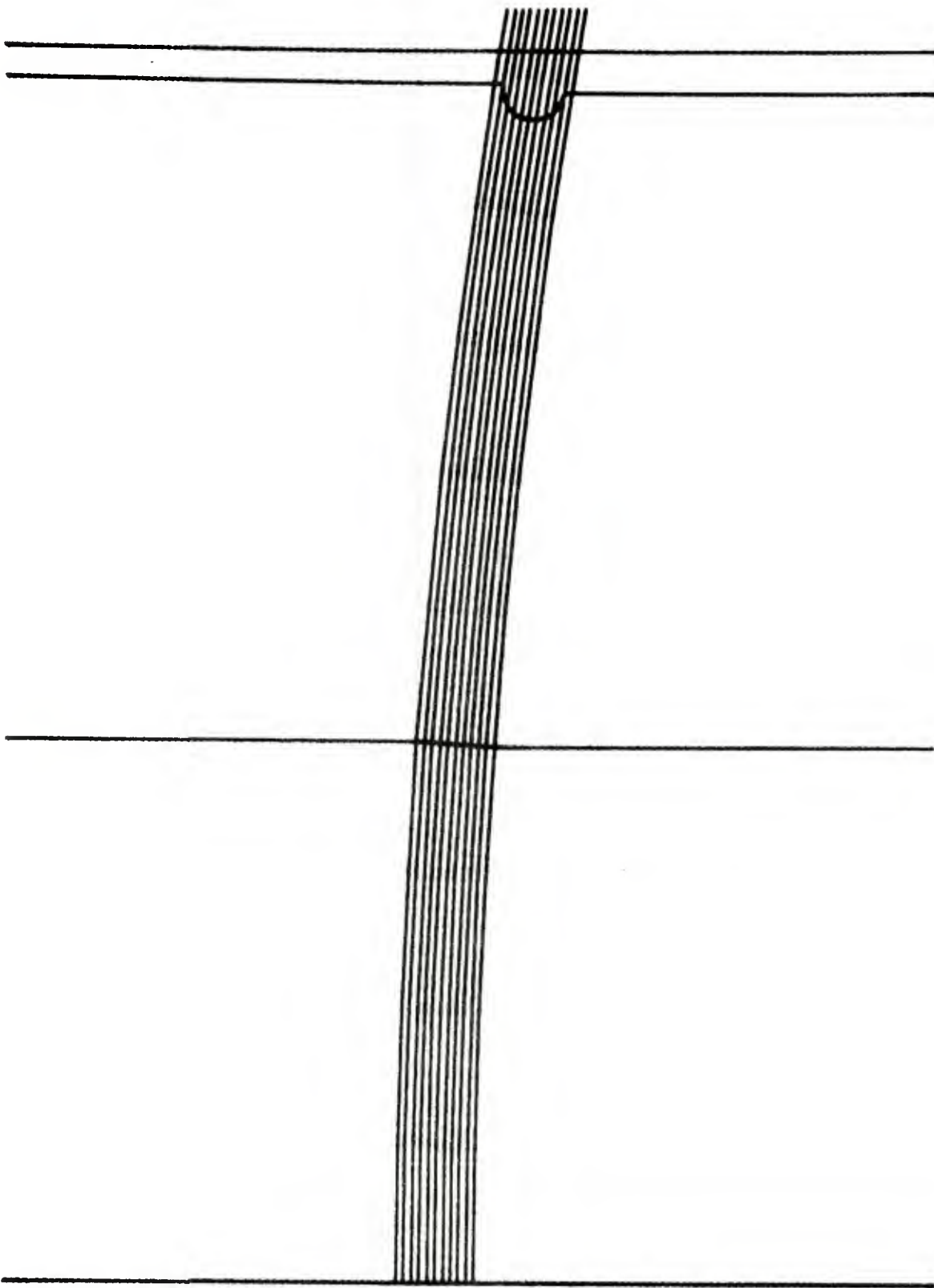


FIG. 6

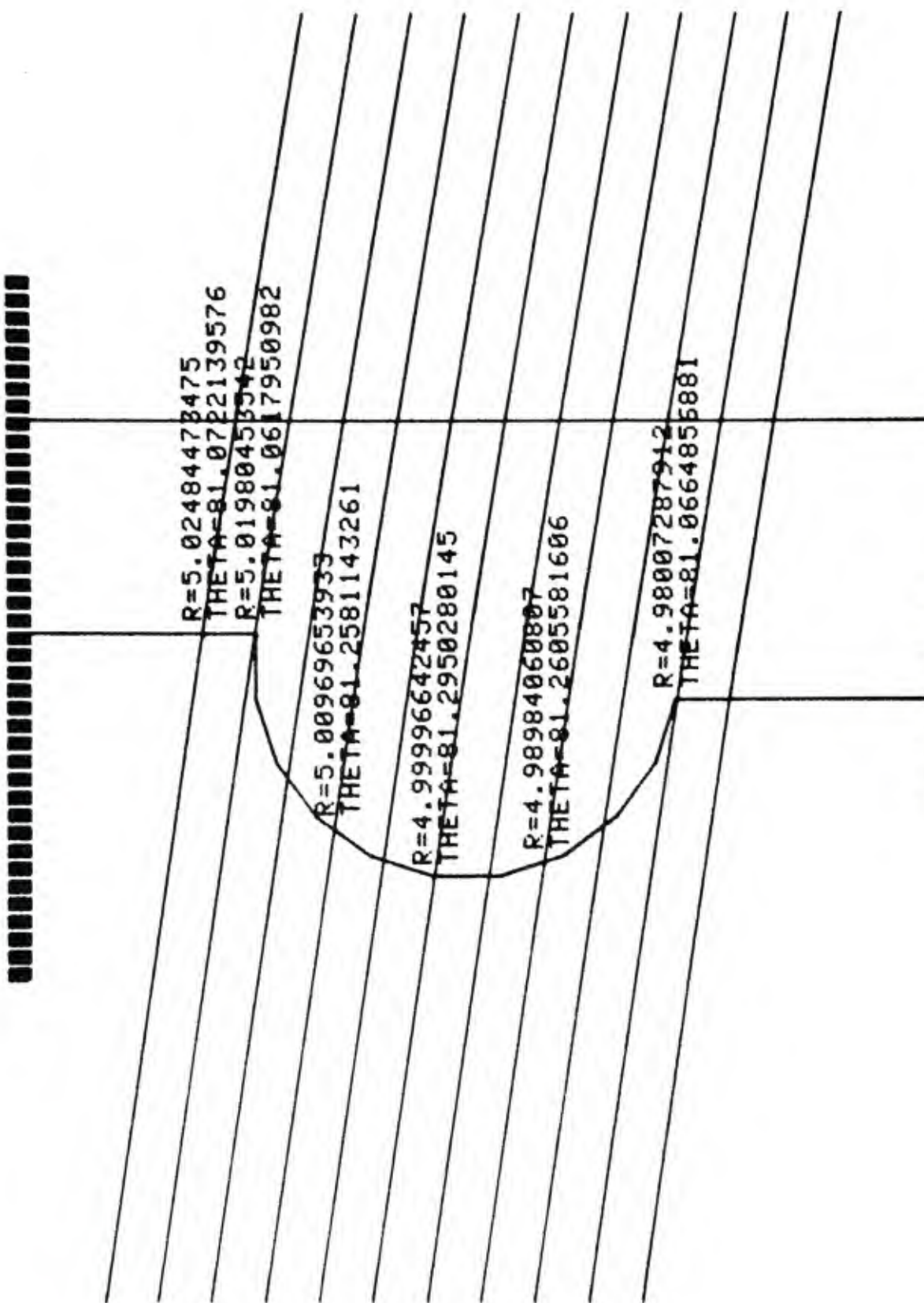
CAD DRAWING OF AMMRC FATIGUE TEST SPECIMEN

FIG. 7





BLOW UP OF FIG. 7
FIG. 8



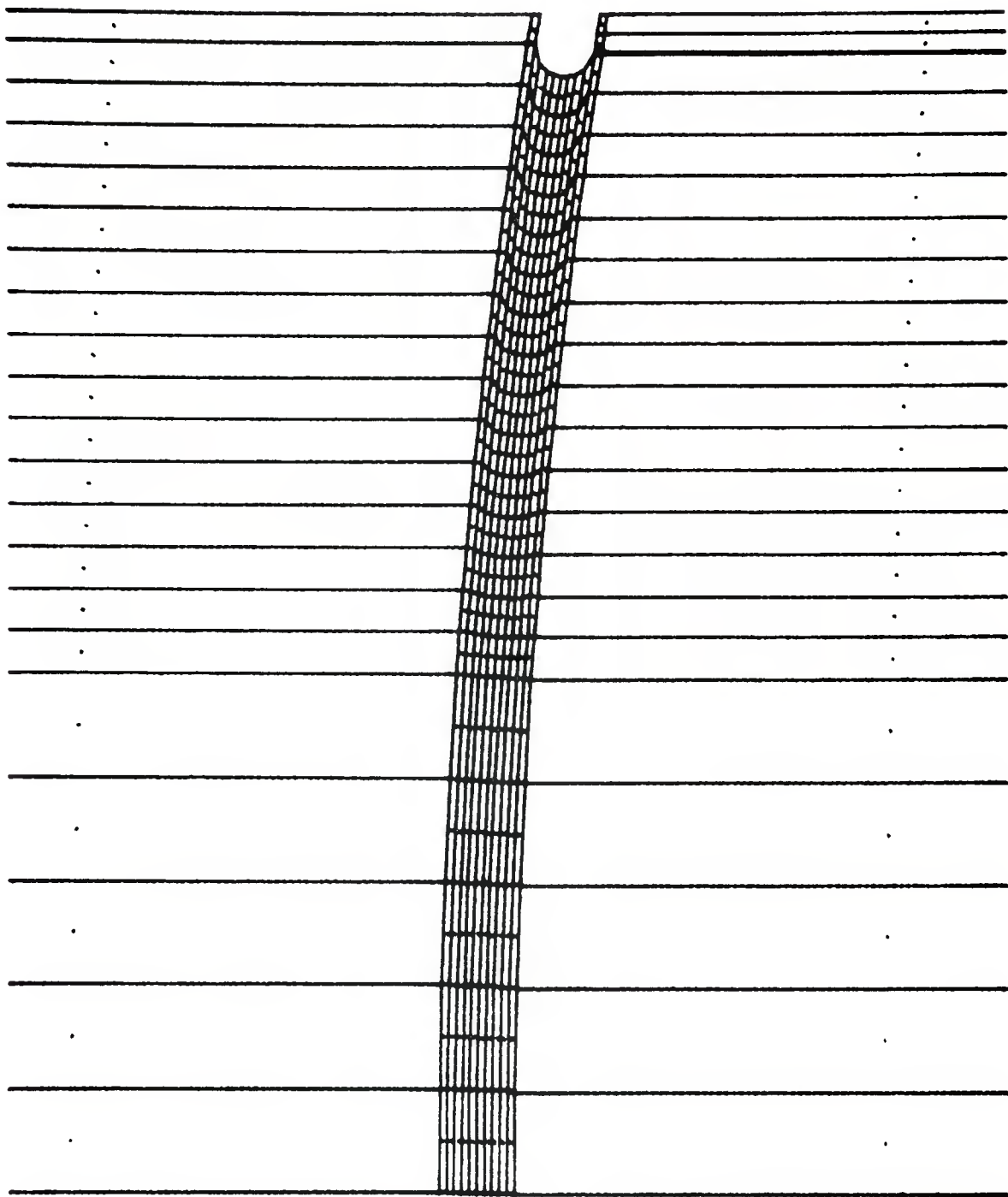
CAD QUERY LOCATION

FIG. 9



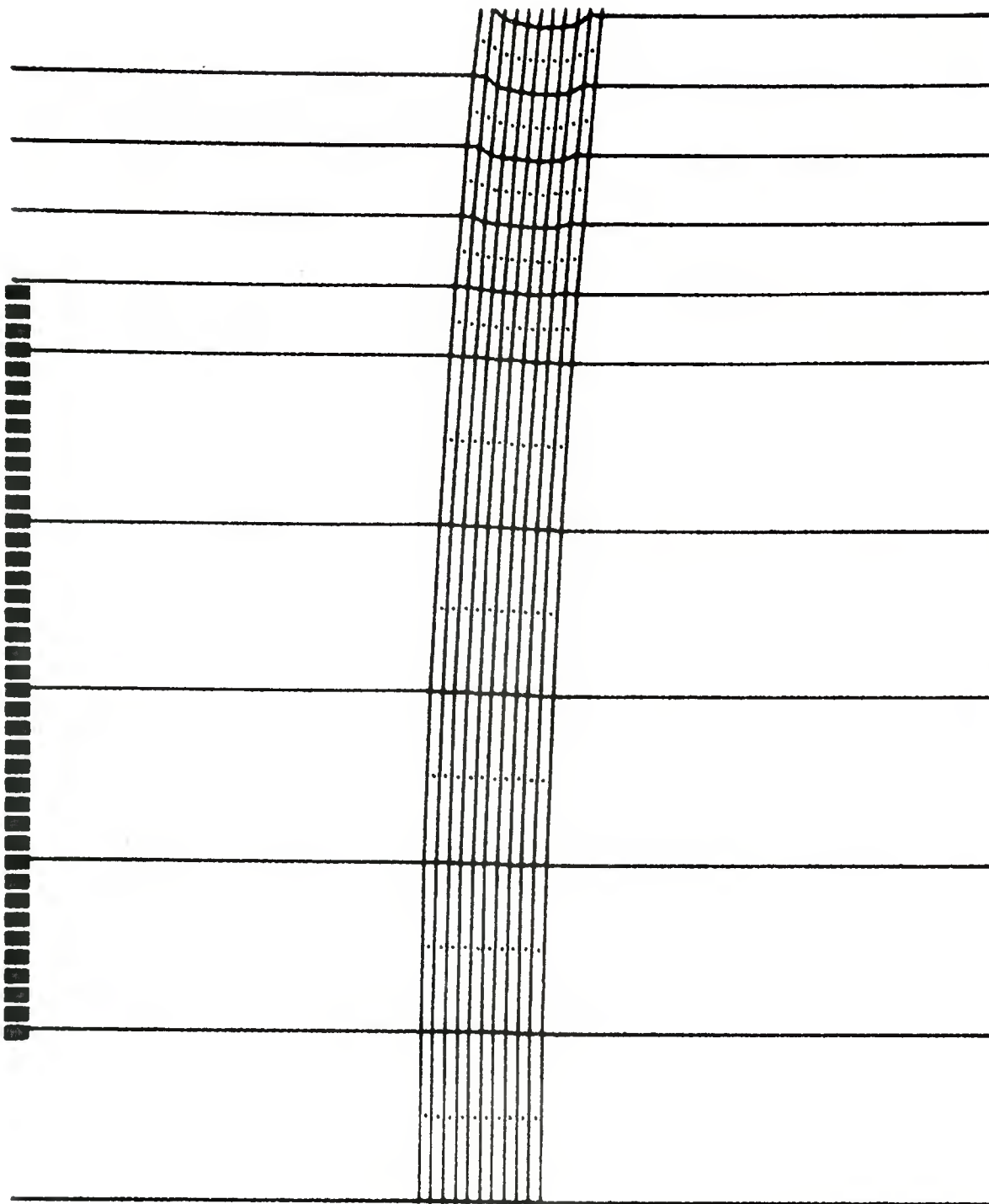
PREVIEW MODEL OF AMMRC FATIGUE SPECIMEN

FIG. 10



BLOW UP OF FIG. 10

FIG. 11

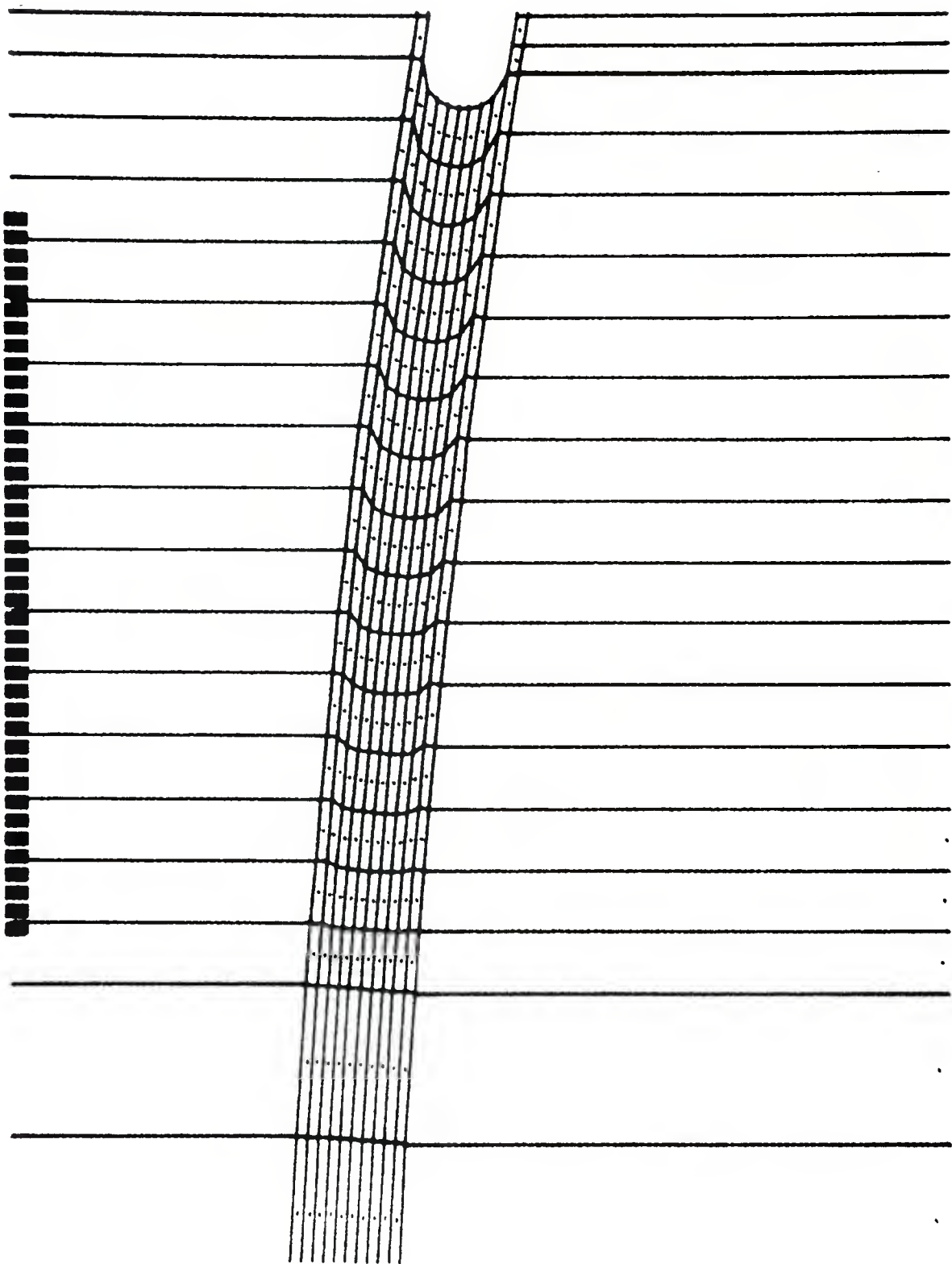


BLOW UP OF FIG. 10

FIG. 12

FIG. 13

BLOW UP OF FIG. 10



SECTION 3.
ANALYSIS OF ENDURANCE STRAINS

The previous section covered the use of the finite element method to determine stresses and strains within a laminated elastomeric bearing. It was explained how each loading case must be compatible with the tangential displacement specified for a single problem run. The result is that when all the individual loading cases shown in the S.E.S. Specification (see Section 1.) are analyzed, the analyst is left with a number of states of stress or strain at each location in the bearing. The task covered by this section is how to use this data to predict the life of the bearing.

The following discussion will show a method for determining the life of an elastomer when subject to a spectrum of non-random loading cases. For each loading case a finite element analysis will, in general, produce several shear strain resultants with similar and/or different geometric and time phase angles. The principal of superposition will be used to allow these resultants to be combined. The usual restriction on superposition of a linear stress-strain relationship, loading that is independent of deformation, etc., of course apply here. Fortunately for the elastomer in a laminated elastomeric bearing these conditions are usually met.

In October, 1968, C.H. Fagan, Senior R & D Engineer, Bell Helicopter, Fort Worth, Texas, published in the American Helicopter Society Periodical, a 5th power relationship

for the endurance life of natural rubber (see Figure 1). (Note, in this report γ will be used to represent the actual shear strain.) In order to find the combined effect of independent loading cases, Miner's Rule will be used. See Appendix I for the specialized case of using Miner's Rule on materials that have a 5th power endurance life relationship. Effective values for the pertinent parameters from the Blackhawk load and motion spectrum (S.E.S.) were calculated and are given in Figure 2.

The analysis of the state of stress and strain for an elastomer is very different from what it would be for most common engineering materials. The strains are usually so large that the analytical basis for small strain analysis is unjustifiable. For relatively incompressible elastomeric materials (Poisson's ratio close to $\frac{1}{2}$) conventional normal stress-strain relationships do not hold up. Shear stress, however, is still directly related to shear strain even for strains that would in other material be past the yield point. When converting from a strain analysis to a stress analysis a troublesome hydrostatic pressure term must be found. In the case of thin elastomer and metal laminates this hydrostatic pressure term can be large. Normally a vibratory hydrostatic stress in-and-of itself does not result in fatigue damage in an elastomeric part. It has been found that some of the best correlations between

experimental and analytical results for elastomers have been based on shear strain (see Figure 1).

One of the problems that an analyst faces in analyzing complex elastomeric bearings is that the state of strain is seldom one-dimensional but, usually two- or three-dimensional. The reason that this poses such a large problem for the analyst is that two- and three-dimensional shear failure theories do not exist for elastomers. The analyst is, therefore, sometimes more interested in finding an "effective" one-dimensional state of strain than he is in obtaining a complete two- or three-dimensional solution to a problem.

It would be thought that the best way to combine states of strain for a superposition solution to a problem would be a tensor addition (See Appendix II). At this point in time, however, this is not necessarily the case. The lack of a two- or three-dimensional endurance failure theory makes it difficult to use tensor results to predict the endurance life of elastomeric parts. Classical solutions to elastomeric bearing problems are normally given in terms of a maximum shear strain and superpositions is made by vector methods. It is easier to visualize the interaction of individual states of strains by looking at their maximum shear strains rather than their tensors.

Shear strains are often combined by vector methods. Shear strains are normally identified by the plane around whose normal line they act. For the case of combining shear strains with coincident normal lines the reader is referred to classical two-dimensional strain analysis for a discussion of Mohr's circle which looks like a "double angle vector". This technique will not be needed for this study. For the case of combining shear strains with noncoincident normal lines, see Figure 3 for the mathematics of combining time dependent vectors. Appendix II shows that for certain important cases the behavior of the strain tensor is the same as a conventional vector.

Normally an analytical analysis of elastomer degradation in an elastomeric bearing is valid only until endurance damage has resulted. After endurance damage the original model used in the analysis is no longer valid. The degradation of the elastomer in an elastomeric bearing has been found to be progressive and noncatastrophic. Actual bearing life is characteristically several times the calculated and observed life to first damage.

It might be thought that because of the larger amount of data that is available on metal fatigue, that the analysis of the endurance life of the metal shells would be less difficult. Determining the stress in the shell of the Blackhawk main

rotor thrust bearing is relatively straight forward but the resulting endurance "S-N" is usually at the low cycle end of the endurance curve making a precise life prediction very difficult. For the Blackhawk main rotor spherical bearing the maximum shell stress results from a combined loading case that has a shifting loading vector. This prevents the use of superposition and a full three-dimensional finite element analysis would be needed.

Percent
Shear Strain

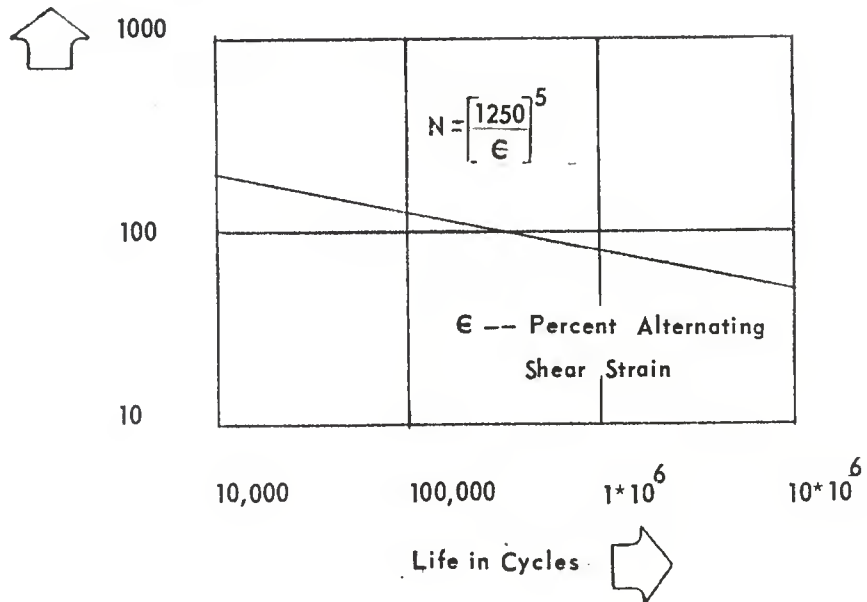


Fig. 1.

EFFECTIVE MAGNITUDES AND PHASE

ANGLES FOR THE S.E.S. SPECTRUM

Vibratory pitch change ($\pm \theta_z$) ----- $\pm 6.54^\circ$ @ 0°

Flap ($\pm \theta_x$)----- $\pm 3.58^\circ$ @ 90°

Lead-lag ($\pm \theta_y$)----- $\pm 1.5^\circ$ @ 90°

Vibratory centrifugal load----- ± 315 lbs. @ 90°

Vibratory out-of-plane load----- $\pm 1,292$ lbs. @ 90°

Normal centrifugal load----- 68,000 lbs.

Over-speed centrifugal load----- 82,000 lbs.

Note 1: The first 5 @ 258 cycles per second

Note 2: The first 5 effective magnitudes

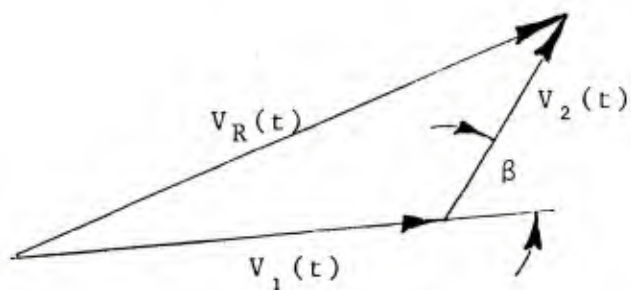
were obtained from the S.E.S. with

the following formula from the Appendix I

$$\theta_e = \sqrt[5]{\frac{\sum_{i=1}^m N_i (\theta_i)^5}{\sum_{i=1}^m N_i}}$$

FIG. 2.

COMBINATION OF TIME DEPENDENT VECTORS



$$v_1(t) = ||v_1|| \sin \omega t$$

$$v_2(t) = ||v_2|| \sin(\omega t + \theta)$$

Where $||v||$ is the maximum value of the vector v .

$$v_R(t) = \pm \sqrt{[||v_1|| \sin \omega t]^2 + [||v_2|| \sin(\omega t + \theta)]^2} \\ + 2 ||v_1|| * ||v_2|| \sin \omega t \sin(\omega t + \theta) \cos \beta$$

PHASE ANGLE θ	VECTOR ANGLE β	MAXIMUM MAGNITUDE $ v_R $
0	0	$ v_1 + v_2 $
0	$\pm 90^\circ$	$\sqrt{ v_1 ^2 + v_2 ^2}$
$\pm 90^\circ$	0	$\sqrt{ v_1 ^2 + v_2 ^2}$
$\pm 90^\circ$	$\pm 90^\circ$	Greater of $ v_1 $ or $ v_2 $
0	180°	$ v_2 - v_1 $
180°	0	$ v_2 - v_1 $

*It is customary in elastomeric strain analysis to also consider the Miner's Rule effect of the smaller vector.

Fig. 3

A P P E N D I X I

PROCEDURE FOR CALCULATING THE ENDURANCE
LIFE OF ELASTOMERS

The following procedure is intended for materials that follow the fifth power life rule (see the body of this report). It is specialized to incorporate Miner's rule for the accumulated latent damage that results from a spectrum of loading conditions.

The fifth power life rule is

$$N = \left(\frac{12.5}{\gamma}\right)^5$$

Where:

γ = Is the shear strain.

N -- Is the life in cycles.

Miner's rule states that apparent damage occurs when

$$\sum_{i=1}^m \frac{N_i}{N_f} = 1$$

Where:

N_i -- Is the number of cycles at the i'th loading

case.

N_f -- Is the number of cycles to apparent damage at

the i'th load.

m -- Is the total number of loading cases in the loading spectrum.

The life of an elastomeric part to first apparent damage then is

$$\text{Life (hours)} = \frac{1}{\sum_{i=1}^m \left(\frac{N_i}{(12.5)^5} \right)}$$

$$\text{Life} = \frac{(12.5)^5}{\sum_{i=1}^m N_i (\gamma_i)^5}$$

Where:

N_i -- Is now the number of loading cycles per hour for the i'th case.

To simplify calculations when a spectrum of strain conditions is given, a single strain can be found that is equivalent to the spectrum in that it will produce a damage equivalent to the spectrum when applied for the same total number of cycles. This equivalent value may be found as follows:

$$\gamma_e = \sqrt[5]{\frac{\sum_{i=1}^m N_i (\gamma_i)^5}{\sum_{i=1}^m N_i}}$$

Where:

γ_e -- Is effective strain magnitude.

Obviously for materials with a linear stress-strain relationship an equivalent value may be found by this procedure for any load or motion that is specified by a spectrum of conditions.

A P P E N D I X II

COMBINATION OF STRAINS BY THE STRAIN TENSOR METHOD

The three - dimensional strain tensor is

$$\begin{bmatrix} \epsilon_x & \frac{1}{2}\gamma_{xy} & \frac{1}{2}\gamma_{xz} \\ \frac{1}{2}\gamma_{xy} & \epsilon_y & \frac{1}{2}\gamma_{yz} \\ \frac{1}{2}\gamma_{xz} & \frac{1}{2}\gamma_{yz} & \epsilon_z \end{bmatrix}$$

where ϵ_x , ϵ_y & ϵ_z are the normal strains along the X, Y & Z axes respectively

and γ_{xy} , γ_{yz} & γ_{xz} are the shear strains acting on X-Y, Y-Z, X-Z planes respectively.

In order to solve for the principal strains and maximum shear strains the following eigenmatrix is used;

$$\begin{bmatrix} (\epsilon_x - P) & \frac{1}{2}\gamma_{xy} & \frac{1}{2}\gamma_{xz} \\ \frac{1}{2}\gamma_{xy} & (\epsilon_y - P) & \frac{1}{2}\gamma_{yz} \\ \frac{1}{2}\gamma_{xz} & \frac{1}{2}\gamma_{yz} & (\epsilon_z - P) \end{bmatrix} = 0$$

where P is a principal strain.

This matrix equation results in the following cubic equation in terms of strain invariants;

$$P^3 - I_1 P^2 + I_2 P - I_3 = 0$$

$$\text{where } I_1 = (\epsilon_x + \epsilon_y + \epsilon_z)$$

$$I_2 = (\epsilon_x \epsilon_y + \epsilon_y \epsilon_z + \epsilon_z \epsilon_x) - \frac{1}{4}(\gamma_{xy}^2 + \gamma_{yz}^2 + \gamma_{xz}^2)$$

$$I_3 = \epsilon_x \epsilon_y \epsilon_z + \frac{1}{4}(\gamma_{xy} \gamma_{yz} \gamma_{xz}) - \epsilon_x \gamma_{yz}^2 - \epsilon_y \gamma_{xz}^2 - \epsilon_z \gamma_{xy}^2$$

The maximum shear strains are

$$\gamma_1 = \text{ABS}(P_1 - P_2); \gamma_2 = \text{ABS}(P_2 - P_3); \gamma_3 = \text{ABS}(P_3 - P_1)$$

where P_1 , P_2 & P_3 are the principal strains (roots of the cubic).

A computer program in Basic to solve these equations is shown in Figure 1. Figure 2. shows some interesting maximum shear strain results for monoplanar, biplanar and triplanar states of shear.

NOTE: The 2nd, 4th, 5th and 6th examples have a maximum shear strain resulting from a biplanar state of shear strain that is equal to the vector combination of the shear strains. The 3rd example shows that this result can not be expanded to the triplanar case.

As an example the maximum shear strain will be calculated for the fourth layer of the spearical bearing at the I.D. for 6 and 12 o'clock positions.

The flap strain tensor is

$$3.58 * \begin{bmatrix} .03400 & -.03205 & -.03518 \\ -.03205 & -.03988 & -.05858 \\ -.03518 & -.05858 & 0 \end{bmatrix}$$

The vibratory in-plane strain tensor is

$$(-1) * \frac{315}{68000} * \begin{bmatrix} -1.314 & -1.358 & 0 \\ -1.358 & 1.343 & 0 \\ 0 & 0 & .0003 \end{bmatrix}$$

The vibratory out-of-plane strain tensor is

$$\begin{bmatrix} -.03417 & -.03521 & .0023 \\ -.03521 & .03509 & .0038 \\ .0023 & .0038 & 0 \end{bmatrix}$$

The combined strain tensor is

$$= \begin{bmatrix} .1217 & .1390 & -.1317 \\ .1390 & -.0870 & -.2163 \\ -.1317 & -.2163 & 0 \end{bmatrix}$$

The principal strains and maximum shear strains resulting from this strain tensor is calculated in Figure 3.

Great care must be excercised with regard to the choice of signs of the tensors since an incorrect sign will completely alter the boundary conditions of the problem.

At this point we must take a large and as of yet unjustified step in using the triplanar maximum as the uniplanar value. The maximum strain of .38001 shown in Figure 3 (triplanar) compares to .379 obtained by vector combination of these states of strain as shown below:

The two-dimensional maximum shear strain from the above tensors are,

$$\gamma_{\text{flap}} = \sqrt{(.03400 - (-.03988))^2 + (-.03205)^2} = .0803$$
$$\gamma_{\text{vibratory in - plane}} = \sqrt{(-1.314 - 1.343)^2 + (-1.358)^2} = 2.9839$$

$$\gamma_{\text{vibratory out-of-plane}} = \sqrt{(-.03417 - .03509)^2 + (-.03521)^2} = .07769$$

The resulting combined shear strain is

$$\begin{aligned}\gamma_{v1} &= 3.58 * .0803 + 2.9839 \left(\frac{315}{68000} \right) + .07769 \\ &= .379\end{aligned}$$

```

100 PRINT "ENTER PRINCIPAL STRAIN - X ";
110 INPUT X
120 PRINT "ENTER EPSILON - Y ";
130 INPUT Y
140 PRINT "ENTER EPSILON - THETA ";
150 INPUT T
160 INPUT GAMMA --- XY ";
170 PRINT "ENTER GAMMA --- XY ";
180 INPUT T0
190 PRINT "ENTER GAMMA --- XTHETA ";
200 INPUT Y0
210 PRINT "ENTER GAMMA --- YTHETA ";
220 INPUT X0
230 I1=-(Y+X+T)
240 I2=Y*X*T+Y*T-(T0*T2+X0*T2+Y0*T2)/4
250 I3=-(X*T+T0*X*Y0-X*X0*T2-Y*Y0*T2-T*T0*T2)/4
260 S=0.3
270 R=((S+I1)*S+I2)*S+I3
280 R1=(3*S+2*I1)*S+I2
290 H=S
300 OH SIZE THEN 330
310 S=S-R/R1
320 IF ABS(R/(CH*R1))>1.0E-12 THEN 270
330 B=I1+S
340 C=(S+I1)*S+I2
350 D=B*B/4-C
360 IF D<-1.0E-3 THEN 450
370 OH SIZE THEN 390
380 D=SQR(D)
390 S1=-B/2-D
400 S2=-B/2+D
410 PRINT "PRINCIPAL STRAINS ",S,S1,S2
420 PRINT "MAXIMUM SHEAR STRAINS "
430 PRINT ABS(S-S1),ABS(S1-S2),ABS(S2-S),",J"

```

FIG. 1

```
449 GO TO 110
450 PRINT "IMPOSSIBLE STATE OF STRAIN J"
460 GO TO 110
470 END
```

FIG. 1 (CONTINUED)

PRINCIPAL STRAIN DETERMINATION

ENTER EPSILON - X 0	ENTER EPSILON - Y 0	ENTER EPSILON - XY 1
ENTER EPSILON - THETA 0	ENTER EPSILON - XY 1	ENTER GAMMA --- XTHETA 0
ENTER GAMMA --- XY 1	ENTER GAMMA --- XTHETA 0	ENTER GAMMA --- YTHETA 0
PRINCIPAL STRAINS		
0.5	-0.5	0
MAXIMUM SHEAR STRAINS		
1	0.5	0.5

ENTER EPSILON - X 0	ENTER EPSILON - Y 0	ENTER EPSILON - XY 1
ENTER EPSILON - THETA 0	ENTER EPSILON - XY 1	ENTER GAMMA --- XTHETA 0
ENTER GAMMA --- XY 1	ENTER GAMMA --- XTHETA 1	ENTER GAMMA --- YTHETA 1/0
PRINCIPAL STRAINS		
0	-0.707106781187	0.707106781187
MAXIMUM SHEAR STRAINS		
0.707106781187	<u>1.41421356237</u>	<u>0.707106781187</u>

ENTER EPSILON - X 0	ENTER EPSILON - Y 0	ENTER EPSILON - XY 1
ENTER EPSILON - THETA 0	ENTER EPSILON - XY 1	ENTER GAMMA --- XTHETA 0
ENTER GAMMA --- XY 1	ENTER GAMMA --- XTHETA 1	ENTER GAMMA --- YTHETA 1/0
PRINCIPAL STRAINS		
-0.499999982831	-0.5000000017169	1
MAXIMUM SHEAR STRAINS		
3.433705587E-8	<u>1.50000001717</u>	<u>1.49999998283</u>

FIG. 2

PRINCIPAL STRAIN DETERMINATION

ENTER EPSILON = X 0			
ENTER EPSILON = Y 0			
ENTER EPSILON = THETA 0			
ENTER GAMMA --- XY 0			
ENTER GAMMA --- XTHETA 1			
ENTER GAMMA --- YTHTA 1/2			
PRINCIPAL STRAINS			
8	-1.11803398875	1.11803398875	
MAXIMUM SHEAR STRAINS	<u>2.2360679775</u>	<u>1.11803398875</u>	<u>1.11803398875</u>
<hr/>			
ENTER EPSILON = X 1			
ENTER EPSILON = Y 1			
ENTER EPSILON = THETA 1			
ENTER GAMMA --- XY 1			
ENTER GAMMA --- XTHETA 2			
ENTER GAMMA --- YTHTA 0			
PRINCIPAL STRAINS			
-8.11803398875	1	2.11803398875	
MAXIMUM SHEAR STRAINS	<u>1.11803398875</u>	<u>1.11803398875</u>	<u>2.2360679775</u>
<hr/>			
ENTER EPSILON = X 1			
ENTER EPSILON = Y 1			
ENTER EPSILON = THETA 1			
ENTER GAMMA --- XY -1			
ENTER GAMMA --- XTHETA 1			
ENTER GAMMA --- YTHTA 0			
PRINCIPAL STRAINS			
8.292893218813	1	1.70710678119	
MAXIMUM SHEAR STRAINS	<u>0.707106781187</u>	<u>0.707106781187</u>	<u>1.41421356237</u>

PRINCIPAL STRAIN DETERMINATION

```
ENTER EPSILON = X .09364
ENTER EPSILON = Y -.18498
ENTER EPSILON = THETA 0
ENTER GAMMA --- XY -.14366
ENTER GAMMA --- XTHETA -.12364
ENTER GAMMA --- YTHETA -.20592
PRINCIPAL STRAINS
0.125984476751 -0.254030749459 0.0376062727086
MAXIMUM SHEAR STRAINS
0.38801522621 0.291637022168 0.088378204042
```

FIG. 3

SECTION 4.
ANALYSIS OF THE AMMRC FATIGUE SPECIMEN

A fatigue specimen has been designed (see 80 6627 in Figure 1). It was designed with an undercut radius at the O.D. of the part that is intended to lower the strain at this critical location. This is normal design practice. The location of this radius is shown in the enlarged section of Fig. 1. Note, the spherical design of the elastomer will minimize the effects of equipment nonparallelism during endurance testing.

A fine mesh model for this specimen was generated and is shown in Figure 2. Note, this model has a small center hole (not obvious) that avoids a mathematical pole in the analysis and is eliminated by the boundary conditions applied to the model. A finite element analysis (F.E.A.) was completed on this model. For this analysis the model was loaded with a compressive force system equal to the half amplitude range to be applied during the fatigue tests. A listing of the input data program is included in Appendix I. The shear strain occurring along the bond line is shown in Figure 3. The location of this bond line strain is shown on the model in Figure 2 as line A-A. The strain along the undercut radius is shown in Figure 4. The location of this radius is shown again on the model in Figure 2 along Curve A-B-C.

Figure 5 is the second model of the fatigue test spec-

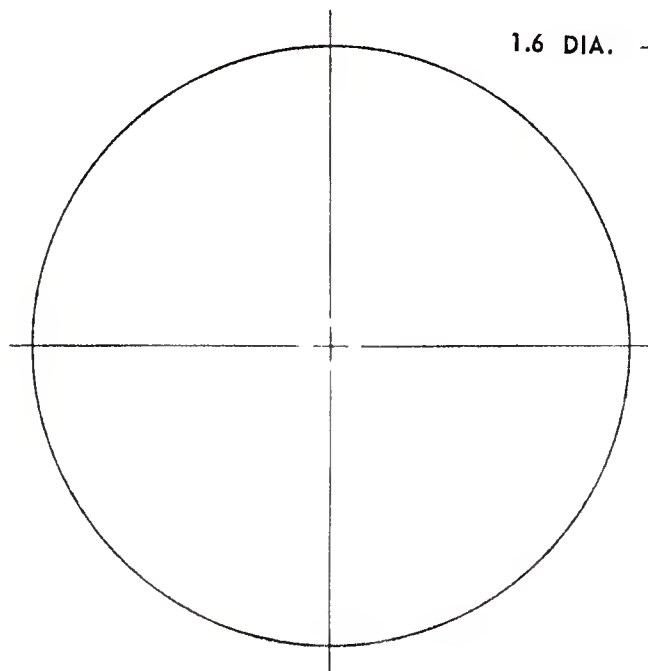
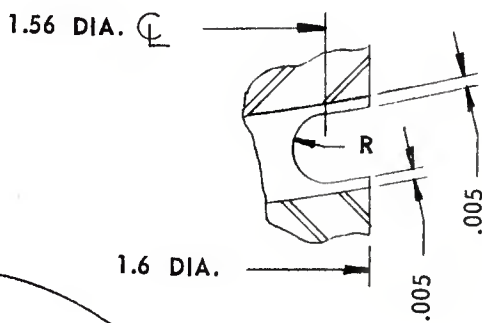
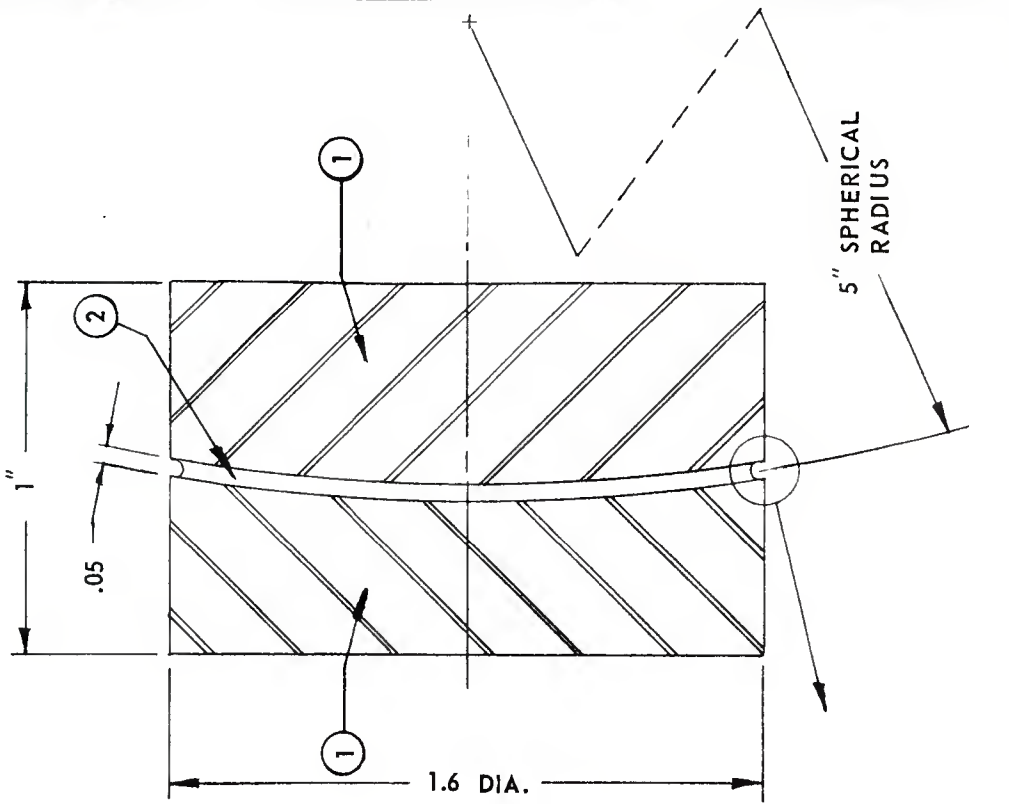
imen. This coarse model was set up with the thickness of the elastomer layer represented by a single element. The elastomer layer is divided so that each of seven elements have the same polar angle width. The bond line shear strain is shown in Figure 6. The program for this analysis is given in Appendix II.

The third model as shown in Figure 7 incorporates a small element at the outside edge to improve the resolution of strain at this critical position. The reasoning behind this procedure is that this finite element analysis program actually only calculates the state of strain at an integration point in the middle of each side. The aim is to get a reading from a "mid-side mode" near the edge of the part. The strain results for this model are given in Figure 8. The program is listed in Appendix III.

The conclusion of the coarse grid modelling study is as follows: The strain reducing effect of a radius undercut at the edge of the layer is missed and hence, elastomer strain results tend to be a little high (conservative). It is safest, especially when strain gradients are high, to incorporate a small element with a width about equal to its thickness at the edges of a layer. When this is done it is felt that a coarse grid model will consistently give results that are slightly conservative.

CR DRAWING NO.	REVISION		
B60 - 80 6627			
149	02	007	10
			80 6627 0

DO NOT SCALE DRAWING
METRIC: 1 in. = 25.4 mm



MATERIALS
 (1) STEEL
 (2) NATURAL RUBBER

C.R. INDUSTRIES		CHICAGO RAWHIDE MFG. CO.		ORDER BY CR PART NO. B60 - 80 6627
		Mechanical Products Division		
CUSTOMER	A.M.M.R.C.	REVISIONS	SCALE	
		LTR DATE	2X	
APPLICATION		DESCRIPTION		
CUSTOMER PART NO.		BY		
		NAME	FATIGUE SPECIMEN	
		DATE	1/12/75	
		DRAWN	4/2/75	
		CHECKED	4/2/75	
		APPROVED	A	

FIG. 1

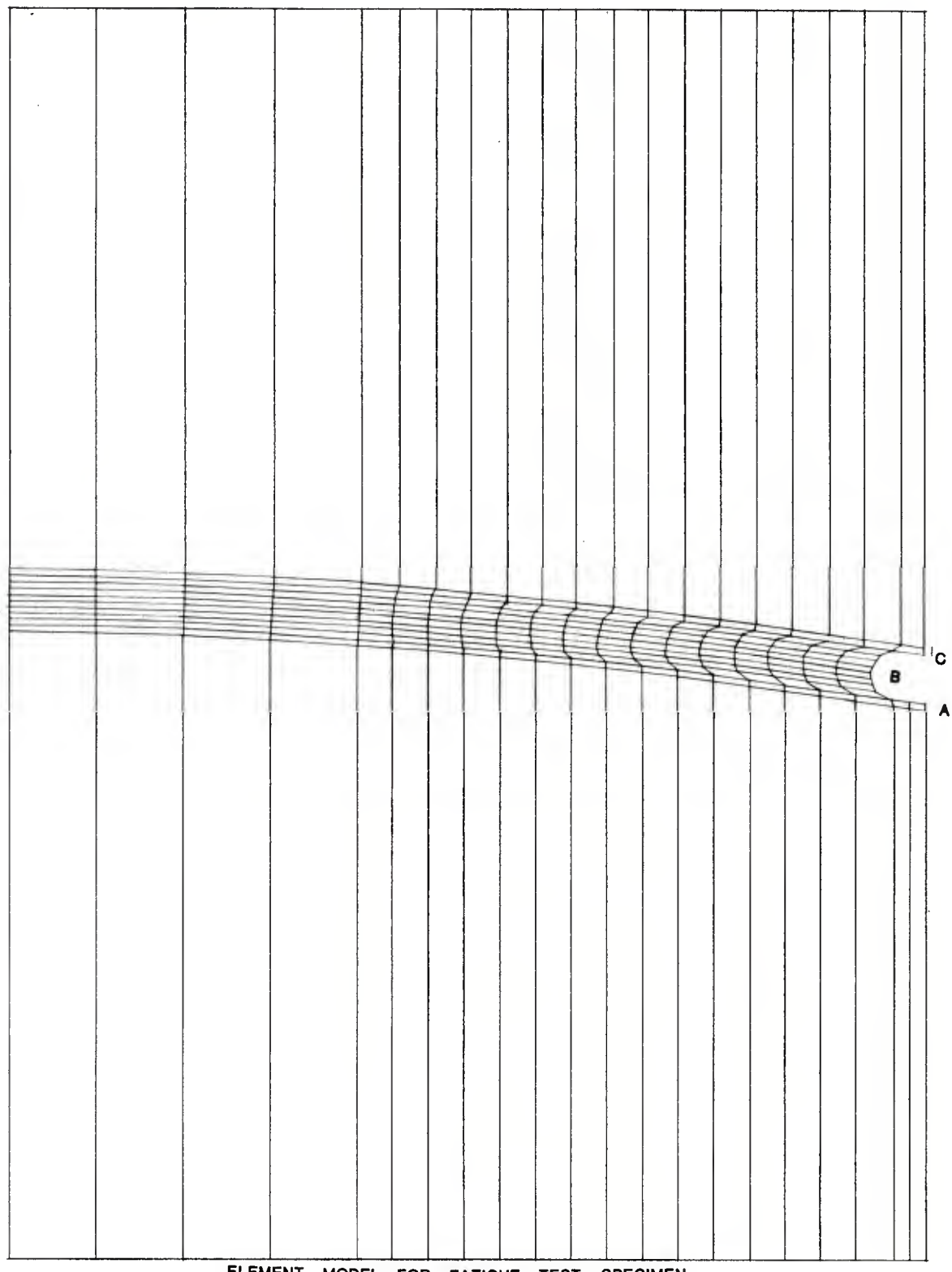
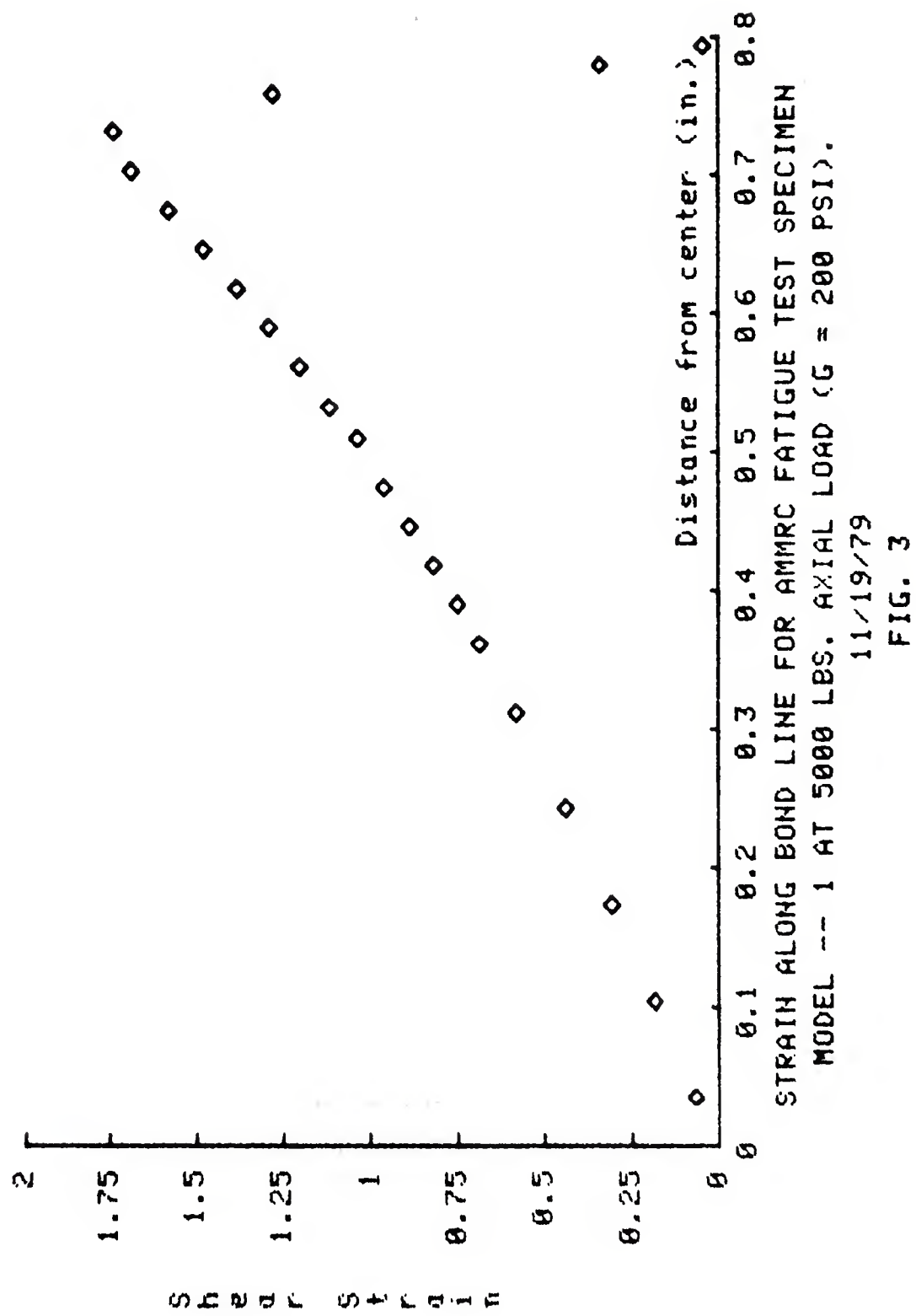
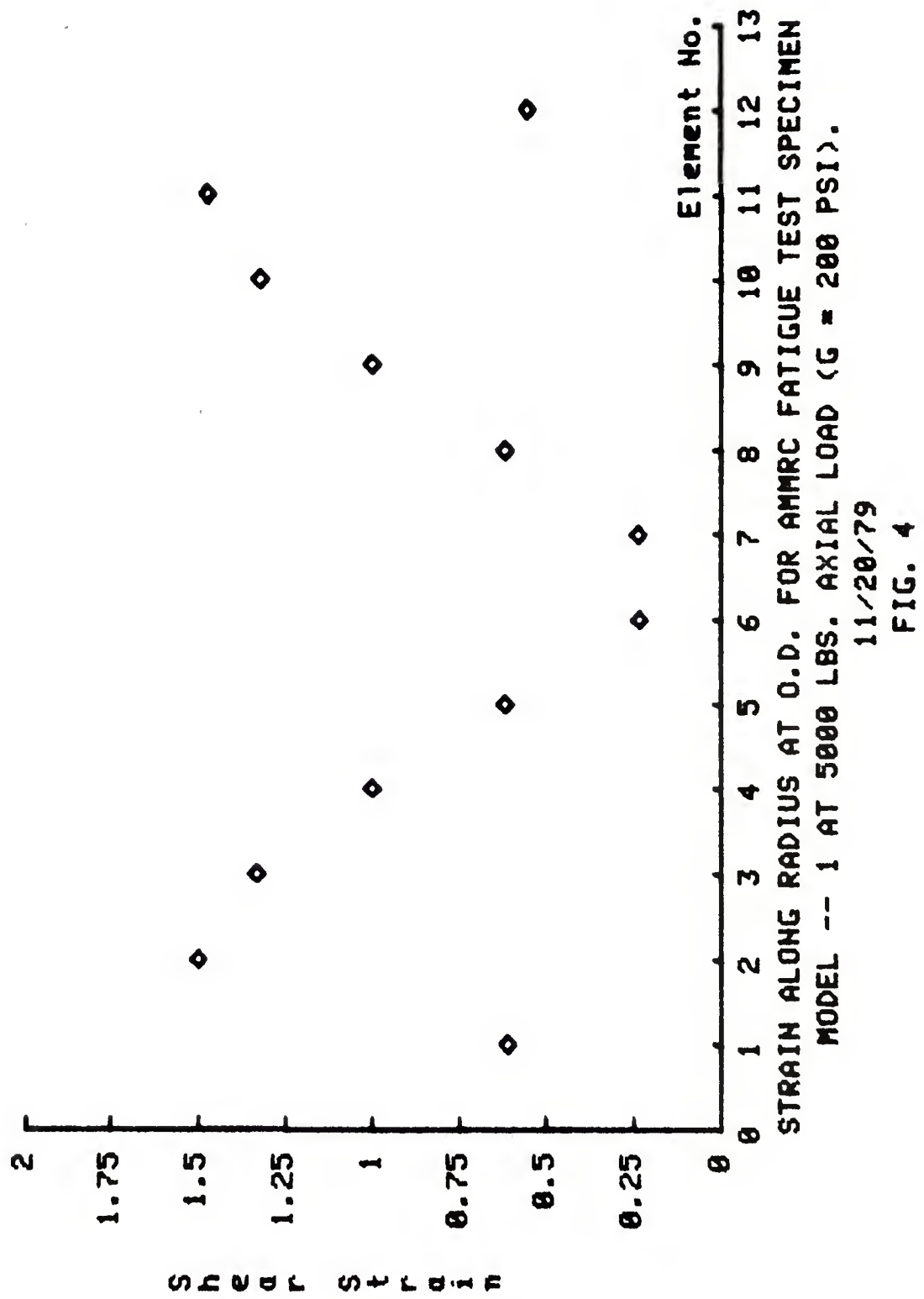


FIG. 2





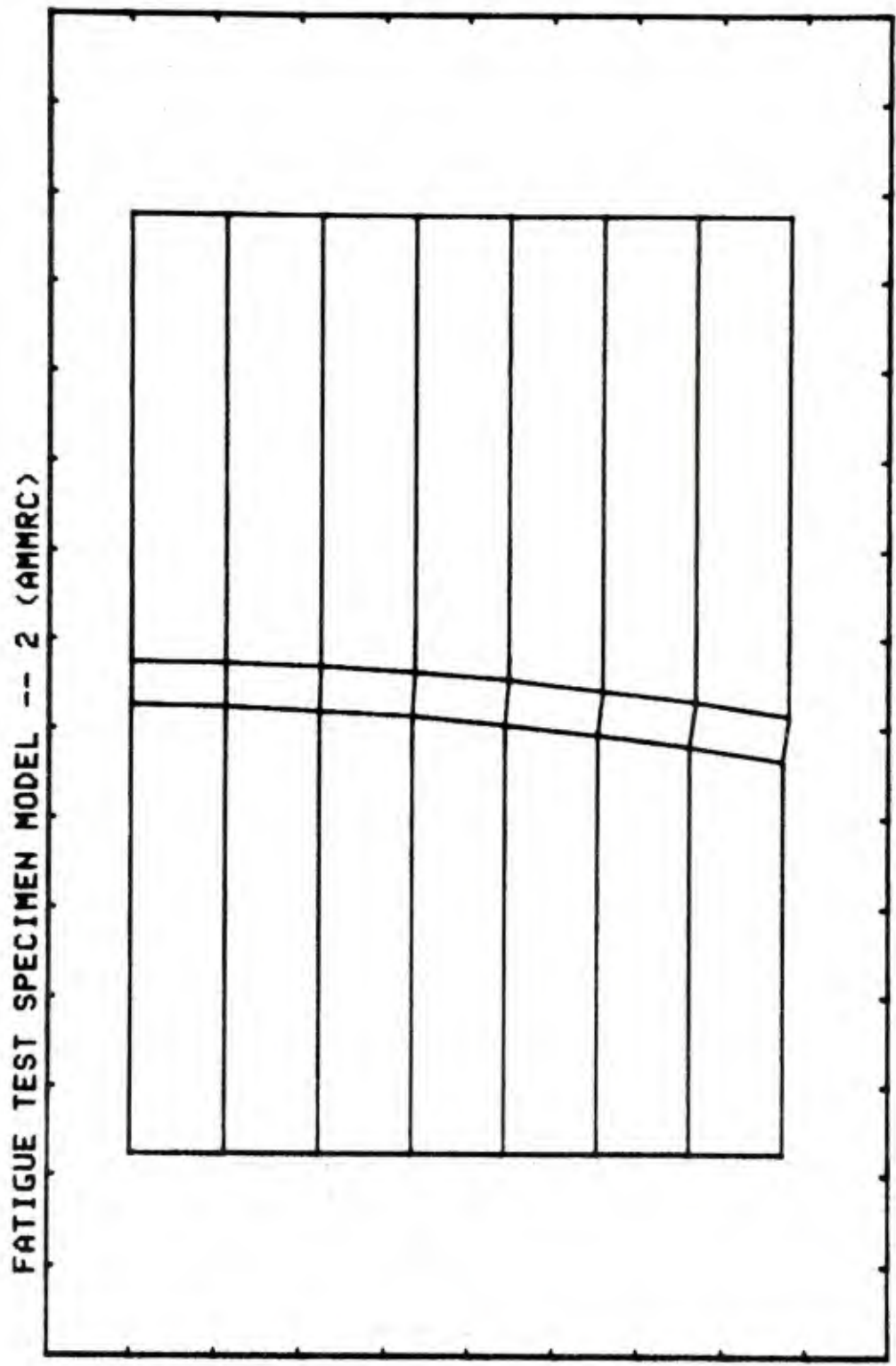


FIG. 5

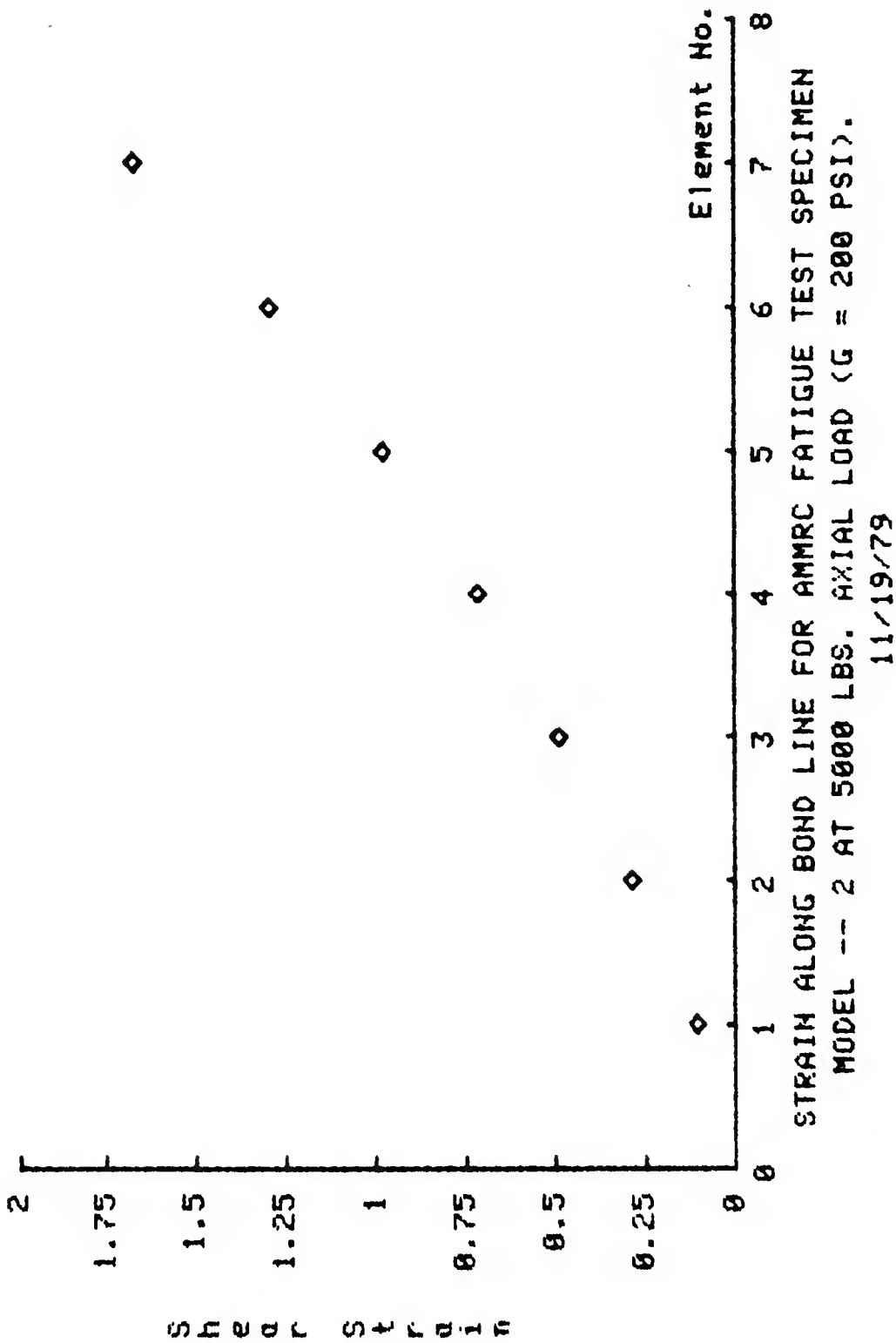


FIG. 6

FATIGUE TEST SPECIMEN MODEL 3 (AMMRC)

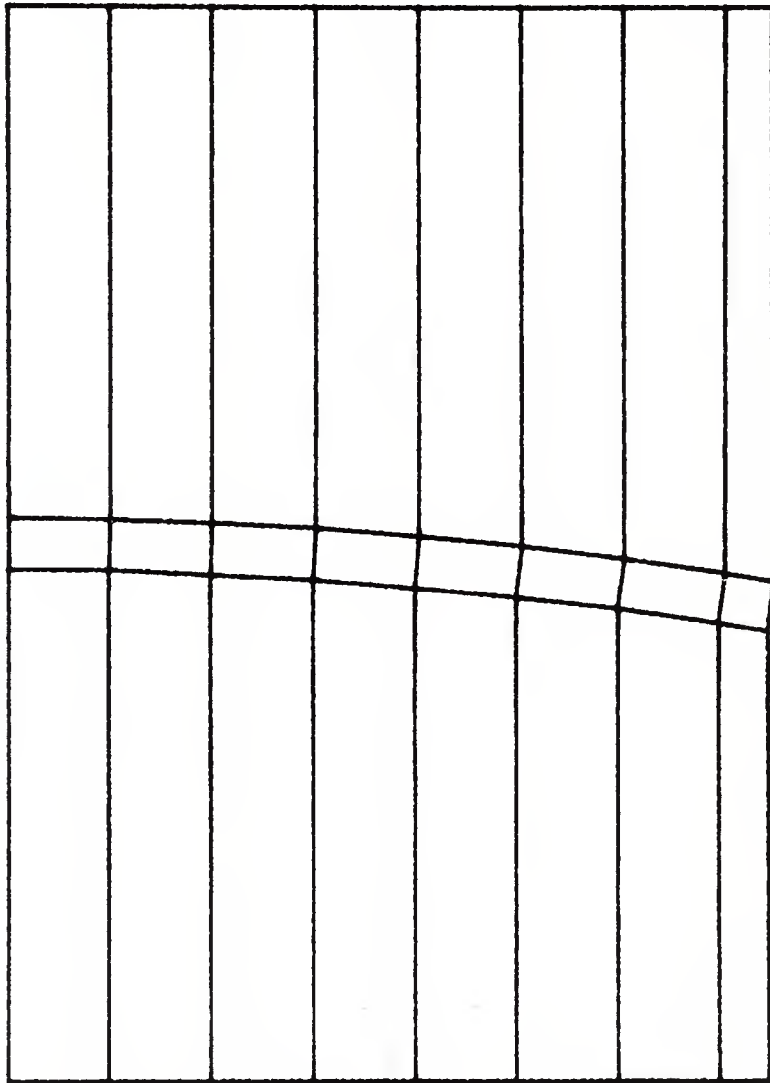
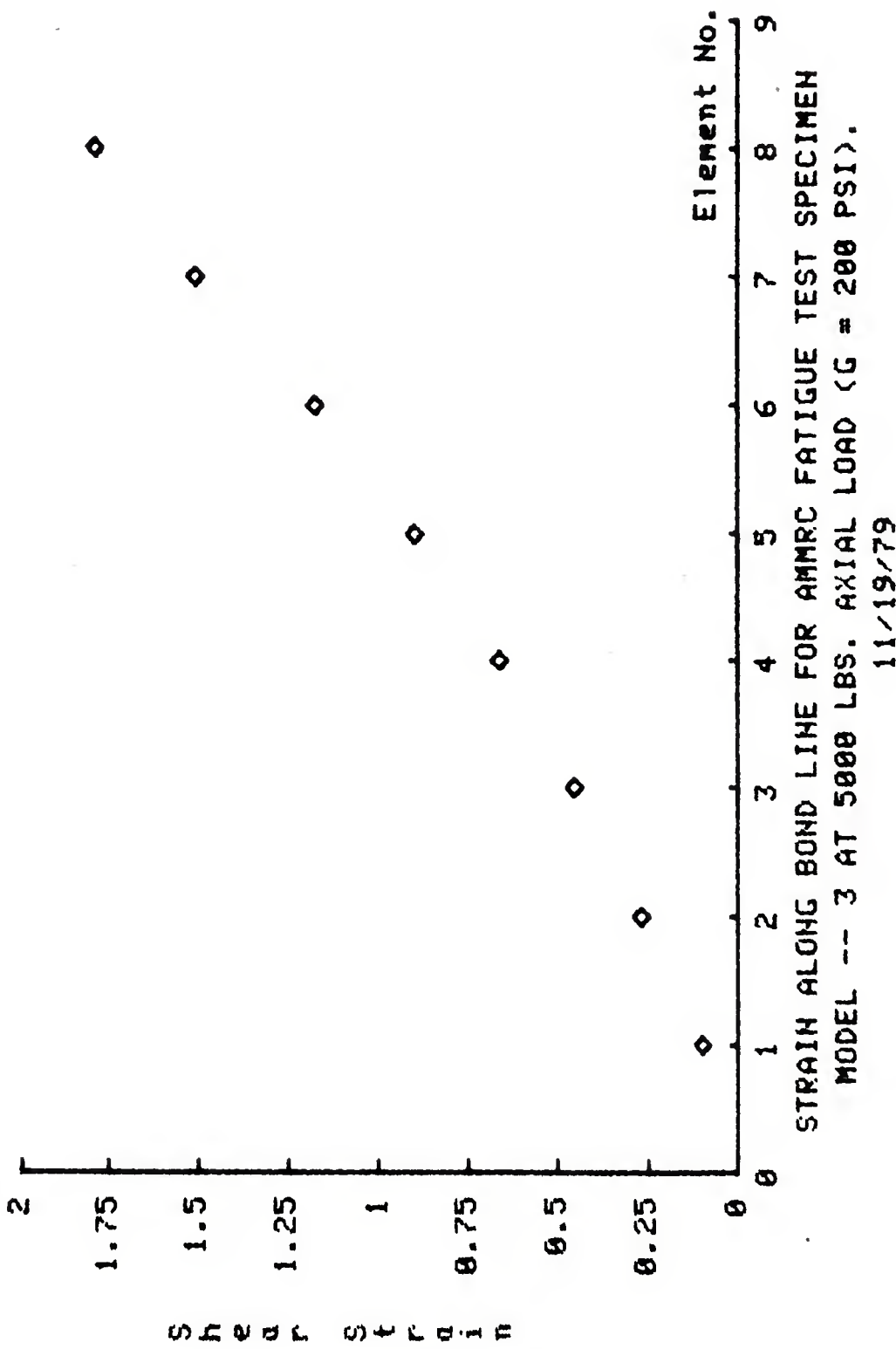


FIG. 7



A P P E N D I X I

1:\$ FATIGUE TEST SPECIMEN AMMRC MODEL 1
 2:SETUP,4,PREScriB,25
 3:RUBBER,1,600,.4995
 4:SSTEEL,2,30E6,.3
 5:END, MATERIAL
 6:1,1,2,1
 ? 0, .06946, .06946, 0
 8:4.47466,4.47466,4.47466,4.47466
 9:3,1,4,1
 18:13891, .20833, .20833, .13891
 11:4.47466,4.47466,4.47466,4.47466
 12:5,1,6,1
 13:27771, .34704, .34704, .27771
 14:4.47466,4.47466,4.47466,4.47466
 15:7,1,8,1
 16:37555, .40405, .40405, .37555
 17:4.47466,4.47466,4.47466,4.47466
 18:9,1,10,1
 19:43254, .46101, .46101, .43254
 20:4.47466,4.47466,4.47466,4.47466
 21:11,1,12,1
 22:48947, .51791, .51791, .48947
 23:4.47466,4.47466,4.47466,4.47466
 24:13,1,14,1
 25:54633, .57474, .57474, .54633
 26:4.47466,4.47466,4.47466,4.47466
 27:15,1,16,1
 28:60312, .63149, .63149, .60312
 29:4.47466,4.47466,4.47466,4.47466
 30:17,1,18,1
 31:65984, .68816, .68816, .65984
 32:4.47466,4.47466,4.47466,4.47466
 33:19,1,20,1
 34:71646, .74474, .74474, .71646

35: 4. 47466, 4. 47466, 4. 47466, 4. 47466
 36: 20, 1, 21, 1
 37: 7, 4474, 77299, 77299, 74474
 38: 4. 47466, 4. 47466, 4. 47466, 4. 47466
 39: 1, 2, 6, 2, 1, 1, 1, 1, POLAR, 0, 0
 40: 4, 975, 4, 975, 4, 980, 4, 980
 41: 98, 86, 86, 98
 42: 6, 2, 21, 3, 1, 1, 1, POLAR, 0, 0
 43: 4, 975, 4, 975, 4, 980, 4, 980
 44: 86, 81, 86143, 81, 86143, 86
 45: 1, 4, 6, 5, 1, 1, 1, 1, POLAR, 0, 0
 46: 4, 985, 4, 985, 4, 990, 4, 990
 47: 98, 86, 86, 98
 48: 6, 4, 21, 5, 1, 1, 1, 1, POLAR, 0, 0
 49: 4, 985, 4, 985, 4, 990, 4, 990
 50: 86, 81, 21308, 81, 25994, 86
 51: 1, 6, 6, 7, 1, 1, 1, 1, POLAR, 0, 0
 52: 4, 995, 4, 995, 5, 5
 53: 98, 86, 86, 98
 54: 6, 6, 21, 7, 1, 1, 1, 1, POLAR, 0, 0
 55: 4, 995, 4, 995, 5, 5
 56: 86, 81, 28326, 81, 29043, 86
 57: 1, 8, 6, 9, 1, 1, 1, 1, POLAR, 0, 0
 58: 5, 885, 5, 885, 5, 816, 5, 816
 59: 98, 86, 86, 98
 60: 6, 8, 21, 9, 1, 1, 1, 1, POLAR, 0, 0
 61: 5, 885, 5, 885, 5, 816, 5, 816
 62: 86, 81, 28318, 81, 25958, 86
 63: 1, 10, 6, 11, 1, 1, 1, 1, POLAR, 0, 0
 64: 5, 815, 5, 815, 5, 820, 5, 820
 65: 98, 86, 86, 98
 66: 6, 10, 21, 11, 1, 1, 1, POLAR, 0, 0
 67: 5, 815, 5, 815, 5, 820, 5, 820
 68: 86, 81, 21265, 81, 86125, 86

69: 1, 11, 6, 12, 1, 1, 1, 1, POLAR, 0, 0
70: 5, 020, 5, 020, 5, 025, 5, 025
71: 90, 86, 86, 90
72: 6, 11, 21, 12, 1, 1, 1, POLAR, 0, 0
73: 5, 020, 5, 020, 5, 025, 5, 025
74: 86, 81, 06125, 81, 06125, 86
75: 1, 13, 2, 13
76: 0, 07016, 07016, 0
77: 5, 5253, 5, 5253, 5, 5253
78: 3, 13, 4, 13
79: 14031, 21043, 21043, 14031
80: 5, 5253, 5, 5253, 5, 5253
81: 5, 13, 6, 13
82: 28050, 35053, 35053, 28050
83: 5, 5253, 5, 5253, 5, 5253
84: 7, 13, 8, 13
85: 37933, 40811, 40811, 37933
86: 5, 5253, 5, 5253, 5, 5253
87: 9, 13, 10, 13
88: 43689, 46565, 46565, 43689
89: 5, 5253, 5, 5253, 5, 5253
90: 11, 13, 12, 13
91: 49439, 52312, 52312, 49439
92: 5, 5253, 5, 5253, 5, 5253
93: 13, 13, 14, 13
94: 55183, 58052, 58052, 55183
95: 5, 5253, 5, 5253, 5, 5253
96: 15, 13, 16, 13
97: 60919, 63785, 63785, 60919
98: 5, 5253, 5, 5253, 5, 5253
99: 17, 13, 18, 13
100: 66648, 69509, 69509, 66648
101: 5, 5253, 5, 5253, 5, 5253
102: 19, 13, 20, 13

103: .72368, .75224, .75224, .72368
104: 5.5253, 5.5253, 5.5253, 5.5253
105: 20, 13, 2, 13
106: .75224, .78078, .78078, .75224
107: 5.5253, 5.5253, 5.5253, 5.5253
108: 21, 11, 22, 12
109: .78, .8, .8, .78077
110: 4.95982, 4.95584, 4.9609, 4.96397
111: 21, 12, 22, 13
112: .78077, .8, .8, .78077
113: 4.96397, 4.9609, 5.5253, 5.5253
114: 21, 1, 23, 2
115: .77299, .8, .8, .77299
116: 4.47466, 4.47466, 4.91026, 4.91458
117: 21, 2, 23, 3
118: .77299, .8, .8, .77301
119: 4.91458, 4.91025, 4.91532, 4.91952
120: EHD, GRID
121: JL00P, 20, 1
122: QUAD, 2, 1, 1
123: IEHD
124: JL00P, 10, 1
125: JL00P, 20, 1
126: QUAD, 1, 1, 2
127: IEHD
128: JEHD
129: JL00P, 20, 1
130: QUAD, 2, 1, 12
131: IEHD
132: QUAD, 1, 21, 11
133: QUAD, 2, 21, 12
134: QUAD, 2, 21, 1
135: QUAD, 2, 22, 1
136: QUAD, 1, 21, 2

```
137: QUAD, 1, 22, 2
138: ILOOP, 22, 1
139: BC, UZ, 1, 1, 1, 0
140: IEND
141: ILOOP, 21, 1
142: BC, PRESSURE, 1, 12, 3, 2486.79
143: IEND
144: END, ELEMENTS
145: PLOT, ELEMENTS, -.25, 4.25, 1, 5.75, 10
146: AXISYM
147: STUP
```

A P P E N D I X II

1: \$ FATIGUE TEST SPECIMEN MODEL -- 2 (AMMRC)
 2: SETUP,4,PREScriB,¹⁰
 3: RUBBER,1,600,.4995
 4: STEEL,2,30E6,.3
 5: END MATERIAL
 6: 1,1,2,1
 7: 0,11089,11089,0
 8: 4.47446,4.47446,4.47446,4.47446
 9: 3,1,4,1
 10: .22172,.33244,.33244,.22172
 11: 4.47446,4.47446,4.47446,4.47446
 12: 5,1,6,1
 13: 44299,55333,55333,44299
 14: 4.47446,4.47446,4.47446,4.47446
 15: 7,1,8,1
 16: .66339,.77312,.77312,.66339
 17: 4.47446,4.47446,4.47446,4.47446
 18: 1,2,8,3,1,1,1,POLAR,0,0
 19: 4.975,4.975,5.025,5.025
 20: 90,81,86,81,86,90
 21: 1,4,2,4
 22: 6,112,112,0
 23: 5.5253,5.5253,5.5253,5.5253
 24: 3,4,4,4
 25: .22394,.33578,.33578,.22394
 26: 5.5253,5.5253,5.5253,5.5253
 27: 5,4,6,4
 28: 4.47446,55889,55889,44744
 29: 5.5253,5.5253,5.5253,5.5253
 30: 7,4,8,4
 31: 67005,78089,78089,67005
 32: 5.5253,5.5253,5.5253,5.5253
 33: END,GRID
 34: ILOOP,7,1

```
35: QUAD, 2, 1, 1
36: IEND
37: ILOOP, ? , 1
38: QUAD, 1, 1, 2
39: IEND
40: ILOOP, ? , 1
41: QUAD, 2, 1, 3
42: IEND
43: ILOOP, ? , 1
44: BC, UZ, 1, 1, 1, 0
45: IEND
46: ILOOP, ? , 1
47: BC, PRESSURE, 1, 3, 3, 2616
48: IEND
49: END, ELEMENTS
50: PLOT, ELEMENTS, - . 1, 4.25, . 9, 5. 75, 10
51: AXISYM
52: STOP
```

A P P E N D I X III

1: \$ FATIGUE TEST SPECIMEN MODEL -- 3 (AMMRC)
 2: SETUP,4,PRESCTRIB,10
 3: RUBBER,1,600,.4995
 4: SSSTEEL,2,30E6,.3
 5: END, MATERIAL
 6: 1,1,2,1
 7: 0,-10375,.10375,0
 8: 4.47446,4.47446,4.47446,4.47446
 9: 3,1,4,1
 10: 20746,-31108,-31108,-20746
 11: 4.47446,4.47446,4.47446,4.47446
 12: 5,1,6,1
 13: 41475,.51787,.51787,.41475
 14: 4.47446,4.47446,4.47446,4.47446
 15: 7,1,8,1
 16: 62095,.72376,.72376,.62095
 17: 4.47446,4.47446,4.47446,4.47446
 18: 8,1,9,1
 19: 72376,.77312,.77312,.72376
 20: 4.47446,4.47446,4.47446,4.47446
 21: 1,2,8,3,1,1,1,POLAR,0,0
 22: 4.975,4.975,5.025,5.025
 23: 98,81,635,81,635,90
 24: 8,2,9,3,1,1,1,POLAR,0,0
 25: 4.975,4.975,5.025,5.025
 26: 81,635,81,06,81,06,81,635
 27: 1,4,2,4
 28: 0,10486,10486,0
 29: 5,5253,5,5253,5,5253,5,5253
 30: 3,4,4,4
 31: 20967,-31140,-31140,-20967
 32: 5,5253,5,5253,5,5253,5,5253
 33: 5,4,6,4
 34: .41898,.52339,.52339,.41898

35: 5. 5253, 5. 5253, 5. 5253, 5. 5253
36: 7. 4. 8, 4
37: . 62756, . 73146, . 73146, . 62756
38: 5. 5253, 5. 5253, 5. 5253, 5. 5253
39: 8. 4, 9, 4
40: . 73146, . 78089, . 78089, . 73146
41: 5. 5253, 5. 5253, 5. 5253, 5. 5253
42: END, GRID
43: ILOOP, 8, 1
44: QUAD, 2, 1, 1
45: IEHD
46: ILOOP, 8, 1
47: QUAD, 1, 1, 2
48: IEND
49: ILOOP, 8, 1
50: QUAD, 2, 1, 3
51: IEND
52: ILOOP, 8, 1
53: BC, UZ, 1, 1, 1, 0
54: IEND
55: ILOOP, 8, 1
56: BC, PRESSURE, 1, 3, 3, 2616
57: IEND
58: END, ELEMENTS
59: PLOT, ELEMENTS, -1, 4. 25, . 9, 5. 75, 10
60: AXISYM
61: STOP

SECTION 5.

EXPERIMENTAL DATA ON THE AMMRC ENDURANCE SPECIMEN

The report in Appendix I. of this section gives experimental results of endurance tests on thirteen AMMRC fatigue specimens (see Table 1 of the Appendix). The data is plotted in Fig. 1. The report gives the following fifth power curve fitted to the life (N) vs. load (L) data;

$$N = \left(\frac{29,500}{L} \right)^5$$

In the previous section we found a maximum shear strain of 1.8 for a load of 5000 lbs. on the coarse grid model, so that the shear strain is given by

$$\gamma = \frac{L}{2778}$$

Substituting we find the life to be

$$N = \left(\frac{10.6}{\gamma} \right)^5$$

Since this experimental endurance curve was obtained from an actual elastomeric bearing based on the materials, analytic and measuring techniques normally used in elastomeric bearings it should be specific to these conditions. It does, however, compare well with a published general relationship listed in Section 3 as

$$N = \left(\frac{12.5}{\gamma} \right)^5$$

A documentation of the criterion of first damage used on the AMMRC endurance specimen is given in Appendix II. Fig. 1 is a photomicrograph of the elastomer edge from the fatigue specimen before test. Fig. 2 is a photomicrograph of the same edge after test. Fig. 3 is a line drawing interpretation of the significance of these photos. Admittedly this criterion of first damage was stringent, but, when scaled up to elastomeric bearings the size of the Blackhawk main rotor bearings, it is felt that this criterion is consistant with that used for the larger bearings.

A P P E N D I X I

Chicago Rawhide Mfg. Co., 2517 Pan Am Blvd., Elk Grove Village, Ill. 60007, 312/595-4620



TEST REPORT

AMMRC Contract DAA-46-78-C-0029

September 27, 1979

by

Emmet M. Skroch

Test Lab Manager

CHICAGO RAWHIDE MANUFACTURING COMPANY

Test Report

Testing of the AMMRC Fatigue Specimens (CR 80 6627) has been completed. A total of 13 specimens were tested, until evidence of first damage was observed.

Compressive axial loading of the test parts was done using a sine wave forcing function at a cycling rate of 4.2 Hz. The minimum compressive axial load for each test specimen was established as 10% of the peak-to-peak cyclic loading.

Table I shows the loading spectrum that was used in testing the fatigue plugs. Figure 1 is a plot of the half amplitude cyclic loading vs. the cycles to first damage. All observation for first damage were made using a microscope with 15 x magnification. The solid line shown in Figure 1 is a 5th power curve derived from the empirical data. The line as shown in Figure 1 is not continuous. For cyclic loads of approximately 1700 lbs. and less a knee is evident. This knee is an indication of infinite fatigue life. The continuous portion of this curve can be described by the following equation:

$$N = \left(\frac{29,500}{L} \right)^5$$

CHICAGO RAWHIDE MANUFACTURING COMPANY

Page 2

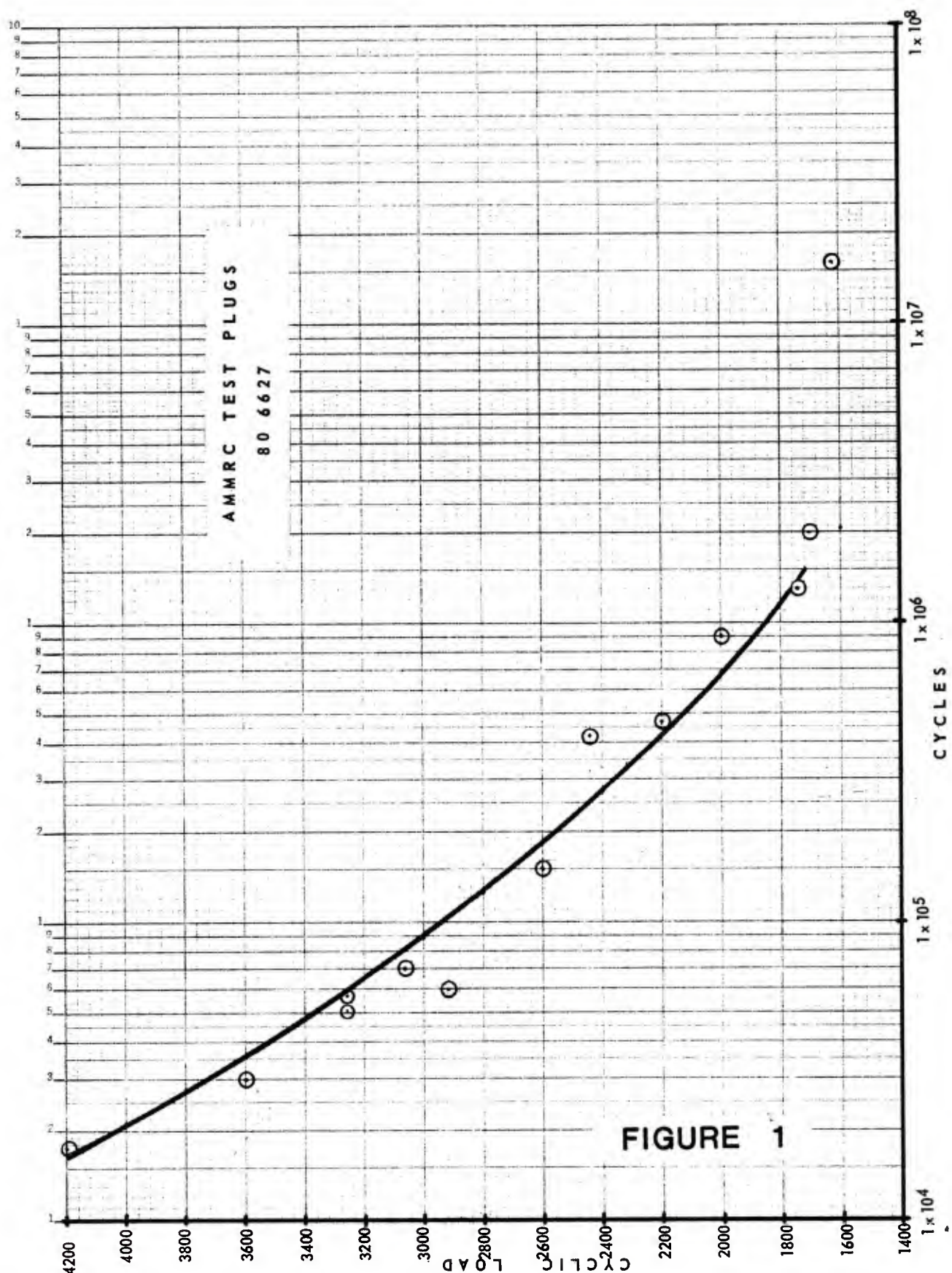
In the above equations

N is the number of cycles

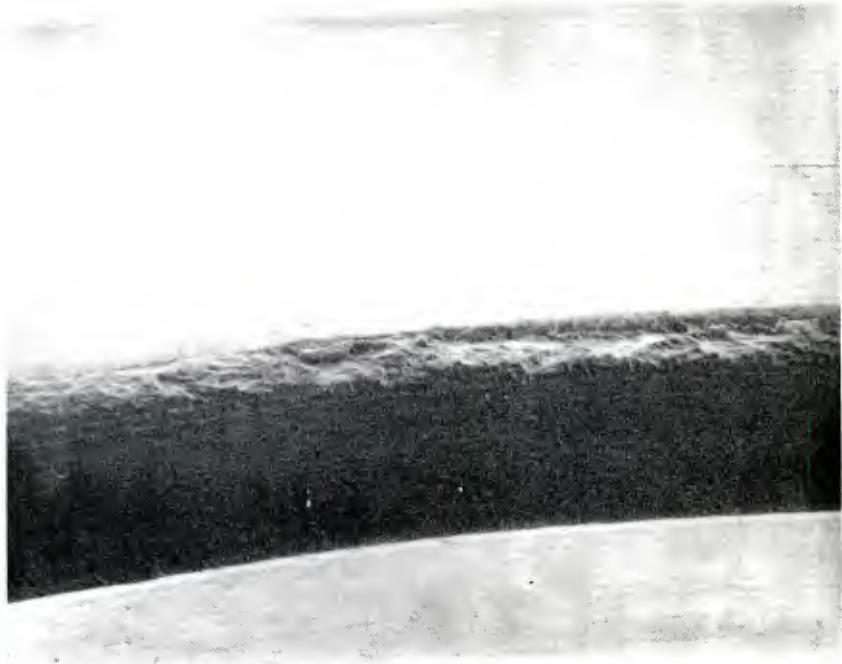
L is the half amplitude cyclic load

L O A D (1bs)	C Y C L E S
1. 5050 ± 4200	1.75 x 10 ⁴
2. 4320 ± 3600	3.00 x 10 ⁴
3. 3900 ± 3250	5.69 x 10 ⁴
4. 3900 ± 3250	5.10 x 10 ⁴
5. 3660 ± 3050	7.00 x 10 ⁴
6. 3510 ± 2925	6.00 x 10 ⁴
7. 3120 ± 2600	1.50 x 10 ⁵
8. 2925 ± 2438	4.20 x 10 ⁵
9. 2640 ± 2200	4.70 x 10 ⁵
10. 2400 ± 2000	9.00 x 10 ⁵
11. 2100 ± 1750	1.30 x 10 ⁶
12. 2040 ± 1700	2.00 x 10 ⁶
13. 1950 ± 1625	1.60 x 10 ⁷

TABLE I



A P P E N D I X II



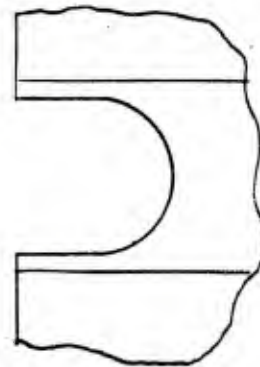
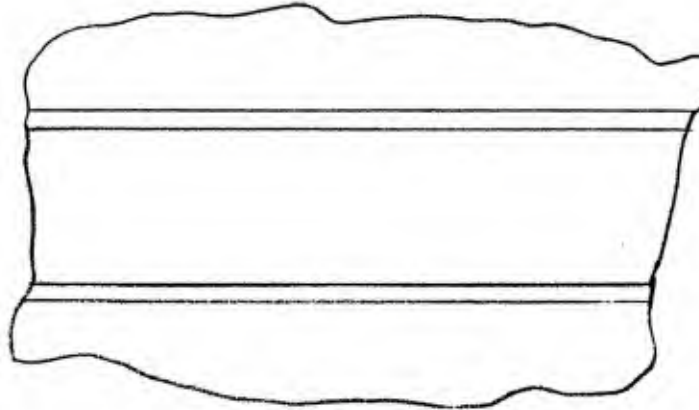
FATIGUE SPECIMEN BEFORE TEST

FIG. 1

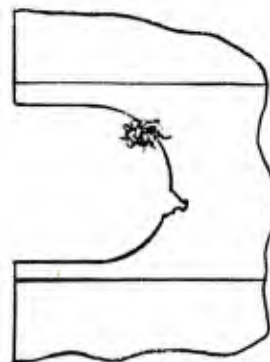
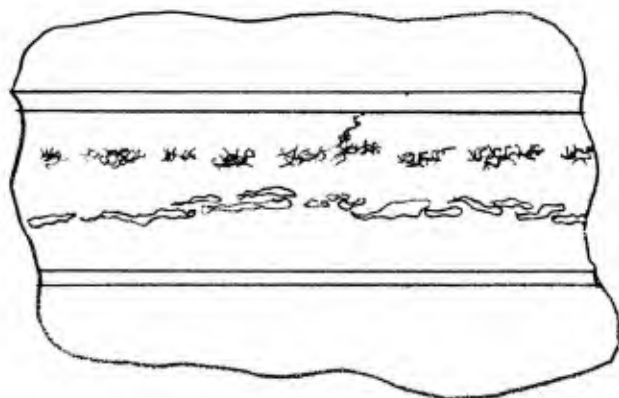


FATIGUE SPECIMEN AFTER TEST

FIG. 2



FATIGUE SPECIMEN ELASTOMER EDGE
BEFORE TEST



FATIGUE SPECIMEN ELASTOMER EDGE
AFTER TEST
FIG. 3

SECTION 6.

ANALYSIS OF THE BLACKHAWK MAIN ROTOR THRUST BEARING

The subject covered in this section is an analysis of the elastomer strain and metal shell stress in the Blackhawk main rotor elastomeric thrust bearing (see Figure 1.) A prediction of the life of the thrust bearing will be given based on this data. As reference it is suggested that the Sections 2 and 3, covering finite element analysis and the use of strain data to predict the life of elastomeric parts, be reviewed.

The analysis of this thrust bearing was straight forward and superposition was not required.

The first model for stress or strain at the I.D. of the thrust bearing is shown in Figure 2 and enlarged sections in Figures 3 and 4. Note, the small element at the I.D. allows "mid-side node" stress or strain values for a location close to the edge. The model for O.D. stress and strain is shown in Figure 5 and blow-ups in Figures 6 and 7. A listing of the programs are given in the Appendix.

The maximum stress in the A-70 C.P. titanium shells for a 68,000 pound C.F. load is shown in Figures 8 and 9 to be 70 ksi. With a 70 ksi yield point the stress in the shells after the first cycle may be considered to be 35 ± 35 ksi. The metal shells, therefore, are not expected to suffer endurance failure within the expected life of this bearing.

The elastomer strain for the 68,000 pound C.F. load is shown in Figures 10 and 11. The elastomer strain due to pitch change can be calculated directly from first principles. For a 1 degree rotation

$$\gamma = \frac{R\theta}{t}$$

$$\gamma_{I.D.} = \frac{1.5 (\pi/180)}{(10*0.025+45*0.030)} = 0.0164$$

$$\gamma_{O.D.} = \frac{2.55 (\pi/180)}{(10*0.025+45*0.030)} = 0.0278$$

Where: γ is the shear strain

θ is the angle of rotation (in radians)

t is the total elastomer thickness

R is the radius

Note; the above may seem like an oversimplification, but is identical to the result obtained by an integral solution. The finite element backup solution is shown in Figure 12.

The spherical and the thrust bearing share the total blade pitch change.

Spring rate of the spherical bearing = 1000 in.-lb./degree

Spring rate of 80 9589 = 120 in.-lb./degree

$$\left(\frac{1000}{1000 + 120} \right) 100 = 89.3\% \text{ of the total pitch change for 80 9589.}$$

The effective pitch change angle found from S.E.S. 701054

Rev. 4 by the method previously described (see Appendix of Section 3) is 6.54 degrees.

The following is a sample calcultaion of the life limiting combination of pitch change and centrifugal force strain calculated for the I.D. of the first layer (see the Appendix of Section 3);

$$\gamma =$$

$$\sqrt[5]{\frac{258*60(6.54*0.893*0.0164)^5 + \left(\frac{7.29}{2} * \frac{82000}{68000}\right)^5 + 2*\left(\frac{7.29}{2}\right)^5}{258*60 + 1.0 + 2.0}}$$

$$\gamma = .717$$

The life limiting strain at the I.D. is shown for all the layers in Figure 13. The results for a similar procedure for the O.D. is shown in Figure 14.

On the basis of this analysis, first damage is predicted at

$$\text{Life} = \left(\frac{10.6}{.717}\right)^5 * \frac{1}{60*258}$$
$$= 46 \text{ hrs}$$

The predicted location for this first damage is at the I.D. of the first layer next to the flanged end fitting (see Figures 13 and 14).

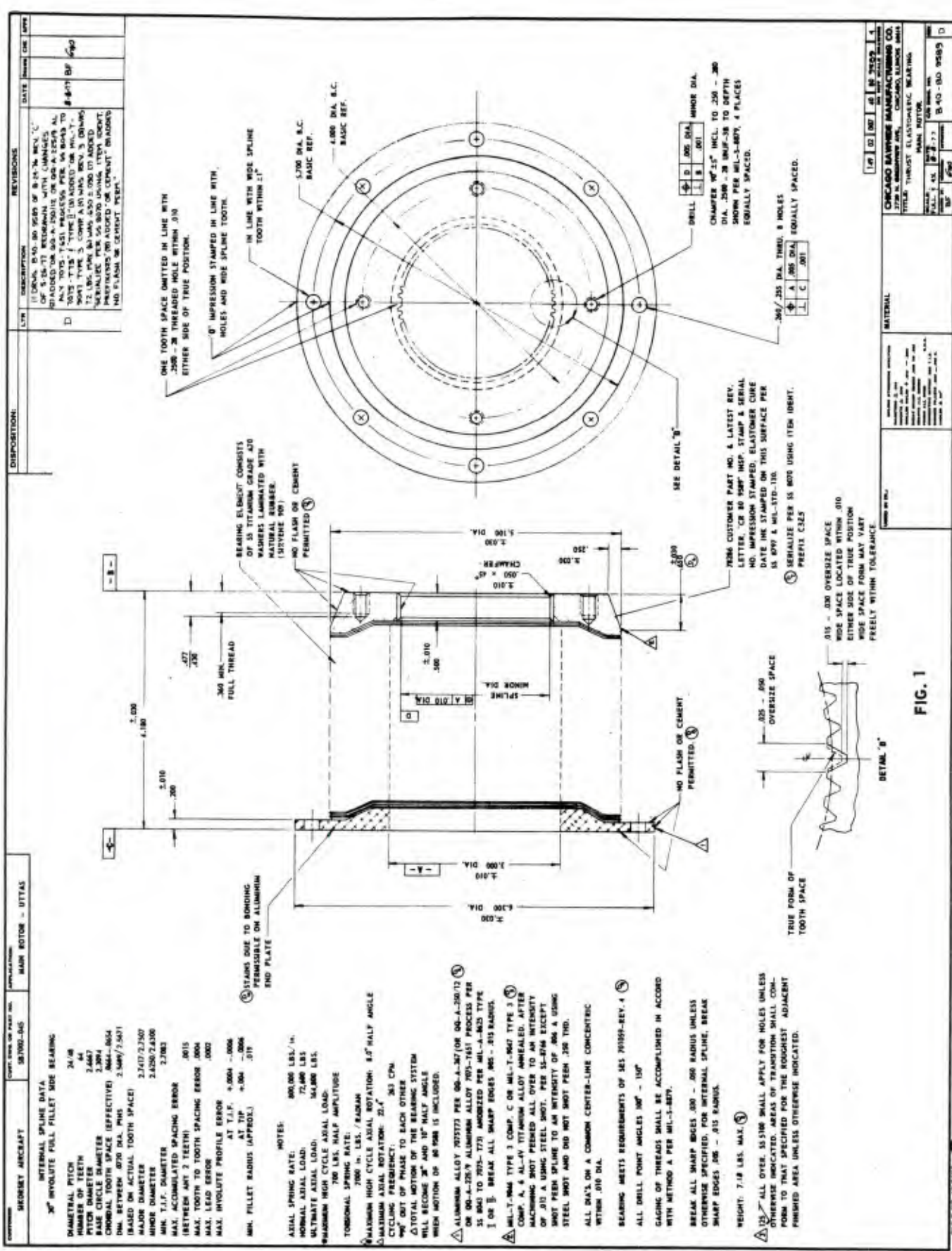


FIG. 1

DISPOSITION:	DATE:	REVISIONS:
LTR	10-60-50	10-60-500 Series of 8014-74 MOD. 1-C CUT 5-1/2" IN. REWORKED WITH CHANGES ADDED ON ONE SIDE N/A TOTS. T451 PROCESS PER A 200-A TOL. TOTS. T451. TYPE 3 (IN) ADDED ON MIL-T- SPEC TYPE 5 (COMP. A IN) WAS REV. 3. (DRILLS T1. 200 PINS. AS WAS 450 ± 0.05 LT ADDED MANUFACTURED ON US AND UNIVIA. ITEM IDENT REFERS TO FORD CEMENT BANDS HAD FASHION & CEMENT PREP.

MATERIAL:	
MIL-A-842	10-60-500 Series of 8014-74 MOD. 1-C CUT 5-1/2" IN. REWORKED WITH CHANGES ADDED ON ONE SIDE N/A TOTS. T451 PROCESS PER A 200-A TOL. TOTS. T451. TYPE 3 (IN) ADDED ON MIL-T- SPEC TYPE 5 (COMP. A IN) WAS REV. 3. (DRILLS T1. 200 PINS. AS WAS 450 ± 0.05 LT ADDED MANUFACTURED ON US AND UNIVIA. ITEM IDENT REFERS TO FORD CEMENT BANDS HAD FASHION & CEMENT PREP.

ITEM 1

REV. 1

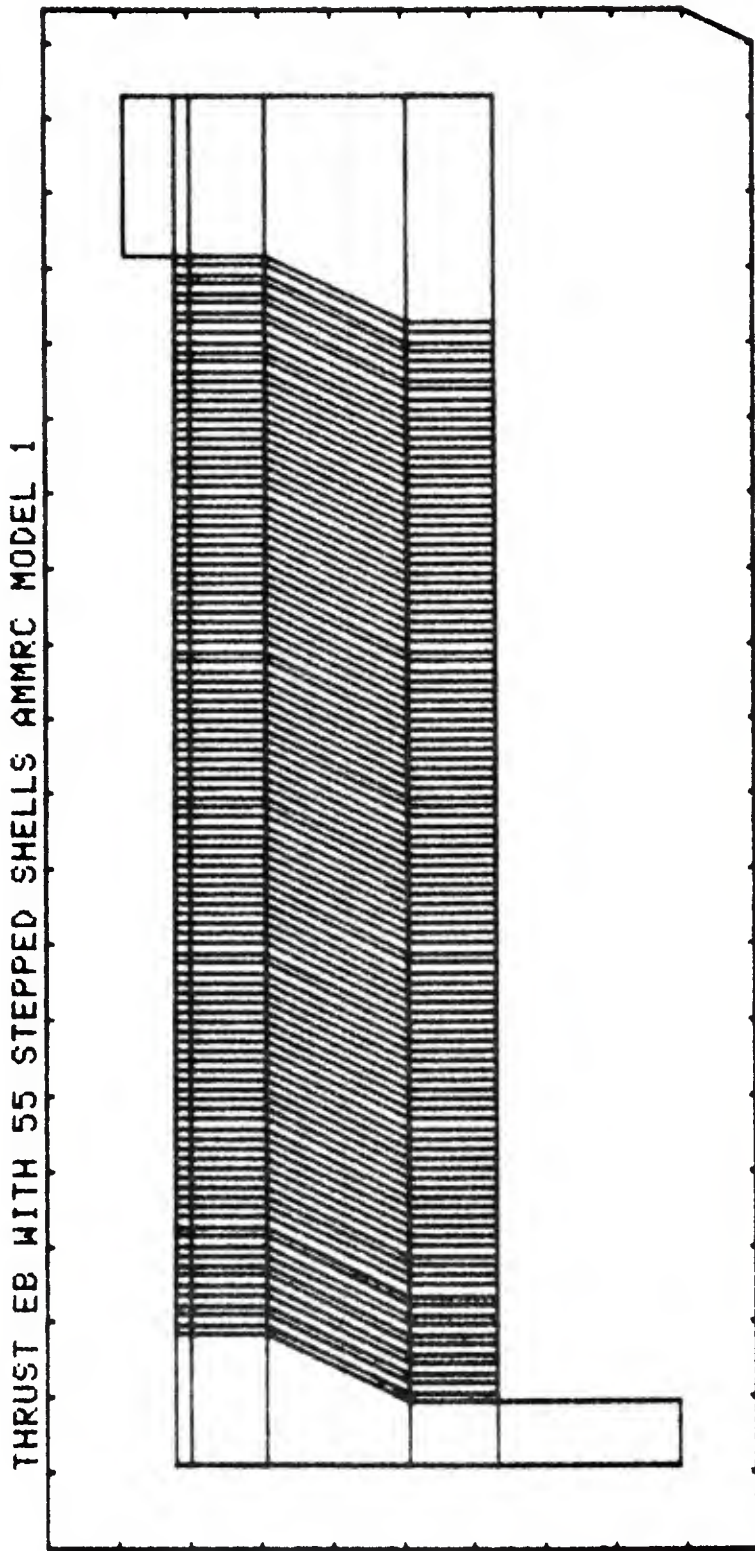
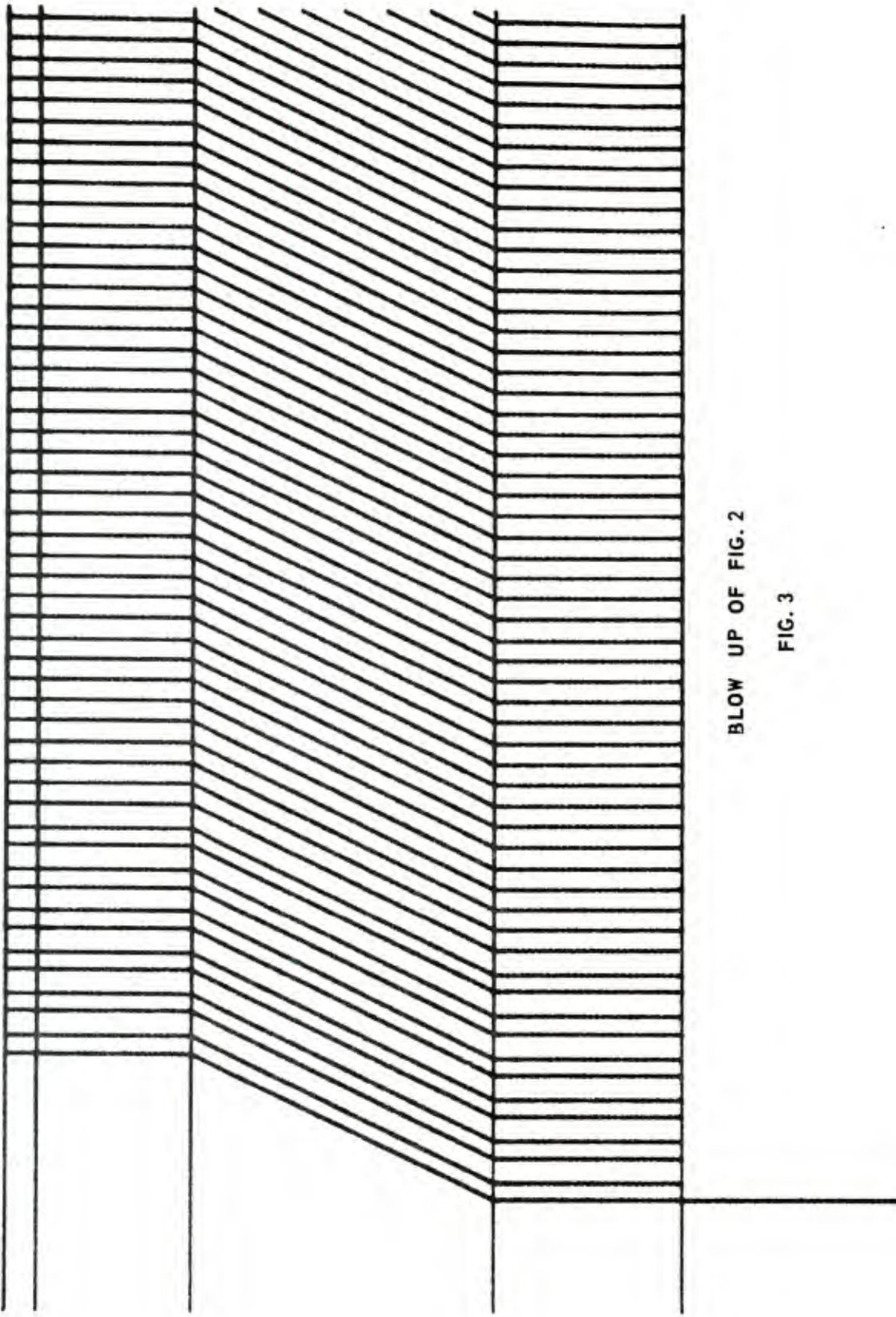
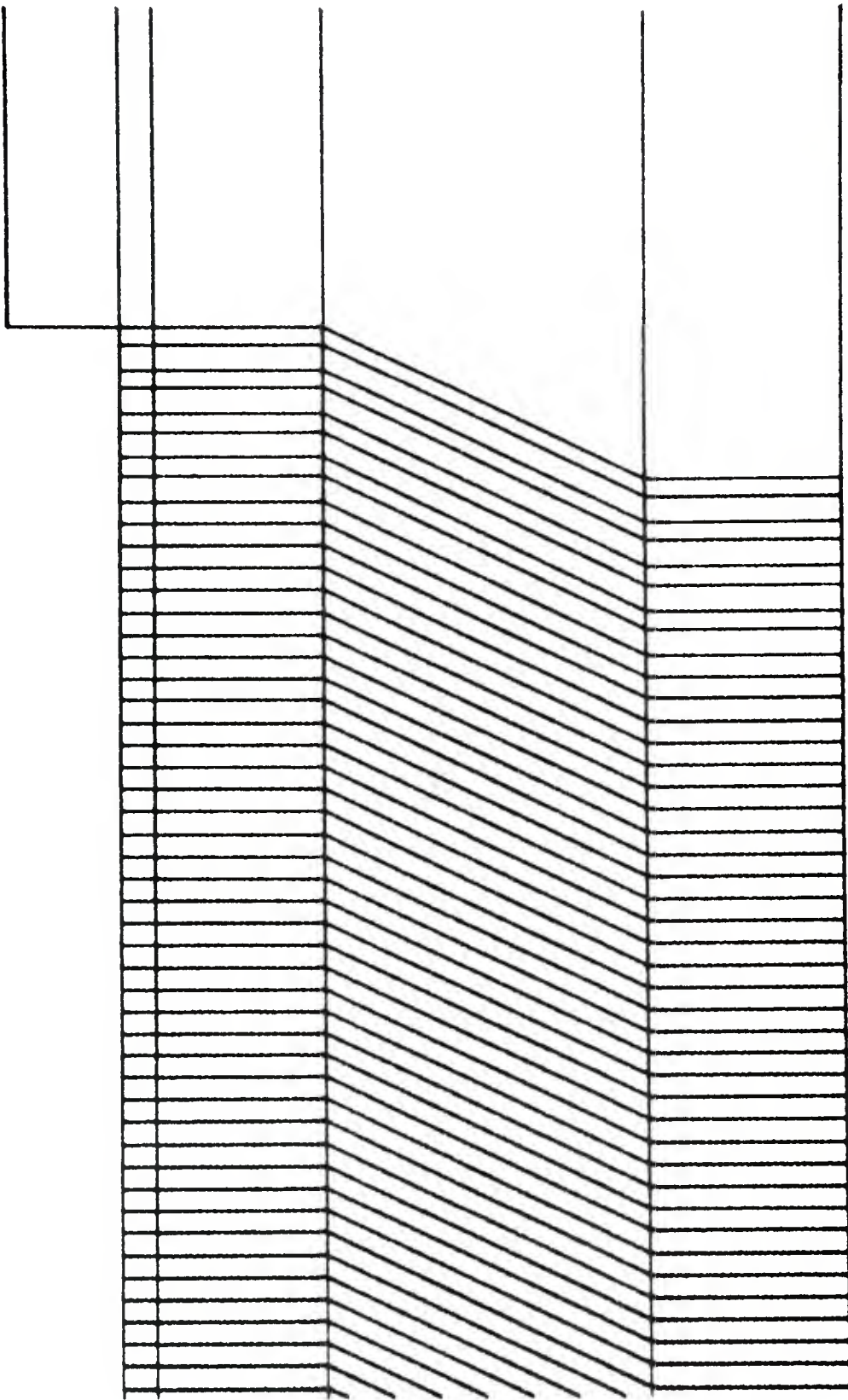


FIG. 2



BLOW UP OF FIG. 2

FIG. 3



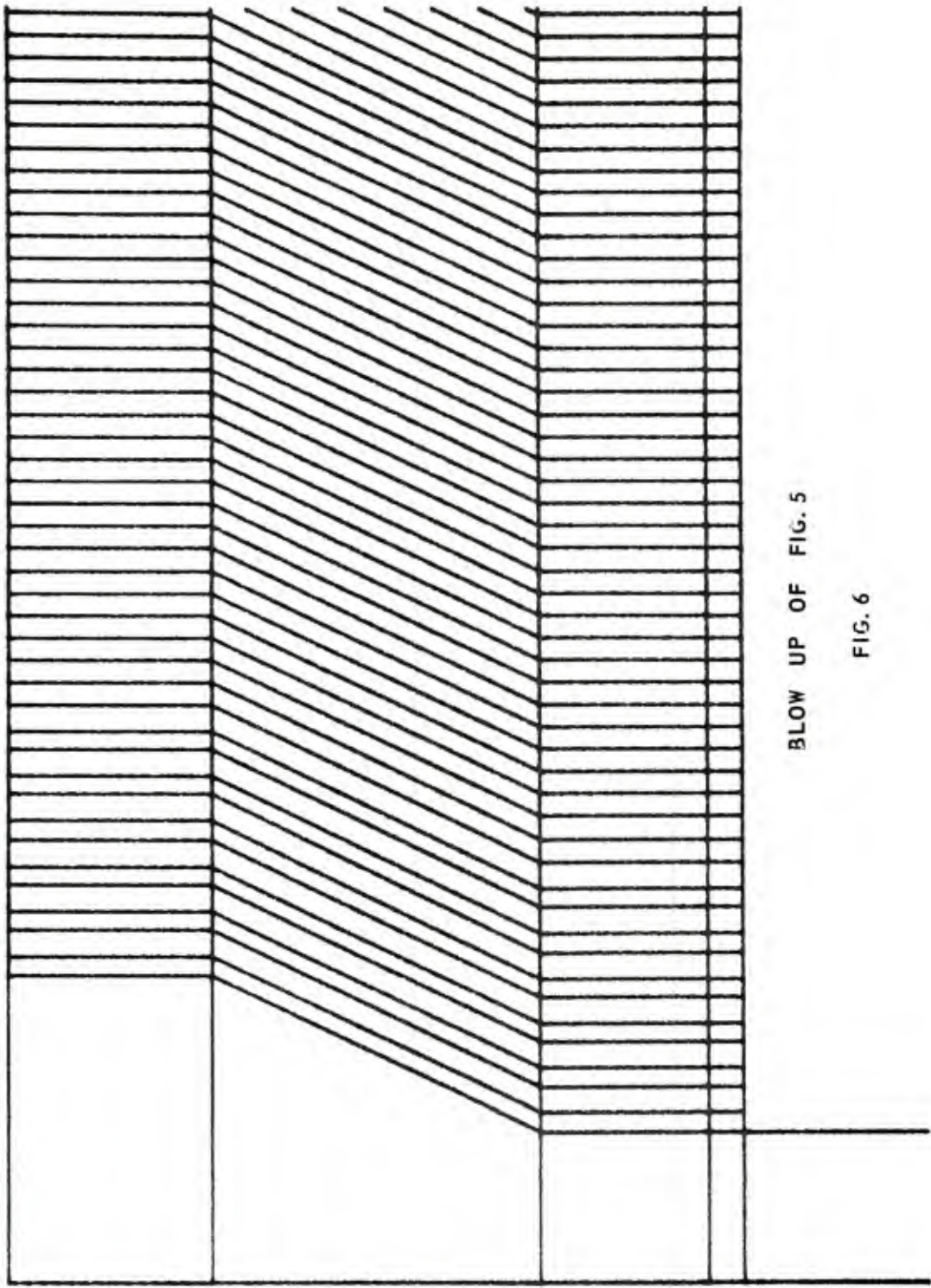
BLOW UP OF FIG. 2

FIG. 4

THRUST EB WITH 55 STEPPED SHELLS AMMRC MODEL 2

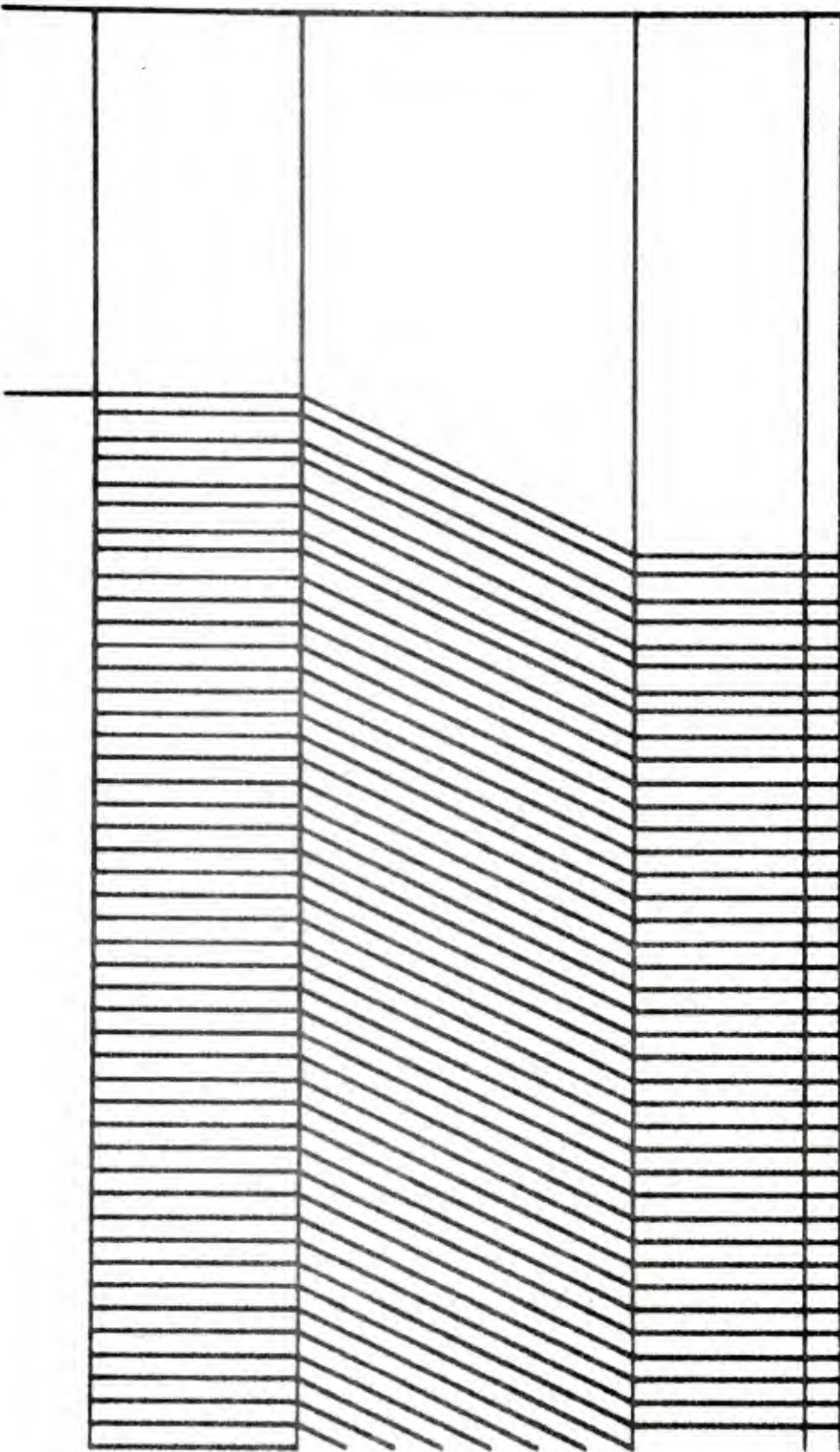


FIG. 5



BLOW UP OF FIG. 5

FIG. 6



SLOW UP OF FIG. 5

FIG. 7

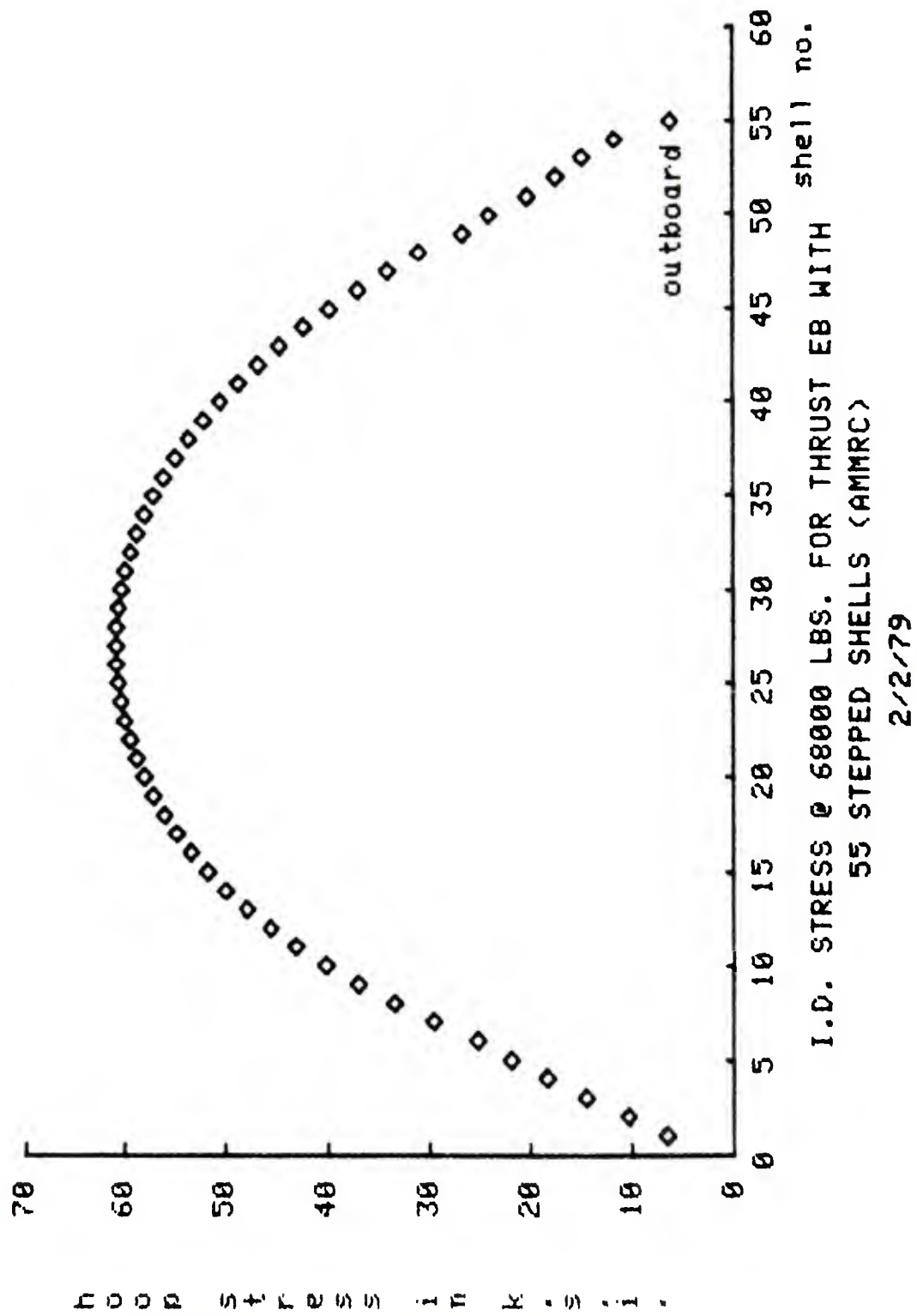


FIG. 8

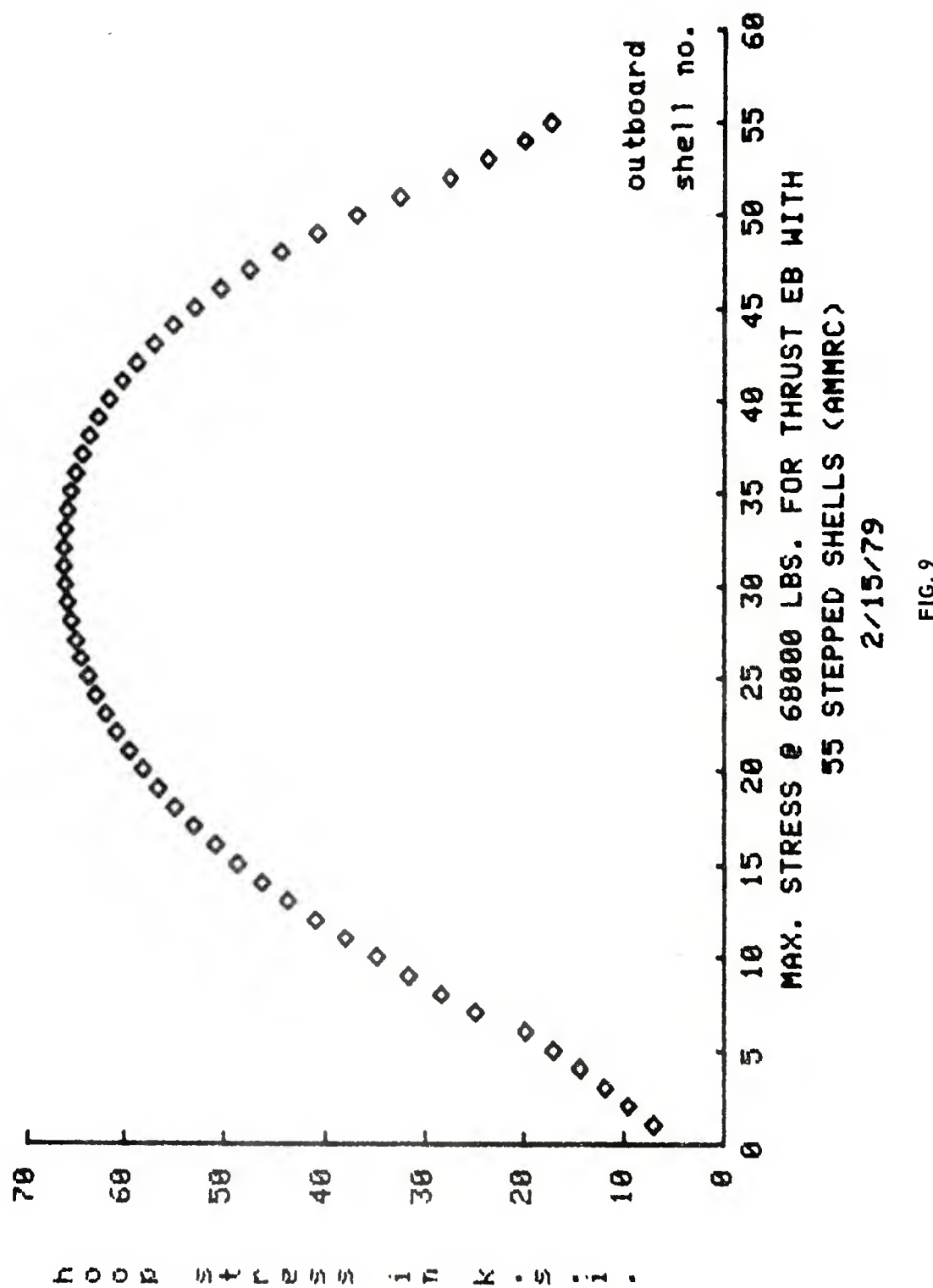
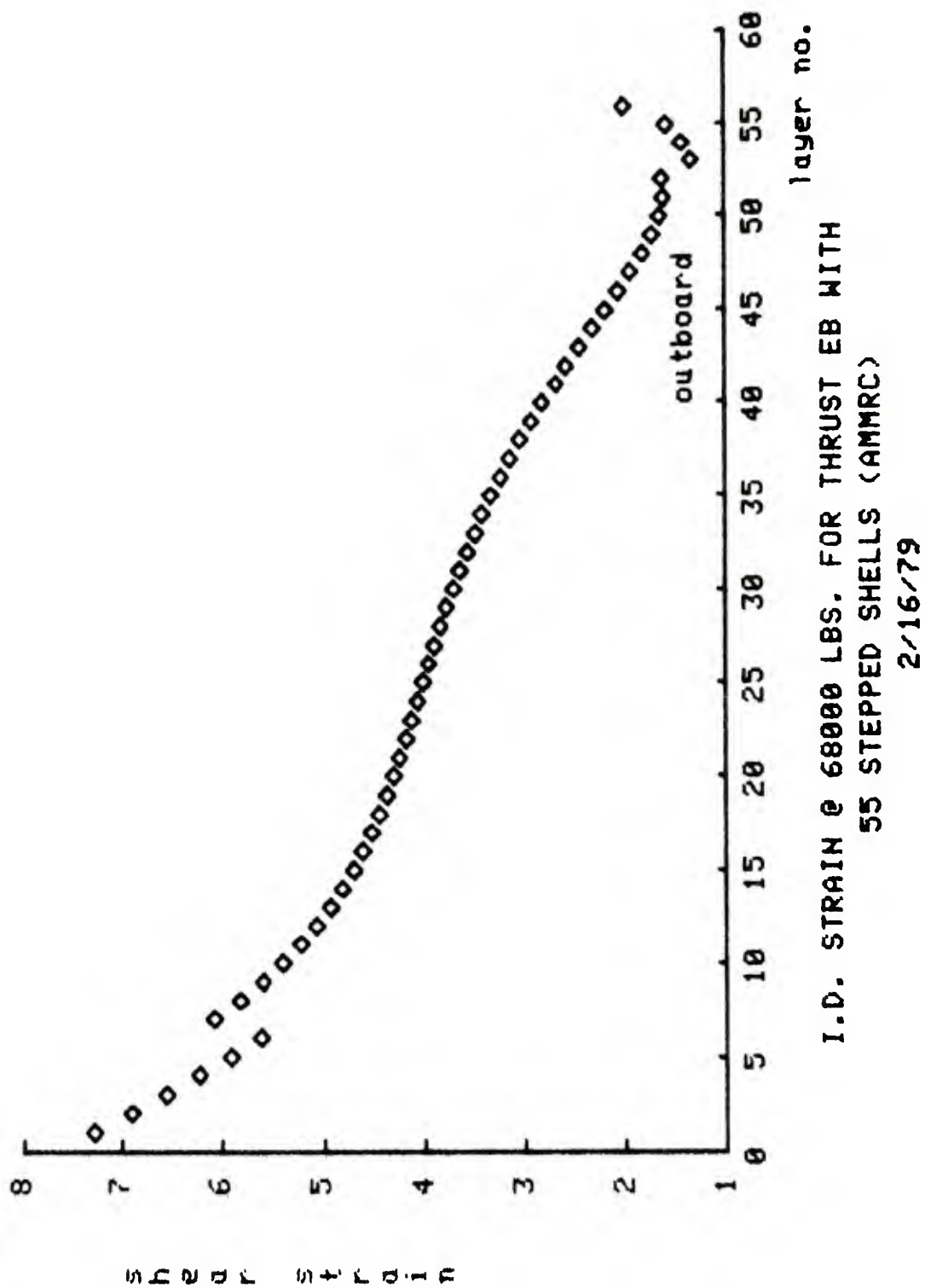


FIG. 9



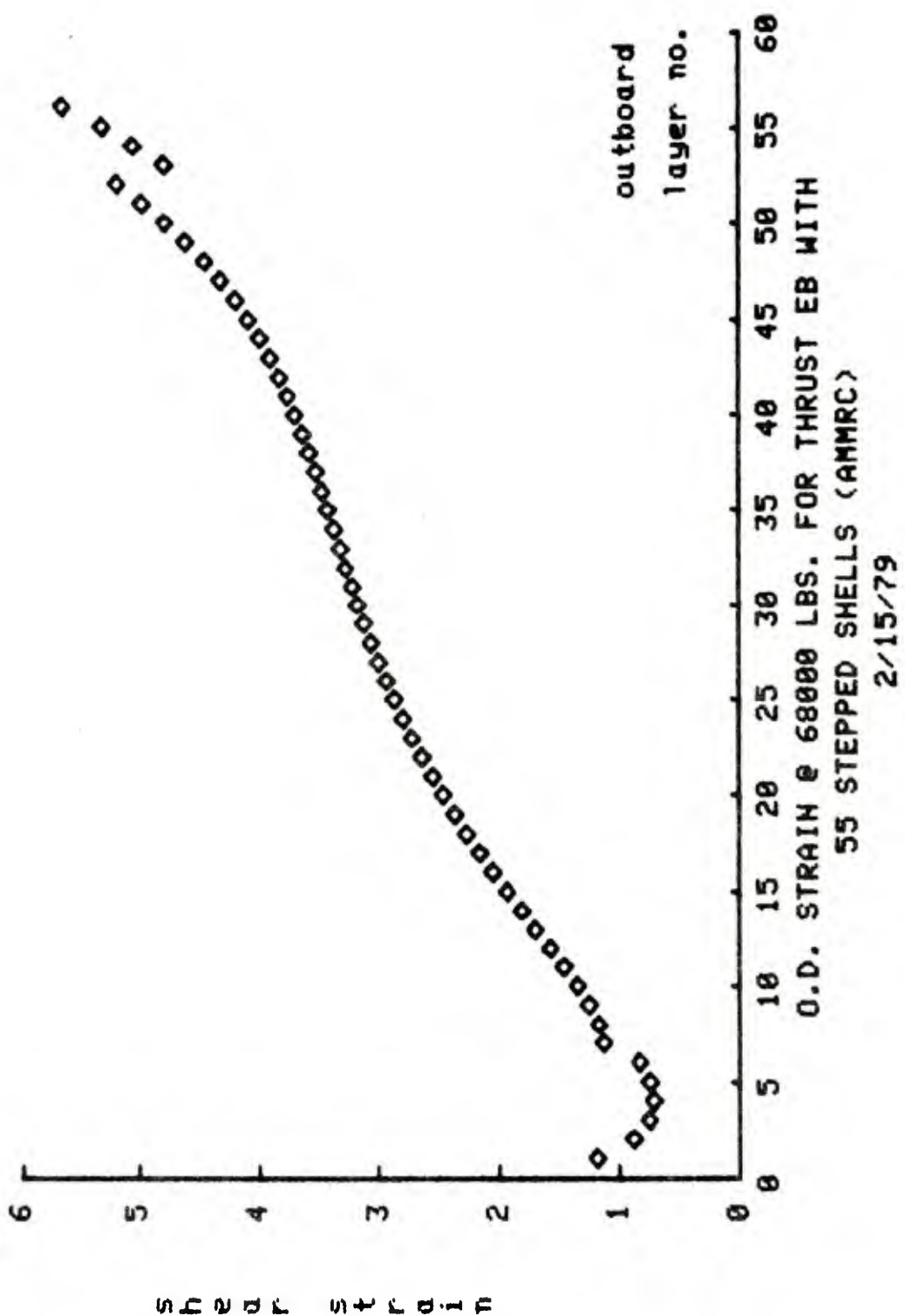


FIG. 11

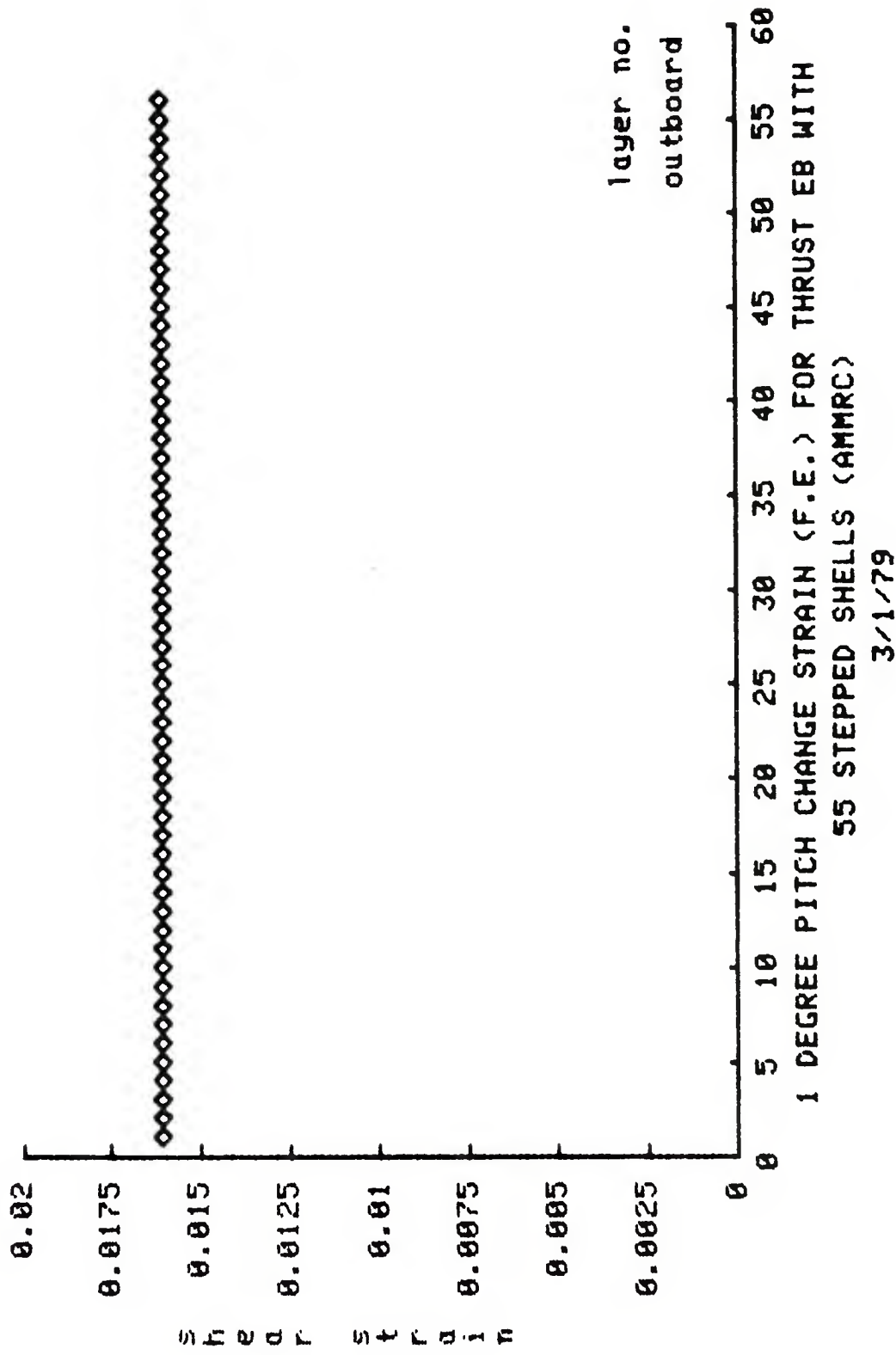
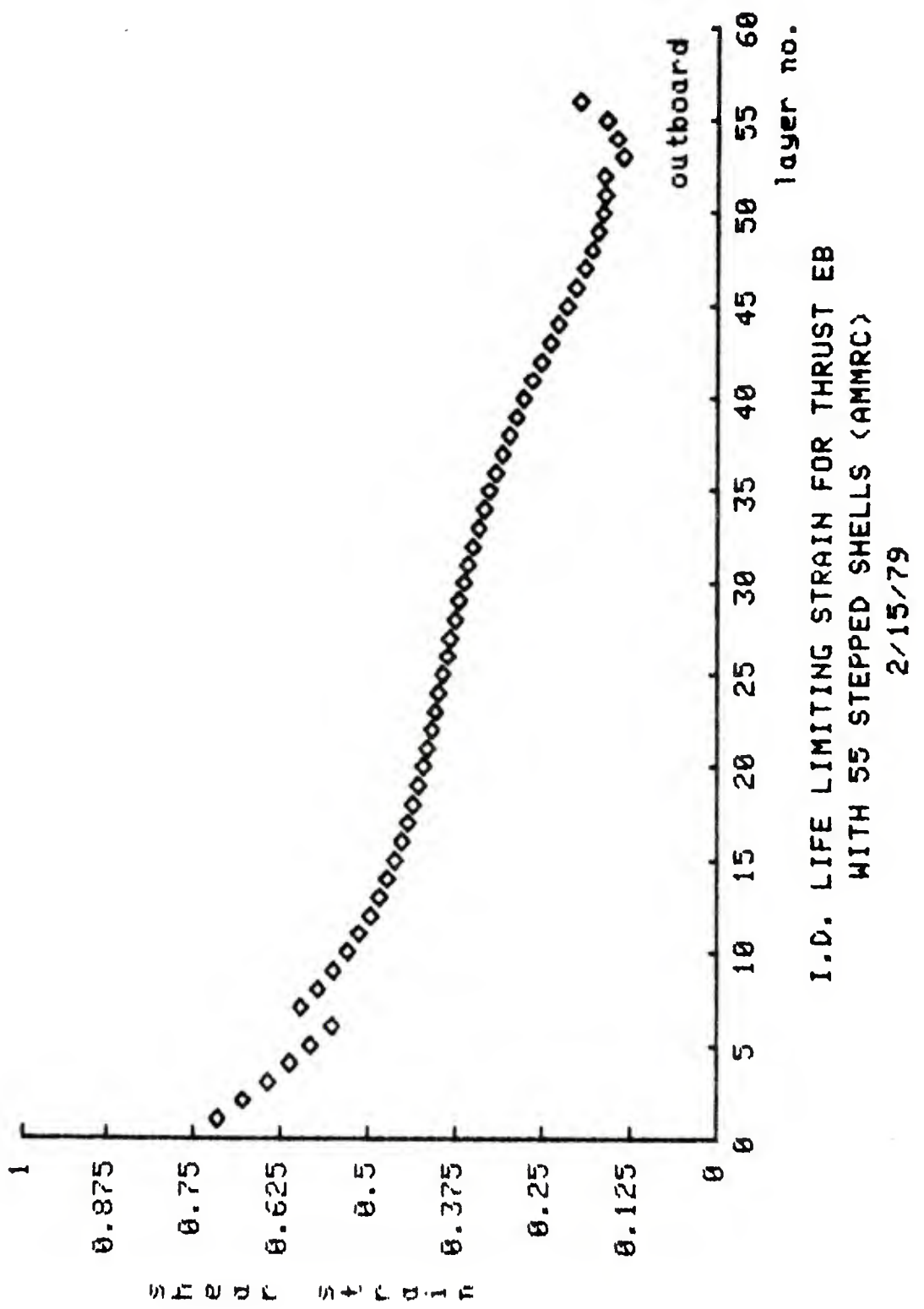


FIG. 12



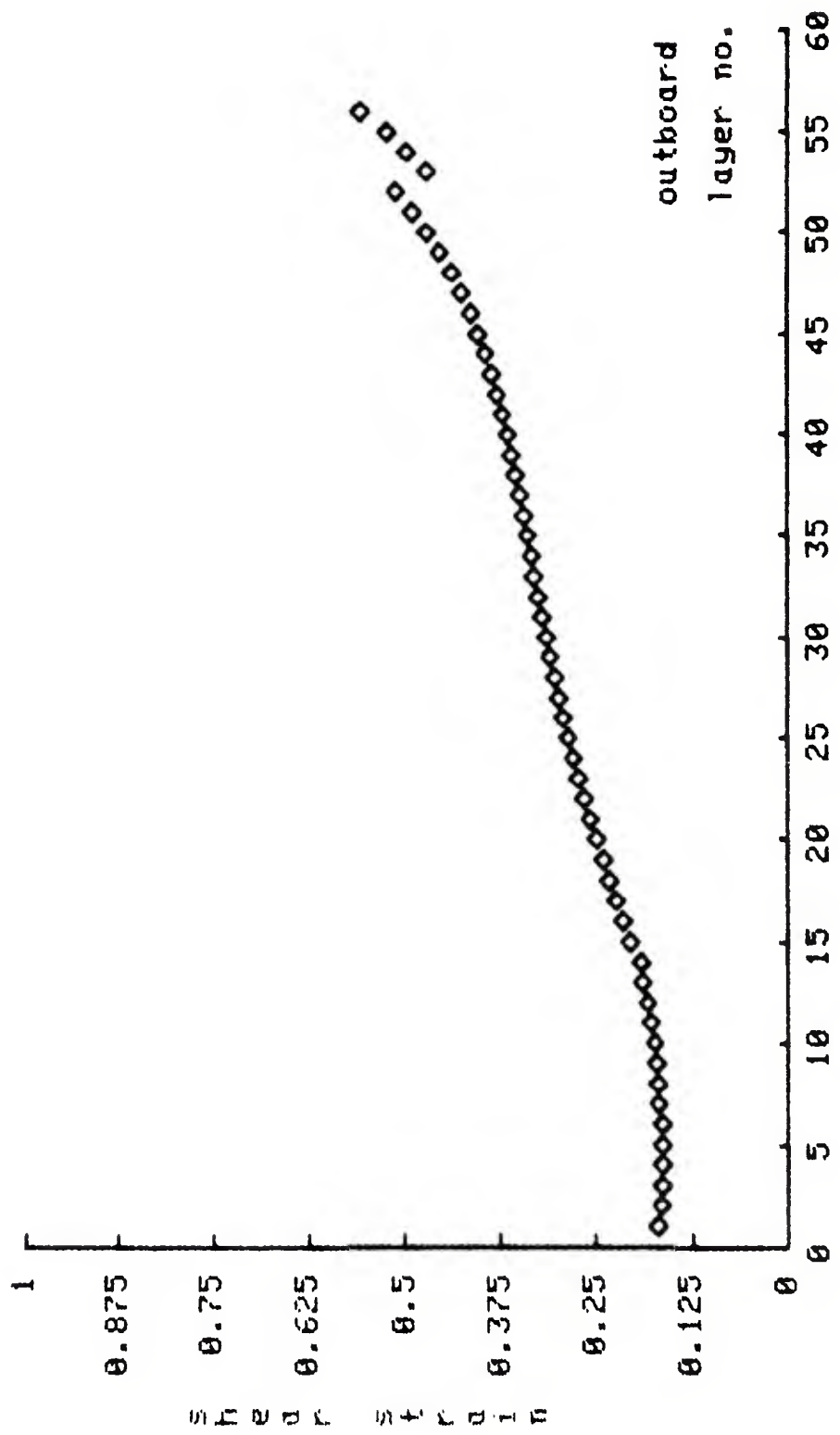
I.D. LIFE LIMITING STRAIN FOR THRUST EB
WITH 55 STEPPED SHELLS (AMMRC)
2/15/79

FIG. 13

FIG. 14

2/15/79

O.D. LIFE LIMITING STRAIN FOR THRUST EB
WITH 55 STEPPED SHELLS (AMMRC)



A P P E N D I X

```

1: $ THRUST EB WITH 55 STEPPED SHELLS AMMRC MODEL 1
2: SETUP,4,PREScriB,10
3: RUBBER,1,.688,-.4995
4: TITANIUM,2,.15E6, .3
5: TITANIUM,3,.15E6, .3
6: ALUMINIUM,4,.18E6, .33
7: END, MATERIAL
8: 1,1,3,2,.2,1,?95,1
9: 1.5,1.795,1.795,1.5
10: 0,0,.41,.41
11: 4,1,5,2
12: 2.261,2.550,2.550,2.261
13: 0,0,.2,.2
14: 5,1,6,2
15: 2.55,3.15,3.15,2.55
16: 0,0,.2,.2
17: 1,3,3,4,.2,1,?2,1
18: 1.5,1.795,1.795,1.5
19: .435,.435,.470,.470
20: 4,3,5,4
21: 2.261,2.550,2.550,2.261
22: 2.225,.225,.260,.260
23: 1,5,3,6,.2,1,?2,1
24: 1.5,1.795,1.795,1.5
25: .495,.495,.530,.530
26: 4,5,5,6
27: 2.261,2.550,2.550,2.261
28: 2.285,.285,.320,.320
29: 1,7,3,8,.2,1,?2,1
30: 1.5,1.795,1.795,1.5
31: .555,.555,.590,.590
32: 4,7,5,8
33: 2.261,2.550,2.550,2.261
34: .345,.345,.380,.380

```

35: 1, 9, 3, 18, 2, 1, 2, 1
 36: 1, 5, 1, 795, 1, 795, 1, 5
 37: 615, 615, 658, 658
 38: 4, 9, 5, 18
 39: 2, 261, 2, 550, 2, 550, 2, 261
 40: 4, 405, 405, 440, 440
 41: 1, 11, 3, 12, 2, 1, 2, 1
 42: 1, 5, 1, 795, 1, 795, 1, 5
 43: 675, 675, 710, 710
 44: 4, 11, 5, 12
 45: 2, 261, 2, 550, 2, 550, 2, 261
 46: 4, 465, 465, 500, 500
 47: 1, 13, 3, 14, 2, 1, 2, 1
 48: 1, 5, 1, 795, 1, 795, 1, 5
 49: 735, 735, 77, 77
 50: 4, 12, 5, 14
 51: 2, 261, 2, 550, 2, 550, 2, 261
 52: 525, 525, 560, 560
 53: 1, 14, 3, 70, 2, 1, 2, 1
 54: 1, 5, 1, 795, 1, 795, 1, 5
 55: 770, 770, 2, 450, 2, 450
 56: 4, 14, 5, 78
 57: 2, 261, 2, 550, 2, 550, 2, 261
 58: 56, 56, 2, 24, 2, 24
 59: 6, 30, 8, 64, 2, 1, 2, 1
 60: 1, 5, 1, 795, 1, 795, 1, 5
 61: 2, 45, 2, 45, 3, 47, 3, 47
 62: 9, 30, 18, 64
 63: 2, 261, 2, 550, 2, 550, 2, 261
 64: 2, 24, 2, 24, 3, 26, 3, 26
 65: 6, 65, 8, 66, 2, 1, 2, 1
 66: 1, 5, 1, 795, 1, 795, 1, 5
 67: 2, 5, 2, 5, 2, 535, 3, 535
 68: 9, 65, 18, 66

69:2.261,2.550,2.550,2.261
70:3.29,3.29,3.325,3.325
71:6,67,8,68,1,2,1,2,1
72:1.5,1.795,1.795,1.5
73:3.56,3.56,3.595,3.595
74:9,67,10,68
75:2.261,2.550,2.550,2.261
76:3.35,3.35,3.385,3.385
77:6,69,8,70,1,2,1,2,1
78:1.5,1.795,1.795,1.5
79:3.62,3.62,3.655,3.655
80:9,69,10,70
81:2.261,2.550,2.550,2.261
82:3.41,3.41,3.445,3.445
83:6,71,8,72,2,1,2,1
84:1.5,1.795,1.795,1.5
85:3.680,3.680,3.715,3.715
86:9,71,10,72
87:2.261,2.550,2.550,2.261
88:3.47,3.47,3.505,3.505
89:5,73,6,74
90:1.33,1.5,1.5,1.33
91:3.74,3.74,4.24,4.24
92:6,73,8,74,1,2,1,2,1
93:1.5,1.795,1.795,1.5
94:2.74,3.74,4.24,4.24
95:9,73,10,74
96:2.261,2.55,2.55,2.261
97:3.53,3.53,4.24,4.24
98:END,GRID
99:LOOP,5,1
100:GUARD,4,1,1
101:END
102:LOOP,4,1

103: BC, SLOPE, 1, 1, 1
104: IEND
105: JLOOP, 33, 2
106: ILOOP, 4, 1
107: QUAD, 1, 1, 2
108: IEHD
109: ILOOP, 4, 1
110: QUAD, 2, 1, 3
111: IEND
112: JEHD
113: ILOOP, 4, 1
114: QUAD, 1, 1, 68
115: IEHD
116: ILOOP, 4, 1
117: QUAD, 2, 1, 69, 2, 69, 7, 30, 6, 30
118: IEND
119: JLOOP, 21, 2
120: ILOOP, 4, 1
121: QUAD, 1, 6, 38
122: IEHD
123: ILOOP, 4, 1
124: QUAD, 2, 6, 31
125: IEHD
126: JEHD
127: ILOOP, 4, 1
128: QUAD, 1, 6, 72
129: IEHD
130: ILOOP, 5, 1
131: QUAD, 3, 5, 73
132: IEHD
133: ILOOP, 4, 1
135: BC, PRESSURE, 6, 73, 3, 5434
136: IEND, ELEMENTS
137: END, ELEMENTS

138:PLOT,ELEMENTS,1.08,-.25,3.4,4.49,10
139:AXISYM
140:STOP

1: \$ THRUST EB WITH 55 STEPPED SHELLS AMMRC MODEL 2
 2: SETUP,4,PREScriB,10
 3: RUBBER,1,600,-4995
 4: TITANM,2,15E6,.3
 5: TITANM,3,15E6,.3
 6: ALUMINM,4,10E6,.33
 7: END, MATERIAL
 8: 1,1,2,.2
 9: 1,5,1,795,1,795,1,5
 10: 0,0,.41,.41
 11: 3,1,5,2,4,886,1,4,886,1
 12: 2,261,2,550,2,550,2,261
 13: 0,0,.2,.2
 14: 5,1,6,2
 15: 2,55,3,15,3,15,2,55
 16: 6,6,.2,.2
 17: 1,3,2,4
 18: 1,5,1,795,1,795,1,5
 19: 4,35,.435,.470,.470
 20: 3,3,5,4,4,886,1,4,886,1
 21: 2,261,2,550,2,550,2,261
 22: 2,25,.225,.260,.260
 23: 1,5,2,6
 24: 1,5,1,795,1,795,1,5
 25: 4,95,.495,.530,.530
 26: 3,5,5,6,4,886,1,4,886,1
 27: 2,261,2,550,2,550,2,261
 28: 2,85,.285,.320,.320
 29: 1,7,2,8
 30: 1,5,1,795,1,795,1,5
 31: 5,55,.555,.590,.590
 32: 7,5,8,4,886,1,4,886,1
 33: 2,261,2,550,2,550,2,261
 34: 345,.345,.380,.380

35: 1, 9, 2, 10
36: 1, 5, 1, 795, 1, 795, 1, 5
37: 3, 615, 615, 650, 650
38: 3, 9, 5, 10, 4, 886, 1, 4, 886, 1
39: 2, 261, 2, 550, 2, 550, 2, 261
40: 405, 405, 440, 440
41: 1, 11, 2, 12
42: 1, 5, 1, 795, 1, 795, 1, 5
43: 675, 675, 710, 710
44: 3, 11, 5, 12, 4, 886, 1, 4, 886, 1
45: 2, 261, 2, 550, 2, 550, 2, 261
46: 465, 465, 500, 500
47: 1, 13, 2, 14
48: 1, 5, 1, 795, 1, 795, 1, 5
49: 735, 735, 77, 77
50: 3, 13, 5, 14, 4, 886, 1, 4, 886, 1
51: 2, 261, 2, 550, 2, 550, 2, 261
52: 525, 525, 560, 560
53: 1, 14, 2, 78
54: 1, 5, 1, 795, 1, 795, 1, 5
55: 770, 770, 2, 450, 2, 450
56: 2, 14, 5, 78, 4, 886, 1, 4, 886, 1
57: 2, 261, 2, 550, 2, 550, 2, 261
58: 56, 56, 2, 24, 2, 24
59: 6, 38, 7, 64
60: 1, 5, 1, 795, 1, 795, 1, 5
61: 2, 45, 2, 45, 3, 47, 3, 47
62: 8, 30, 10, 64, 4, 886, 1, 4, 886, 1
63: 2, 261, 2, 550, 2, 550, 2, 261
64: 2, 24, 2, 24, 3, 26, 3, 26
65: 6, 65, 7, 66
66: 1, 5, 1, 795, 1, 795, 1, 5
67: 3, 5, 3, 5, 3, 535, 3, 535
68: 8, 65, 10, 66, 4, 886, 1, 4, 886, 1

69: 2.261, 2.550, 3.325, 3.325
 70: 3.29, 3.29, 3.325, 3.325
 71: 6.67, 7.68
 72: 1.5, 1.795, 1.795, 1.5
 73: 3.56, 3.56, 3.595, 3.595
 74: 8.67, 10.68, 4.886, 1.4.886, 1
 75: 2.261, 2.550, 2.550, 2.261
 76: 3.35, 3.35, 3.385, 3.385
 77: 6.69, 7.70
 78: 1.5, 1.795, 1.795, 1.5
 79: 3.62, 3.62, 3.655, 3.655
 80: 8.69, 10.70, 4.886, 1.4.886, 1
 81: 2.261, 2.550, 2.550, 2.261
 82: 3.41, 3.41, 3.445, 3.445
 83: 6.71, 7.72
 84: 1.5, 1.795, 1.795, 1.5
 85: 3.680, 3.680, 3.715, 3.715
 86: 8.71, 10.72, 4.886, 1.4.886, 1
 87: 2.261, 2.550, 2.550, 2.261
 88: 3.47, 3.47, 3.505, 3.505
 89: 5.73, 6.74
 90: 1.33, 1.5, 1.5, 1.33
 91: 3.74, 3.74, 4.24, 4.24
 92: 6.73, 7.74
 93: 1.5, 1.795, 1.795, 1.5
 94: 3.74, 3.74, 4.24, 4.24
 95: 8.73, 10.74, 4.886, 1.4.886, 1
 96: 2.261, 2.55, 2.55, 2.261
 97: 3.53, 3.53, 4.24, 4.24
 98: END, GRID
 99: ILOOP, 5, 1
 100: QUD, 4, 1, 1
 101: IEHD
 102: ILOOP, 4, 1

103: BC, SLOPE, 1, 1, 1
104: IEND
105: JLOOP, 33, 2
106: ILOOP, 4, 1
107: QUAD, 1, 1, 2
108: IEND
109: ILOOP, 4, 1
110: QUAD, 2, 1, 3
111: IEND
112: JEHD
113: ILOOP, 4, 1
114: QUAD, 1, 1, 68
115: IEND
116: ILOOP, 4, 1
117: QUAD, 2, 1, 69, 2, 69, 7, 30, 6, 30
118: IEND
119: JLOOP, 21, 2
120: ILOOP, 4, 1
121: QUAD, 1, 6, 30
122: IEHD
123: ILOOP, 4, 1
124: QUAD, 2, 6, 31
125: IEHD
126: JEHD
127: ILOOP, 4, 1
128: QUAD, 1, 6, 72
129: IEHD
130: ILOOP, 5, 1
131: QUAD, 3, 5, 73
132: IEHD
133: ILOOP, 4, 1
134: BC, PRESSURE, 6, 73, 3, 5434
135: IEHD
136: EHD, ELEMENTS

137:PLOT,ELEMENTS,1.08,-.25,3.4,4.49,10
138:AXISYM
139:STOP

SECTION 7.

ANALYSIS OF THE SHELL STRESSES IN AN ALTERNATE
BLACKHAWK MAIN ROTOR THRUST BEARING

The stress in the metal shells of an alternate Blackhawk main rotor thrust bearing (see SK4-80 9590 in Fig. 1) will be analyzed in this section. This analysis can be accomplished with a single finite element problem run without the use of superposition.

The analysis of this thrust bearing begins with the model shown in Figure 2. Even with the coarse modeling technique previously developed, computational limits on the number of available elements prevent a generous representation of the shell radii at the center of the shell where the peak stress occurs. This limitation also restricts the number of shells modeled to 35 -- the real bearing has 52. A small element (see the enlarged view in Figure 3.) is used to check the stress at the transition point in this model. Figure 4 shows the stress that results in this element for a 68,000 pound thrust load.

As a result of the nice plateau on the previous result, the number of shells was further reduced to 17 to study the effect of length on shell stress. The model is shown in Figure 5, a blowup in Figure 6 and the results in Figure 7. The model shown in Figure 8 again has 17 shells but, has a good representation of the center radius. The stress values are shown in Figure 9.

The similarity of Figure 7 and Figure 9 would indicate

that the crude radius representation is giving useful results. The increase in peak stress from Figure 7 to Figure 4, representing an increase from 17 to 35 shells, would suggest an estimate of 115 ksi for the peak stress in the real bearing with 52 shells. In the interest of weight reduction it is intended that the shells for the test bearing be made of A-70 C.P. Titanium. The stress results from the application of the C.F. load should be nonreversing and, hence, it is anticipated that the first loading cycle will locally yield the 70 ksi yield strength titanium so that the stress for subsequent cycles might be considered to be 12.5 ± 57.5 ksi. Fatigue failure of this part is, therefore, predicted at a reasonably low number of cycles. In service the loading spectrum is somewhat more complicated but, the total number of cycles expected is less than 20,000.

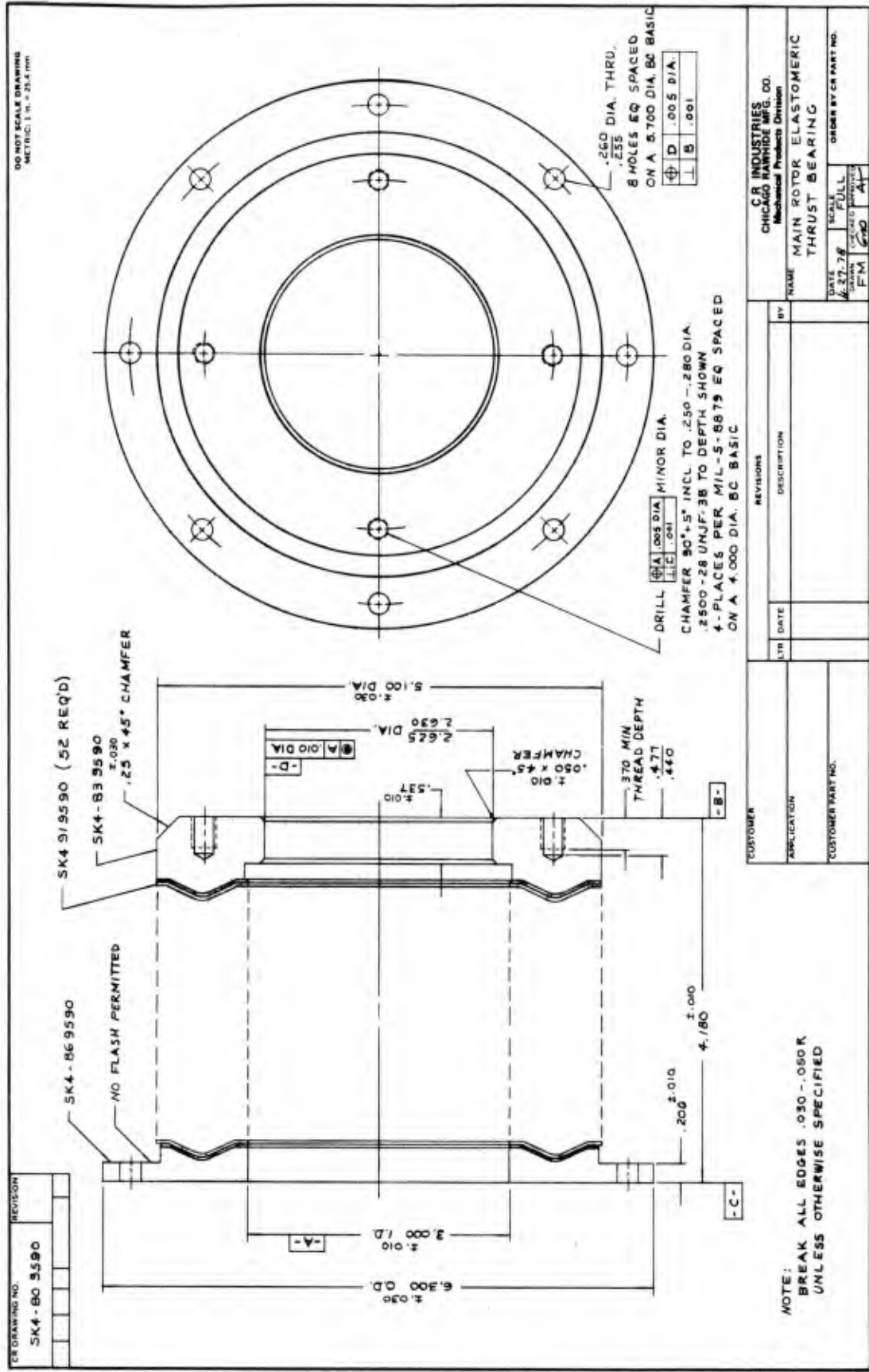


FIG. 1

METAL FATIGUE THRUST EB AMMRC MODEL 1

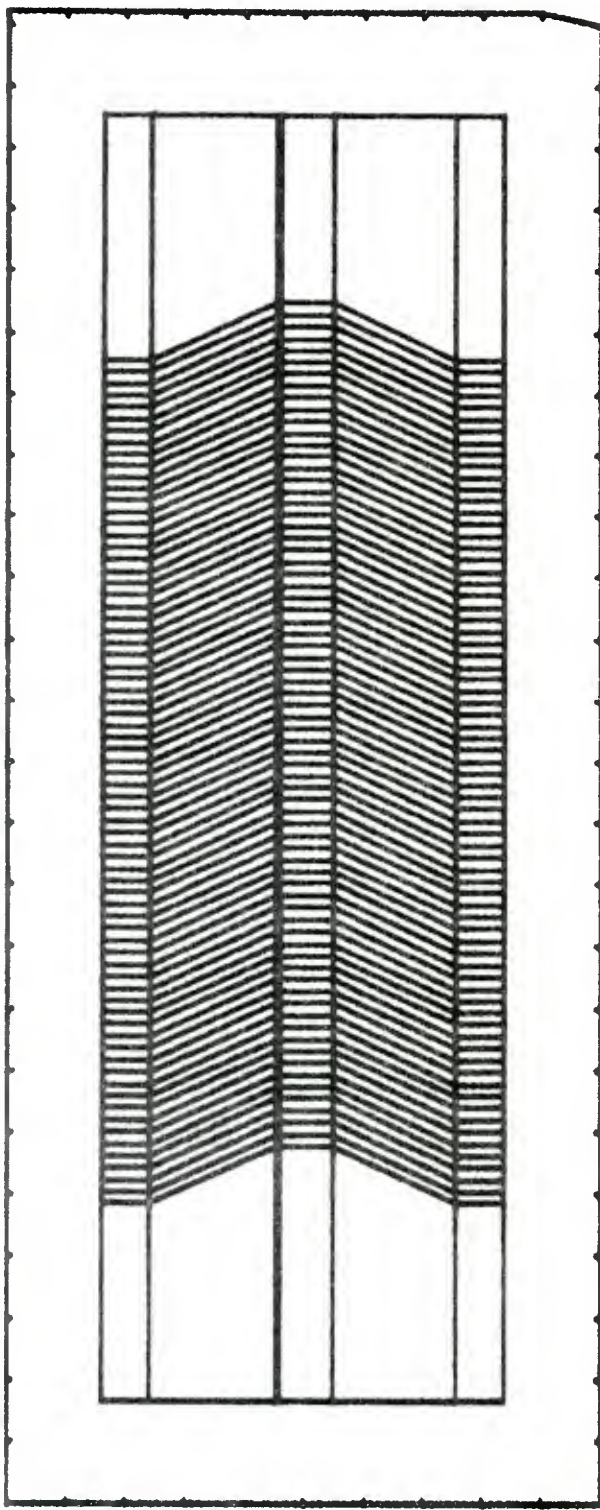
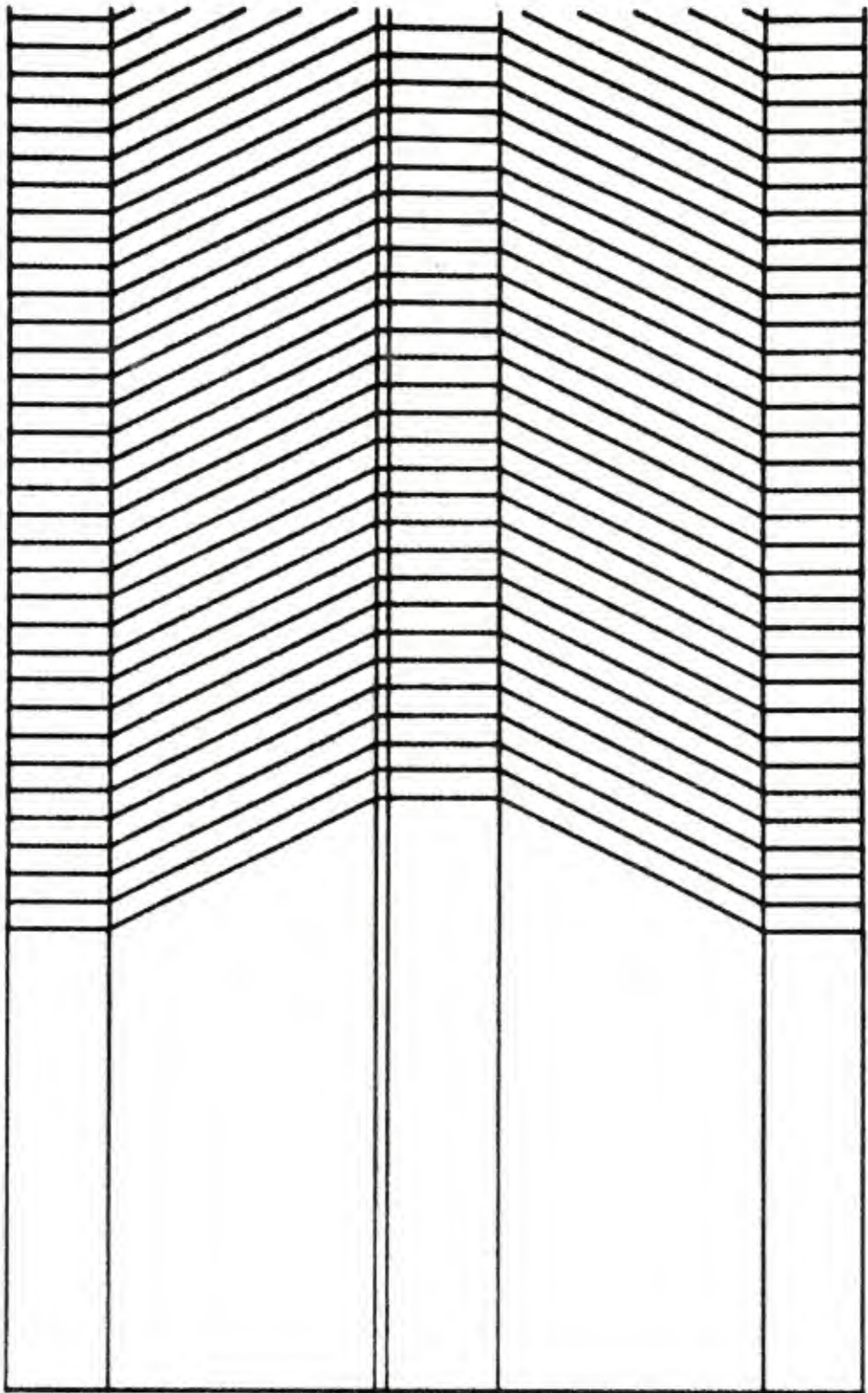


FIG. 2



BLOW UP OF FIG. 2

FIG. 3

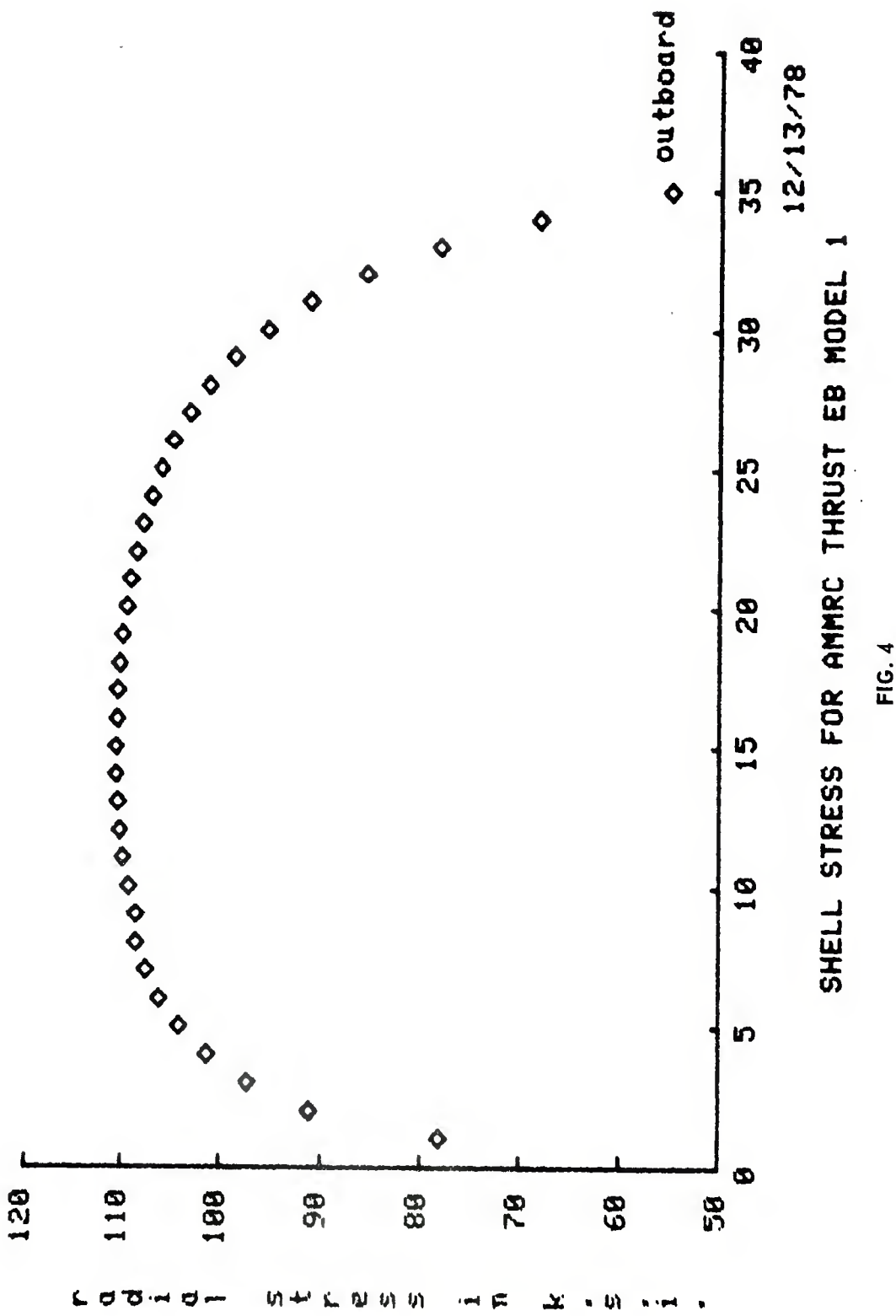


FIG. 4

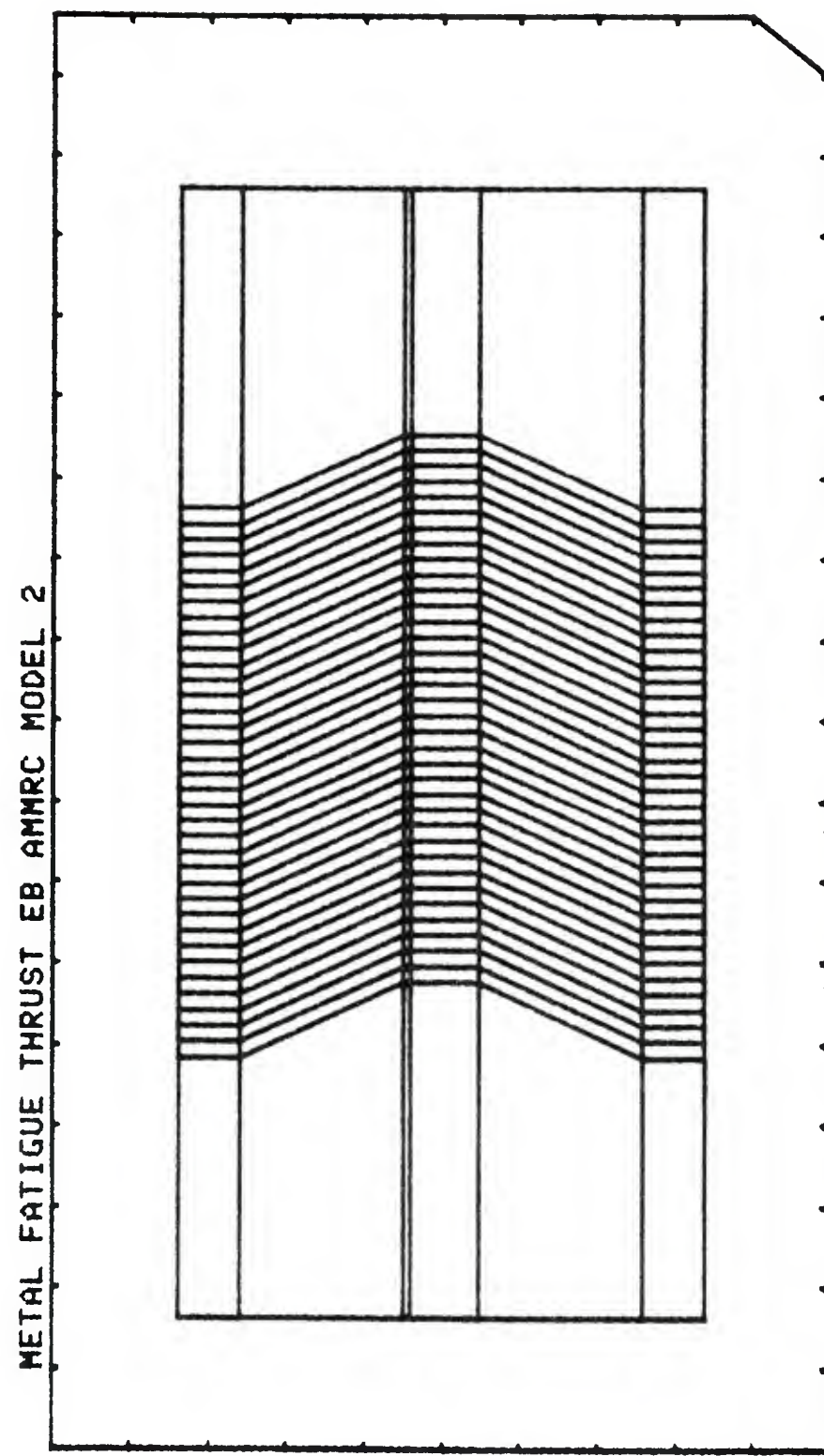
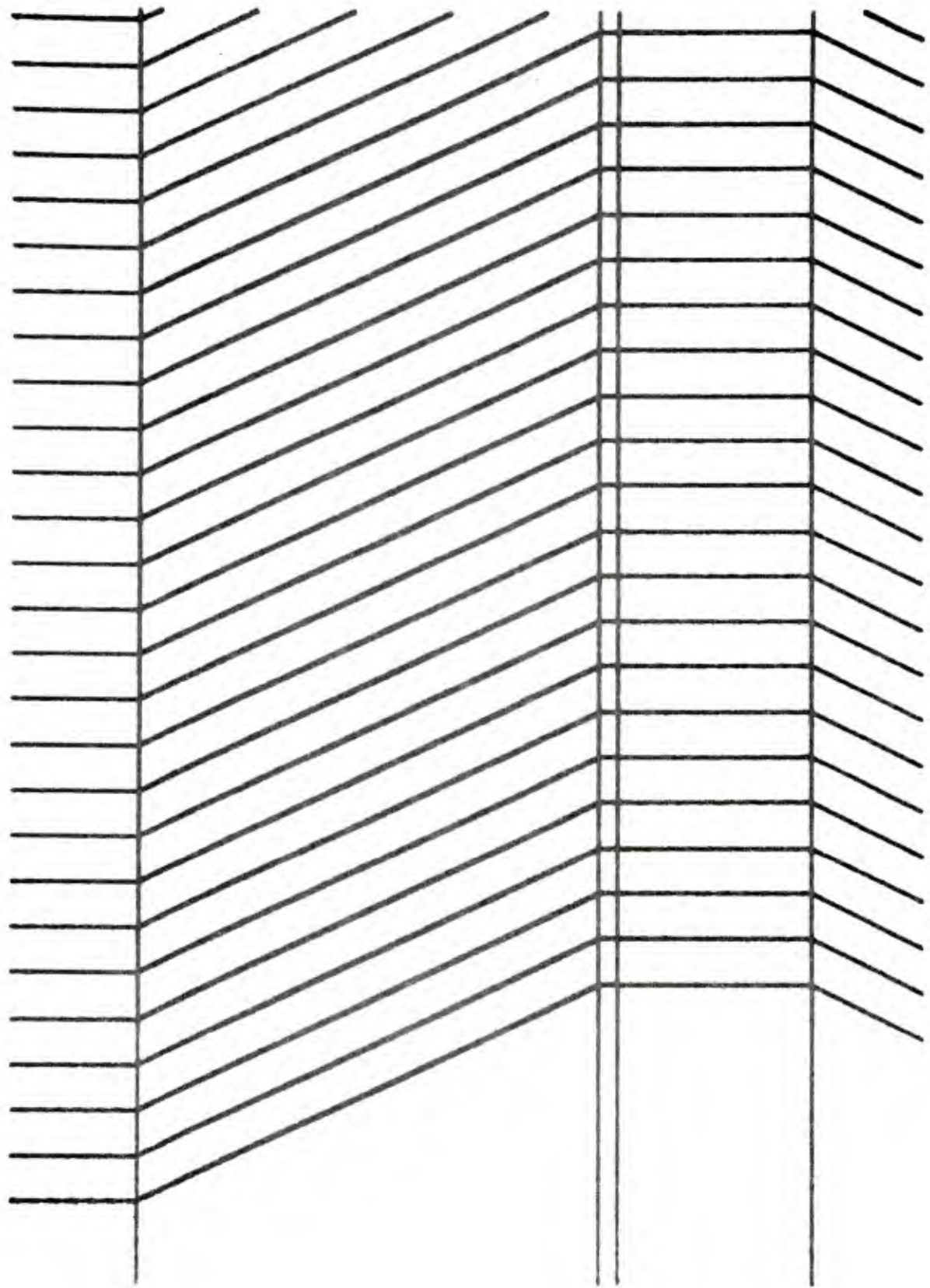
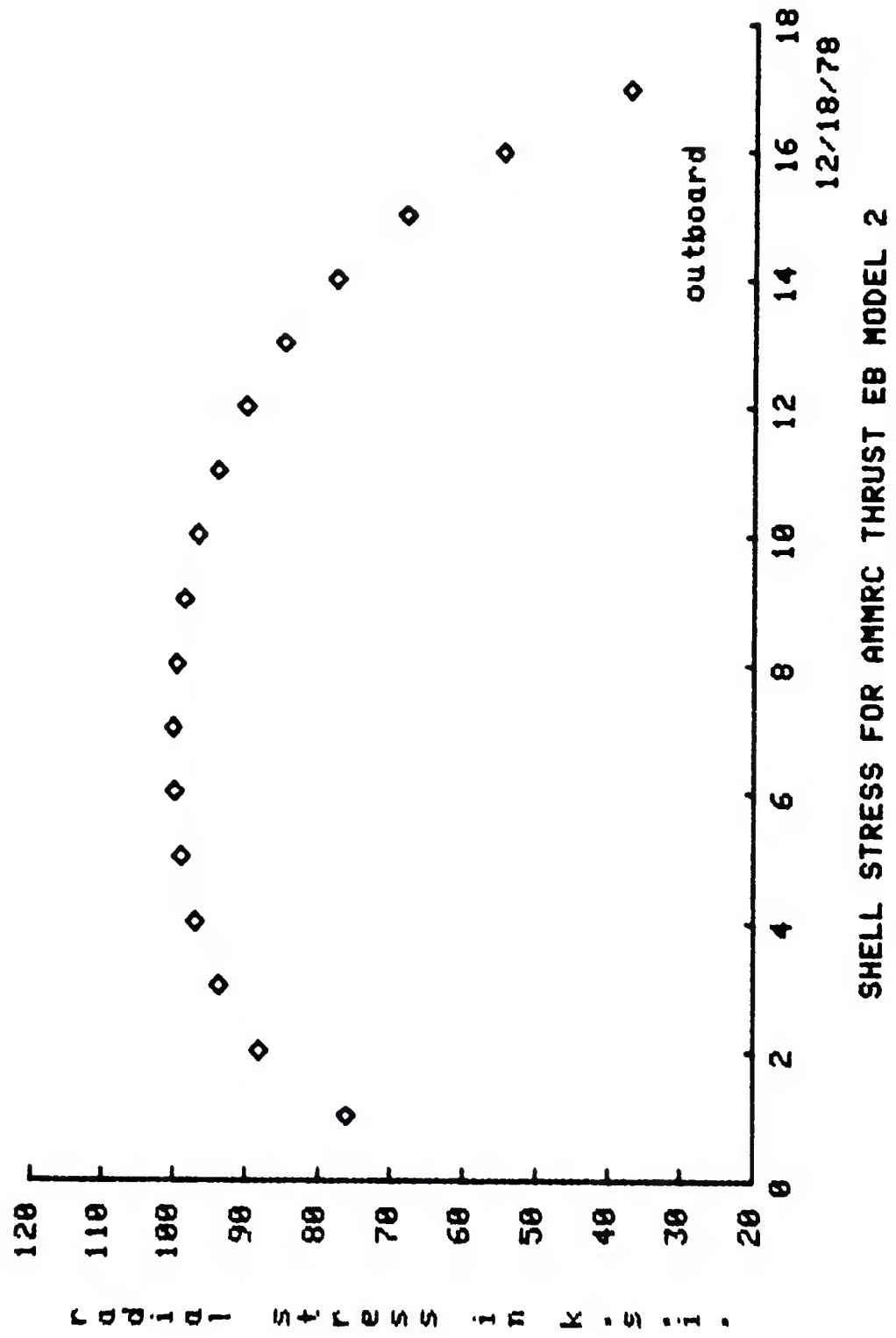


FIG. 5



BLOW UP OF FIG. 5

FIG. 6



METAL FATIGUE THRUST EB AMRC MODEL 3

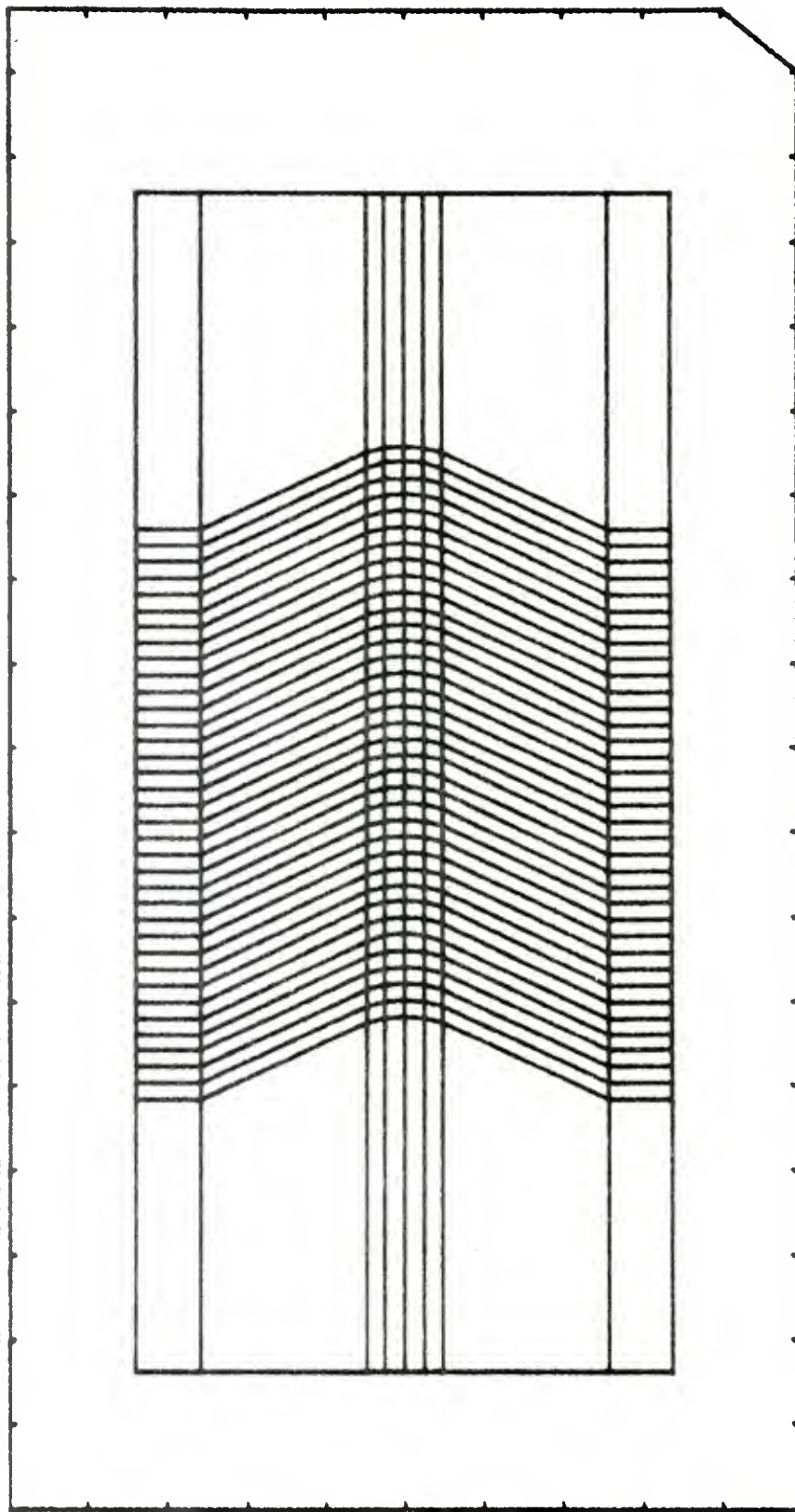


FIG. 8

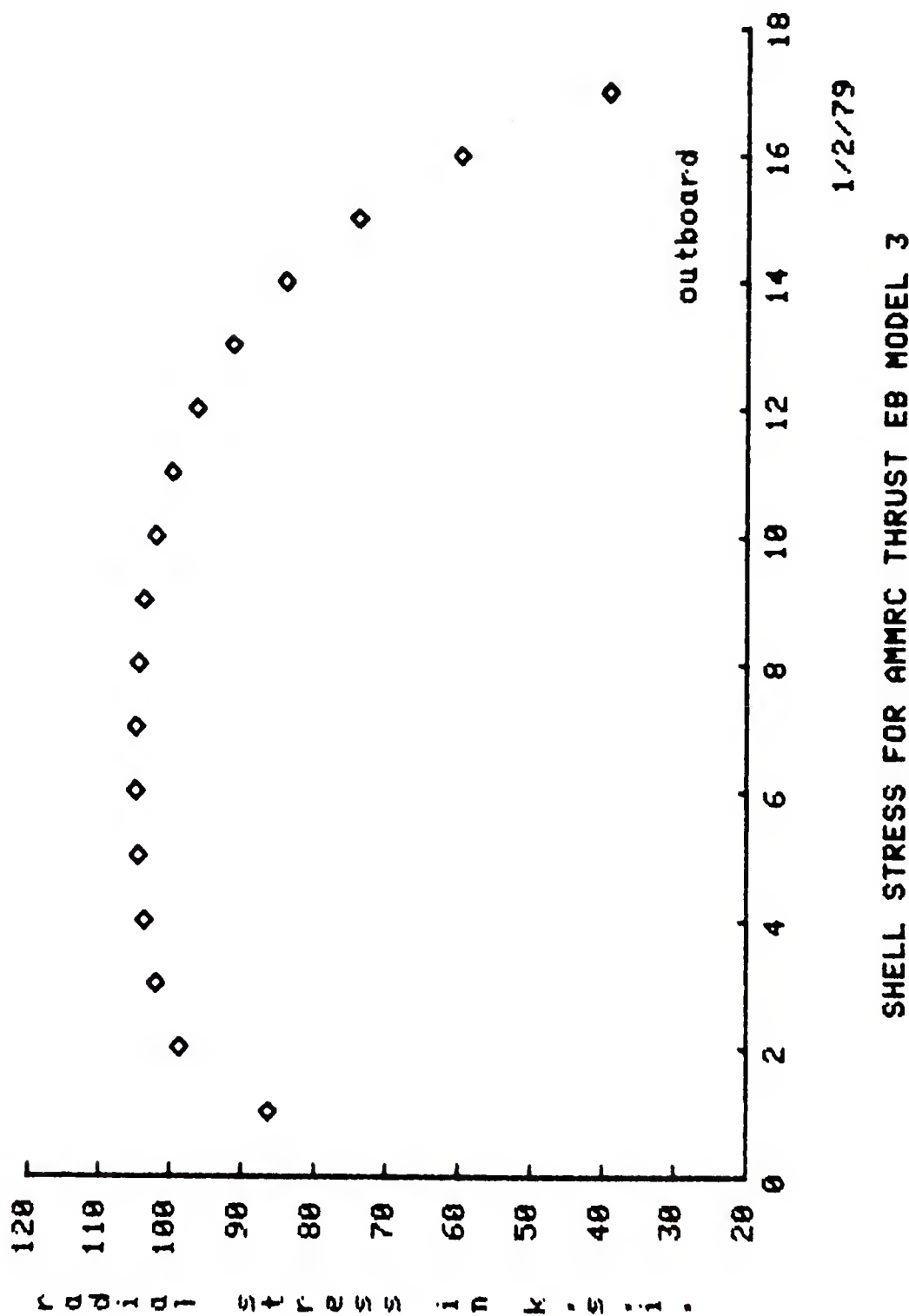


FIG. 9

A P P E N D I X I

1:\$ METAL FATIGUE THRUST EB AMMRC MODEL 1
2:\$ SETUP,4,
3:\$ RUBBER,1,600,.4995
4:\$ STEEL,2,30E6,.3
5:\$ TITAN,3,15E6,.3
6:\$ END, MATERIAL
7:1,1,2,2
8:1.5,1.625,1.625,1.5
9:0,0,.5,.5
10:3,1.5,2,1,1,1,1
11:1.95,2,1,2,1,1.95
12:0,0,.644,.644
13:6,1,7,2
14:2.425,2.55,2.55,2.425
15:0,0,.5,.5
16:1,2,2,73
17:1.5,1.625,1.625,1.5
18:1.5,.5,2.63,2.62
19:3,2,5,73,.1,1,1,1
20:1.95,2,1,2,1,1.95
21:1.644,.644,2.774,2.774
22:6,2,7,73
23:2.425,2.55,2.55,2.425
24:1.5,.5,2.63,2.63
25:1,73,2,74
26:1.5,1.625,1.625,1.5
27:2.63,2.63,3.25,3.25
28:3,73,5,74,.1,1,1,1
29:1.95,2,1,2,1,1.95
30:2.774,2.774,3.25,3.25

31: 6, 73, 7, 74
32: 2, 425, 2, 55, 2, 55, 2, 425
33: 2, 63, 2, 63, 3, 25, 3, 25
34: END, GRID
35: ILOOP, 6, 1
36: QUAD, 3, 1, 1
37: QUAD, 1, 1, 2
38: JLOOP, 35, 2
39: QUAD, 2, 1, 3
40: QUAD, 1, 1, 4
41: JEHD
42: QUAD, 3, 1, 73
43: IEND
44: ILOOP, 6, 1
45: BC, SLOPE, 1, 1, 1
46: BC, PRESSURE, 1, 73, 3, 5434
47: IEND
48: END, ELEMENTS
49: PLOT, ELEMENTS, 1, 25, -, 25, 2, 8, 3, 5, 10
50: AXISYN
51: STOP

A P P E N D I X II

1:\$ METAL FATIGUE THRUST EB AMMRC MODEL 2
2:SETUP,4,?
3:RUBBER,1,600,.4995
4:STEEL,2,30E6,.3
5:TITANW,3,15E6,.3
6:END, MATERIAL
7:1,1,2,2
8:1,5,1,625,1,625,1,5
9:0,0,.5,.5
10:3,1,5,2,1,1,1,1
11:1,95,2,1,2,1,1,95
12:0,0,-644,-644
13:6,1,7,2
14:2,425,2,55,2,425
15:0,0,.5,.5
16:1,2,2,3?
17:1,5,1,625,1,625,1,5
18:5,5,1,55,1,55
19:3,2,5,37,1,1,1,1
20:1,95,2,1,2,1,1,95
21:-644,-644,1,694,1,694
22:6,2,7,37
23:2,425,2,55,2,425
24:5,5,1,55,1,55
25:1,37,2,38
26:1,5,1,625,1,625,1,5
27:1,55,1,55,2,17,2,17
28:3,37,5,38,1,1,1,1
29:1,95,2,1,2,1,1,95
30:1,694,1,694,2,170,2,170
31:6,37,7,38
32:2,425,2,55,2,425
33:1,55,1,55,2,17,2,17
34:END,GRID

35: ILOOP,6,1
36: QUAD,3,1,1
37: QUAD,1,1,2
38: JLOOP,17,2
39: QUAD,2,1,3
40: QUAD,1,1,4
41: JEHD
42: QUAD,3,1,37
43: IEND
44: ILOOP,6,1
45: BC,SLOPE,1,1,1
46: BC,PRESSURE,1,37,3,5434
47: IEND
48: END,ELEMENTS
49: PLOT,ELEMENTS,1,.25,-.25,2.8,2.5,10
50: AXISYM
51: STOP

A P P E N D I X III

```

1: $ METAL FATIGUE THRUST EB AMMRC MODEL 3
2: SETUP,4,10
3: RUBBER,1,600,.4995
4: STEEL,2,30E6,.3
5: TITANM,3,15E6,.3
6: END, MATERIAL
7: 1,1,2,2
8: 1,5,1,625,1,625,1,5
9: 0,0,.5,.5
10: 3,1,4,2
11: 1,95,1,9875,1,9875,1,95
12: 0,0,.6527,.644
13: 5,1,5,2
14: 2,025,2,025,2,025,2,025
15: 0,0,.6555,.6555
16: 6,1,7,2
17: 2,0625,2,1,2,1,2,0625
18: 0,0,.644,.6527
19: 8,1,9,2
20: 2,425,2,55,2,55,2,425
21: 0,0,.5,.5
22: 1,2,2,3?
23: 1,5,1,625,1,625,1,55
24: .5,.5,1,55,1,55
25: 3,2,4,37
26: 1,95,1,9875,1,9875,1,95
27: 644,.6527,1,7027,1,694
28: 5,2,5,37
29: 2,025,2,025,2,025,2,025
30: .655,.655,1,7055,1,7055
31: 6,2,7,37
32: 2,0625,2,1,2,1,2,0625
33: .6527,.644,1,694,1,7027

```

```

34: 8, 2, 9, 37
35: 2, 425, 2, 55, 2, 55, 2, 425
36: .5, 5, 1, 55, 1, 55
37: 1, 37, 2, 38
38: 1, 5, 1, 625, 1, 625, 1, 5
39: 1, 55, 1, 55, 2, 17, 2, 17
40: 3, 37, 4, 38
41: 1, 95, 1, 9875, 1, 9875, 1, 95
42: 1, 694, 1, 7627, 2, 17, 2, 17
43: 5, 37, 5, 38
44: 2, 825, 2, 825, 2, 825, 2, 825
45: 1, 7055, 1, 7055, 2, 17, 2, 17
46: 6, 37, 7, 38
47: 2, 8625, 2, 1, 2, 1, 2, 8625
48: 1, 7627, 1, 694, 2, 17, 2, 17
49: 8, 37, 9, 38
50: 2, 425, 2, 55, 2, 55, 2, 425
51: 1, 55, 1, 55, 2, 17, 2, 17
52: END, GRID
53: ILOOP, 8, 1
54: GUAD, 3, 1, 1
55: GUAD, 1, 1, 2
56: JLOOP, 17, 2
57: GUAD, 2, 1, 3
58: GUAD, 1, 1, 4
59: JEHD
60: GUAD, 3, 1, 37
61: IEHD
62: ILOOP, 8, 1
63: BC, SLOPE, 1, 1, 1
64: BC, PRESSURE, 1, 37, 3, 5434
65: IEHD
66: END, ELEMENTS

```

67:PLOT,ELEMENTS,1.25,-.25,2.8,2.5,10
68:AXISM
69:STOP

SECTION 8.

ANALYSIS OF THE BLACKHAWK MAIN ROTOR SPHERICAL BEARING

The subject covered in this section is an analysis of the elastomer strain in the Blackhawk main rotor spherical elastomeric bearing (see Figure 1) and a prediction of the life of this bearing. It is suggested that the two sections, covering finite element analysis and determining the life of elastomeric parts based on strain, be reviewed.

The model for the spherical bearing is shown in Figure 2 and an enlargement in Figure 3. A listing of the input program is shown in Appendix I. In order to generate the nodal data for this program a mesh generator program was written in Basic language for our Tektronix 4051 mini-computer. This program is included in Appendix II.

The strain resulting from a 68,000 pound axial C.F. load is shown for the I.D. in Figure 4 and for the O.D. in Figure 5. At the 6 and 12 o'clock positions the strain for an out-of-plane load of 1,292 pounds is shown in Figure 6 for the I.D. and Figure 7 for the O.D.. For this load at the 3 and 9 o'clock positions the strain at the I.D. is shown in Figure 8 and for the O.D. in Figure 9. The strain at the 6 and 12 o'clock position for a 1 degree flapping cock is shown in Figure 10 for the I.D. and Figure 11 for the O.D. The 3 and 9 o'clock strains are shown in Figures 12 and 13.

The strain due to pitch change may be calculated directly from first principals. The relationships are derived in Appendix III and a Basic language computer program is listed in Appendix IV. The calculated I.D. strain for 1 degree of pitch change rotation is given in Figure 14. The finite element solution is shown in Figure 15. It can be seen that at the I.D. the agreement is very good. At the O.D. there is an approximate 10% difference. The O.D. finite element results are given in Figure 16. The spherical and the thrust bearing share the total pitch change motion.

Spring rate of the spherical bearing 1000 in-lbs./degree.

Spring rate of the thrust bearing 120 in-lbs./degree.

$$\left(\frac{120}{1000 + 120} \right) 100 = 10.7\% \text{ of the pitch change for the spherical bearing.}$$

The following is a sample calculation of the life limiting strain for the 6 and 12 o'clock position on the I.D. of the fourth layer:

The vibratory strain vectors due to flap ($\pm \theta_x$), inplane load ($\pm v_c$) and vibratory out-of-plane load ($\pm v_n$) are all in the same direction and phase. The strain magnitudes are, therefore, directly additive.

$$\gamma_{v_1} = 3.58 * 0.0803 + 2.984 * \left(\frac{315}{68000} \right) + 0.0777$$

$$\gamma_{v_1} = 0.379$$

Note: Pitch change strain did not enter the above calculation because it is 90° out of phase in both geometry and time but, its Miner's Rule effect will be considered in the following vector:

$$\gamma_{v_2} = 0.0385 * 6.54 * 0.107 = 0.0269$$

The life limiting strain is (see Appendix of Section 3)

$$\gamma = \sqrt[5]{\frac{258 * 60 \left[\gamma_{v_1}^5 + \gamma_{v_2}^5 \right] + \left(\frac{\gamma_{cf}}{2} * \frac{82000}{68000} \right)^5 + 2 * \left(\frac{\gamma_{cf}}{2} \right)^5}{258 * 60 + 1 + 2}}$$

$$\gamma = \sqrt[5]{\frac{258 * 60 (.379^5 + .0269^5) + \left(\frac{2.984 * 82000}{2 * 68000} \right)^5 + 2 * \left(\frac{2.984}{2} \right)^5}{258 * 60 + 3}}$$

$$\gamma = 0.398$$

Note: lead-lag motion causes negligible damage at this location.

A plot of life limiting strain for the 6 and 12 o'clock position of each layer is given in Figure 17.

The following is a sample calculation of the life limiting strain for the 6 or 12 o'clock position on the O.D. of the fourth layer:

The vibratory strain vectors due to flap ($\pm \theta_x$), inplane load ($\pm v_c$) and vibratory out-of-plane load ($\pm v_n$) are all in the same direction and phase. The strain magnitudes are, therefore, directly additive.

$$\gamma_{v_1} = 3.58 * 0.0761 + 1,652 * \left(\frac{315}{68000} \right) + 0.0709$$

$$\gamma_{v_1} = 0.351$$

Note: Pitch change strain did not enter the above calculation because it is 90° out of phase in both geometry and time but, its Miner's Rule effect will be considered in the following vector:

$$\gamma_{v_2} = 0.05077 * 6.54 * 0.107 = 0.0355$$

The life limiting strain is

$$\gamma = \sqrt[5]{\frac{258 * 60 \left[\gamma_{v_1}^5 + \gamma_{v_2}^5 \right] + \left(\frac{\gamma_{cf}}{2} * \frac{82000}{68000} \right)^5 + 2 * \left(\frac{\gamma_{cf}}{2} \right)^5}{258 * 60 + 1 + 2}}$$

$$\gamma = \sqrt[5]{\frac{258 * 60 (.351^5 + .0355^5) + \left(\frac{1.652}{2} * \frac{82000}{68000} \right)^5 + 2 * \left(\frac{1.652}{2} \right)^5}{258 * 60 + 3}}$$

$$\gamma = 0.352$$

Note: Lead-lag motion causes negligible damage at this location.

This life limiting strain is plotted for all layers in Figure 18.

The following is a sample calculation of the life limiting strain for the 3 and 9 o'clock position on the I.D. of the fourth layer:

The strain due to blade flapping is

$$\gamma_f = 3.58 * 0.0581 = 0.207$$

The strain due to vibratory C.F. is

$$\gamma_{cf} = \left(\frac{2.984}{2}\right) * \left(\frac{315}{68000}\right) = 0.0069$$

The strain due to lead-lag motion is

$$\gamma_{ll} = 1.5 * 0.0803 = 0.120$$

The strain due to pitch change is

$$\gamma_{pc} = 0.0385 * 6.54 * 0.107 = 0.0269$$

These strains can be combined as shown in the following table;

STRAIN	TIME PHASE	DIRECTION	MAGNITUDE
γ_{pc}	0°	0°	0.0269
γ_{11}	0°	90°	0.120
In-phase resultant*	0°	90°	0.123
γ_f	90°	90°	0.207
γ_{cf}	90°	90°	0.0069
Out-of-phase resultant*	90°	90°	0.214

* Conventional vector combination

The resulting effective strain is

$$\gamma = \sqrt{(0.214)^2 + (0.123)^2} = 0.247$$

Note: in the general case of non-perpendicular phase resultants obtaining this effective strain vector is more complicated.

The life limiting strain is

$$\gamma = \sqrt[5]{\frac{258*60(0.247^5) + \left(\frac{2.984*82000}{68000}\right)^5 + 2*\left(\frac{2.984}{2}\right)^5}{258*60 + 3}}$$

$$\gamma = .315$$

A plot of the life limiting strain for this location on all the shells is given in Figure 19. A plot for the O.D. is given in Figure 20.

On the basis of this analysis, first damage is predicted at

$$\text{LIFE} = \left(\frac{10.6}{0.398} \right)^{\frac{5}{3}} \quad 60 * 258$$
$$= 866 \text{ HR.}$$

The predicted location for first damage is the I.D. of the fourth layer. This location for first damage agrees with previous test results.

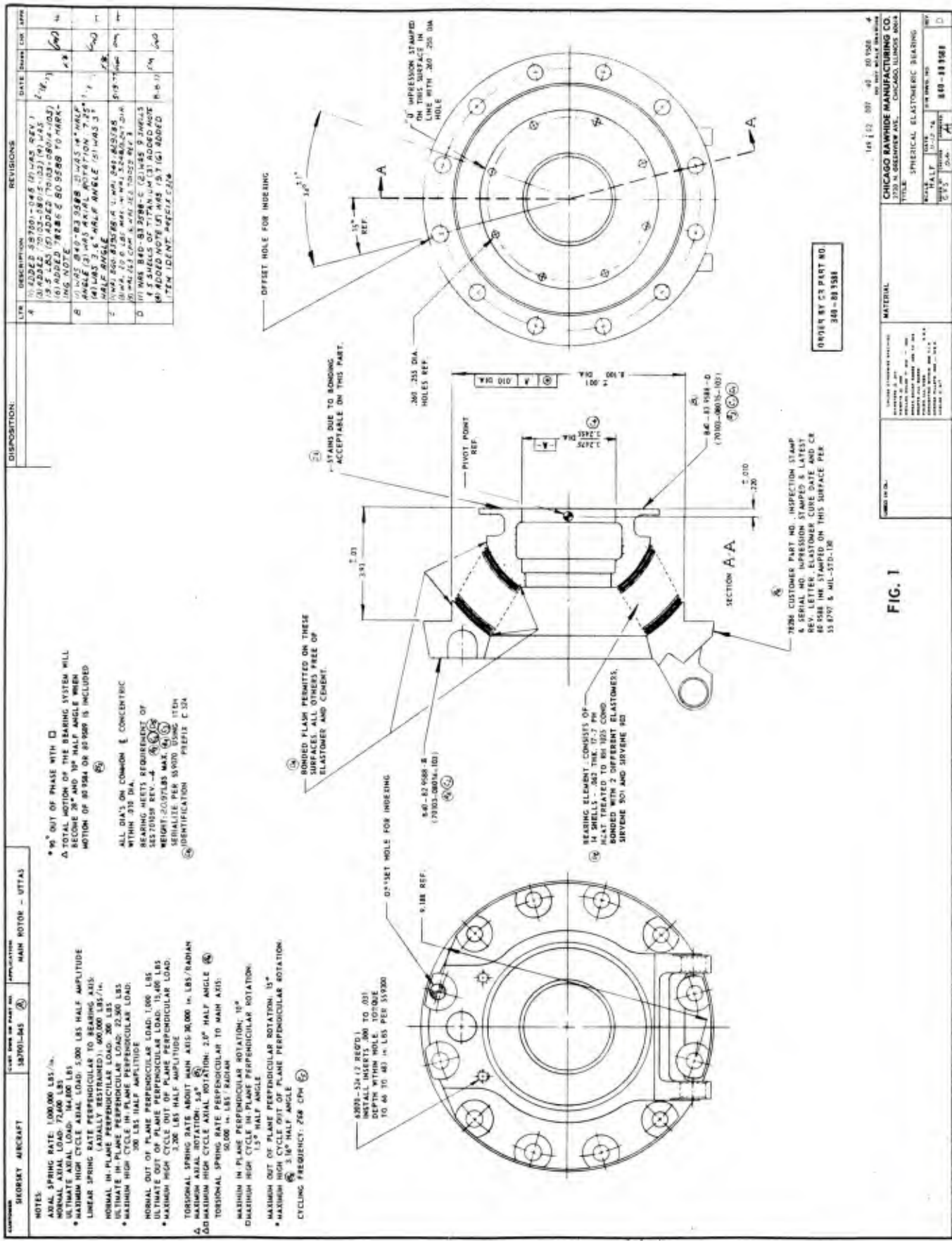


FIG. 1

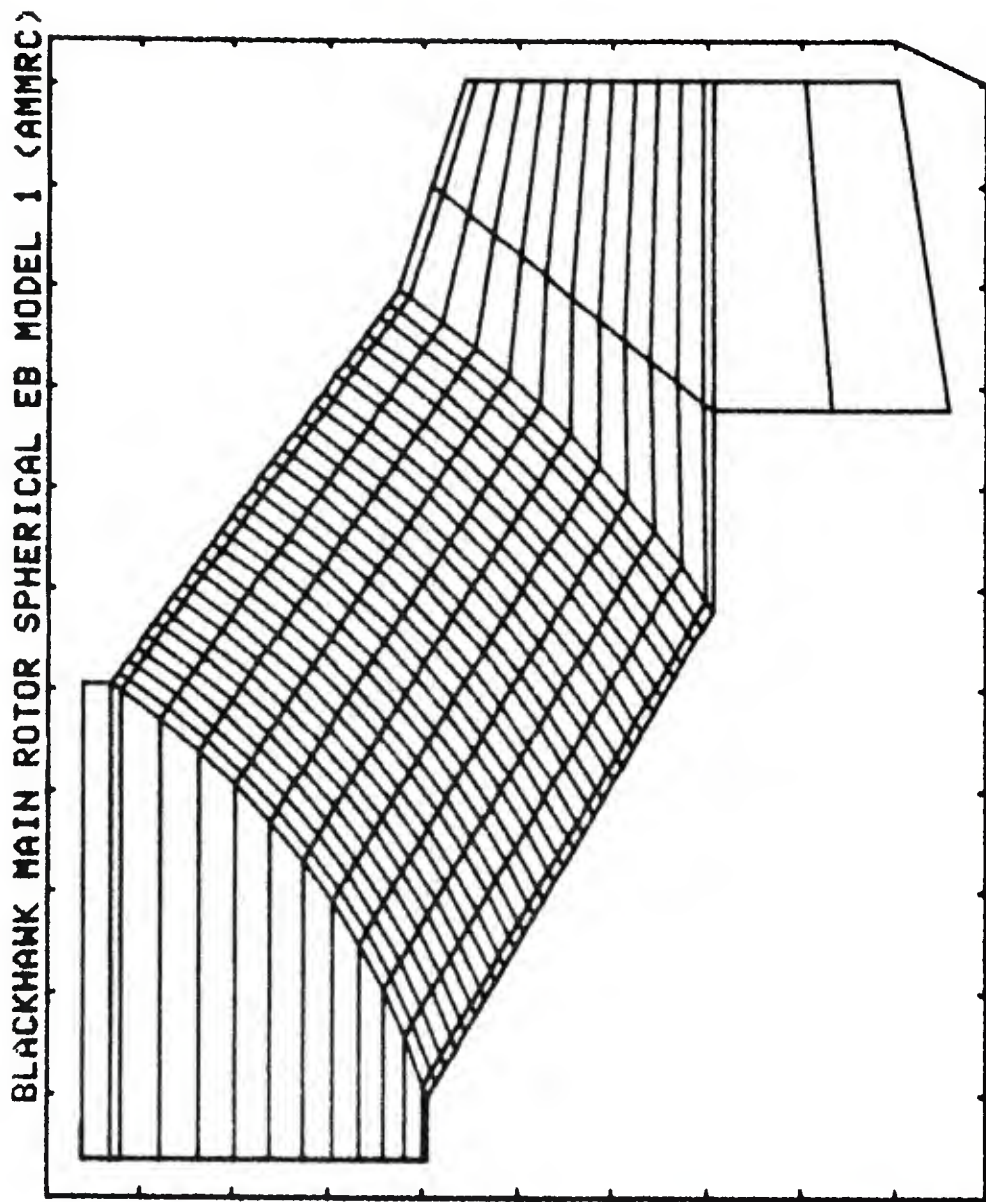
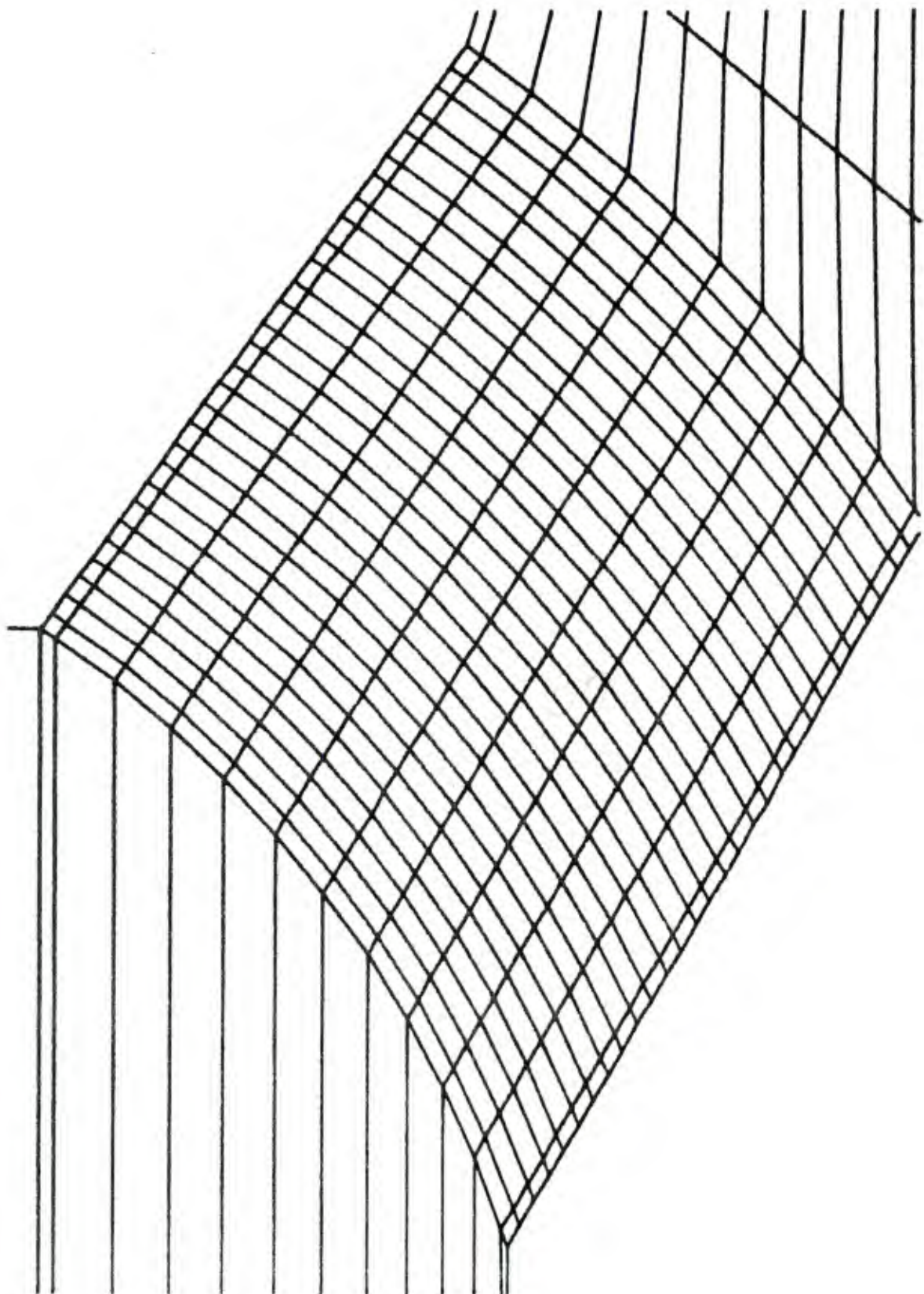
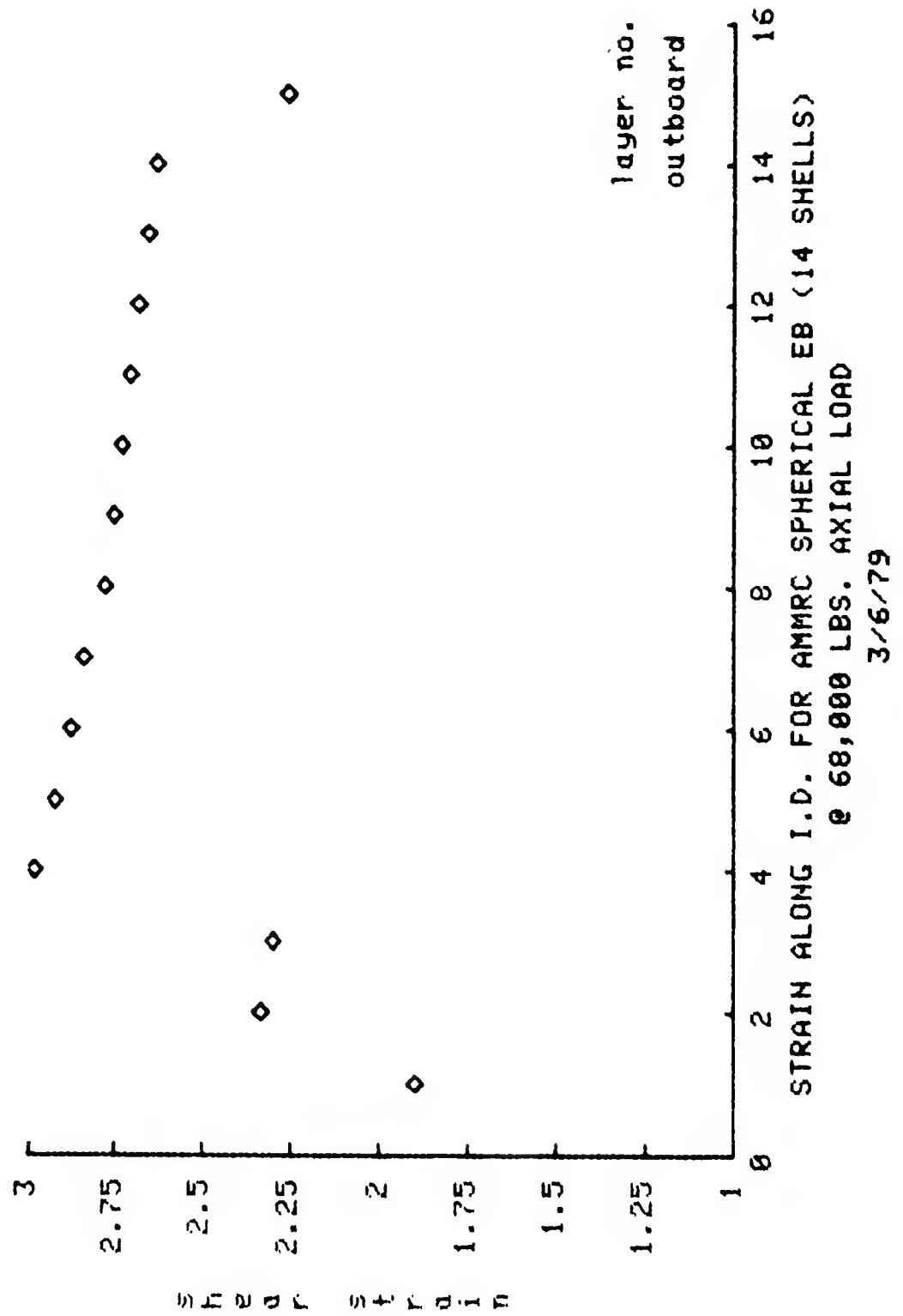


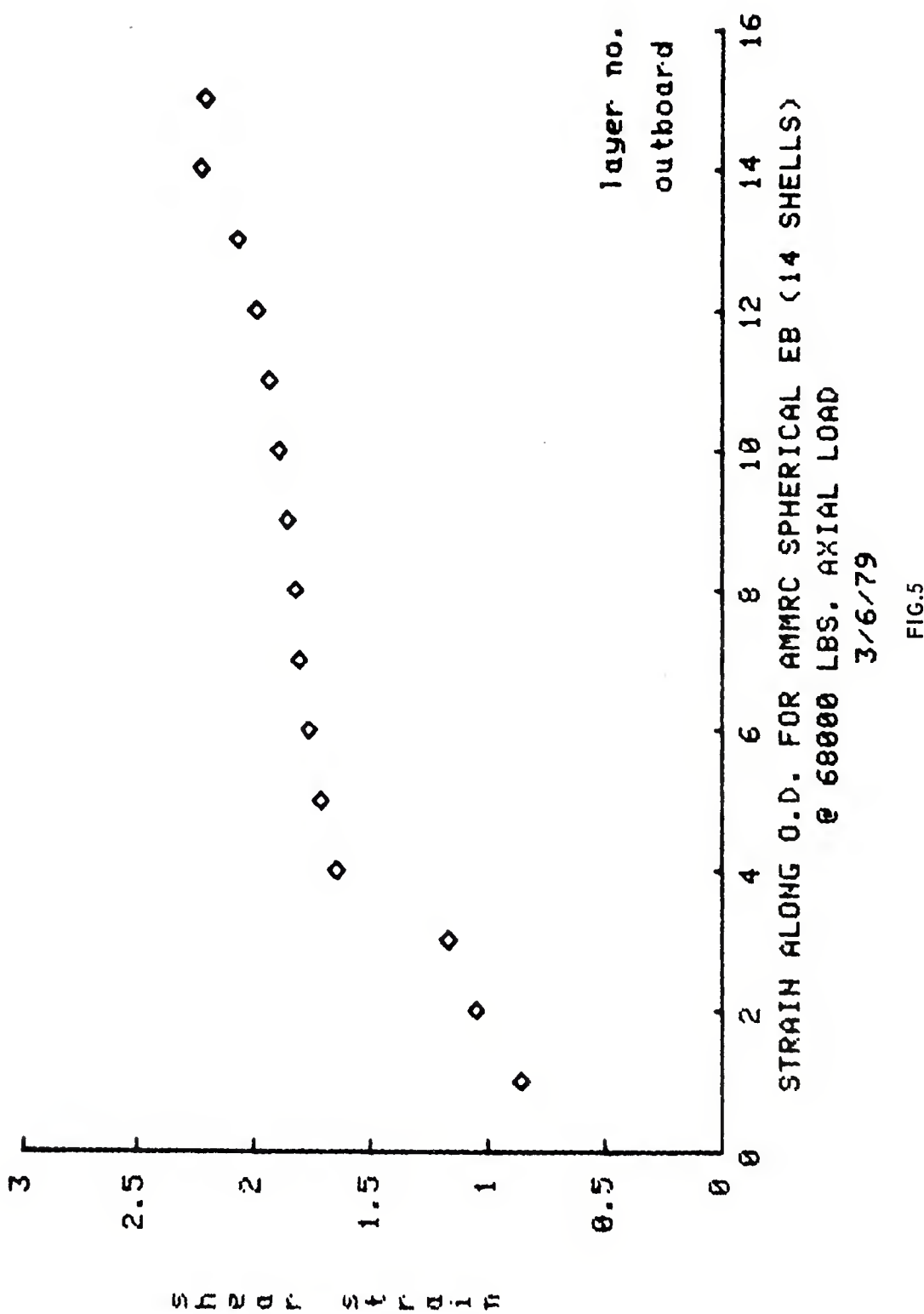
FIG. 2

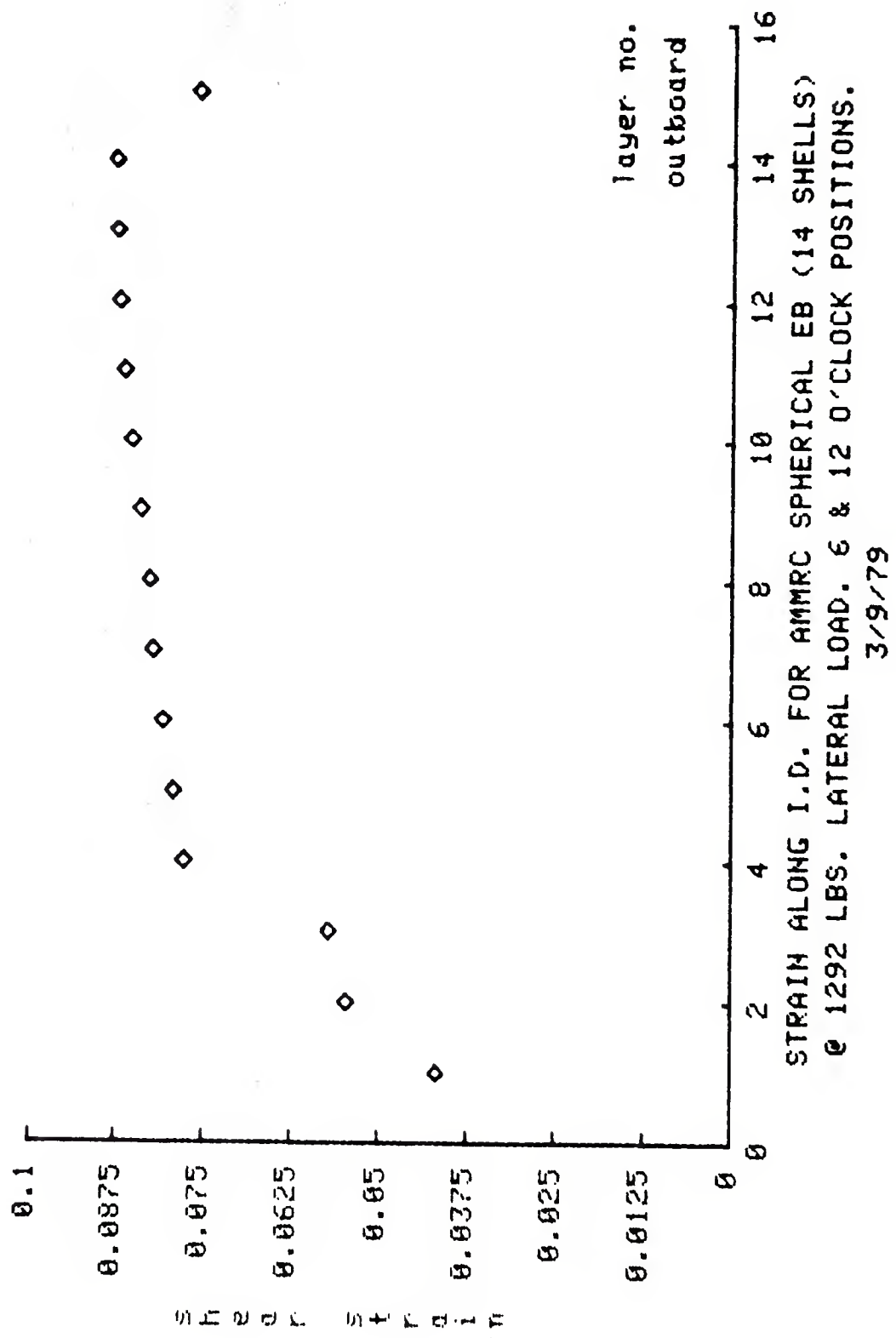


BLOW UP OF FIG. 2

FIG. 3







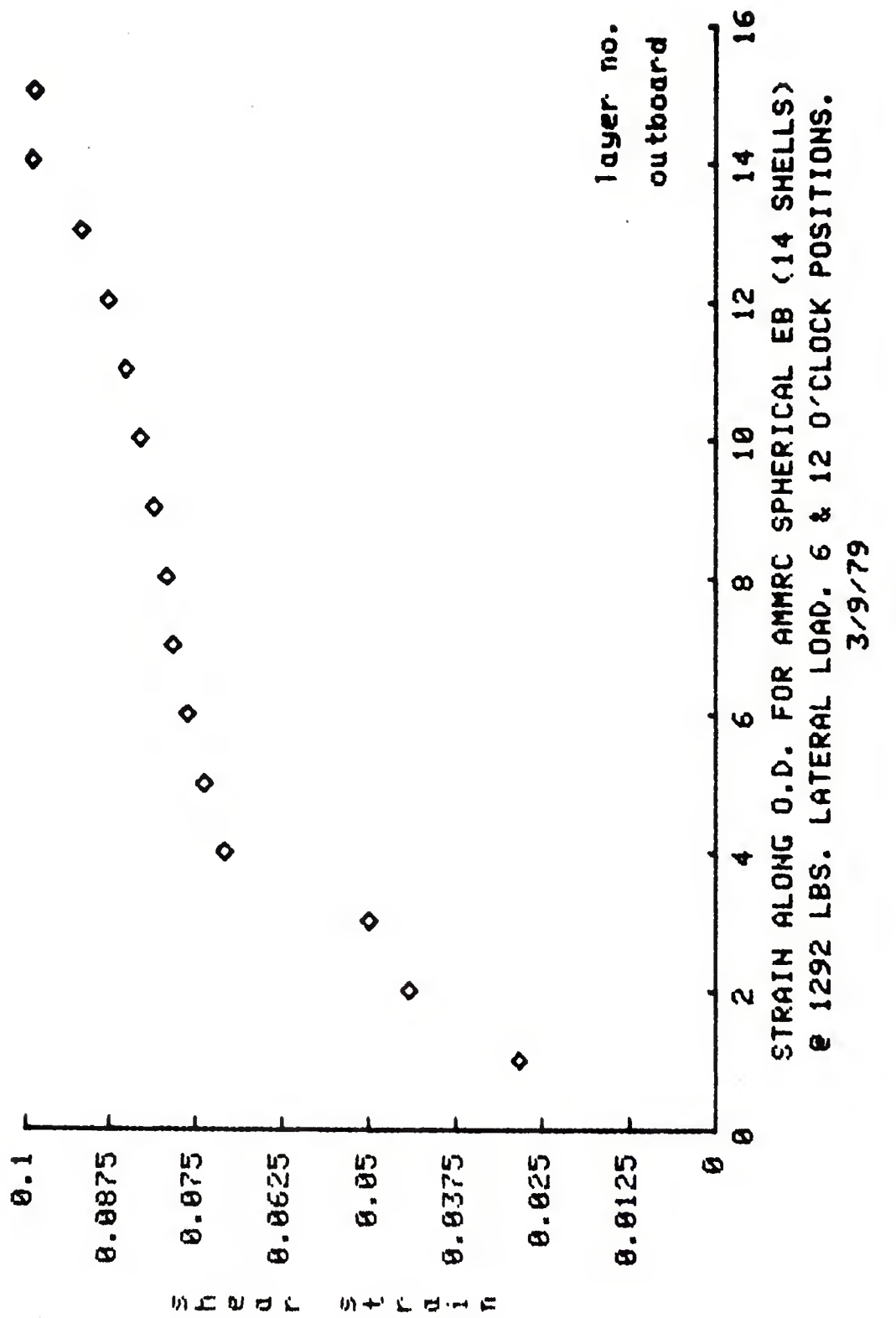


FIG. 7

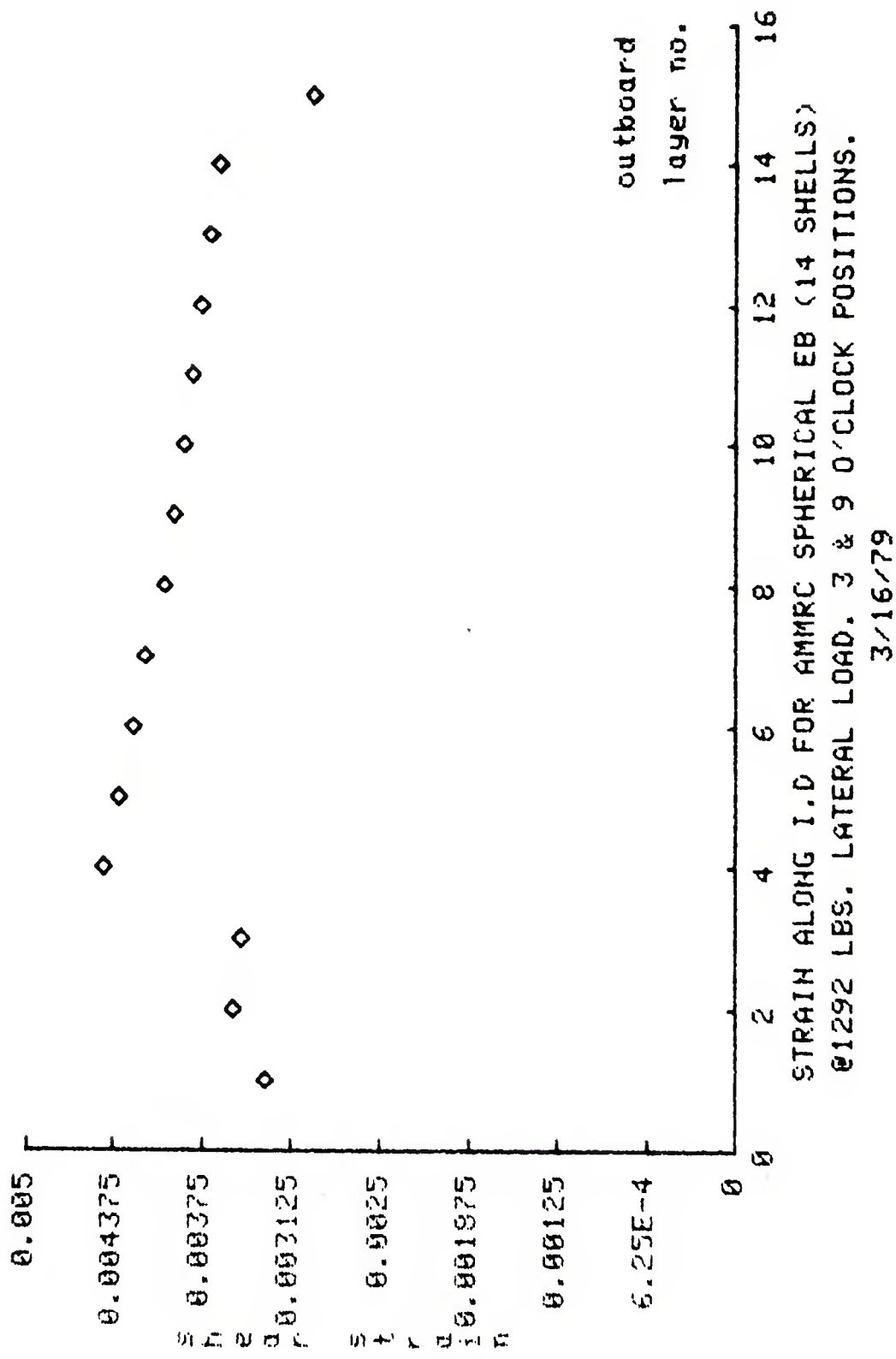


FIG. 8

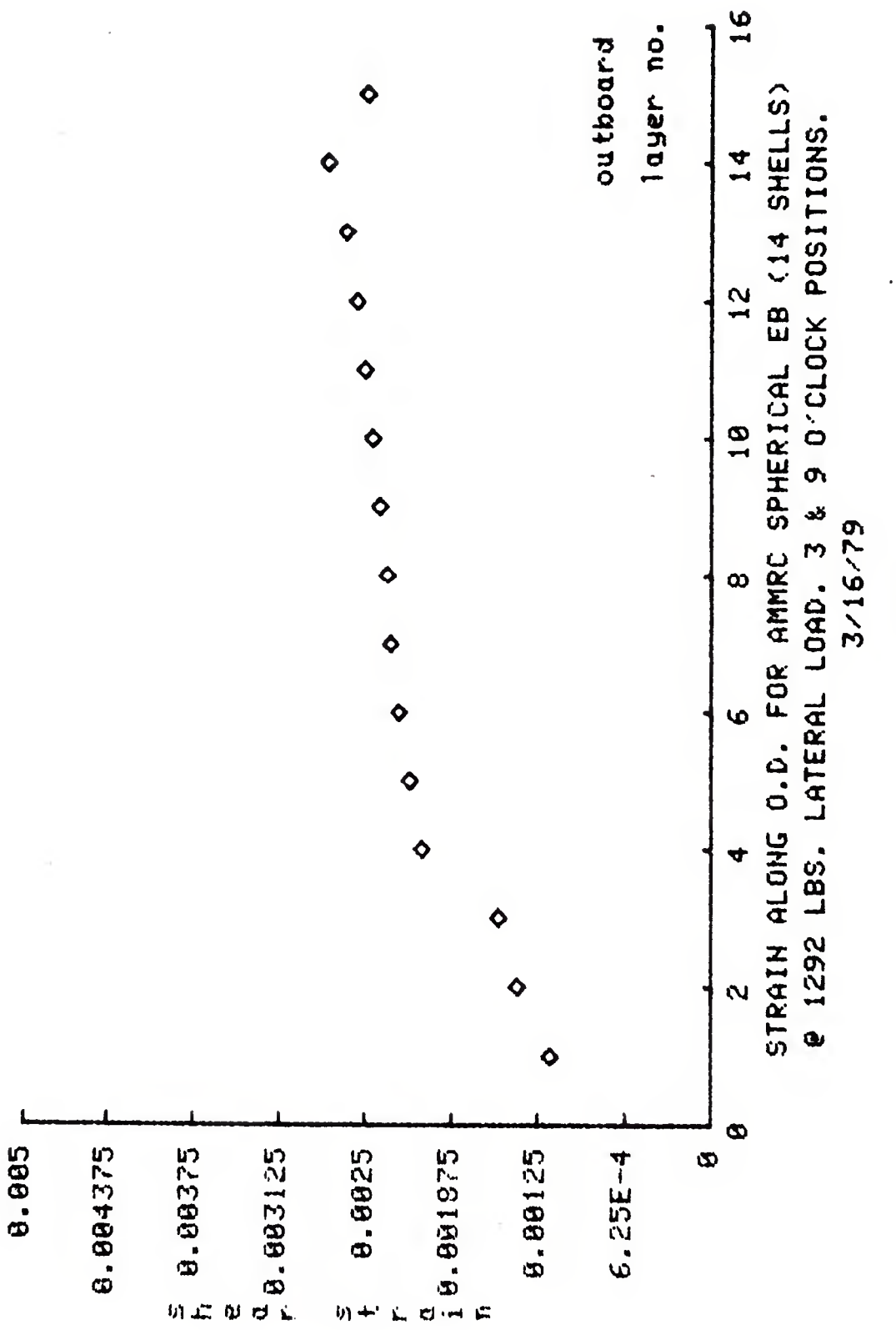
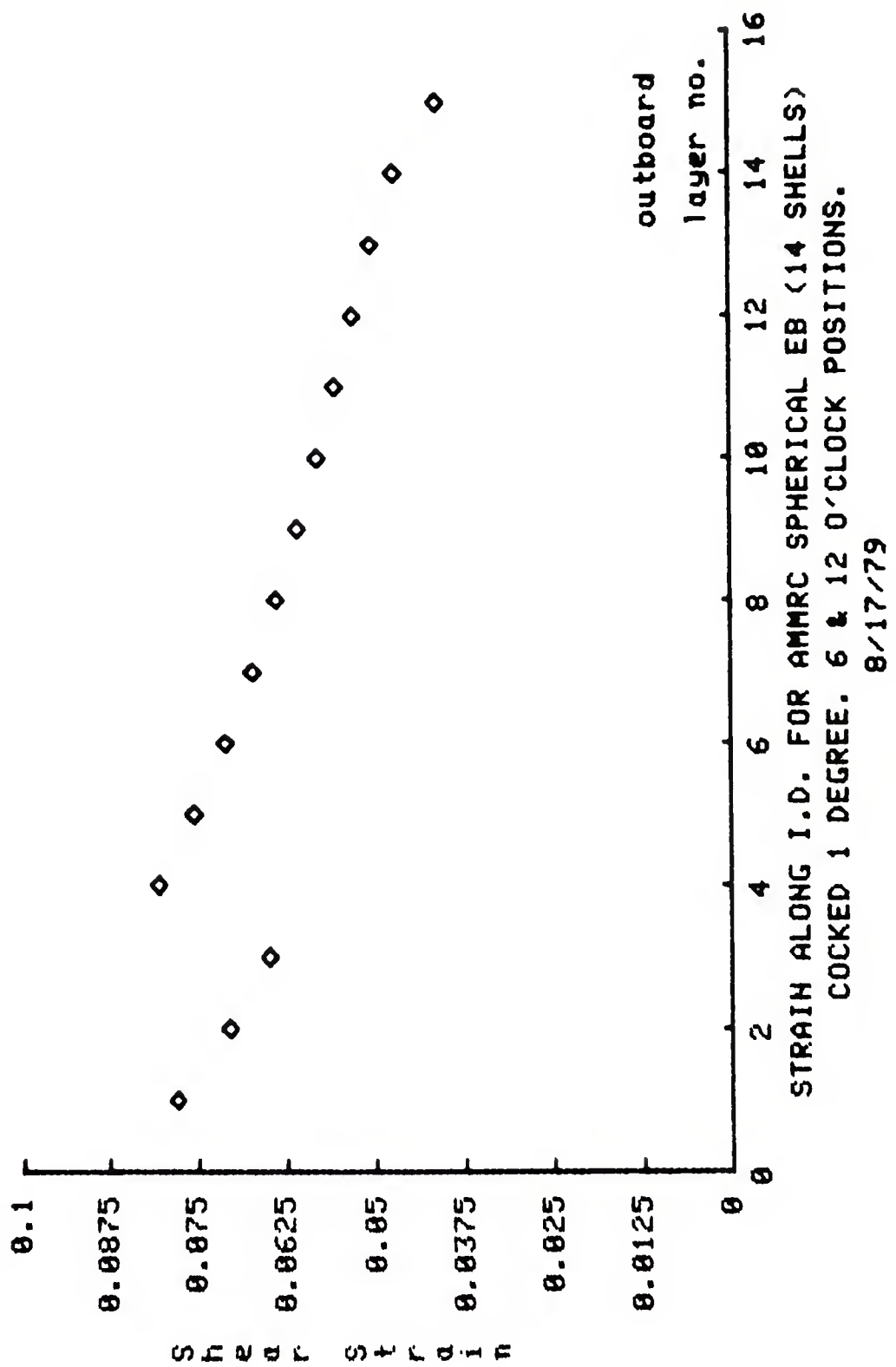


FIG. 9



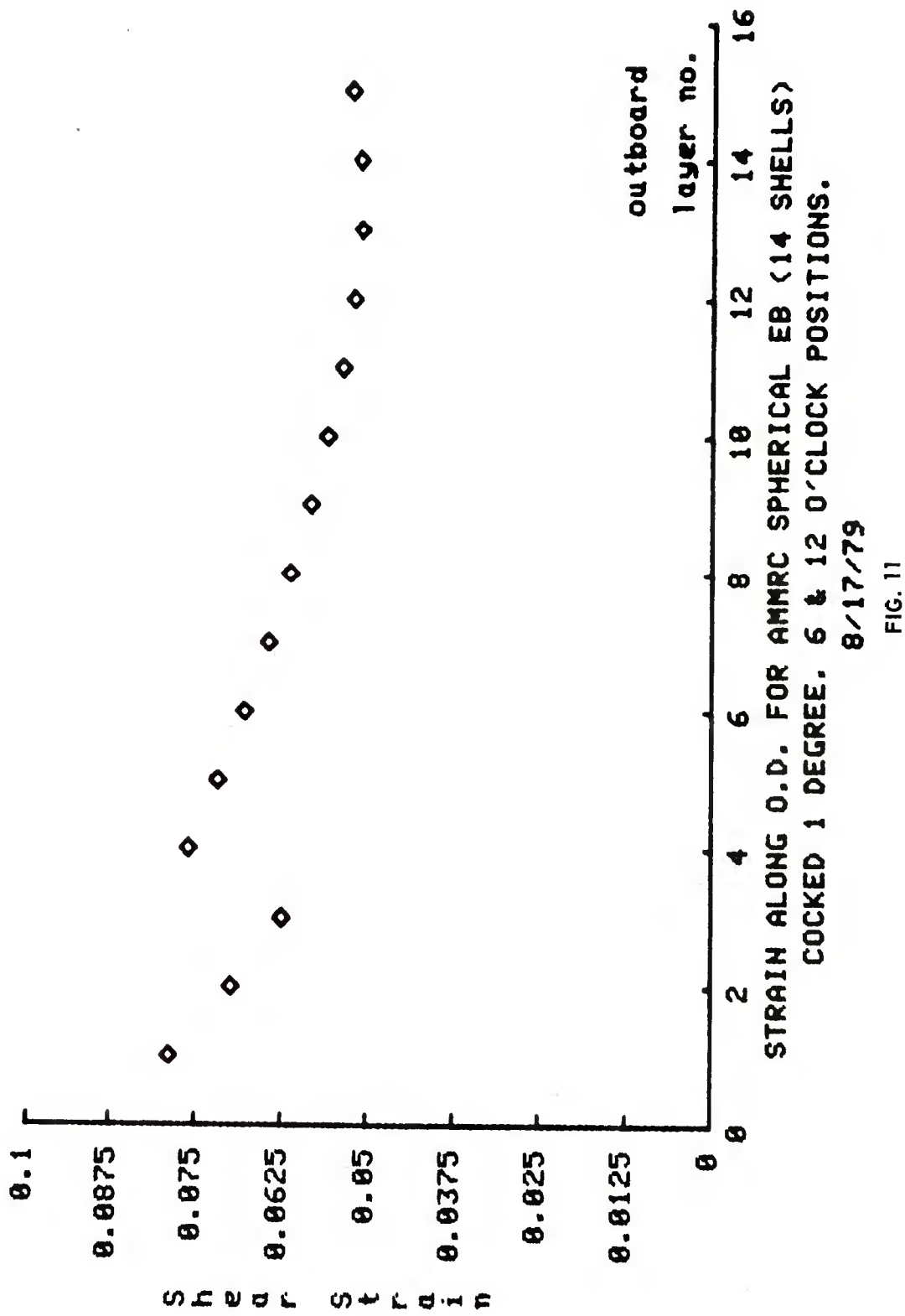
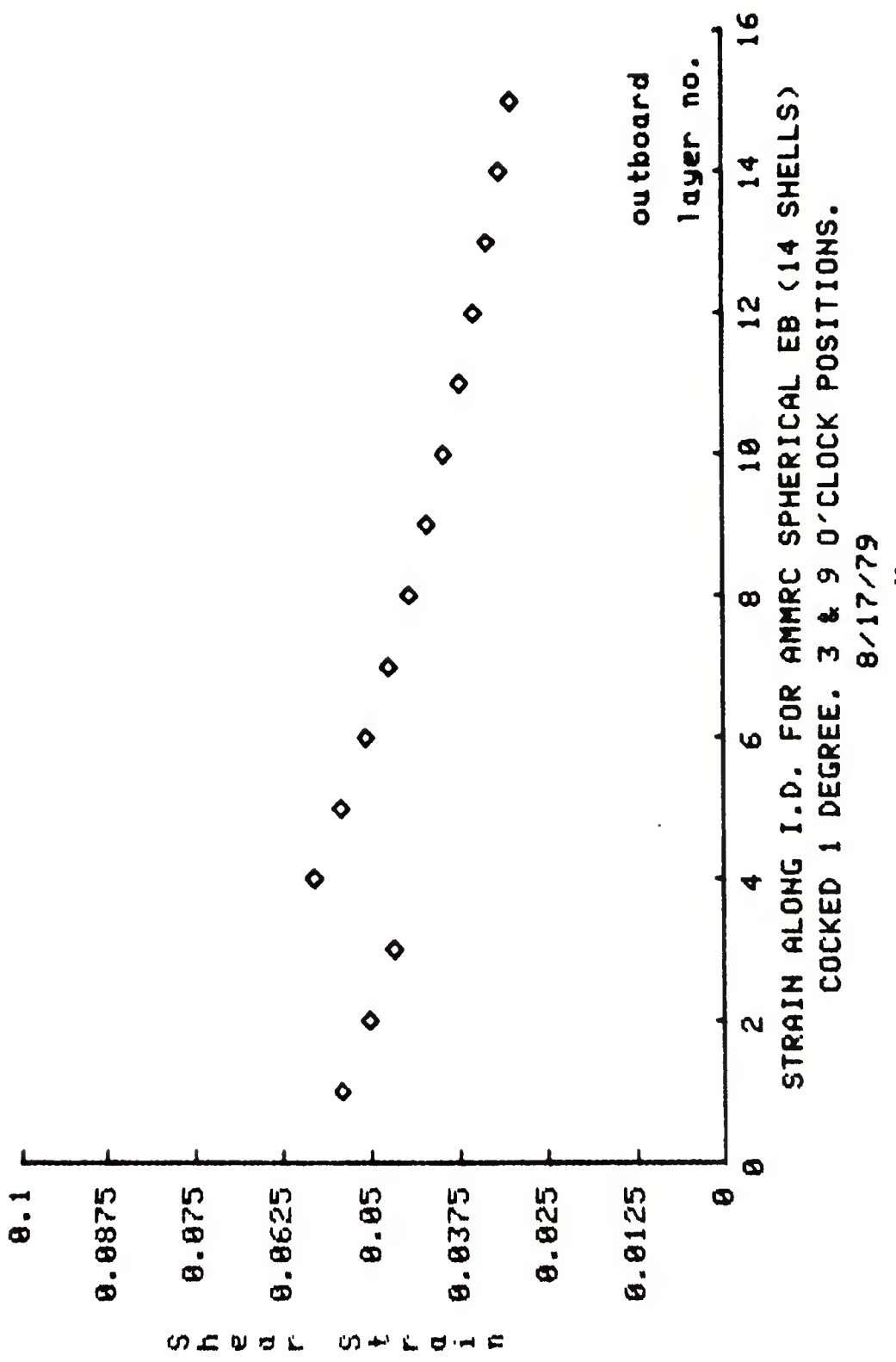
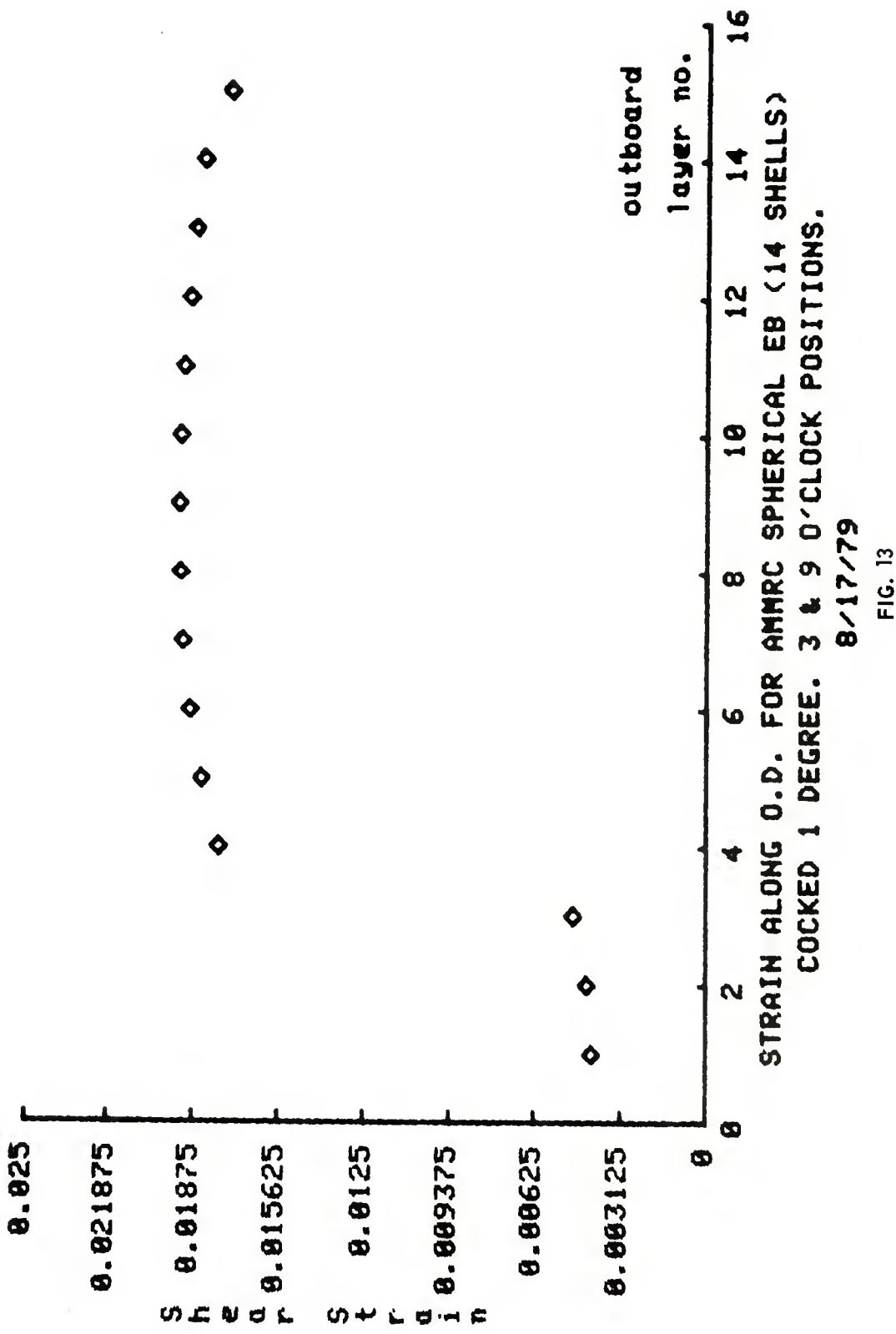
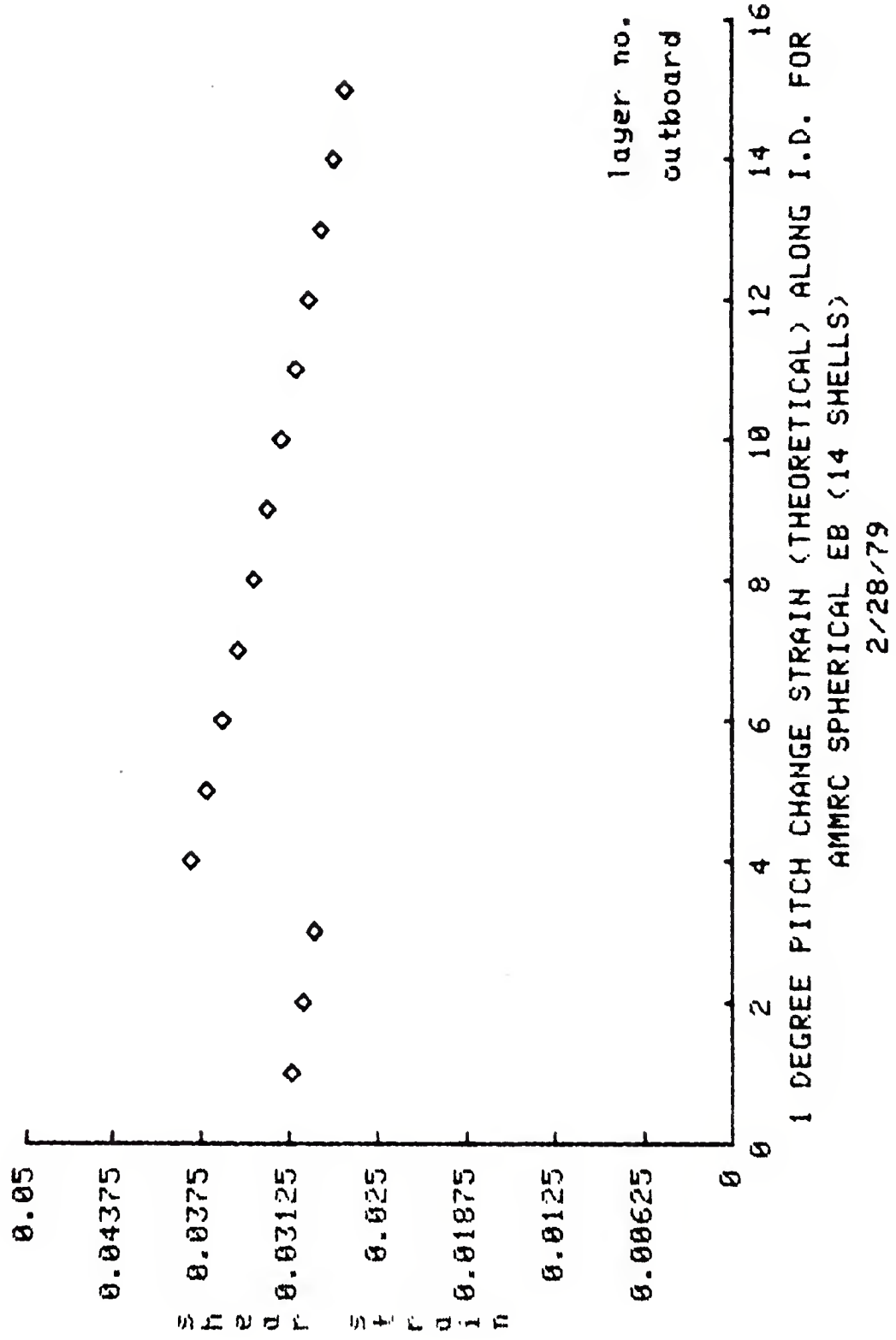


FIG. 11







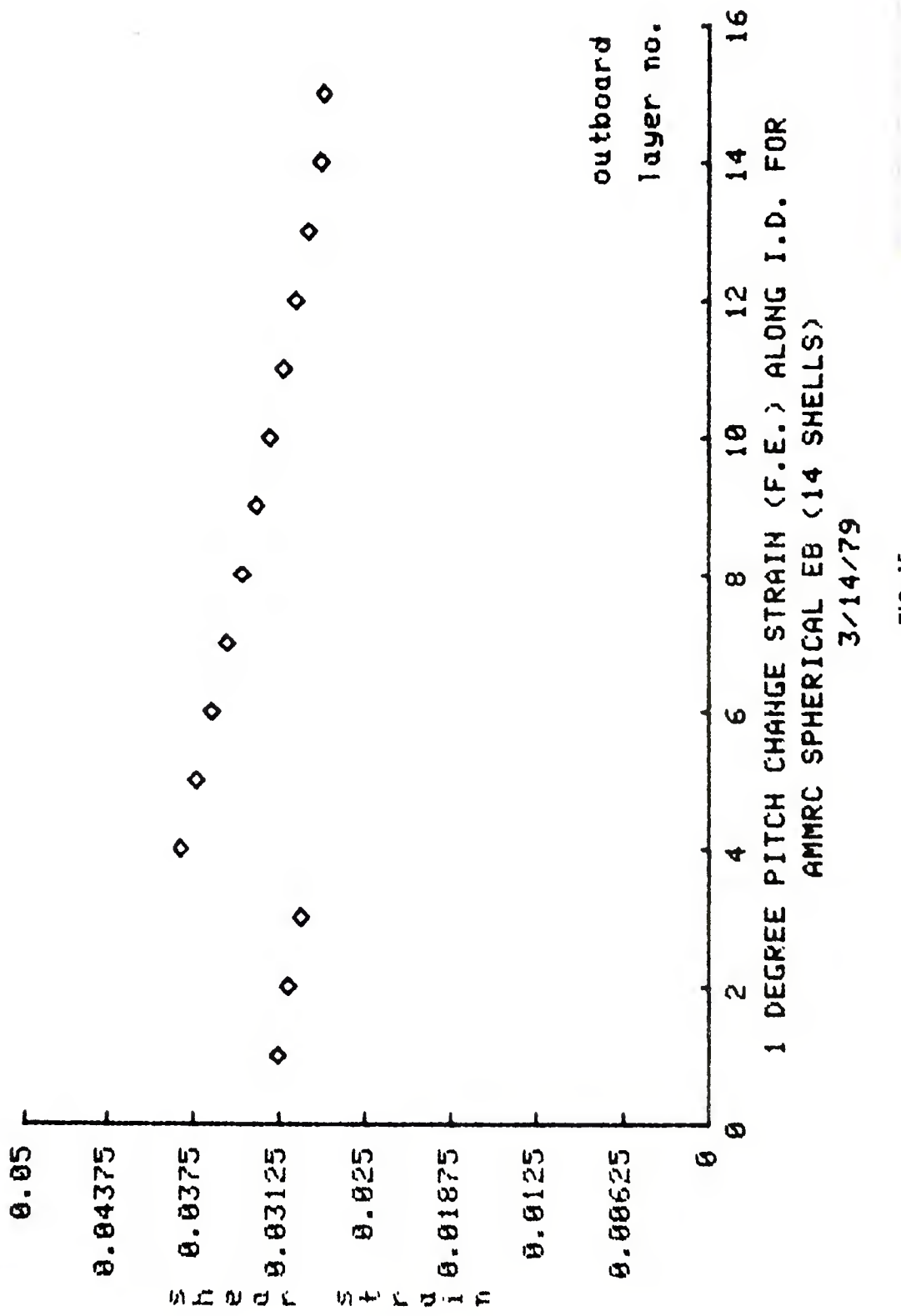
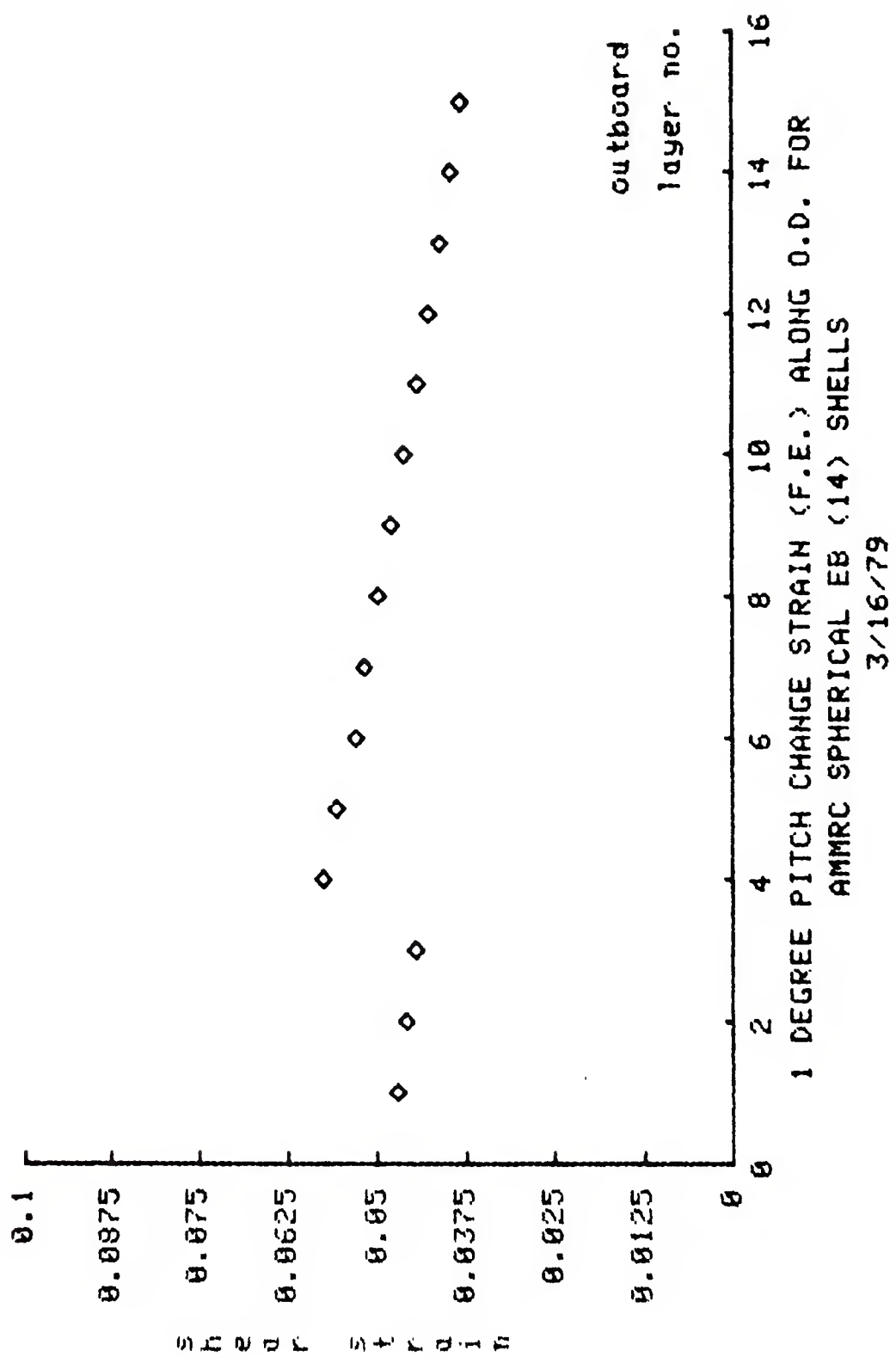


FIG. 15



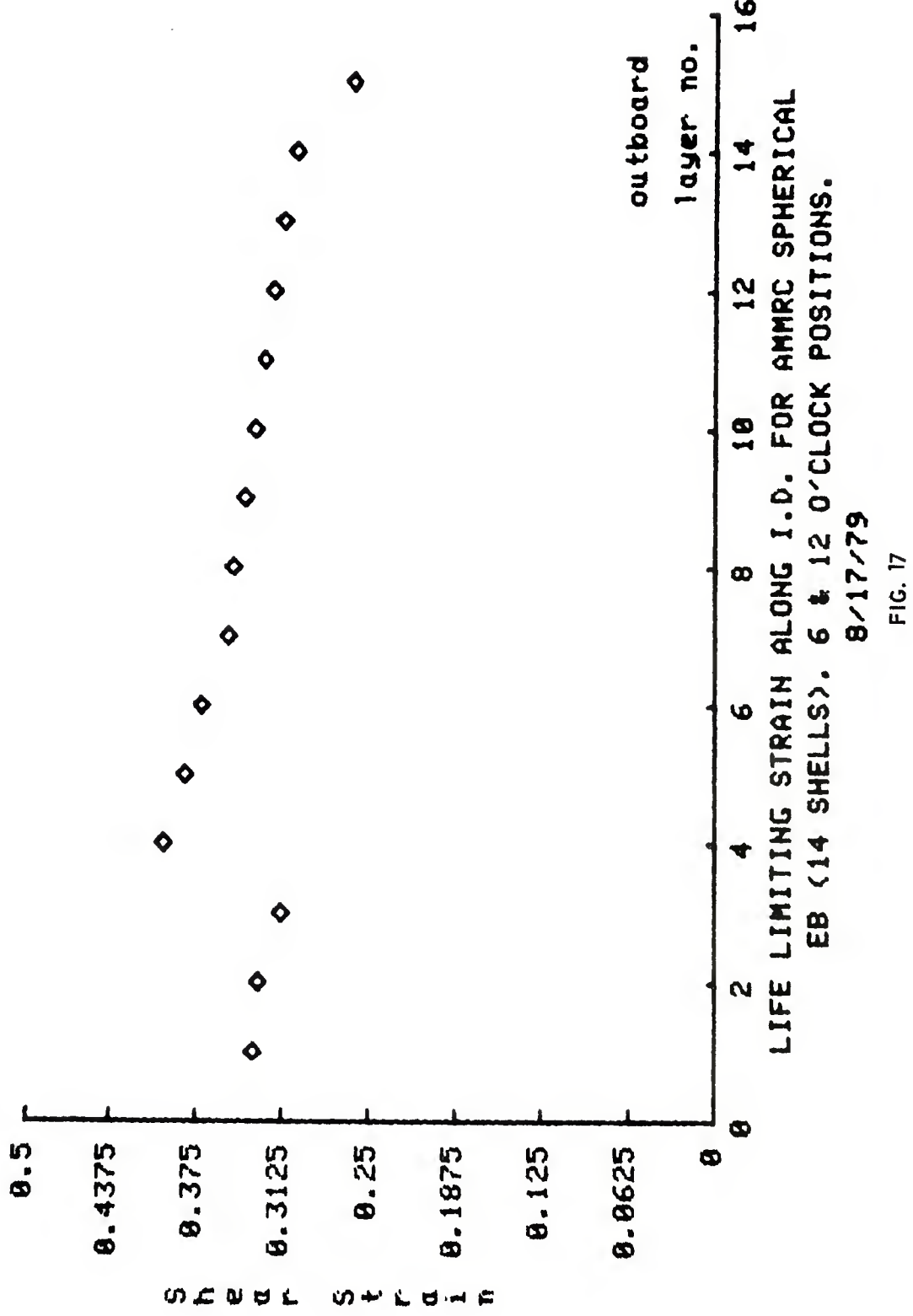


FIG. 17

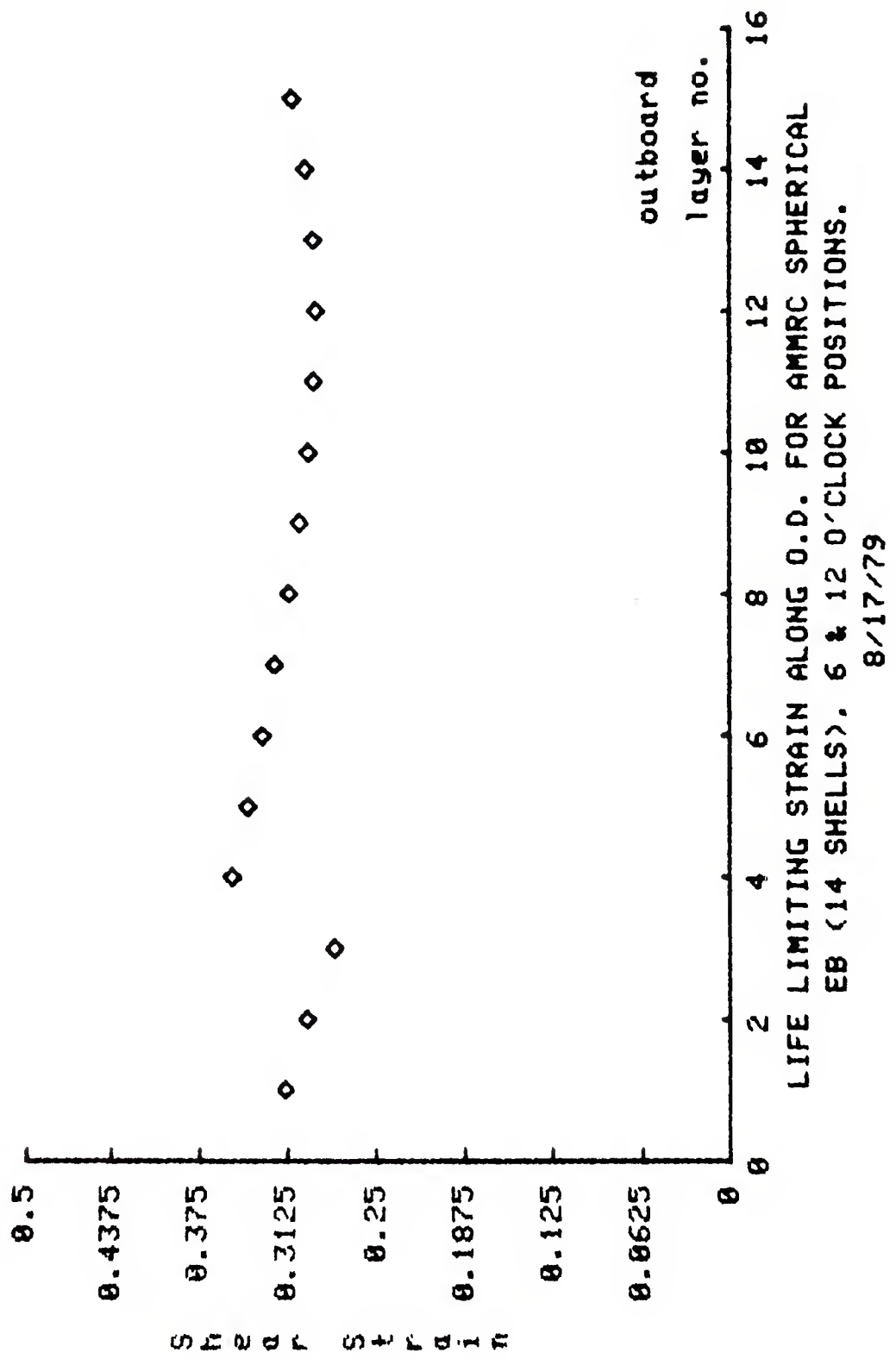
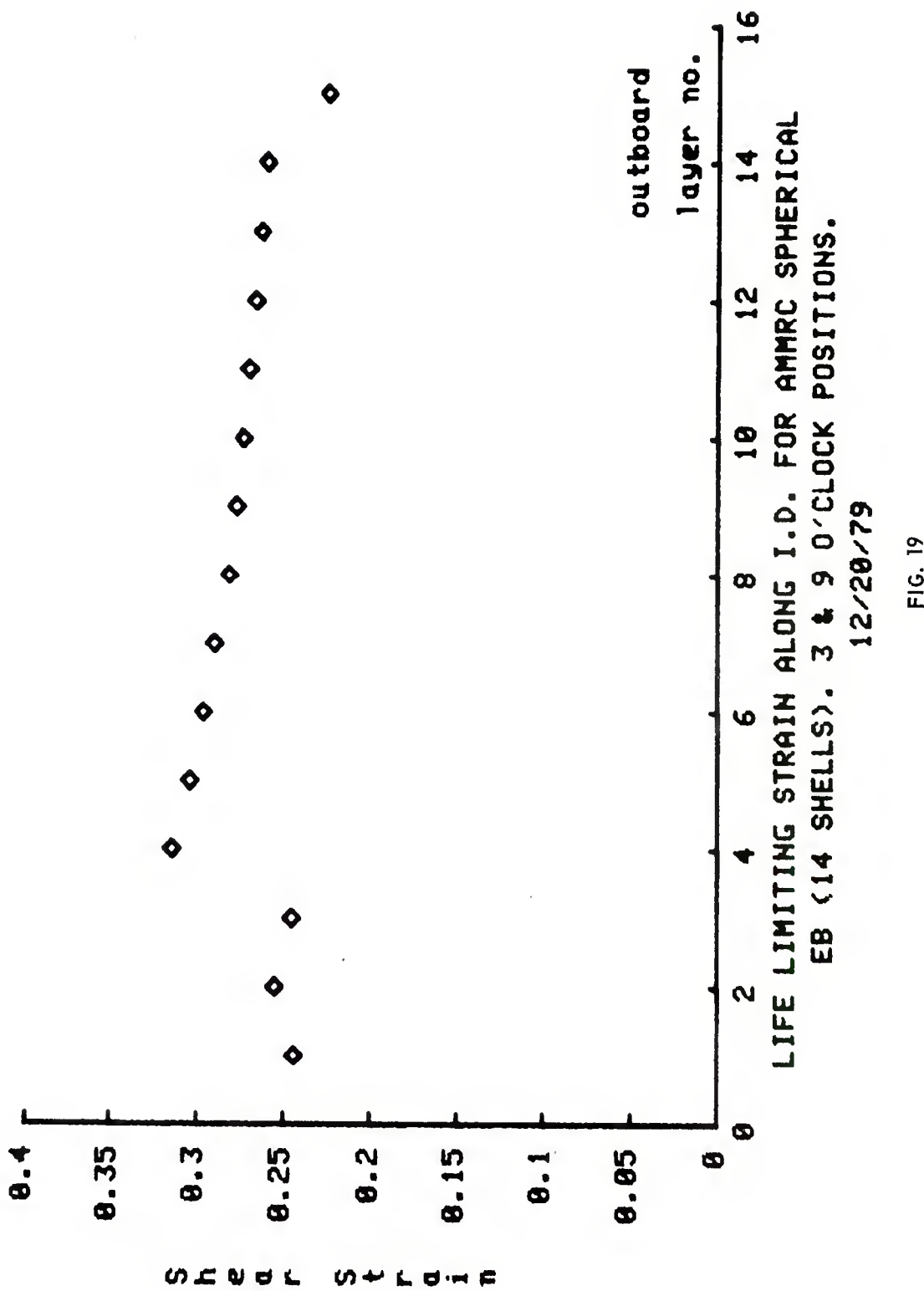


FIG. 18



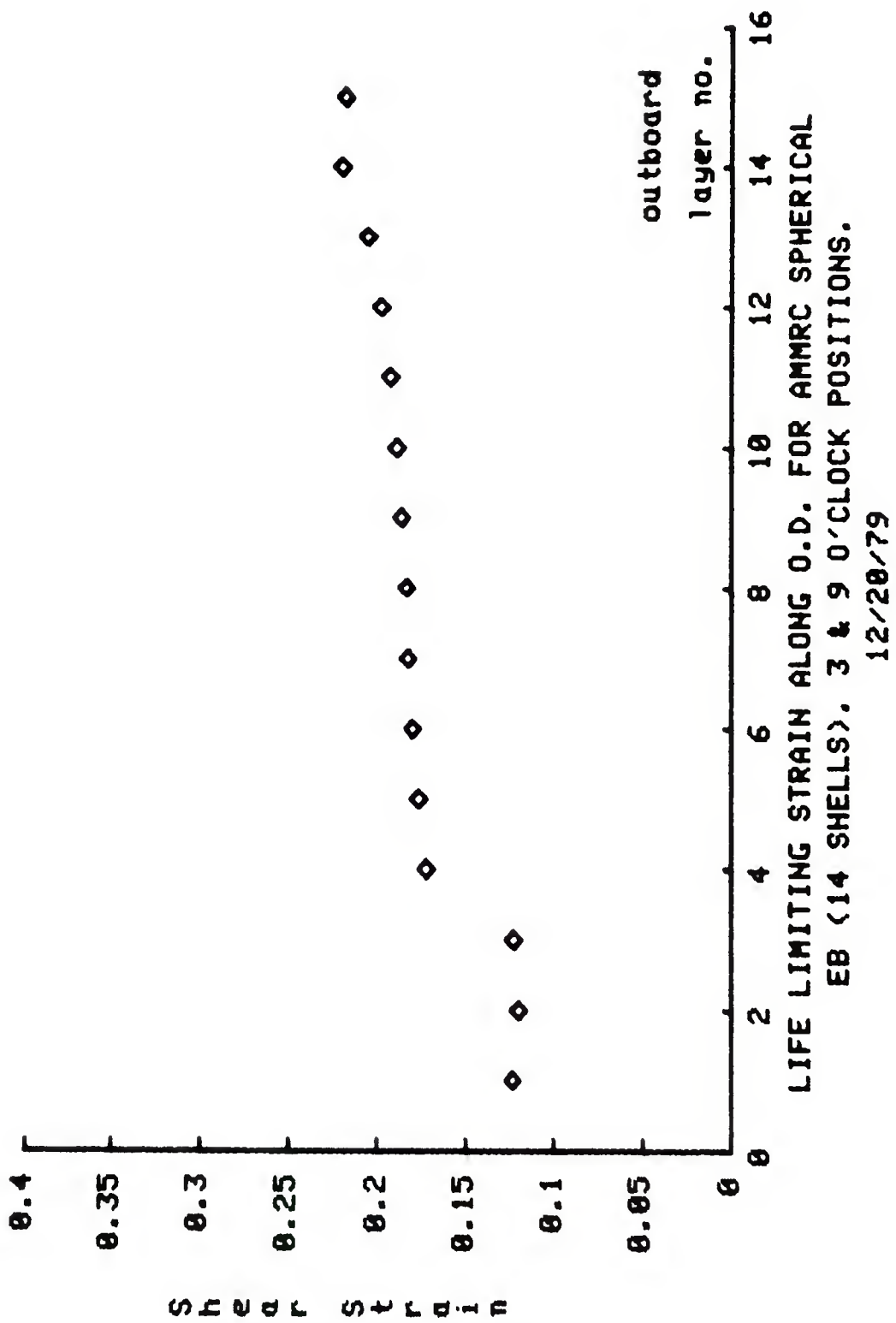


FIG. 20

A P P E N D I X I

```

1: $ BLACKHAWK MAIN ROTOR SPHERICAL EB MODEL 1 (AMMRC)
2: SETUP,4,PRESCRIB,18
3: RUBBER,1,600,.4995
4: RUBBER,2,450,.4996
5: ALUMINM,3,10E6,.33
6: SSSTEEL,4,28E6,.3
7: TITANM,5,15E6,.3
8: END, MATERIAL
9: 1,1,2,2
10: 1,375,1.5,1.5,1,375
11: .744,.744,2.61,2.61
12: 2,1,3,1
13: 1.5,1.543,1.543,1.5
14: .744,.744,.744,.744
15: 4,1,5,1
16: 1.716,1.881,1.881,1.716
17: .744,.744,.744,.744
18: 6,1,7,1
19: 2.837,2.184,2.184,2.037
20: .744,.744,.744,.744
21: 8,1,9,1
22: 2.326,2.445,2.445,2.320
23: .744,.744,.744,.744
24: 10,1,1,1
25: 2.560,2.662,2.662,2.560
26: .744,.744,.744,.744
27: 12,1,13,1
28: 2.752,2.829,2.829,2.752
29: .744,.744,.744,.744
30: 13,1,14,1
31: 2.829,2.8455,2.8455,2.829
32: .744,.744,.744,.744
33: 2,2,3,3,1,1,1,POLAR,0,0
34: 3.010,3.010,3.062,3.062

```

35: 60. 110, 59. 158, 59. 038, 59. 974
 36: 3. 12, 13, 3, 1, 1, 1, POLAR, 0, 0
 37: 3. 010, 3. 010, 3. 062, 3. 062
 38: 59. 158, 19. 982, 20. 742, 59. 038
 39: 13. 12, 14, 3, 1, 1, 1, POLAR, 0, 0
 40: 3. 010, 3. 010, 3. 062, 3. 062
 41: 19. 982, 19. 030, 19. 812, 20. 742
 42: 2, 4, 3, 5, 1, 1, 1, POLAR, 0, 0
 43: 3. 124, 3. 124, 3. 188, 3. 188
 44: 59. 017, 58. 980, 58. 764, 59. 662
 45: 3. 124, 3. 124, 3. 188, 3. 188
 46: 3. 124, 3. 124, 3. 188, 3. 188
 47: 58. 980, 21. 687, 22. 455, 58. 764
 48: 13, 4, 14, 5, 1, 1, 1, POLAR, 0, 0
 49: 3. 124, 3. 124, 3. 188, 3. 188
 50: 21. 687, 28. 780, 21. 578, 22. 455
 51: 2, 6, 3, 1, 1, 1, 1, POLAR, 0, 0
 52: 3. 250, 3. 250, 3. 316, 3. 316
 53: 59. 517, 58. 636, 58. 586, 59. 370
 54: 3, 6, 13, 7, 1, 1, 1, POLAR, 0, 0
 55: 3. 250, 3. 250, 3. 316, 3. 316
 56: 58. 636, 23. 236, 24. 028, 58. 506
 57: 13, 6, 14, 7, 1, 1, 1, POLAR, 0, 0
 58: 3. 250, 3. 250, 3. 316, 3. 316
 59: 23. 236, 22. 371, 23. 184, 24. 028
 60: 2, 8, 3, 9, 1, 1, 1, POLAR, 0, 0
 61: 3. 378, 3. 378, 3. 446, 3. 446
 62: 59. 236, 58. 389, 58. 265, 59. 095
 63: 3, 8, 13, 9, 1, 1, 1, POLAR, 0, 0
 64: 3. 378, 3. 378, 3. 446, 3. 446
 65: 58. 389, 24. 738, 25. 481, 58. 265
 66: 13, 8, 14, 9, 1, 1, 1, POLAR, 0, 0
 67: 3. 378, 3. 378, 3. 446, 3. 446
 68: 24. 738, 23. 911, 24. 672, 25. 481

69:	2,10,	3.508	,3.508	,3.578	,3.578	,1,1,	,1,1,	,1,1,	,1,1,	POLAR,	0,0
70:	3.58.	972	.58.	156	.58.	037	.58.	837			
71:	3,10,	13,11,	1,1,	1,1,	1,1,	1,1,	1,1,	1,1,	1,1,	POLAR,	0,0
72:	3,508	,3,508	,3,578	,3,578							
73:	3,58.	156	,26,	128	,26,	826	,58.	837			
74:	3,58.	14,	1,	1,	1,	1,	1,	1,	1,	POLAR,	0,0
75:	3,508	,3,508	,3,578	,3,578							
76:	3,57.	936	,27,	418	,28,	676	,57.	823	,58.	594	
77:	26,	128	,25,	334	,26,	049	,26,	826			
78:	2,	12,	3,	13,	1,	1,	1,	1,	1,	POLAR,	0,0
79:	3,	640	,3,	640	,3,	712	,3,	712			
80:	3,	58.	723	,57.	936	,57.	823	,58.	594		
81:	3,	12,	13,	13,	1,	1,	1,	1,	1,	POLAR,	0,0
82:	3,	640	,3,	640	,3,	712	,3,	712			
83:	57.	936	,27,	418	,28,	676	,57.	823			
84:	13,	12,	14,	14,	1,	1,	1,	1,	1,	POLAR,	0,0
85:	3,	640	,3,	640	,3,	712	,3,	712			
86:	27,	418	,26,	655	,27,	329	,28,	876			
87:	2,	14,	3,	15,	1,	1,	1,	1,	1,	POLAR,	0,0
88:	3,	774	,3,	774	,3,	848	,3,	848			
89:	58.	488	,57.	729	,57.	621	,58.	365			
90:	3,	14,	13,	15,	1,	1,	1,	1,	1,	POLAR,	0,0
91:	3,	774	,3,	774	,3,	848	,3,	848			
92:	57.	729	,28,	628	,29,	242	,57.	621			
93:	13,	14,	14,	15,	1,	1,	1,	1,	1,	POLAR,	0,0
94:	3,	774	,3,	774	,3,	848	,3,	848			
95:	28,	628	,27,	884	,28,	521	,29,	242			
96:	2,	16,	3,	17,	1,	1,	1,	1,	1,	POLAR,	0,0
97:	3,	910	,3,	910	,3,	985	,3,	985			
98:	58.	266	,57.	534	,57.	432	,58.	150			
99:	3,	16,	13,	17,	1,	1,	1,	1,	1,	POLAR,	0,0
100:	3,	910	,3,	910	,3,	985	,3,	985			
101:	57.	534	,29,	743	,30,	324	,57.	432			
102:	13,	16,	14,	17,	1,	1,	1,	1,	1,	POLAR,	0,0

183:	3.910	3.910	3.985	3.985
184:	29.743	29.032	29.627	30.324
185:	2.18	3.19	1.1	1, POLAR, 0, 0
186:	4.047	4.047	4.124	4.124
187:	58.058	57.350	57.253	57.947
188:	3.18	13.19	1.1	1, POLAR, 0, 0
189:	4.047	4.047	4.124	4.124
190:	57.350	30.787	31.339	57.253
191:	13.18	14.19	1.1	1, POLAR, 0, 0
192:	4.047	4.047	4.124	4.124
193:	30.787	30.099	30.663	31.339
194:	2.28	3.21	1.1	1, POLAR, 0, 0
195:	4.186	4.196	4.265	4.265
196:	57.868	57.176	57.083	57.754
197:	3.20	13.21	1.1	1, POLAR, 0, 0
198:	4.186	4.186	4.265	4.265
199:	57.176	31.767	32.292	57.083
200:	13.20	14.21	1.1	1, POLAR, 0, 0
201:	4.186	4.186	4.265	4.265
202:	31.767	31.180	31.637	32.292
203:	2.22	3.23	1.1	1, POLAR, 0, 0
204:	4.327	4.327	4.408	4.408
205:	57.673	57.011	56.921	57.571
206:	3.22	13.22	1.1	1, POLAR, 0, 0
207:	4.327	4.327	4.408	4.408
208:	57.011	32.689	33.190	56.921
209:	13.22	14.23	1.1	1, POLAR, 0, 0
210:	4.327	4.327	4.408	4.408
211:	32.689	32.042	32.553	33.190
212:	2.24	3.25	1.1	1, POLAR, 0, 0
213:	4.470	4.470	4.553	4.553
214:	57.495	56.855	56.768	57.397
215:	3.24	13.25	1.1	1, POLAR, 0, 0
216:	4.470	4.470	4.553	4.553

137:	56.	855	33.559, 34.036, 56.768	
138:	13.	24.	14.25, 1, 1, 1, POLAR, 0, 0	
139:	4.	470	4.47, 4.553	
140:	33.	559	32.930, 33.417, 34.036	
141:	2.	26,	3, 27, 1, 1, 1, POLAR, 0, 0	
142:	4.	615	4.615, 4.700, 4.700	
143:	57.	326,	56.706, 56.623, 57.232	
144:	3.	26,	13, 27, 1, 1, 1, POLAR, 0, 0	
145:	4.	615	4.615, 4.700, 4.700	
146:	56.	706	34.380, 34.836, 56.623	
147:	13.	26,	14.27, 1, 1, 1, POLAR, 0, 0	
148:	4.	615	4.615, 4.700, 4.700	
149:	34.	398	33.768, 34.233, 34.836	
150:	2.	28,	3, 29, 1, 1, 1, POLAR, 0, 0	
151:	4.	762	4.762, 4.849, 4.849	
152:	57.	166	56.564, 56.484, 57.075	
153:	3.	28,	13, 29, 1, 1, 1, POLAR, 0, 0	
154:	4.	762	4.762, 4.849, 4.849	
155:	56.	564	35.157, 35.592, 56.484	
156:	13.	28,	14, 29, 1, 1, 1, POLAR, 0, 0	
157:	4.	762	4.762, 4.849, 4.849	
158:	35.	157	34.560, 35.605, 35.592	
159:	2.	36,	3, 31, 1, 1, 1, POLAR, 0, 0	
160:	4.	911	4.911, 4.985, 4.985	
161:	57.	013	56.429, 56.365, 56.940	
162:	3.	30,	13, 31, 1, 1, 1, POLAR, 0, 0	
163:	4.	911	4.911, 4.985, 4.985	
164:	56.	429	35.892, 36.240, 56.365	
165:	13.	30,	14, 31, 1, 1, 1, POLAR, 0, 0	
166:	4.	911	4.911, 4.985, 4.985	
167:	35.	892	35.311, 35.665, 36.240	
168:	2.	32,	3, 33, 35, 36, 37	
169:	2.	8597	2.9017, 3.042, 3	
170:	4.	593	4.4659, 5.0088, 5.008	

171:3,32,13,33
172:2,9017,4,008,4,008,3,042
173:4,5659,3,7281,5,008,5,008
174:13,32,14,33
175:4,008,4,05,4,05,4,008
176:3,7281,3,701,5,008,5,008
177:14,32,16,33
178:4,05,5,065,4,835,4,05
179:3,701,3,701,5,008,5,008
180:END,GRID
181:ILOOP,13,1
182:QUAD,3,1,1
183:IEHD
184:ILOOP,13,1
185:BC,PRESSURE,1,1,1,3487,63
186:IEHD
187:JLOOP,3,2
188:ILOOP,12,1
189:QUAD,1,2,2
190:IEHD
191:ILOOP,12,1
192:QUAD,4,2,3
193:IEHD
194:JEHD
195:JLOOP,11,2
196:ILOOP,12,1
197:QUAD,2,2,8
198:IEHD
199:ILOOP,12,1
200:QUAD,4,2,9
201:IEHD
202:JEHD
203:ILOOP,12,1
204:QUAD,2,2,30

```
205: IEND
206: JLOOP,2,1
207: ILOOP,12,1
208: QUAD,5,2,31
209: IEHD
210: JEHD
211: QUAD,5,14,32
212: QUAD,5,15,32
213: ILOOP,2,1
214: BC,UR,14,32,1,0
215: BC,U2,14,32,1,0
216: IEHD
217: ILOOP,14,1
218: BC,U2,2,32,3,0
219: IEHD
220: PLOT,ELEMENTS,1.225,.594,5.215,5.128,10
221: END,ELEMENTS
222: AXISYM
223: STOP
```

A P P E N D I X II

```

100 PAGE ****SPHERICAL EB MODEL GENERATOR*****"J
110 PRINT " WHICH FILE DO YOU WANT THE DATA TO BE STORED IN? ";
120 INPUT D
130 INPUT J
140 PRINT "NUMBER OF SHELLS =";
150 INPUT F
160 L=F+1
170 SET RADIAN S
180 PRINT "-----FIRST I.D. POINT-----";
190 PRINT "-----SPHERICAL RADIUS 1 =";;
200 INPUT RI
210 PRINT "I.D. 1 =";;
220 INPUT MI
230 X1=M1^2
240 Y1=SQR(R1*R1-X1*X1)
250 PRINT "-----SECOND I.D. POINT-----";
260 PRINT "-----SPHERICAL RADIUS 2 =";;
270 INPUT R2
280 PRINT "I.D. 2 =";;
290 INPUT M2
300 X2=M2^2
310 Y2=SQR(R2*R2-X2*X2)
320 REM S'S ARE SLOPES & C'S ARE INTERCEPTS
330 S1=(Y1-Y2)/(X1-X2)
340 C1=Y1-S1*X1
350 REM ANGLE FOR .05 ELEMENT
360 Q=ACOS(X1/R1)-0.05/R1
370 Y1=R1*SIN(Q)
380 X1=R1*COS(Q)
390 Q=ACOS(X2/R2)-0.05/R2
400 Y2=R2*SIN(Q)
410 X2=R2*COS(Q)
420 S2=(Y1-Y2)/(X1-X2)
430 C2=Y1-S2*X1

```

```

440 PRINT "J-----FIRST O.D. POINT-----";
450 PRINT "O.D. 1=";
460 INPUT M1
470 X1=M1/2
480 Y1=SQR(R1*R1-X1**X1)
490 PRINT "J-----SECOND O.D. POINT-----";
500 PRINT "O.D. 2 =" ;
510 INPUT M2
520 PAGE
530 X2=M2/2
540 Y2=SQR(R2*R2-X2**X2)
550 S3=(Y1-Y2)/(X1-X2)
560 C3=Y1-S3*X1
570 REM ANGLE FOR .05 END ELEMENT ON 00
580 Q=ACOS(X1/R1)+0.05/R1
590 Y1=R1*SIN(Q)
600 X1=R1*COS(Q)
610 Q=ACOS(X2/R2)+0.05/R2
620 Y2=R2*SIN(Q)
630 X2=R2*COS(Q)
640 S4=(Y1-Y2)/(X1-X2)
650 C4=Y1-S4*X1
660 REM OUTPUT FORMATTING
670 FIND D
680 SET DEGREES
690 REM SUBROUTINE FOR RADII & ANGLES
700 P=1
710 PRINT "JINSIDE RADIUS=";
720 INPUT R1
730 PRINT "JOUTSIDE RADIUS =";
740 INPUT R2
750 C$="1,1,1,1,POLAR,0,0"
760 PRINT @33: USING 70:"2","," ,P+1," , " , " 3" , " , " , " , " , P+2,C$"
770 IMAGE 2A,A,2D,A,18A
780 PRINT @33: USING 790:R1," , " , " , R2," , " , R2

```

```

790 IMAGE D. 3D, A, D. 3D, A, D. 3D, A, D. 3D
800 A=C1
810 B=S1
820 Y=A*B/(B*B+1)
830 X=SQR(Y**Y+(R1*R1-A*A)/(B*B+1))-Y
840 REM Z'S ARE ANGLES
850 Z1=ACS(X/R1)
860 X=SQR(Y**Y+(R2*R2-A*A)/(B*B+1))-Y
870 Z2=ACS(X/R2)
880 REM REPEATING FOR C2 & S2
890 A=C2
900 B=S2
910 Y=A*B/(B*B+1)
920 X=SQR(Y**Y+(R1*R1-A*A)/(B*B+1))-Y
930 Z3=ACS(X/R1)
940 X=SQR(Y**Y+(R2*R2-A*A)/(B*B+1))-Y
950 Z4=ACS(X/R2)
960 REM REPEATING FOR C4 & S4
970 A=C4
980 B=S4
990 Y=A*B/(B*B+1)
1000 X=SQR(Y**Y+(R1*R1-A*A)/(B*B+1))-Y
1010 Z5=ACS(X/R1)
1020 X=SQR(Y**Y+(R2*R2-A*A)/(B*B+1))-Y
1030 Z6=ACS(X/R2)
1040 REM REPEATING FOR C3 & S3
1050 A=C3
1060 B=S3
1070 Y=A*B/(B*B+1)
1080 X=SQR(Y**Y+(R1*R1-A*A)/(B*B+1))-Y
1090 Z7=ACS(X/R1)
1100 X=SQR(Y**Y+(R2*R2-A*A)/(B*B+1))-Y
1110 Z8=ACS(X/R2)
1120 PRIHT 033: USING 1130:21,"23","24","","",Z2
1130 IMAGE 2D.3D,A,2D.3D,A,2D.3D

```

```

1140 PRINT @33: USING 770: "3", "P+1", "13", "R2", "P+2, C#
1150 PRINT @33: USING 790: R1, "R1", "R2", "R2"
1160 PRINT @33: USING 1130: Z3, "Z3", "Z5", "Z6", "Z4
1170 PRINT @33: USING 770: "13", "P+1", "14", "R2", "P+2, C#
1180 PRINT @33: USING 790: R1, "R1", "R2", "R2"
1190 PRINT @33: USING 1130: Z5, "Z7", "Z8", "Z6
1200 P=P+2
1210 G=2*L+1
1220 IF P=G THEN 1300
1230 IF P=9 THEN 1270
1240 IF P=15 THEN 1270
1250 IF P=21 THEN 1270
1260 GO TO 710
1270 PAGE
1280 GO TO 710
1290 CLOSE
1300 END

```

A P P E N D I X III

NOMENCLATURE

K = A linear spring rate.

K_T = A torsional spring rate.

d = The differential operator.

A = Area.

G = The shear modulus.

T = Torque.

t = The perpendicular layer thickness.

R = The spherical radius.

\bar{R} = The moment arm or distance to the bearing axis.

\bar{R}_o = The largest moment arm in a layer.

H = The axial distance from a point to the spherical axis.

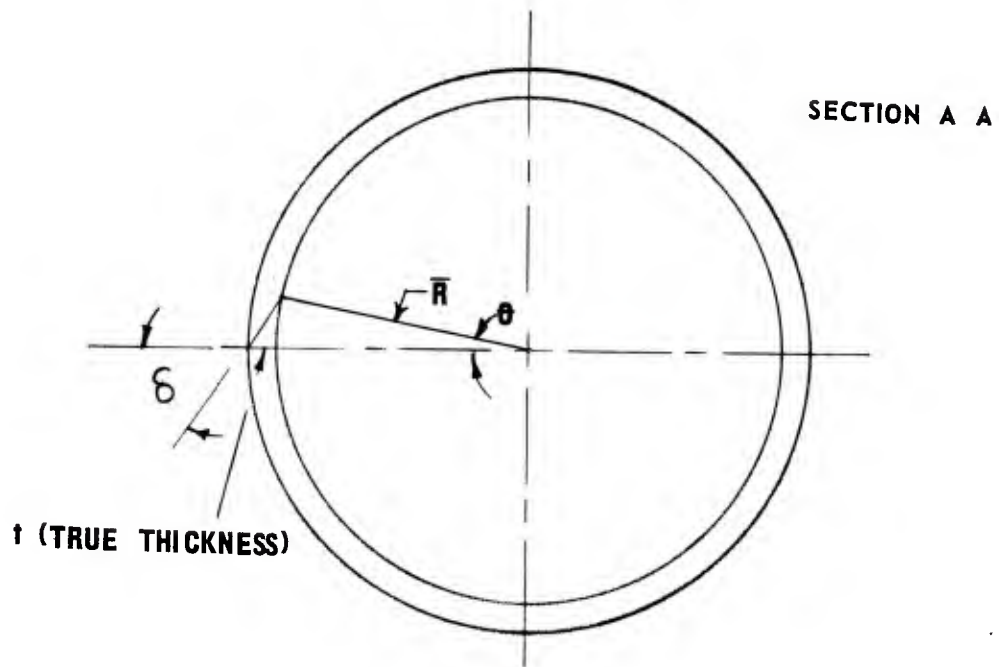
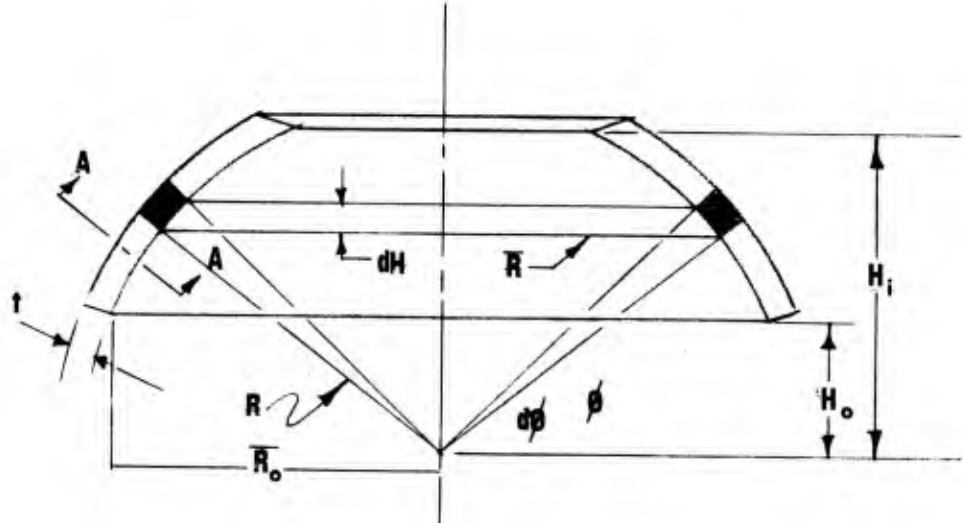
H_o = The axial distance of the O.D. of a layer to the spherical axis.

H_i = The axial distance of the I.D. of a layer to the spherical axis.

θ = The torsional angle of relative rotation for the layer.

ϕ = An arbitrary angle of integration.

γ = The shear strain.



AXIAL TORSION ON A POLAR SPHERICAL E.B.

AXIAL TORSION ON A POLAR SPHERICAL E.B.

The shear spring rate of an elastomeric layer is

$$K = F/\delta = \frac{GA}{t}$$

For a layer with constant thickness and modulus the rate of change of spring rate is

$$dK = (G/t)dA$$

The rate of change in torsional rate is

$$dK_T = \frac{GR^2}{t} dA$$

The differential area for a polar spherical layer (See Figure) is

$$dA = 2\pi\bar{R}Rd\phi$$

$$\phi = \sin^{-1}(H/R)$$

$$d\phi = \frac{dH}{\sqrt{R^2 - H^2}}$$

$$\bar{R} = \sqrt{R^2 - H^2}$$

$$dA = 2\pi R dH$$

Substituting in the spring rate equation

$$dK_T = \frac{2\pi GR}{t} (R^2 - H^2) dH$$

$$K_T = \frac{2\pi GR}{t} \int_{H_i}^{H_o} (R^2 - H^2) dH$$

$$K_T = \frac{2\pi GR}{t} \left[R^2(H_o - H_i) - (H_i^3 - H_o^3)/3 \right]$$

The definition of torsional spring rate is

$$K_T = T/\theta$$

The shear strain (See Figure) is

$$\gamma = \frac{\bar{R}\theta}{t}$$

$$\gamma = \frac{\bar{R}T}{tK_T}$$

$$\gamma = \frac{T \sqrt{R^2 - H^2}}{tK_T}$$

$$\gamma = \frac{T \sqrt{R^2 - H^2}}{2\pi GR} \left[\frac{1}{R^2(H_i - H_o) - (H_i^3 - H_o^3)/3} \right]$$

The pitch change shear strain is seen to be a function of position but, has a maximum at the O.D. of each layer of

$$\gamma_{MAX} = \frac{T}{2\pi G} \left[\frac{\sqrt{1 - (H_o/R)^2}}{R^2(H_i - H_o) - (H_i^3 - H_o^3)/3} \right]$$

The composite rotation for a multi-layer bearing is

$$\theta = \sum \frac{t \gamma_{MAX}}{\bar{R}_o}$$

$$= \frac{T}{2\pi} \sum \frac{1}{GR} \left[\frac{t}{R^2(H_i - H_o) - (H_i^3 - H_o^3)/3} \right]$$

A P P E N D I X IV

```

100 PAGE
110 INIT
120 PRINT "***** PITCH CHANGE STRAIN CALCULATIONS *****"
130 PRINT "***** for spherical EB with 2 different elastomers *****"
140 PRINT "layer no. from mushroom end at which elastomer changes---";
150 INPUT L
160 PRINT "FIRST SHEAR MODULUS,G1----";
170 INPUT G1
180 PRINT "SECOND SHEAR MODULUS,G2----";
190 INPUT G2
200 PRINT "NUMBER OF SHELLS-----";
210 INPUT J
220 PRINT "APPLIED TORQUE = ";
230 INPUT T
240 DIM F(50),P(50),R1(50),U(50)
250 PRINT "----- FIRST I.D. POINT -----"
260 PRINT "----- JSPHERICAL RADIUS 1 = ";
270 INPUT R
280 PRINT "I.D. 1 = ";
290 INPUT M1
300 X1=M1/2
310 Y1=SQR(R*R-X1*X1)
320 PRINT "----- SECOND I.D. POINT -----"
330 PRINT "----- JSPHERICAL RADIUS 2 = ";
340 INPUT R2
350 PRINT "I.D. 2 = ";
360 INPUT M2
370 X2=M2/2
380 Y2=SQR(R2*R2-X2*X2)
390 REM S'S ARE SLOPES & C'S ARE INTERCEPTS
400 S1=(Y1-Y2)/(X1-X2)
410 C1=Y1-S1*X1
420 PRINT "----- FIRST O.D. POINT -----"
430 PRINT "O.D. 1 = ";

```

```

440 INPUT M1
450 X1=M1/2
460 Y1=SQR(R*R-X1*X1)
470 PRINT "J----- SECOND O.D. POINT -----"
480 PRINT "O.D. 2 = ";
490 INPUT M2
500 X2=M2/2
510 PAGE
520 Y2=SQR(R2*R2-X2*X2)
530 S2=(Y1-Y2)/(X1-X2)
540 C2=Y1-S2*X1
550 I=1
560 G=G1
570 PRINT "INSIDE SPHERICAL RADIUS OF THE LAYER CONSIDERED";
580 INPUT R1(I)
590 Z=C1*S1/(S1*S1+1)
600 X=SQR(Z*Z+(R1(I)*R1(I)-C1*C1)/(S1*S1+1))-Z
610 H1=C1+S1*X
620 REM REPEATING FOR C2 & S2
630 Z=C2*S2/(S2*S2+1)
640 X=SQR(Z*Z+(R1(I)*R1(I)-C2*C2)/(S2*S2+1))-Z
650 H2=C2+S2*X
660 D=R1(I)*R1(I)*(H1-H2)-(H1+3-H2+3)/3
670 U=SQR(1-(H1/R1(I))^2)
680 F(I)=U*T/(D*D*PI*G)
690 PRINT "VERTICAL THICKNESS OF THE LAYER = ";
700 INPUT U(I)
710 P(I)=90*U(I)*T/(PI*PI*G*D*R1(I))
720 IF I<=L-1 THEN 740
730 G=G2
740 I=I+1
750 IF I<J+2 THEN 570
760 K=0
770 PAGE
780 PRINT USING "70";"---";

```

```

798 PRINT " PITCH CHANGE PARAMETERS"
800 PRINT USING "70";"";
810 PRINT USING 820;"NO.;";"LAYER";"INSIDE";"GAMMA";"THETA"
820 IMAGE3T,FA,10T,FA,21T,FA,31T,FA,41T,FA,
830 PRINT USING 820;"";"THICK";"RADIIUS";"STRAIN";"LAYER"
840 PRINT USING "70";"";
850 K=0
860 FOR I=1 TO J+1
870 K=K+P(I)
880 PRINT USING 890:I,U(I),R1(I),F(I),P(I)
890 IMAGE 3T,2D,10T,D,3D,21T,D,3D,31T,D,4D,41T,D,4D
900 NEXT I
910 PRINT USING "70";"";
920 PRINT "JTOTAL ANGLE OF TWIST IN DEGREES (THETA)----";
930 PRINT K
940 PRINT "JAPPLIED TORQUE IN LB.-INCHES-----";
950 PRINT T
960 END

```

SECTION 9.

TEST RESULTS ON THE BLACKHAWK MAIN ROTOR BEARINGS

Enclosed in the Appendix is a test report covering the testing of a pair of Blackhawk main rotor spherical and thrust elastomeric bearings as outlined in Section 1. These results should be correlated with previous analytical results.

The agreement between experimental and analytical predictions is reasonably good for the thrust bearing. See that Figures 4 and 5 of the Appendix confirm the location of first damage predicted in Section 6. The analytical prediction of time to first damage was 46 hours, whereas, first damage was actually reported as occurring between 200 and 300 hours. The test substantiated the analytical prediction that elastomer damage would occur before metal fatigue.

For the spherical bearing the agreement between experimental and theoretical predictions is again reasonably good for the elastomer. Photograph 2 shows the I.D. of the first layer as the location of first damage. The I.D. of the fourth layer is the location predicted in Section 8. The first damage life was between 300 and 400 hours vs. a predicted 866 hours. Remember that no prediction of the endurance life of the metal shells could be made in section 8.

It is important to recognize that "first damage" as defined here is the first sign of damage visible under laboratory conditions and that elastomer damage in an elastomeric bearing is slowly progressive and noncatastrophic. The justification for this statement is Sikorsky Aircraft's 2000 hr. qualification test with these bearings. While laboratory level damage was observed on these bearings relatively early in the test they continued on for from 10 to 20 times the laboratory first damage life shown here without excessive damage.

A P P E N D I X

CR INDUSTRIES

TEST REPORT

AMMRC Contract DAA-46-78-C-0029

May 22, 1979

By

Emmet M. Skroch

Test Lab Manager

TEST REPORT

This test consisted of endurance testing two Blackhawk Main Rotor Elastomeric Bearings per the plan described in the AMMRC test proposal of September 15, 1978.

Prior to any endurance testing all samples were acceptance tested according to their respective Sikorsky approved ATP's (ATP No. 4014 for 80 9588, Sikorsky SB7001-045 and ATP No. 4015 for 80 9589, Sikorsky SB7002-045).

For the spherical bearings (P/N 80 9588), slight modification to the end fitting had to be made (Figure 1.1) to fixture them in our test rig (Figure 1.2). Thermocouples were attached at the 6 o'clock and 9 o'clock position, both inside and outside, at the inner race. For the thrust bearing (P/N 80 9589), a thermocouple was attached to the outer center part of the bearing.

All loads and motions of the test were applied in 100 hour blocks as specified in the Blackhawk Main Rotor E. B. Endurance Life Test Blocks I through III.

Testing of the spherical bearing (P/N 80 9588), has been terminated after a total of 4 blocks of testing or 400 flight hours. First damage was observed at the first rubber layer (smallest spherical radius) at the 5 and 11 o'clock positions when flapping was applied through the 6 and 12 o'clock axis. Figures 2 and 3 show the degree of damage of each bearing. The recorded temperatures of the test ranged from 91°F to 109°F.

The loss of measured axial spring rates ranged from 2.4% to 3.4% for the 400 flight hour period.

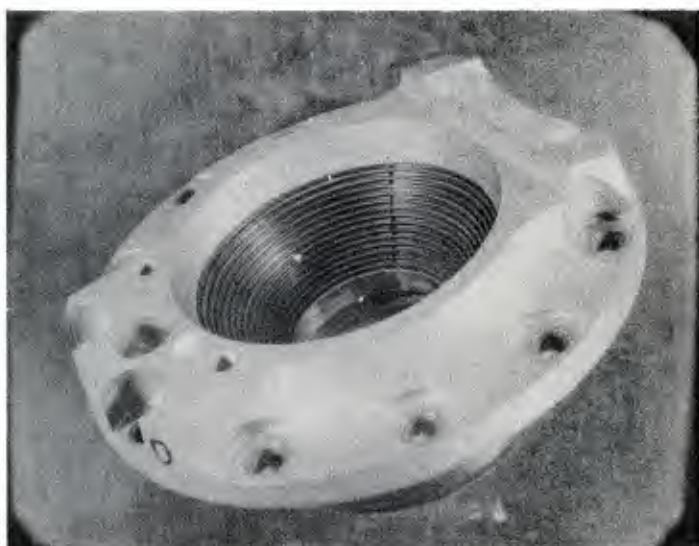
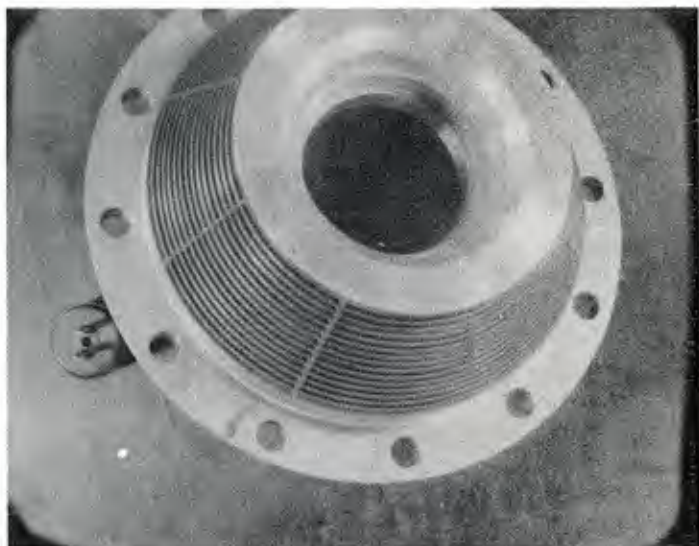
Testing of the thrust bearing (P/N 80 9588) has been terminated after a total of 3 blocks of testing or 300 flight hours. First damage was observed at the O.D. of the bearing on the spline side and at the I.D. on the flanged side. Figures 4 and 5 show the degree of the damage.

The recorded temperatures during the test ranged from 116°F to 120°F.

The loss of measured axial spring rates for the two bearings was as follows:

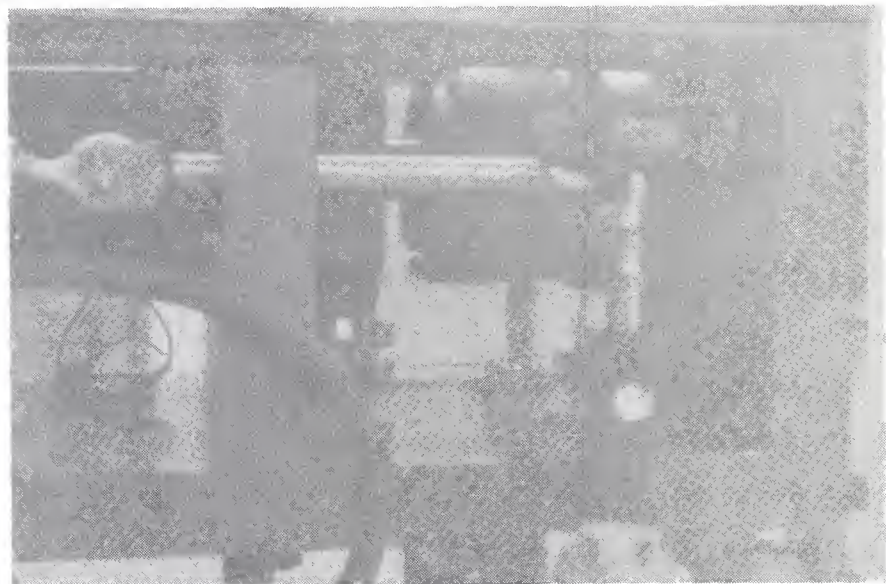
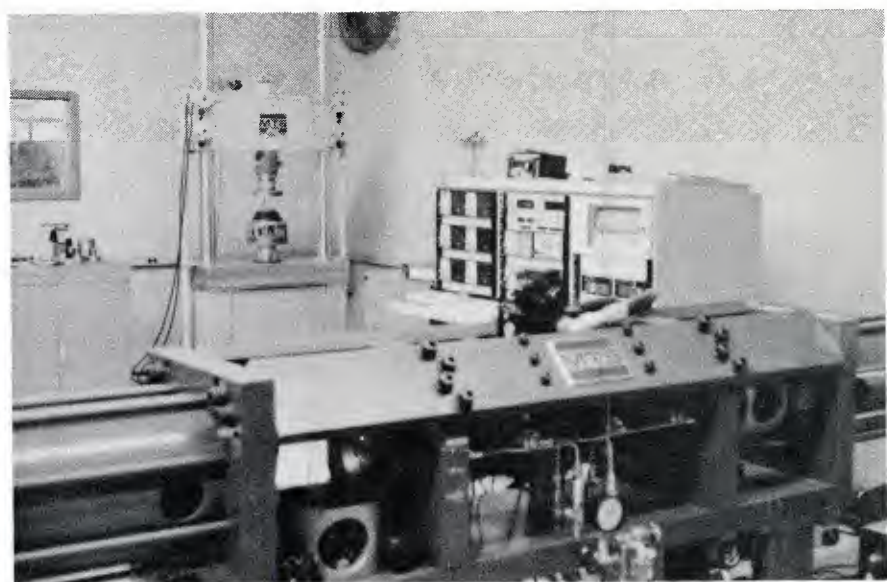
% Spring Rate Change

Flight Hours	SN 00049	SN 00051
New	-	-
200	1.3	2.6
300	1.3	5.1



MODIFIED SPHERICAL BEARING

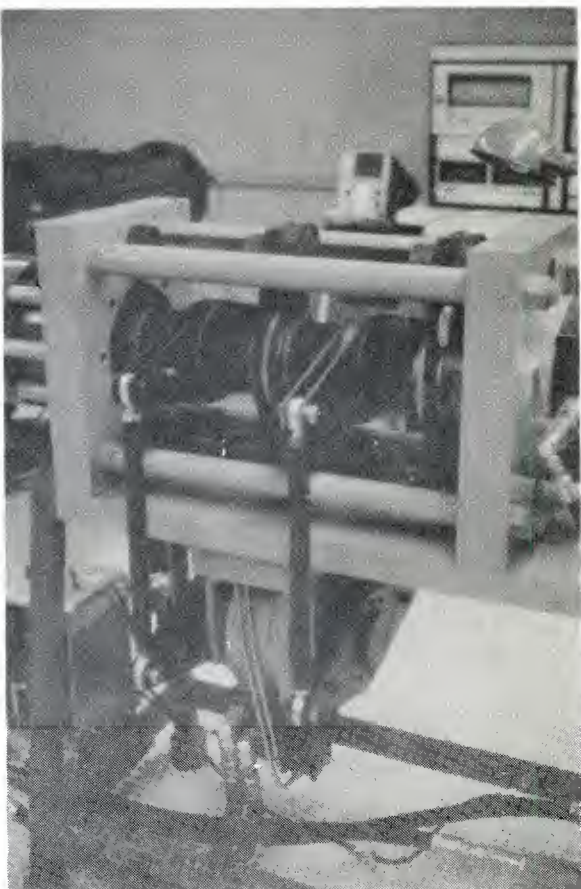
FIGURE 1.1



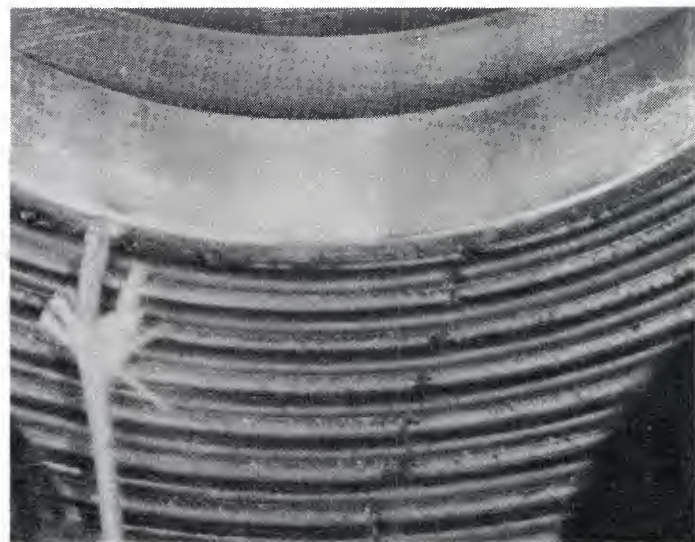
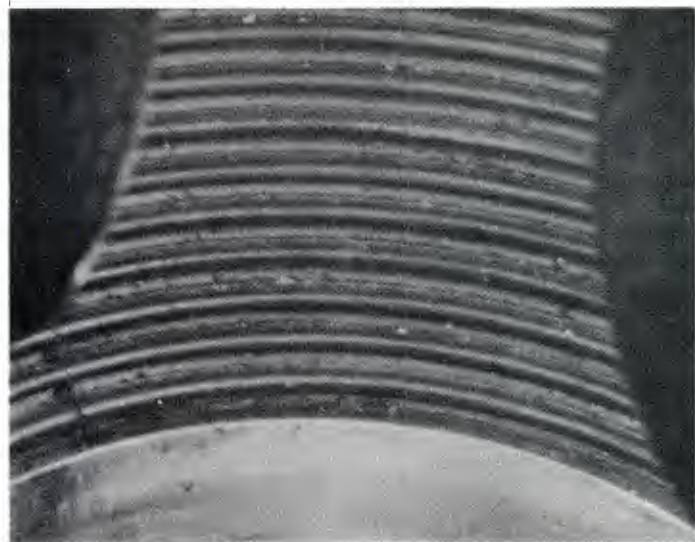
SPHERICAL BEARING

TEST RIG.

FIGURE 1.2



**THRUST BEARING
TEST RIG.
FIGURE 1.3**



C.R. 80 9588 (SN 00005) SPHERICAL
BEARING I.D. AFTER 400 FLIGHT
HOURS.

FIGURE 2



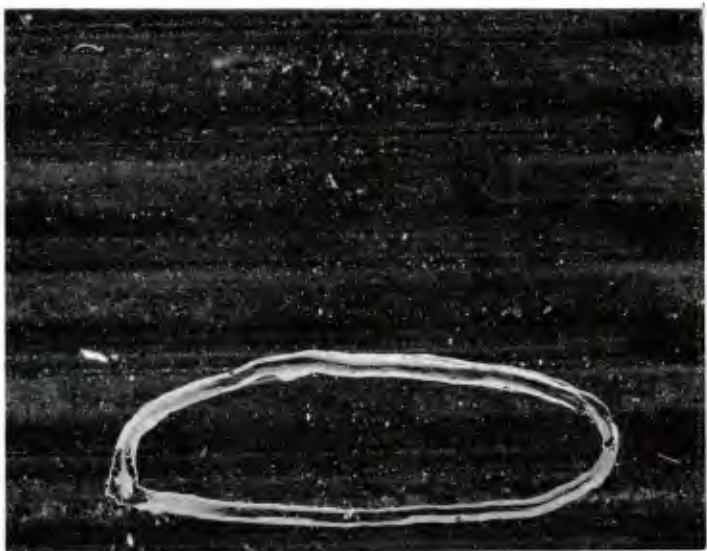
C.R. 80 9588 (SN 00004) SPHERICAL
BEARING I.D. AFTER 400 FLIGHT
HOURS.

FIGURE 3



THRUST BEARING I.D.

FIGURE 4



THRUST BEARING O.D.

FIGURE 5

SECTION 10.

TEST RESULTS ON THE BLACKHAWK MAIN ROTOR SPHERICAL BEARING
WITH ON-OFF CENTRIFUGAL FORCE AS THE ONLY LOADING MODE

In order to obtain some correlation between analytical and experimental results for shell stress in a spherical bearing, a sample was tested with on-off centrifugal force as the only loading (see test report in the Appendix). This test case can be completely analyzed by one program run of our quasi three-dimensional finite element analysis program. Fig. 1 shows the shell stress at the I.D. for this loading case and Fig. 2 shows it for the O.D. This loading case is not expected to produce failure in the 17-7 PH stainless steel shells. Shell failure was not observed in this test.

From results in Section 8, the predicted elastomer life under this loading condition is

$$\left(\frac{10.6}{2.95/2} \right)^5 = 19,200 \text{ cycles}$$

with first damage predicted for the I.D. of the fourth layer. First damage was experimentally noted at 55,000 cycles at the bearing I.D. in the zone of the 3rd to 5th layers.

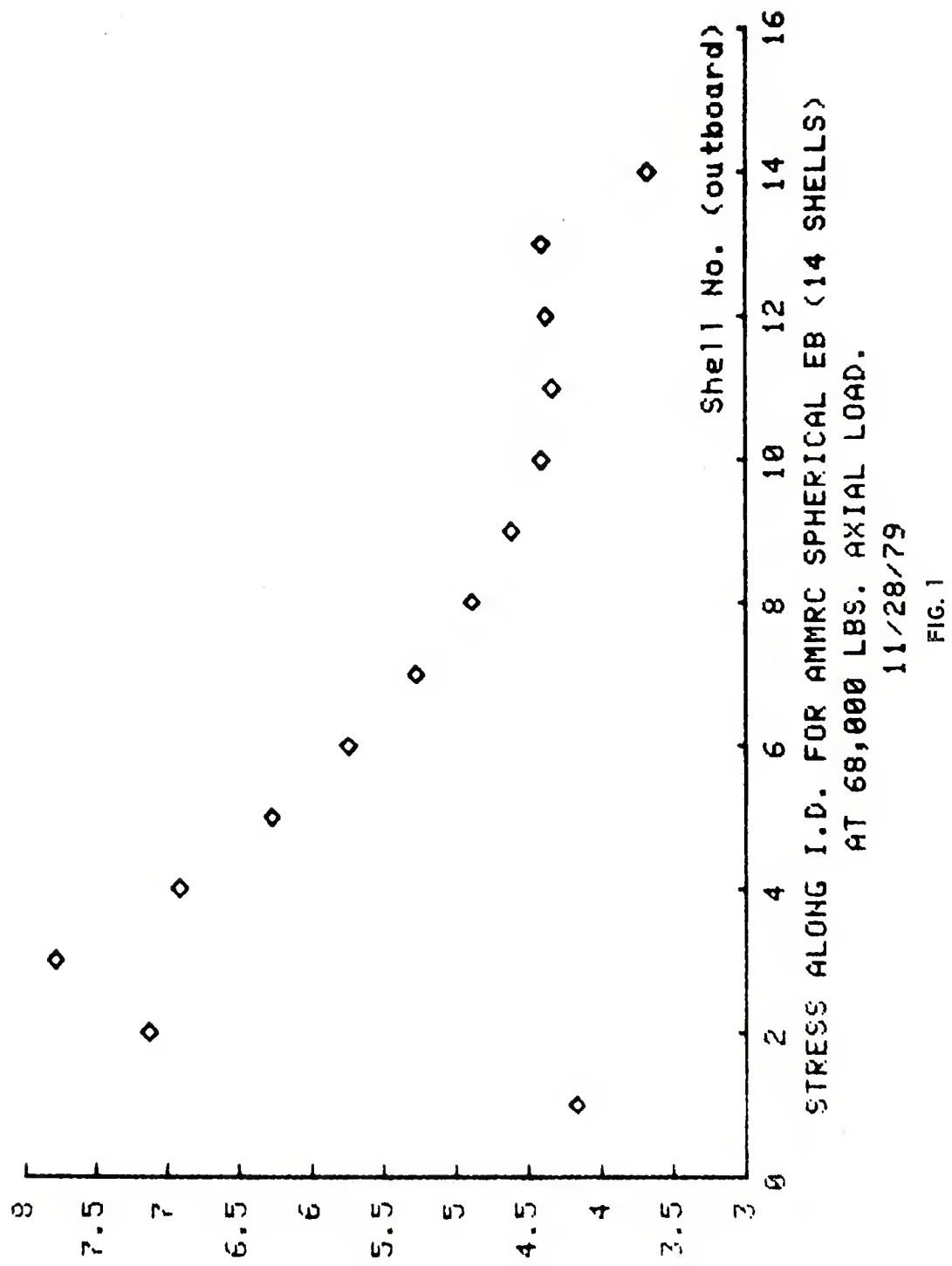


FIG. 1

H C C Q O + L N D V H T K - U - A -

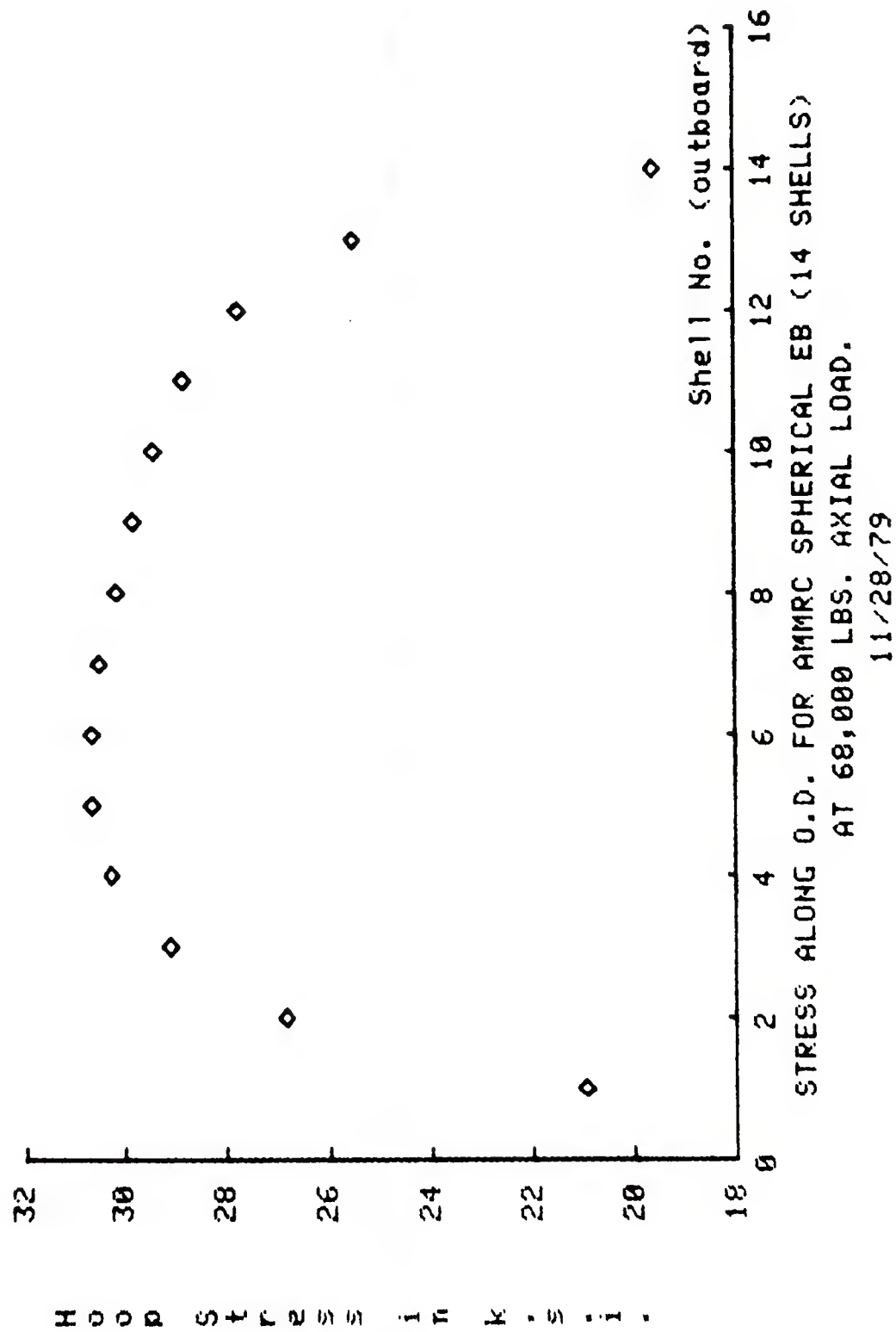


FIG. 2

APPENDIX

Chicago Rawhide Mfg. Co., 2517 Pan Am Blvd., Elk Grove Village, Ill. 60007, 312/595-4620



Test Report

AMMRC Contract DAA-46-78-C-0029

May 29, 1979

by

Emmet M. Skroch

Test Lab Manager

CHICAGO RAWHIDE MANUFACTURING COMPANY

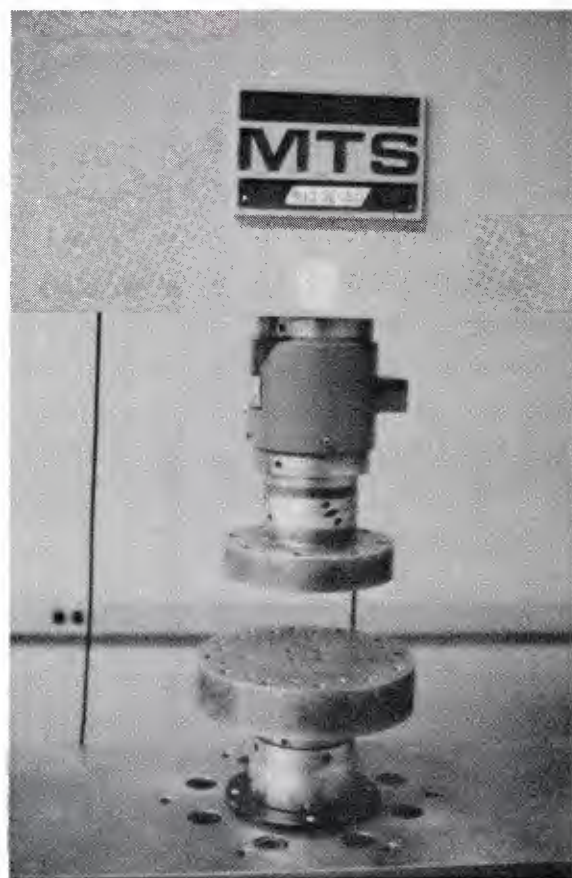
Test Report

This test consisted of endurance testing a Blackhawk Main Rotor Elastomeric Bearing by "on-off" C.F. loading.

Prior to any endurance testing, the sample was acceptance tested according to its' respective Sikorsky approved ATP (ATP No. 4014 for 80 9588, Sikorsky SB7001-045).

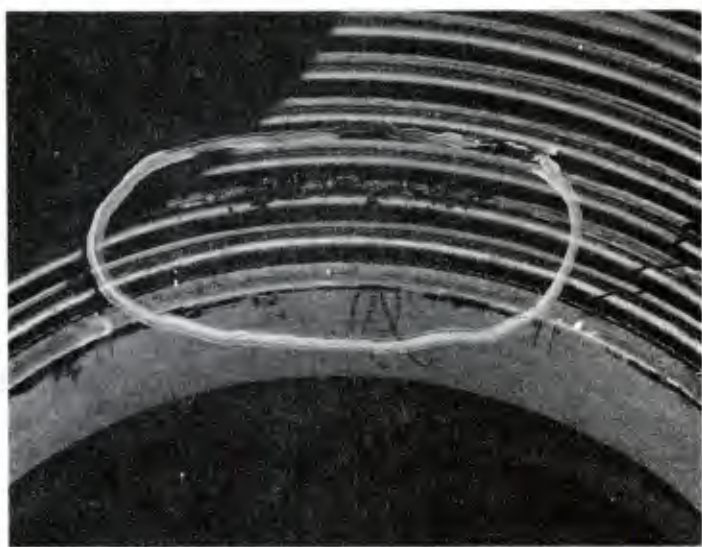
A spherical bearing (P/N 80 9588) was axially loaded and unloaded from 0 to 68,000 lbs. at a cycling rate of 20 cycles per minute (CPM). The test part was loaded in our 100 KIP test rig, see Figure 1.

First damage was observed after 55,000 on-off cycles or the equivalent of 27,500 flight hours as described in the AMMRC test proposal of September 15, 1978, Black Hawk Rotor E.B. Endurance Life Test Block III. The damaged area consisted of the first 10 elastomeric layers (smallest spherical radius being the 1st layer) at the I.D., in varying degree. Figure 2 shows the predominant damage which occurred in the zone of the 3rd through 5th layers.



AXIAL TEST RIG

FIGURE 1



I.D. OF 80 9588 (SPHERICAL BEARING)

FIGURE 2

SECTION 11.

TEST RESULTS ON THE ALTERNATE BLACKHAWK MAIN ROTOR THRUST
BEARING WITH ON-OFF CENTRIFUGAL FORCE AS THE ONLY LOADING
MODE.

In order to demonstrate the ability of finite element analysis to predict the endurance life of the metal shells in laminate elastomeric bearings a marginal bearing design was analyzed in Section 7 (see Fig. 1) and tested. The test report is included in the appendix. The analysis of this test case did not require the use of superposition. The correlation between analytic and test results should, therefore, be good. The correlation between analytic and test results is seen to be good -- the shells cracked about as predicted.

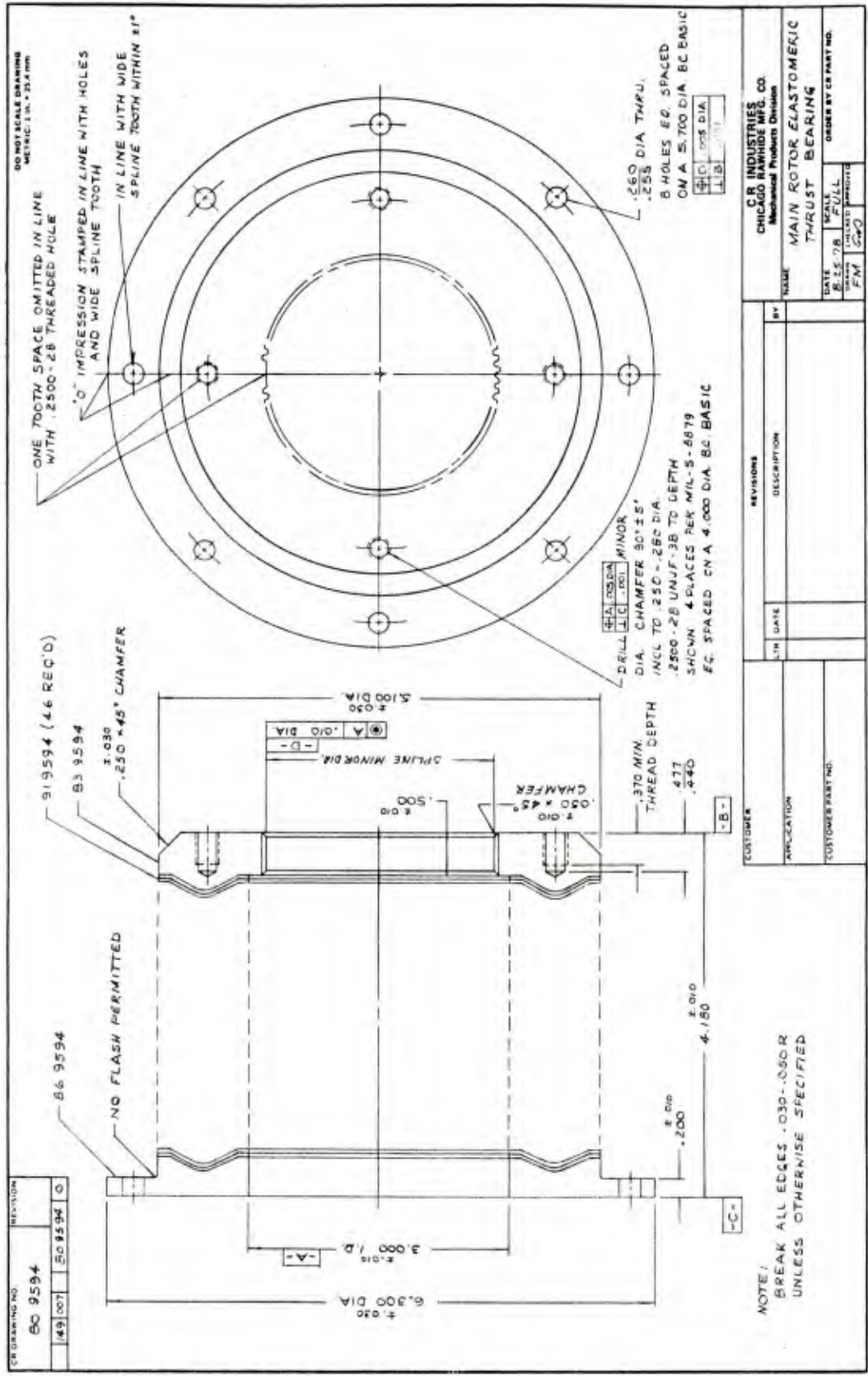


FIG. 1

APPENDIX

CHICAGO RAWHIDE MANUFACTURING COMPANY

July 2, 1979

F I N A L T E S T R E P O R T

AMMRC - Chevron Washer
SK5-80 9590

Thrust Bearing
H90112-1

The bearing tested January 17-19, 1979 was pulled to destruction and then soaked in toluene to remove the rubber and observe the washers.

In the layer that broke in the pull test, about 80% of the rubber was destroyed by fatigue damage. The pull test values were:

	<u>Test Piece</u>	<u>Control Piece</u>
Breaking Load	1,400 lbs.	8,200 lbs.
Extension	0.1 in.	0.15 in.
Mode of Failure	100R	90R 10 unfill

The cleaned washers were examined for cracks. (Flange end-1-52-Spline end)

One radial crack in washer #22 intersected the O.D..

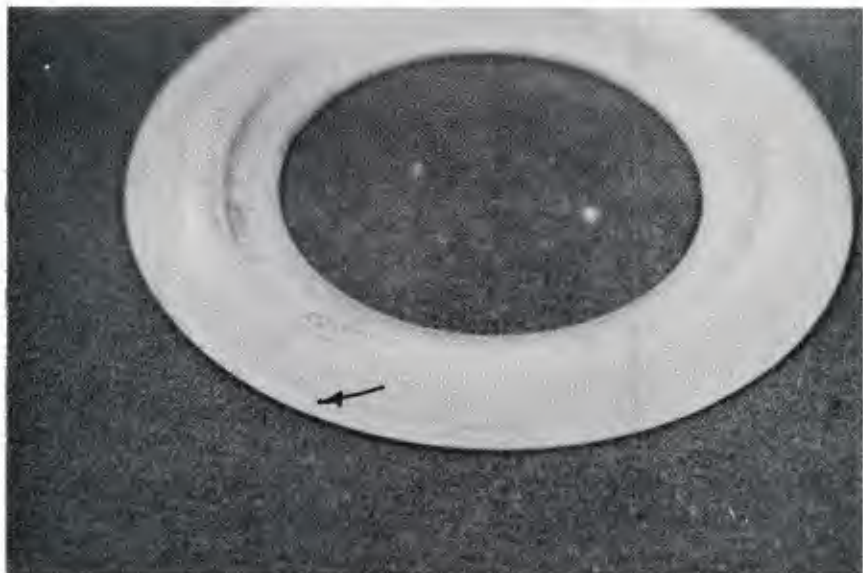
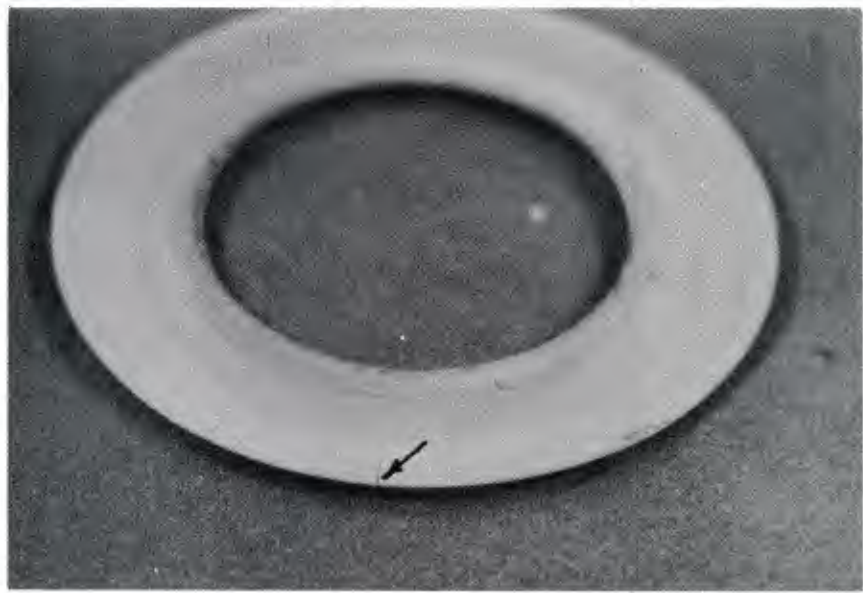
Nine washers exhibited tangential cracks along the top of the chevron. (#13, 18, 19, 20, 23, 24, 27, 29, 38)

Photographs of the cracked washers are attached.

Tom Mueller

Tom Mueller

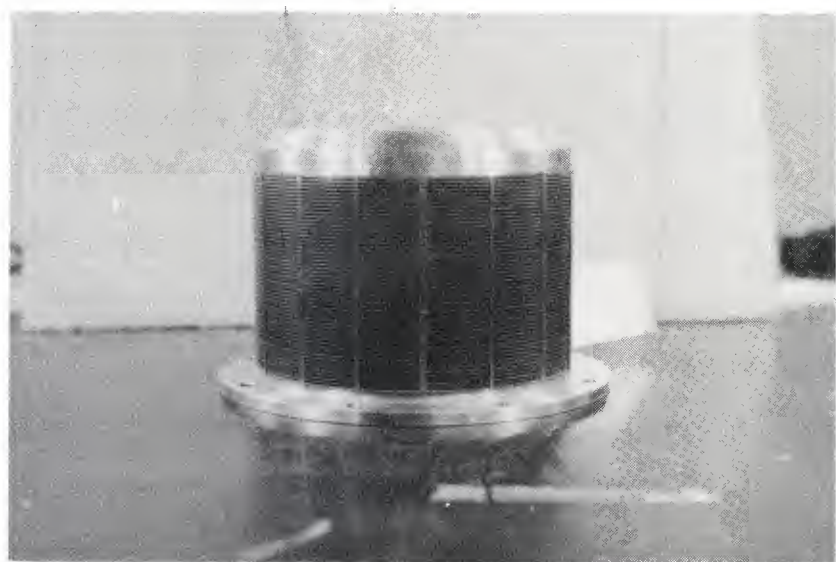
TM:lk
Enclosures



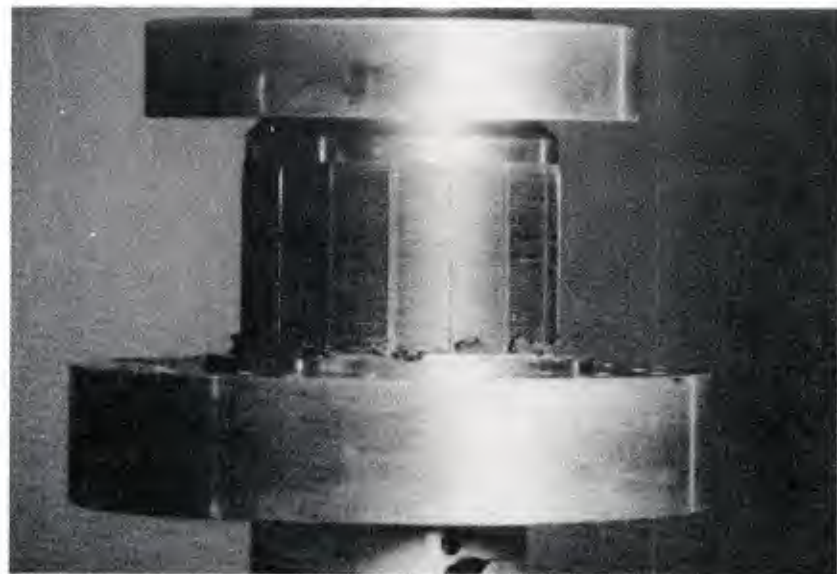
RADIAL CRACK



TANGENTIAL CRACK



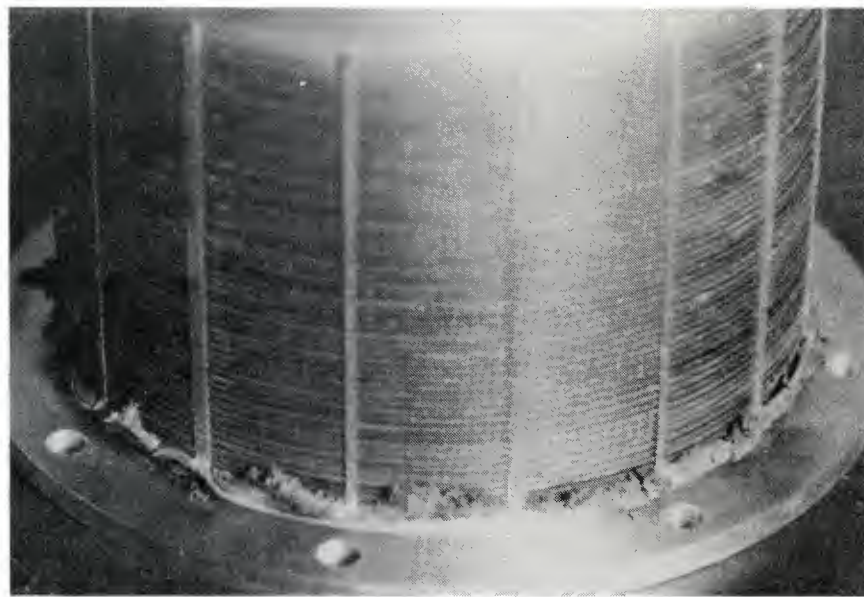
BEFORE



AFTER



I.D. DAMAGE



O.D. DAMAGE



O.D. CRACK

CHICAGO RAWHIDE MANUFACTURING COMPANY

January 23, 1979

TEST REPORT

AMMRC - Chevron Washer Thrust Bearing
SK5-80 9590 H90112-1

Test Start: 2:00 P.M. January 17, 1979
Stop: 7:46 P.M. January 19, 1979

At 51,300 GAG cycles a cracked washer was observed on the O.D. of the bearing.

The last inspection prior to the observation of the crack was at 45,800 GAG cycles.

A "clicking" sound was heard about the 43,000 cycle mark and went away.

The test has been stopped to get photographs of the cracked washer and to decide on further actions to be taken.

A table of axial spring rates is attached.

Tom Mueller

Tom Mueller

TM:lk
Enclosure

cc: J. Morley
A. Hatch
E. Skroch

SK5-80 9590
H90112-1

Axial Spring Rate

<u># Cycles</u>	<u>Deflection to 68,000 #</u> <u>Inches</u>	<u>40,000-68,000 #</u> <u>Lbs./In.</u>	<u>Tangent 68,000 #</u> <u>Lbs./In.</u>
0	0.100	933,000	1,000,000
15,000	0.110	830,000	1,000,000
25,000	0.112	830,000	950,000
30,000	0.115	830,000	950,000
45,000	0.115	830,000	890,000
50,000	0.115	830,000	890,000

Initial Ht. 50,000 ~ Δ_{HT}
4.202 4.180 .022

T.G.M.
1-23-79

The initial Chevron Washer Endurance Test for the AMMRC Contract was started at 2:00 P.M. January 17, 1979.

The test is running with the following parameters:

- | | |
|----------------------|--------------------------------|
| 1. Cyclic axial load | 100/68,000/100 lbs. |
| 2. Frequency | 20 cpm. |
| 3. Length of test | Until washer failure observed. |
| 4. Inspection period | At least twice daily. |
| 5. Documentation | Color photographs |
| | a) Initial condition. |
| | b) At point of washer failure. |

This is a modified SK5-80 9590 thrust bearing molded in the 80 9589 mold with modifications. It has 52 Titanium A70 washers of .030 thickness and .245 radius (see drawing attached). The end fittings are steel.

The bonding process on the Titanium was done per P-7554, which is the current production process on the Sikorsky main rotor bearings for Titanium.

Weight: 9.25#
Height: 4.202 in.

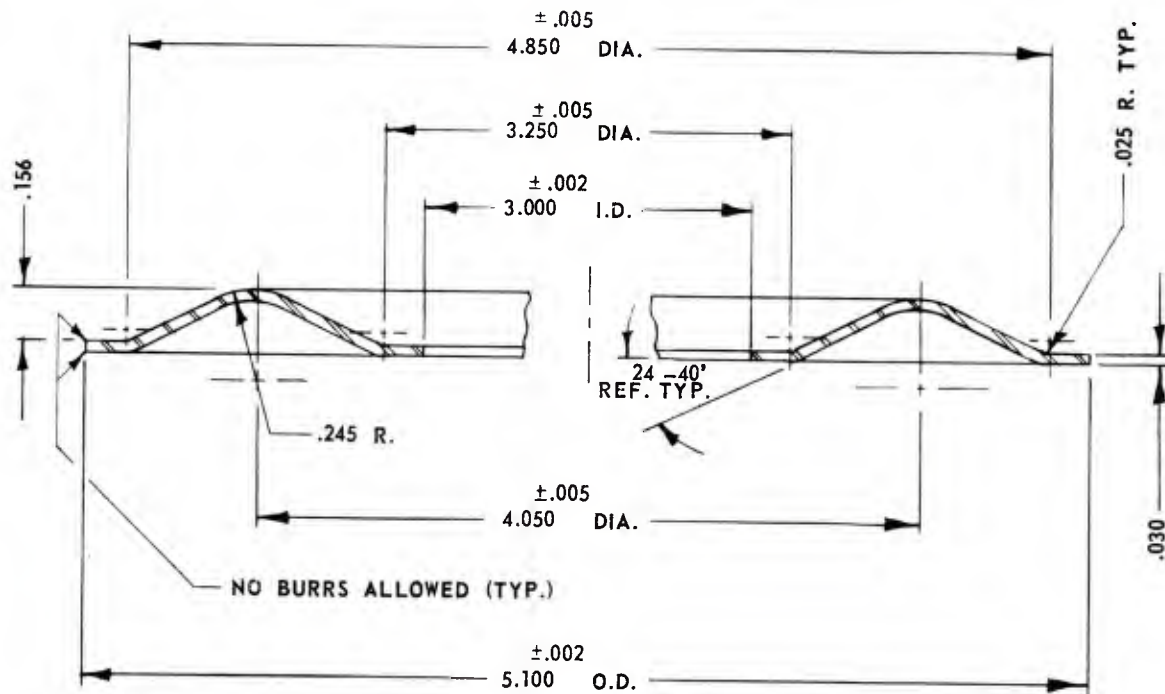
Tom Mueller

Tom Mueller

TM:1k

cc: J. Morley, A. Hatch, E. Skroch

DISPOSITION:	REVISIONS					
	LTR	DESCRIPTION	DATE	DRAWN	CHK	APPR



NOTES:

1. I.D. & O.D. MUST BE CONCENTRIC WITHIN .003 T.I.R.
2. MUST BE FLAT WITHIN .005 T.I.R.

USED IN DL:	METRIC: 1 IN. = 25.4 mm UNLESS OTHERWISE SPECIFIED DIAMETER $\pm .010$ HEIGHTS $\pm .005$ DRILLED HOLES + .010 - .000 BREAK SHARP EDGES .005 TO .015 REMOVE ALL BURRS FINISH ALL OVER R.M.S. CONCENTRIC WITHIN .006 T.I.R. CORNER FILLETS .006 - .015 R. ANGLES $\pm 30^{\circ}$	MATERIAL TITANIUM AMS 4901 OR ASTM B265 GRADE 4	C R INDUSTRIES CHICAGO RAWHIDE MFG. CO. Mechanical Products Division			
			NAME: WASHER	SCALE: 2x	DATE: 8-3-78	CR DWG. NO. SK 5-91 9590
			DRAWN BY: RZ	CHECKED: GIL	APPROVED: AT	REV.

SECTION 12.

SUMMARY AND CONCLUSIONS

An analytical method for predicting the service life of laminated elastomeric bearings based on finite element analysis has been demonstrated. This method has shown generally good agreement with experimental results. The analytical method makes use of superposition to combine out-of-phase strain vectors and quasi three-dimensional strain analysis to find the endurance strain of complex bearings undergoing complex loadings. Limitations on superposition were indicated (shell stress in the spherical bearing). Finally a specific elastomer endurance relationship was drawn from test data on a fatigue specimen. With this background the analytic analysis provided a reasonable estimate of the location and time of first damage on the Blackhawk main rotor spherical and thrust bearings tested as part of this program. Good results were obtained in predicting the endurance life of the metal shells in the thrust bearing but, a prediction was not possible for the spherical bearing.

Future investigations in elastomeric bearing analysis could involve the study of some of the following areas:

- A) Three-dimensional finite element analysis.
- B) The effect of the bias strain on endurance life.
- C) The effect of temperature on endurance life.
- D) The effect of strain rate on endurance life.
- E) The strain-relaxation characteristics of elastomers under constant and varying loads.

- F) The effect of environmental media on the endurance life of elastomers.
- G) The measurement and control of the physical properties of the elastomer.
- H) The development of a three-dimensional shear strain endurance life criterion for elastomers.

DISTRIBUTION LIST

No. of Copies	To
	Commander, U.S. Army Aviation Research and Development Command, P.O. Box 209, St. Louis, Missouri 63166
10	ATTN: DRDAV-EGX
1	DRDAV-D
1	DRDAV-N
	Project Manager, Advanced Attack Helicopter, P.O. Box 209, St. Louis, Missouri 63166
2	ATTN: DRCPM-AAH-TM
1	DRCPM-AAH-TP
	Project Manager, Black Hawk, P.O. Box 209, St. Louis, Missouri 63166
2	ATTN: DRCPM-BH-T
	Project Manager, CH-47 Modernization, P.O. Box 209, St. Louis, Missouri 63166
2	ATTN: DRCPM-CH-47-MT
	Project Manager, Aircraft Survivability Equipment, P.O. Box 209, St. Louis, Missouri 63166
2	ATTN: DRCPM-ASE-TM
	Project Manager, Cobra, P.O. Box 209, St. Louis, Missouri 63166
2	ATTN: DRCPM-CO-T
	Project Manager, Advanced Scout Helicopter, P.O. Box 209, St. Louis, Missouri 63166
2	ATTN: DRCPM-ASH
	Project Manager, Navigation/Control Systems, Fort Monmouth, New Jersey 07703
2	ATTN: DRCPM-NC-TM
	Project Manager, Tactical Airborne Remotely Piloted Vehicle/Drone Systems, P.O. Box 209, St. Louis, Missouri 63166
2	ATTN: DRCPM-RPV
	Commander, U.S. Army Materiel Development and Readiness Command, 5001 Eisenhower Avenue, Alexandria, Virginia 22333
1	ATTN: DRCM
1	DRCPM
	Director, Applied Technology Laboratory, Research and Technology Laboratories (AVRADCOM), Fort Eustis, Virginia 23604
1	ATTN: DAVDL-ATL-ATS
	Director, Research and Technology Laboratories (AVRADCOM), Moffett Field, California 94035
1	ATTN: DAVDL-AL-D

No. of Copies	To
	Director, Langley Directorate, U.S. Army Air Mobility Research and Development Laboratories (AVRADCOM), Hampton, Virginia 23365
1	ATTN: DAVDL-LA, Mail Stop 266
	Commander, U.S. Army Avionics Research and Development Activity, Fort Monmouth, New Jersey 07703
1	ATTN: DAVA-A-O
	Director, Lewis Directorate, U.S. Army Air Mobility Research and Development Laboratories, 21000 Brookpark Road, Cleveland, Ohio 44135
1	ATTN: DAVDL-LE
	Director, U.S. Army Materials and Mechanics Research Center Watertown, Massachusetts 02172
2	ATTN: DRXMR-PL
1	DRXMR-PR
1	DRXMR-PD
1	DRXMR-AP
1	DRXMR-PMT
8	DRXMR-RC, Mr. B. Halpin
	Director, U.S. Army Industrial Base Engineering Activity, Rock Island Arsenal, Rock Island, Illinois 61299
2	ATTN: DRXIB-MT
	Commander, U.S. Army Troop Support and Aviation Materiel Readiness Command, 4300 Goodfellow Boulevard, St. Louis, Missouri 63120
1	ATTN: DRSTS-PLC
1	DRSTS-ME
1	DRSTS-DIL
	Office of the Under Secretary of Defense for Research and Engineering, The Pentagon, Washington, D.C. 20301
1	ATTN: Dr. L. L. Lehn, Room 3D 1079
12	Commander, Defense Technical Information Center, Cameron Station, Alexandria, Virginia 22314
	Defense Industrial Resources Office, DIRSO, Dwyer Building, Cameron Station, Alexandria, Virginia 22314
1	ATTN: Mr. C. P. Downer
	Headquarters, Department of the Army, Washington, D.C. 20310
1	ATTN: DAMA-CSS, Dr. J. Bryant
1	DAMA-PPP, Mr. R. Vawter
	Director, Defense Advanced Research Projects Agency, 1400 Wilson Boulevard, Arlington, Virginia 22209
1	ATTN: Dr. A. Bement

No. of Copies	To
	Commander, U.S. Army Missile Command, Redstone Arsenal, Alabama 35809
1	ATTN: DRSMI-ET
1	DRSMI-RBLD, Redstone Scientific Information Center
1	DRSMI-NSS
	Commander, U.S. Army Tank-Automotive Research and Development Command, Warren, Michigan 48090
1	ATTN: DRDTA-R
1	DRDTA-RCKM, Dr. J. Chevalier
1	Technical Library
	Commander, U.S. Army Tank-Automotive Materiel Readiness Command, Warren, Michigan 48090
1	ATTN: DRSTA-EB
	Commander, U.S. Army Armament Research and Development Command, Dover, New Jersey 07801
1	ATTN: DRDAR-PML
1	Technical Library
1	Mr. Harry E. Pebly, Jr., PLASTEC, Director
	Commander, U.S. Army Armament Research and Development Command, Watervliet, New York 12189
1	ATTN: DRDAR-LCB-S
1	SARWV-PPPI
	Commander, U.S. Army Armament Materiel Readiness Command, Rock Island, Illinois 61299
1	ATTN: DRSAR-IRB
1	DRSAR-IMC
1	Technical Library
	Commander, U.S. Army Foreign Science and Technology Center, 220 7th Street, N.E., Charlottesville, Virginia 22901
1	ATTN: DRXST-SD3
	Commander, U.S. Army Electronics Research and Development Command, Fort Monmouth, New Jersey 07703
1	ATTN: DELET-DS
	Commander, U.S. Army Electronics Research and Development Command, 2800 Powder Mill Road, Adelphi, Maryland 20783
1	ATTN: DRDEL-BC
	Commander, U.S. Army Depot Systems Command, Chambersburg, Pennsylvania 17201
1	ATTN: DRSDS-PMI
	Commander, U.S. Army Test and Evaluation Command, Aberdeen Proving Ground, Maryland 21005
1	ATTN: DRSTE-ME

No. of Copies	To
	Commander, U.S. Army Communications and Electronics Materiel Readiness Command, Fort Monmouth, New Jersey 07703
1	ATTN: DRSEL-LE-R
	Commander, U.S. Army Communications Research and Development Command, Fort Monmouth, New Jersey 07703
1	ATTN: DRDCO-PPA-TP
	Director, U.S. Army Ballistic Research Laboratory, Aberdeen Proving Ground, Maryland 21005
1	ATTN: DRDAR-TSB-S (STINFO)
	Chief of Naval Research, Arlington, Virginia 22217
1	ATTN: Code 472
	Headquarters, Naval Material Command, Washington, D.C. 20360
1	ATTN: Code MAT-042M
	Headquarters, Naval Air Systems Command, Washington, D.C. 20361
1	ATTN: Code 5203
	Headquarters, Naval Sea Systems Command, 1941 Jefferson Davis Highway, Arlington, Virginia 22376
1	ATTN: Code 035
	Headquarters, Naval Electronics Systems Command, Washington, D.C. 20360
1	ATTN: Code 504
	Director, Naval Material Command, Industrial Resources Detachment, Building 75-2, Naval Base, Philadelphia, Pennsylvania 19112
1	ATTN: Technical Director
	Commander, U.S. Air Force Wright Aeronautical Laboratories, Wright-Patterson Air Force Base, Ohio 45433
1	ATTN: AFWAL/MLTN
1	AFWAL/MLTM
1	AFWAL/MLTE
1	AFWAL/MLTC
	National Aeronautics and Space Administration, Washington, D.C. 20546
1	ATTN: AFSS-AD, Office of Scientific and Technical Information
	National Aeronautics and Space Administration, Marshall Space Flight Center, Huntsville, Alabama 35812
1	ATTN: R. J. Schwinghammer, EH01, Dir., M&P Lab
1	Mr. W. A. Wilson, EH41, Bldg. 4612
	Metals and Ceramics Information Center, Battelle Columbus Laboratories, 505 King Avenue, Columbus, Ohio 43201

No. of Copies	To
	Hughes Helicopters-Summa, M/S T-419, Centinella Avenue and Teale Street, Culver City, California 90230
1	ATTN: Mr. R. E. Moore, Bldg. 314
	Sikorsky Aircraft Division, United Aircraft Corporation, Stratford, Connecticut 06497
1	ATTN: Mr. Melvin M. Schwartz, Chief, Manufacturing Technology
	Bell Helicopter Textron, Division of Textron, Inc., P.O. Box 482, Fort Worth, Texas 76101
1	ATTN: Mr. P. Baumgartner, Chief, Manufacturing Technology
1	Mr. Robert Phinney; Rotor Design Group
	Kaman Aerospace Corporation, Bloomfield, Connecticut 06002
1	ATTN: Mr. A. S. Falcone, Chief, Materials Engineering
	Boeing Vertol Company, Box 16858, Philadelphia, Pennsylvania 19142
1	ATTN: R. Pinckney, Manufacturing Technology
1	R. Drago, Advanced Drive Systems Technology
	Detroit Diesel Allison Division, General Motors Corporation, P.O. Box 894, Indianapolis, Indiana 46206
1	ATTN: James E. Knott, General Manager
	General Electric Company, 10449 St. Charles Rock Road, St. Ann, Missouri 63074
1	ATTN: Mr. H. Franzen
	AVCO-Lycoming Corporation, 550 South Main Street, Stratford, Connecticut 08497
1	ATTN: Mr. V. Strautman, Manager, Process Technology Laboratory
	United Technologies Corporation, Pratt & Whitney Aircraft Division, Manufacturing Research and Development, East Hartford, Connecticut 06108
1	ATTN: Mr. Ray Traynor
	Grumman Aerospace Corporation, Plant 2, Bethpage, New York 11714
1	ATTN: Richard Cyphers, Manager, Manufacturing Technology
1	Albert Grenci, Manufacturing Engineer, Department 231
	Lockheed Missiles and Space Company, Inc., Manufacturing Research, 1111 Lockheed Way, Sunnyvale, California 94088
1	ATTN: H. Dorfman, Research Specialist
	Lockheed Missiles and Space Company, Inc., P.O. Box 504, Sunnyvale, California 94086
1	ATTN: D. M. Schwartz, Dept. 55-10, Bldg. 572
	Barry Controls, 700 Pleasant Street, Watertown, Massachusetts 02172
1	ATTN: R. R. Peterson, Technical Director

Army Materials and Mechanics Research Center,
Watertown, Massachusetts 02172
SERVICE LIFE DETERMINATION FOR
UH-60A (BLACKHAWK) HELICOPTER
ELASTOMERIC BEARINGS

Technical Report AVRACOM-80-F-8, April 1980,
270 pp-illus-table,D/A Project: 1757095
AMCMS Code 1498.94.587095 (YY5)

A method is shown for using finite element strain data and elastomer endurance data to predict the service life of elastomeric bearings. The method was demonstrated on the UH-60A (Blackhawk) helicopter main rotor bearings. These bearings were then tested to determine the degree of correlation between analytical and test results. Photographic documentation is given for the damage seen on the elastomeric bearings as a guide in establishing a bearing life criterion based on bearing appearance.

AD UNCLASSIFIED
UNLIMITED DISTRIBUTION
UH-60A (BLACKHAWK) HELICOPTER
ELASTOMERIC BEARINGS

Key Words
UH-60 Helicopter
Elastomeric-Bearings
Life expectancy

AD UNCLASSIFIED
UNLIMITED DISTRIBUTION
UH-60A (BLACKHAWK) HELICOPTER
ELASTOMERIC BEARINGS

Key Words
UH-60 Helicopter
Elastomeric-Bearings
Life expectancy

Army Materials and Mechanics Research Center,
Watertown, Massachusetts 02172
SERVICE LIFE DETERMINATION FOR
UH-60A (BLACKHAWK) HELICOPTER
ELASTOMERIC BEARINGS

Technical Report AVRACOM-80-F-8, April 1980,
270 pp-illus-table,D/A Project: 1757095
AMCMS Code 1498.94.587095 (YY5)

AD UNCLASSIFIED
UNLIMITED DISTRIBUTION
UH-60A (BLACKHAWK) HELICOPTER
ELASTOMERIC BEARINGS

Key Words
UH-60 Helicopter
Elastomeric-Bearings
Life expectancy

AD UNCLASSIFIED
UNLIMITED DISTRIBUTION
UH-60A (BLACKHAWK) HELICOPTER
ELASTOMERIC BEARINGS

Key Words
UH-60 Helicopter
Elastomeric-Bearings
Life expectancy

A method is shown for using finite element strain data and elastomer endurance data to predict the service life of elastomeric bearings. The method was demonstrated on the UH-60A (Blackhawk) helicopter main rotor bearings. These bearings were then tested to determine the degree of correlation between analytical and test results. Photographic documentation is given for the damage seen on the elastomeric bearings as a guide in establishing a bearing life criterion based on bearing appearance.

A method is shown for using finite element strain data and elastomer endurance data to predict the service life of elastomeric bearings. The method was demonstrated on the UH-60A (Blackhawk) helicopter main rotor bearings. These bearings were then tested to determine the degree of correlation between analytical and test results. Photographic documentation is given for the damage seen on the elastomeric bearings as a guide in establishing a bearing life criterion based on bearing appearance.